The role of residues Tyr381 to Val387, in transmembrane domain six of the rat M_1 muscarinic acetylcholine receptor, in agonist binding and receptor activation.

Stuart D. C. Ward

A thesis submitted in fulfilment of the requirements of the University of London for the degree of Doctor of Philosophy.

1999

National Institute for Medical Research,
The Ridgeway,
Mill Hill,
London NW7 1AA

University College London,
Gower Street,
London WC1E 6BT

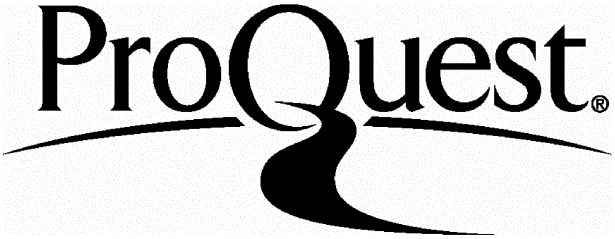

Abstract.

The aim of this project was to investigate the role of residues Tyr381 to Val387 in transmembrane domain six of the rat M_1 muscarinic acetylcholine receptor. Scanning mutagenesis was used. The mutant receptors were characterised by radioligand binding studies and phosphoinositide turnover assays giving measurements of both acetylcholine binding and the acetylcholine induced functional response. Tyr381Ala and Asn382Ala gave the greatest effects. Interestingly, Tyr381 and Asn382 are both conserved in, and specific to the muscarinic acetylcholine receptors and are, therefore, likely to have important functions. The role of these two residues was investigated further by (i) using three series of agonist and antagonist analogues (ACh analogues, azanorbornane- and quinuclidine-based ligands and atropine analogues) as pharmacological probes and, (ii) making the Tyr381Phe mutation to analyse the function of the hydroxyl group and benzene ring of Tyr381. The results indicated that Tyr381 was important in forming interactions with agonists and subsequent receptor activation, whereas Asn382 seemed to be more important for antagonist, especially atropine analogue, binding. Additionally, both residues may form intra-molecular interactions which help to stabilise receptor folding. In the receptor's ground state, the hydroxyl group of Tyr381 forms a hydrogen-bond interaction with the ester-moiety present in the side-chain of acetylcholine, whereas, the benzene ring of Tyr381 is critical for stabilisation or formation of the receptor's activated state, probably by forming a cation-π interaction with the positively charged head-group. The Tyr381 residue made similar interactions with the azanorbornane- and quinuclidine-based ligands, although with a different balance between ground and activated states. In the case of antagonists related to atropine, Tyr381 made both head-group and side-chain interactions in the receptor's ground state. However, Asn382 seemed to play a bigger role, than Tyr381, in the binding of these compounds, via the formation of a hydrogen-bond interaction with their ester moiety.

Table of Contents.

List of Figures.

List of Tables.

List of Abbreviations.

αK	intrinsic efficacy
α-MEM	α-minimal essential medium
[^{3}H]-NMS	(–)-[^{3}H]*N*-methylscopolamine
[^{3}H]-QNB	(–)-[^{3}H]quinuclidinylbenzilate
[^{35}S]-GTPγS	[^{35}S]-guanosine 5'-O-(3-thiotriphosphate)
ACh	acetylcholine
ACh-N(Et)$_2$	N,N-diethyl-N-methyl-aminoethyl acetate iodide
ACh-reversed ester	methyl-(N,N-dimethyl-3-amino)propionate methiodide
Ac-N-Me-Quin	3-acetoxy-N-methyl quinuclidine iodide
ATP	adenosine 5'-triphosphate
bp	base pair
CHO	Chinese hamster ovary
COS-7	African Green monkey kidney cell
cGMP	cyclic guanosine 5'-monophosphate
DAG	diacylglycerol
dLoop	loop deletion construct (residues 225-353 are removed)
DMSO	dimethylsulfoxide
DNA	deoxyribonucleic acid
dpm	disintegrations per minute
EC_{50}	drug concentration that produces 50 % of the maximum response
E.coli	*Escherichia coli*
EDTA	ethylenediaminetetraacetic acid
FPLC	fast protein/polypeptide/polynucleotide liquid chromatography
G protein	guanine nucleotide binding protein
GDP	guanosine 5'-diphosphate
GPCR	G protein-coupled receptor
GRK	G protein-coupled receptor kinase
GTP	guanosine 5'-triphosphate
GTPase	guanosine 5'-triphosphatase
GTPγS	guanosine 5'-O-(3-thiotriphosphate)
HEPES	N-[2-hydroxyethyl]piperazine-N'-[2-ethansulphonic acid]
IC_{50}	drug concentration that inhibits the maximum response by 50 %
K_A	association constant

K_B	competitive antagonist association constant
K_D	dissociation constant
L-658,903	3-(3-methyl-1,2,4-oxadiazol-5-yl)quinuclidine hydrochloride
L-661,319	3-(4-methylfuran-2-yl)quinuclidine hydrochloride
L-661,326	3-(2-methylfuran-4-yl)quinuclidine hydrochloride
L-683,355	(S)-3-(4-methyloxazol-2-yl)quinuclidine hydrochloride
L-683,356	(R)-3-(4-methyloxazol-2-yl)quinuclidine hydrochloride
L-693,046	3-(3-pyridyl)quinuclidine hydrochloride
L-698,583	(R)-3-(3-methyl-1,2,4-oxadiazol-5-yl)-1-azabicyclo[2.2.1]heptane hydrochloride
mAChR	muscarinic acetylcholine receptor
mRNA	messenger ribonucleic acid
nAChR	nicotinic acetylcholine receptor
n_H	Hill Coefficient
N.M.B.	no measurable binding
NMR	nuclear magnetic resonance
NMS	*N*-methylscopolamine
pX	- Log (X)
PCR	polymerase chain reaction
PI	phosphoinositide
pIns-4,5-P_2	phosphatidylinositol-4,5-bisphosphate
pIns-1,4,5-P_3	phosphatidylinositol-1,4,5-trisphosphate
PKA	protein kinase A
PKC	protein kinase C
RAMP	receptor-activity modifying protein
RGS proteins	regulators of G protein signalling proteins
rpm	revolutions per minute
SDS	sodium dodecyl sulfate
S.E.M.	standard error of the mean
SV40	Simian virus 40
TAE	tris-acetate/EDTA buffer
TM	transmembrane

1. Introduction.

Sir Henry Dale, in 1914, produced a definition classifying the two types of receptors that were stimulated by acetylcholine (Dale, 1914). One type could be stimulated by nicotine and inhibited by curare whilst the other could be stimulated by muscarine and inhibited by atropine. These observations led to the two classes of receptors becoming known as the nicotinic and muscarinic acetylcholine receptors. It is now known, however, that the muscarinic and nicotinic receptors are members of different receptor superfamilies, even though they have the same ligand stimulating them.

The nicotinic acetylcholine receptor (nAChR) is a member of the ligand-gated ion channel superfamily. The structure of the nAChR is made up of five subunits, all crossing the membrane, and in an arrangement which produces a central pore. The binding of acetylcholine (ACh) causes the central pore to open and allow sodium and potassium ions to pass through the channel. The response to ACh is fast and the flux of ions causes the membrane to depolarise.

The muscarinic acetylcholine receptor (mAChR) is a member of the guanine nucleotide binding protein (G protein) -coupled receptor superfamily. The response caused by ACh stimulating the mAChR, compared to the nAChR, is much slower with the signal taking milliseconds to seconds to be produced. The mAChR is described in more detail below.

1.1 The muscarinic acetylcholine receptor.

As already mentioned, the mAChR is a member of the G protein-coupled receptor (GPCR) superfamily. The GPCR superfamily is composed of membrane spanning proteins each with seven transmembrane (TM) helices, i.e., the polypeptide chain crosses the lipid bilayer seven times. When an agonist binds to the extracellular side of the protein, this causes the receptor to undergo a conformational change, which in turn leads to the binding and activation of G proteins on the cytoplasmic side. The activated G protein can then go on to cause activation of a second messenger pathway. The complete process allows signals to be transmitted across cell membranes from the extracellular side to the cytoplasm and cell nucleus.

Using molecular biological techniques, five different genes coding for mammalian mAChRs have been found to date. Firstly, the M_1 and M_2 mAChRs were cloned (Kubo, *et al.*, 1986a; Kubo, *et al.*, 1986b) and then the M_3, M_4 and M_5 subtypes (Bonner, *et al.*, 1987; Peralta, *et al.*, 1987; Bonner, *et al.*, 1988). There have also been muscarinic subtypes cloned from non-mammalian sources *Drosophila melanogaster* (Shapiro, *et al.*, 1989), *Xenopus laevis* (Herrera, *et al.*, 1994) and chicken (Tietje, *et al.*, 1990; Tietje and Nathanson, 1991; Gadbut and Galper, 1994).

Initially, the nomenclature used to define the mAChR subtypes is 'M' for the receptors defined by physiological/pharmacological studies and 'm' for the cloned receptors. However, when the cloned receptor has been shown to be identical to the physiological/pharmacological receptor, it is normally given an uppercase letter (Alexander and Peters, 1998). It has recently been decided that there is enough evidence to name all five muscarinic subtypes with an uppercase 'M' (Caulfield and Birdsall, 1998) and it is this nomenclature that will be used in this thesis.

1.1.1 Localisation of the subtypes.

The localisation of the mAChR subtypes has mainly been determined by immunological and nucleic acid hybridisation studies. There have been some pharmacological studies carried out to try to determine subtype localisation. However, the ability of muscarinic ligands to differentiate the individual subtypes is limited, although selectivity is improving and toxins have been found in mambas, African snakes of the genus *Dendroaspis*, that are highly selective for M_1 and M_4 subtypes (Adem and Karlsson, 1997).

The mAChRs are found both in the brain/central nervous system (CNS) and peripheral tissues (for reviews see: Caulfield (1993); Levey (1993); Wess (1996)). All five mAChR subtypes have been found in the brain whilst in the peripheral tissues the muscarinic responses tend to be mediated by specific subtypes.

The mRNAs for all five mAChR subtypes have also been found in the brain (Weiner, *et al.*, 1990). Immunological studies have shown that the subtypes have specific distributions, for example, in the rat hippocampus (Levey, *et al.*, 1995) and striatum (Hersch, *et al.*, 1994) where the subtypes are expressed on specific neuronal

populations and therefore are thought to have specific functional roles in a particular region. The M_1 mAChR seems to be the subtype most widely expressed.

In the peripheral tissues, the M_2 mAChR has been shown to be the main subtype present in the heart, by immunological techniques (Dörje, *et al.*, 1991) and blot hybridisation detecting mRNA expression (Maeda, *et al.*, 1988). In smooth muscle, pharmacological studies (Candell, *et al.*, 1990) and mRNA hybridisation assays (Maeda, *et al.*, 1988) have shown that M_2 and M_3 subtypes are present, but only M_2 mAChR protein has been detected in substantial quantities (Dörje, *et al.*, 1991). The M_4 mAChR is the predominant subtype in rabbit lung, as indicated by pharmacological studies (Lazareno, *et al.*, 1990), although both M_4 and M_2 subtype proteins are present (Dörje, *et al.*, 1991). The exocrine glands contain the mRNAs (Maeda, *et al.*, 1988) and proteins (Dörje, *et al.*, 1991) for the M_1 and M_3 mAChRs.

1.2 The structure of G protein-coupled receptors.

The mAChRs are members of the GPCR superfamily. As mentioned above, all GPCRs are membrane spanning proteins and are involved in transferring an extracellular stimulus into an intracellular signal via G proteins. The GPCR superfamily is extensive and the primary structures of over five hundred G protein-linked receptors are known. The receptors fall into sub-families, classified according to the homology between their primary sequences, and by specific characteristics, e.g., the length of extra- and intra-cellular segments and the identity of specific residues. There are five different sub-families (Horn, *et al.*, 1998): Class A - rhodopsin-like, Class B - secretin-like, Class C - metabotropic glutamate like, Class D - pheromone and Class E - cAMP receptors (Dictyostelium). The mAChRs are one of the types of monoamine receptors that are members of the rhodopsin-like sub-family. The structural features that will be discussed are shown in Figure 1.1.

1.2.1 Structural features common to all GPCRs.

Hydrophobicity analysis has shown that GPCR proteins contain seven hydrophobic stretches corresponding to membrane spanning α-helices (Trumpp-Kallmeyer, *et al.*, 1992), although TM 7 is usually less hydrophobic than the others. The use of

Figure 1.1: Structural features of the rat M_1 mAChR.

The rat M_1 mAChR consists of seven transmembrane domains, which are linked by alternating intracellular and extracellular loops. There is a conserved disulfide bond which links the first extracellular loop to the second extracellular loop, an extracellular amino-terminal domain that is N-glycosylated and a cytoplasmic carboxyl-terminus that has a palmitoylation domain. There are one or more G protein receptor kinase (GRK) sites as well as protein kinase A and protein kinase C sites (not shown) in the third intracellular loop. Asp105, in TM 3, is highlighted in green and residues Tyr381 to Val387, analysed in this study, are highlighted in yellow.

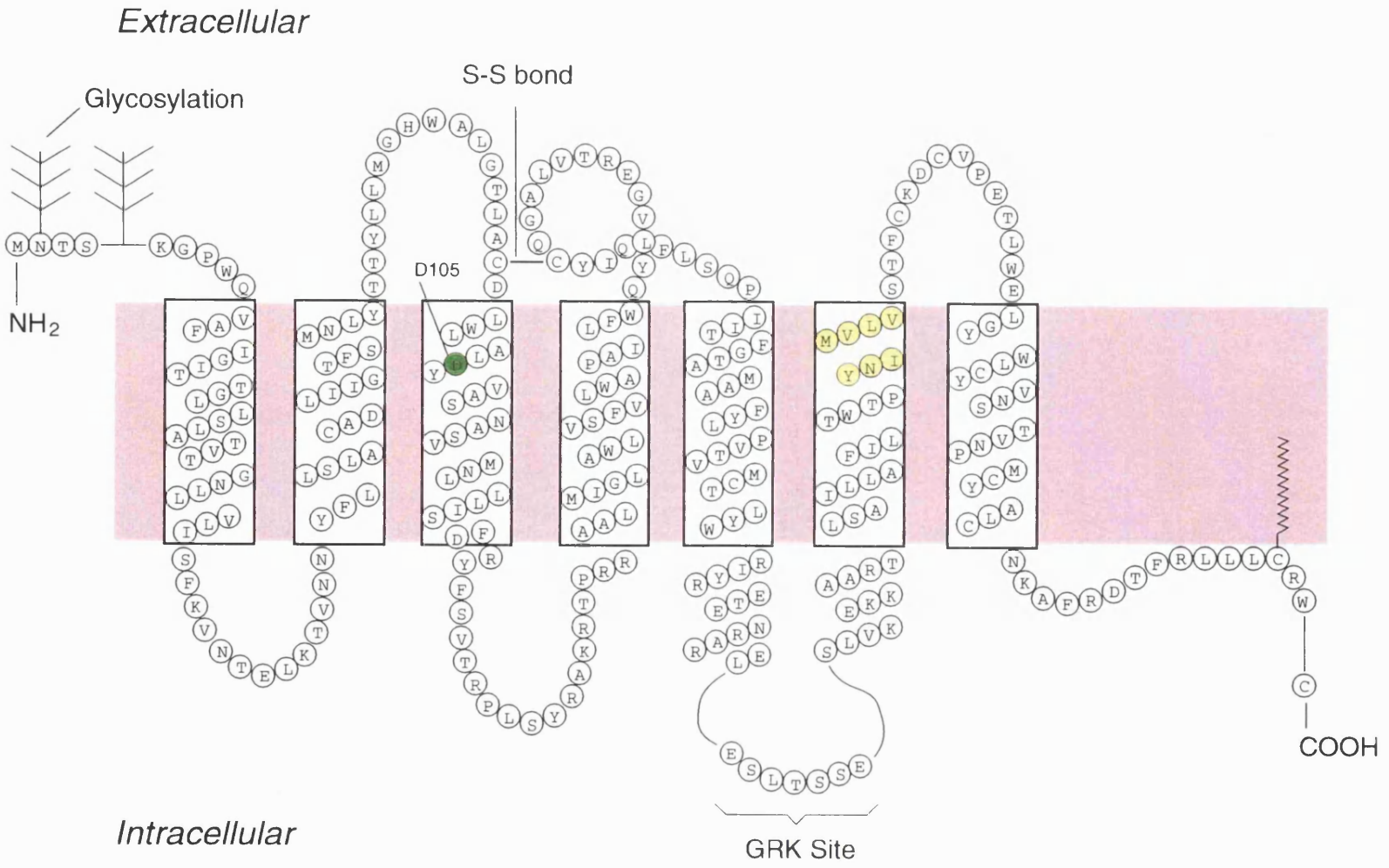
Extracellular
S-S bond
Glycosylation
D105
NH2
COOH
Intracellular
GRK Site

antibodies raised against sections of the β_2-adrenergic receptor has also shown that GPCRs are made from a single polypeptide chain which crosses the plasma membrane seven times, with an extracellular amino-terminus and an intracellular carboxy-terminus (Wang, *et al.*, 1989). A study using insertional mutagenesis supports these findings (Borjigin and Nathans, 1994). The M_1 mAChR has been shown, by antibody-binding studies, to have an intracellular carboxy-tail (Lu, *et al.*, 1997).

The molecular weight of GPCRs is frequently higher than the protein sequence would predict. Protein glycosylation would account for these differences and it has been shown that most GPCRs have one or more asparagine residues in the N-terminal domain that are in a glycosylation consensus sequence: Asn-X-Ser/Thr where X can be any amino acid except proline or aspartate (for details see Kornfeld and Kornfeld (1985) and references therein). All the mAChRs have potential glycosylation sites in their amino-teminal domains (van Koppen and Nathanson, 1990; Ohara, *et al.*, 1990).

Amino-terminal N-glycosylation is thought to play a important role in GPCR expression and function. However, the glycosylation in mAChRs has been removed both by site-directed mutagenesis to remove the asparagine residues in the amino-terminal domain (van Koppen and Nathanson, 1990) and by enzymatic deglycosylation (Ohara, *et al.*, 1990). Each study showed that the amino-terminal glycosylation does not seem to play a role in receptor expression and function. A study carried out on rhodopsin concluded that glycosylation is required for correct receptor expression and function (Kaushal, *et al.*, 1994). However, investigations using the β-adrenergic receptor have displayed conflicting results about whether glycosylation is necessary (Cervantes-Olivier, *et al.*, 1988) or not required (George, *et al.*, 1986) for correct receptor expression and function. These different results could be due to secondary effects, i.e., the deglycosylation enzymes may alter the glycosylation of other proteins associated with the receptor, e.g., proteins involved in the signalling pathway or in receptor processing. Therefore, the function of the receptor may not be directly altered but other events are changed to give a result that appears to be caused by a receptor modification. Since investigations have given conflicting results, the exact function of glycosylation remains unclear.

Recently a family of proteins called receptor-activity modifying proteins (RAMPs) have been identified (McLatchie, *et al.*, 1998). Data have suggested that they play a role in transport of the calcitonin-receptor-like receptor to the membrane, and in regulating the specificity of the ligand that binds to the receptor. It seems that RAMPs may carry out their role by altering the glycosylation of the calcitonin-receptor-like receptor. There might be similar processes regulating receptor function, by altering glycosylation, occurring for the other GPCRs.

Another feature that all GPCRs share is that they have conserved cysteine residues in the first and second extracellular loops. Studies using site-directed mutagenesis followed by chemical modification with [^{3}H]iodoacetic acid have shown that in the rhodopsin photoreceptor, a disulfide bond is formed between the first and second extracellular loops (Karnik and Khorana, 1990). This disulfide bond is necessary to maintain receptor structure and function, particularly it is required for formation of the light-activated metarhodopsin II state (Davidson, *et al.*, 1994).

Investigations using [^{3}H]*N*-ethylmaleimide labelled rat brain mAChRs showed the presence of cysteines that probably were forming a disulfide bond between the extracellular loops (Curtis, *et al.*, 1989; Kurtenbach, *et al.*, 1990). Further analysis using site-directed mutagenesis supported the hypothesis that a disulfide bond was formed between the first and second extracellular loops of the receptor, similar to the situation in rhodopsin, that serves to maintain correct protein folding and the structure of the ligand binding pocket (Savarese, *et al.*, 1992).

Interestingly, the β_2-adrenergic receptor seems to have two disulfide bonds (Noda, *et al.*, 1994). As well as one being formed between the first and second extracellular loops there is also a disulfide bond formed between two cysteines in the second extracellular loop.

1.2.2 The three-dimensional structure of rhodopsin-like receptors.

To date, the direct determination of the atomic structure of any member of the rhodopsin family of GPCRs, by X-ray crystallography or electron microscopy, has not been achieved.

Therefore, receptor structure prediction has been carried out mainly by the alignment and analysis of sequences from members of the GPCR superfamily and their superposition on low-resolution electron density maps derived from cryo-electron microscopy of two-dimensional crystals. Hydrophobicity analysis, as already described, has been used to determine the residues that are in the seven TM domains. A Fourier transformation method was then used by Donnelly, *et al.*, (1993) to determine whether the TM domains were α-helical, and to distinguish the residues that face the lipid bilayer from those that do not. It seems that residues which face the lipid bilayer are less conserved than those that face a polar domain.

Probably the most accurate model of the three-dimensional structure of the rhodopsin family of GPCRs available at present, with an effective resolution of 7.5 Å in the membrane plane and 16.5 Å perpendicular to it, is the one produced by Baldwin, *et al.*, (1997) - see Figure 1.2. The position of the seven TM domains is based on data from a low-resolution electron density map of frog rhodopsin (Unger, *et al.*, 1997).The location of the residues on the α-helices was determined by methods described above which involved the alignment of ~500 sequences.

Whilst the model by Baldwin, *et al.*, (1997) gives a detailed picture of the relative position of the axes of the α-helices, it assumes that the more hydrophobic sides of the various TM domains face towards the lipid bilayer. To try to investigate the orientation of the TM domains, with respect to the lipid bilayer and to each other, mutational studies have been carried out. In the mAChR and rhodopsin, it has been shown that TM domains 1 and 7 are in close proximity (Liu, *et al.*, 1996; Yang, *et al.*, 1996). It has also been shown, for rhodopsin, that TM 3 is close to TM 6 (Farrens, *et al.*, 1996). The TM domains have also been shown to be arranged in an anti-clockwise manner, as viewed from the extracellular side (Mizobe, *et al.*, 1996; Elling and Schwartz, 1996). So far, all the data obtained agrees with the model produced by Baldwin, *et al.*, and the assumptions made therein.

1.3 The ligand binding domains.

The rhodopsin sub-family of GPCRs can be divided into classes of receptors depending on the type of ligands they interact with, e.g., chemokine, protease, protein,

Figure 1.2: Three-dimensional model of the rat M_1 mAChR.

A) This stereo view is based on the rhodopsin model produced by Baldwin, *et al.*, (1997). The model shows the arrangement of the seven TM helices, from the extracellular side of the membrane, as determined from a low-resolution electron density map of frog rhodopsin. The positions of residues in the mAChRs that are important for agonist binding are shown in red, for antagonist binding are shown in blue and for both agonist and antagonist binding in green (detail is described in the text).

B) A figure showing the seven TM helices with the residues highlighted using the same colour scheme described above.

A)

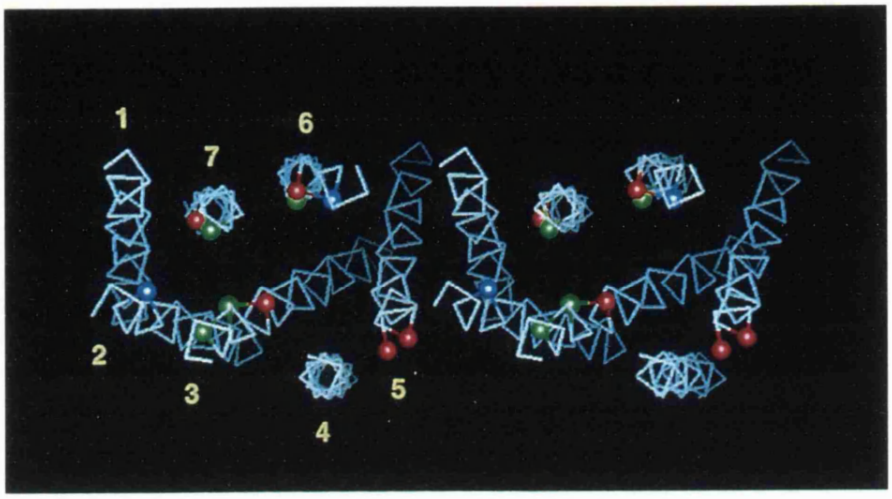

B)

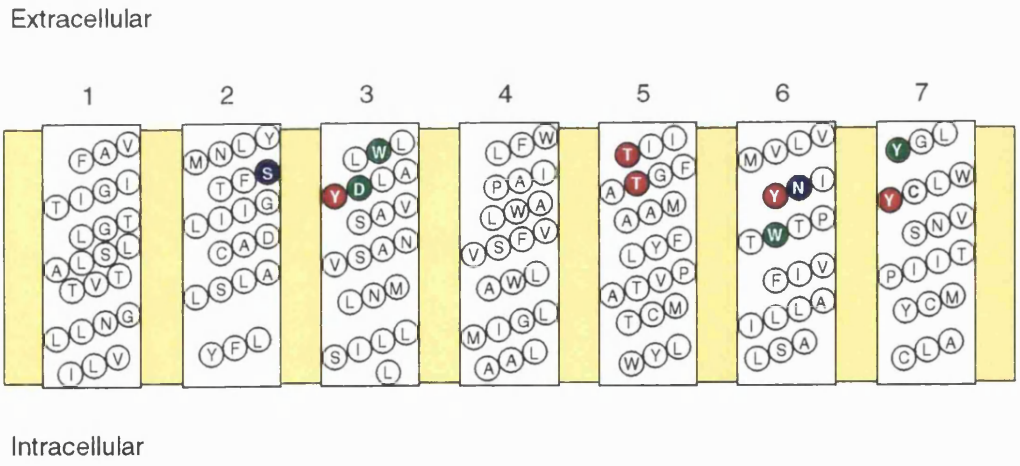

Figure 1.3: Structural features of ACh necessary for binding to and activation of mAChRs.

A figure showing ACh with the characteristics required for binding to and activation of mAChRs. This figure is based on data obtained by Schulman, *et al.*, (1983) who showed that the position of the quaternary nitrogen and ether-oxygen were important for agonist activity by probably interacting with sites 'P' and 'Q' on the receptor that were modelled to be 30 nm and 12 nm from the respective ACh moieties and 66-68 nm apart (PQ). The angle 'τ' was modelled to be between 100 and 117 °. If the distance (PC) between site 'P' and the methyl group, at the end of the ACh side-chain, was greater than 85 nm then the ligand acted as a partial agonist. This figure is adapted from the one by Ringdahl, (1989).

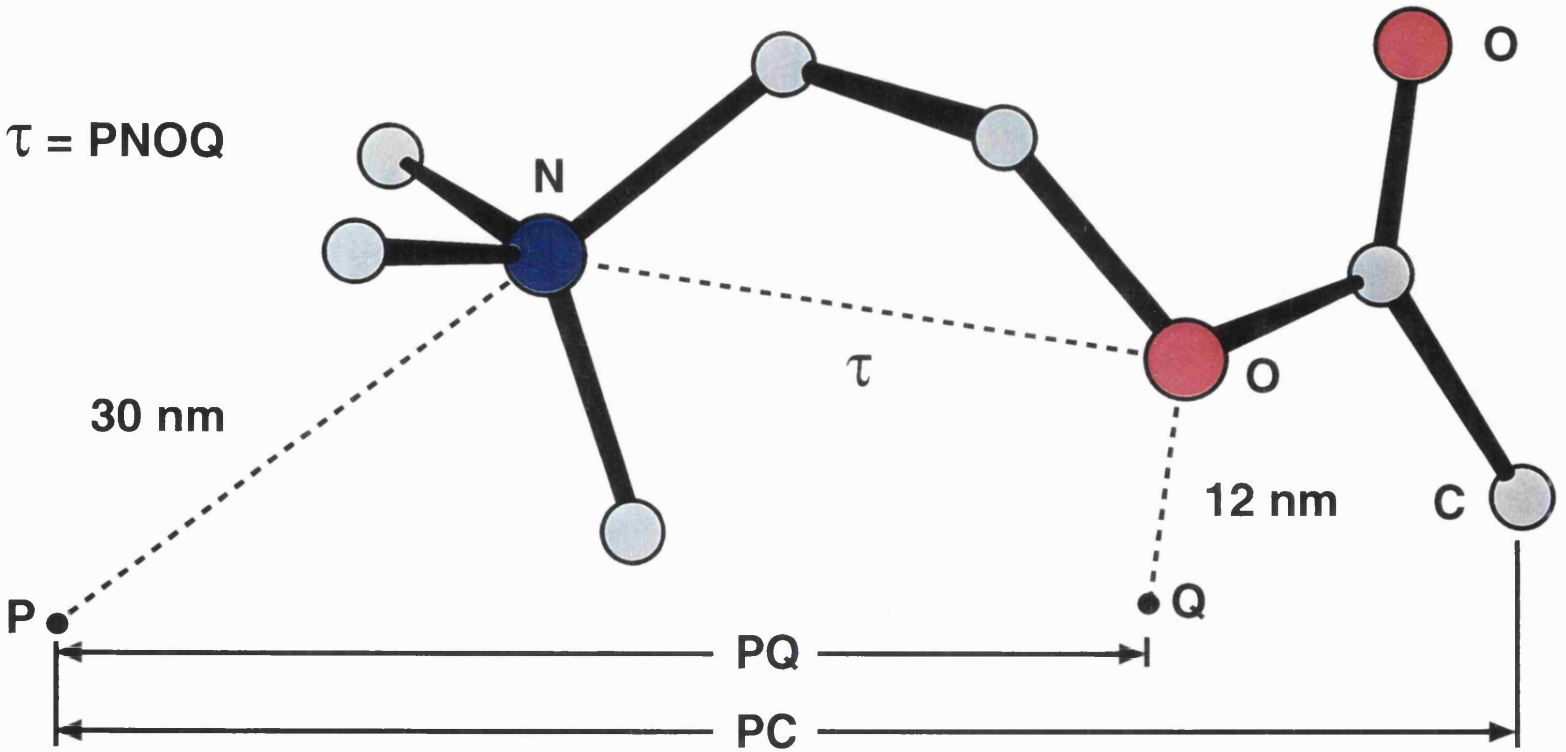
τ = PNOQ
N
O
O
τ
30 nm
12 nm
C
P
Q
PQ
PC

peptide and monoamine receptors. There have been extensive studies investigating the ligand binding domains of GPCRs and it has been shown that they vary considerably between classes (see reviews by Beck-Sickinger (1996); van Rhee and Jacobson (1996)). Therefore, only the ligand binding domains of the monoamine receptors will be reviewed, with emphasis placed on the mAChRs.

1.3.1 The agonist binding domain.

Agonists are described as ligands that bind to receptors and alter the number of receptors in the active state, therefore causing a biological response (Jenkinson, *et al.*, 1998). There are both conventional and inverse agonists that increase and decrease the number of receptors in the active state, respectively.

The first insight to what the mAChR binding domain required came from modelling the muscarinic ligands (Barlow, 1964; Schulman, *et al.*, 1983). These studies analysed a number of agonists and hypothesised what was required in cholinergic agonists for binding to the mAChR. The relative positions of the quaternary nitrogen (polar head-group) and ether-oxygen were shown to be important in binding suggesting that there would be residues in the mAChRs that would interact with these moieties (Figure 1.3).

Since the development of molecular biology techniques, a considerable amount of information has been obtained on the agonist binding domain of the monoamine class of GPCRs. A study using the β-adrenergic receptor showed that deletion of the intracellular and extracellular loops did not have an adverse effect on the binding of agonists (Dixon, *et al.*, 1987). This study implied that it was the TM domains that were involved in agonist binding. However, this deletion strategy could not be applied to investigate the agonist binding site in more detail.

Chimeric β_1/β_2-adrenergic receptors did help to provide more data about which TM domains were important in agonist binding (Frielle, *et al.*, 1988; Dixon, *et al.*, 1989). These studies showed that TM domains 4 and 5 determined subtype specificity, and therefore were involved in agonist binding.

The majority of information about the agonist binding pocket, and other receptor features, has come from analysis of the residues making up the receptor and carrying

out site-directed mutagenesis on the residues that seem to be interesting. It has been shown that all of the monoamine receptors have a conserved aspartate in TM 3 (Asp105 in the M_1 mAChR) which is thought to interact with the polar head-group of amine ligands, which include acetylcholine.

Investigations have shown that Asp105, in the M_1 mAChR, is specifically alkylated by [^{3}H]-ACh mustard suggesting that it forms a direct interaction during agonist binding (Spalding, *et al.*, 1994). When Asp105 is mutated to either an uncharged residue or a residue with a larger side-chain, agonist binding is strongly inhibited (Fraser, *et al.*, 1989; Page, *et al.*, 1995; Hulme, *et al.*, 1995). Similar observations were made with the M_2 mAChR (Page, *et al.*, 1995; Schwarz, *et al.*, 1995). This suggests that the aspartate is making an interaction with the positively charged head-group, as initially hypothesised by Strader, *et al.*, (1987). Studies carried out on the homologous aspartate in other monoamine receptors (for example, β-adrenergic (Strader, *et al.*, 1988; Strader, *et al.*, 1989), dopamine (Mansour, *et al.*, 1992) and 5-hydroxytryptamine receptors (Wang, *et al.*, 1993)) have also shown that agonist binding is affected when it is mutated.

Interestingly, in both the μ-opiate and SST_2 somatostatin receptors, that are rhodopsin-like GPCRs, there is an aspartate residue found in TM 3 which is important in agonist binding (Surratt, *et al.*, 1994; Strnad and Hadcock, 1995). This shows that the presence of an aspartate in TM 3 that is important in the agonist binding domain is not solely a feature of the monoamine receptors.

Since there is a conserved aspartate in all of the monoamine receptors, it was hypothesised that there must be other residues which give specificity to the mAChRs, i.e., that there must be other residues in the receptor that specifically interact with ACh and other muscarinic ligands. There are conserved amino-acids (serine, thronine and tyrosine) among all mAChRs that are rarely conserved in other GPCRs which could potentially form hydrogen-bonds with ACh. These conserved amino-acids are also in the same plane as the conserved aspartate in TM 3 that has been shown to be involved in agonist binding. A site-directed mutagenesis strategy, in the M_3 mAChR, showed that the majority of the conserved tyrosine and threonine residues, in the mAChRs, did play a role in agonist binding (Wess, *et al.*, 1991). Further analysis of

the residues shown to be involved in agonist binding (Thr231, Thr234, Tyr148, Tyr506, Tyr529 and Tyr533 in the M3 mAChR) with a series of ACh analogues indicated that the tyrosine and threonine residues create a polar environment, part of which may be interacting with the ester moiety of ACh (Wess, *et al.*, 1992). The same study showed that Thr234 (in TM 5) and Tyr506 (in TM 6), when mutated to alanine and phenylalanine, respectively, caused the largest decreases in agonist binding affinities. This indicated that these residues play a major role in binding of ACh, although the study failed to identify specific interactions which might be made.

Investigations looking at some of the tyrosine and threonine residues in mAChRs subtypes other than the M_3 mAChR have shown similar results. Experiments on Tyr404, in the M_1 mAChR, which is homologous to Tyr529 in the M_3 mAChR, showed that its mutation to phenylalanine or alanine, reduced agonist affinity (Matsui, *et al.*, 1995). Another study using the M_1 mAChR, showed that mutation of Thr192 (the homologous residue to Thr234 in the M_3 mAChR), to cysteine inhibited agonist binding, and further analysis indicated that it was able to react with bromoacetylcholine, a sulfhydryl-alkylating ACh analogue (Allman, *et al.*, 1997). This suggests that Thr192, and probably the homologous residues in the other mAChRs, may interact with the acetyl methyl group of ACh instead of or in addition to the ester moiety.

The residues in other monoamine receptors at the same TM domain positions as the conserved tyrosine and threonine residues in the mAChRs have also been shown to be involved in binding their respective agonists. For example, the residue corresponding to Thr192 in the M_1 mAChR is a serine in the catecholamine receptors (5-hydroxtryptamine, adrenergic and dopamine receptors). Site-directed mutagenesis has shown that this serine is also involved in agonist binding, possibly by interacting with the ligand via one of the hydroxyl groups present on the phenyl ring (Wang, *et al.*, 1991; Ho, *et al.*, 1992; Pollock, *et al.*, 1992). This illustrates one way in which receptors can manifest specificity for their respective ligand, i.e., a particular position in the receptor structure may be important for agonist binding but the exact residue present at that position determines specificity for the ligand.

The other way receptors are specific for their ligands is that different agonists may have altered modes of interaction. In these cases totally different residue positions are used to bind ligands, therefore producing specificity. At a gross level this can be seen by comparing the peptide and monoamine receptors. The peptide receptor agonist binding domain tends to be in the amino-terminal domain and extracellular loops, whereas in the monoamine receptors it resides mostly within the TM domains (Beck-Sickinger, 1996).

It has also been found that tryptophan residues, that are conserved in the TM domains of most GPCRs, are important for agonist binding (Wess, *et al.*, 1993). This study by Wess, *et al.*, on the M_3 mAChR, showed that the mutations of Trp192 (TM 4) and Trp503 (TM 6) to phenylalanine, reduced agonist binding affinities. A separate study, using the M_1 mAChR, showed that the mutation of Trp101 in TM 3 to alanine, caused a significant reduction in agonist binding affinity (Matsui, *et al.*, 1995). However, the mutation of Trp101 to phenylalanine had little effect on ACh binding which suggested that this residue required an aromatic group to interact with ACh. Models have shown that the tryptophan residues involved in agonist binding in the mAChRs tend to be close to the conserved aspartate in TM 3, which is involved in interacting with the polar head-group of ACh. It has been hypothesised that the conserved tryptophan (or other aromatic) residues near to the conserved aspartate form a cage around the positively charged head-group of the agonist to stabilise the ion-ion interaction with the negatively charged carboxylate group (Trumpp-Kallmeyer, *et al.*, 1992).

Tryptophan residues also seem to play an important role in the potassium channel (Doyle, *et al.*, 1998). The tryptophan residues surround the selectivity filter and are positioned so that they extend into the lipid bilayer close to the membrane-water interface. The suggested role for these residues is to provide support and maintain the selectivity filter at the correct aperture and in the correct orientation. This function is similar to the role that the tryptophan residues in the mAChRs may carry out, i.e., support the receptor architecture.

1.3.2 The antagonist binding domain.

An antagonist is a ligand that reduces the effect of an agonist (Jenkinson, *et al.*, 1998). An antagonist can have its effect by sterically preventing an agonist getting to its

binding domain, i.e., by 'volume exclusion.' Therefore, residues involved in agonist binding do not necessarily have to be precisely identical to those in the antagonist binding domain. However, muscarinic antagonists have similar structural properties to those found in agonists, for example, all potent antagonists have a positively charged head-group. Therefore, some residues shown to be important in agonist binding do also have a role in antagonist binding.

The conserved aspartate in TM3 (Asp105 in M_1 mAChR), that has been shown to be involved in agonist binding, has also been shown to interact with antagonists. Studies have shown that Asp105 can be covalently modified by [^{3}H]propylbenzilylcholine mustard (Curtis, *et al.*, 1989; Kurtenbach, *et al.*, 1990). The results obtained also supports the hypothesis that the aspartate is involved in forming an ion-ion interaction with the ligand. The binding affinities of antagonists have also been shown to be affected by site-directed mutation of Asp105 (Fraser, *et al.*, 1989; Hulme, *et al.*, 1995). These data further suggest that Asp105, in TM 3, is involved in the binding of antagonists, especially those with polar binding moieties.

There are other residues that seem to be involved in the binding of both antagonists and agonists. Trp143 (TM 3), Trp503 (TM 6) and Tyr529 (TM 7), in the M_3 mAChR and the homologous residues in the M_1 mAChR, have been shown to play dual binding roles (Wess, *et al.*, 1993; Matsui, *et al.*, 1995). The study by Matsui, *et al.*, (1995) also showed that mutation of Trp101 (TM3) or Tyr404 (TM 7), in the M_1 mAChR, (which are homologous to Trp143 and Tyr529 in the M_3 mAChR) to alanine, reduced antagonist binding affinity by 10-100 fold, when compared to wild-type. However, when either of these residues was mutated to phenylalanine, antagonist binding affinities were unaffected. These results suggest that it is the aromatic nature of these residues that is important for antagonist binding. Therefore, it seems that the tryptophan in TM 3 and tyrosine in TM 7 could be carrying out a similar role in the binding of both agonists and antagonists, in that they may be involved in stabilising the ion-ion interaction between the conserved aspartate in TM 3 and the positively charged head-group found in the majority of muscarinic agonists and antagonists.

Other residues have also been found that seem to only play a role in antagonist binding. There is a serine residue in TM 2 that is conserved among all mAChRs. In the M_3 mAChR, mutation of this residue (Ser120) to alanine causes a 10 fold reduction in antagonist binding but has little effect on agonist binding (Wess, *et al.*, 1991). Another study has shown that an asparagine (Asn507 in the M_3 mAChR) present in TM 6 of all mAChR subtypes plays a role in antagonist binding (Blüml, *et al.*, 1994). The mutation of this residue to alanine, serine or asparate reduced antagonist binding affinities but had smaller effects on ACh binding. The effects on antagonist binding varied depending on the ligand's structure. Atropine-like ligands and tricyclic compounds such as pirenzepine had their binding affinities significantly reduced, whilst the binding affinities of antagonists with different structural characteristics, for example, (-)-quinuclidinylbenzilate, were only slightly affected by the asparagine mutations. These data suggest that the asparagine may be interacting with specific moieties present in the antagonists, although there is not enough data, as yet, to draw any firm conclusions.

The positions of residues involved in antagonist binding in the mAChRs do not always relate to those of the residues involved in antagonist binding in the other GPCRs (van Rhee and Jacobson, 1996). The probable reason for this is that, as mentioned before, the mode of binding of an antagonist does not have to be as specific as that of an agonist for the antagonist to still exert its effect. Nevertheless, there are subtype-selective antagonists, which indicates that specific binding interactions do take place with some ligands (Melchiorre, *et al.*, 1995). However, to date, there have been few investigations into the nature of the specific interactions which occur in these cases.

1.3.3 The allosteric ligand binding domain.

The concept of allosteric modulation was first described by Monod, *et al.*, (1965), in the context of enzymes. An allosteric ligand is able to bind to the receptor at a location other than the agonist binding site and alter the induction of the receptor's conformational change caused by the agonist binding to the receptor. The allosteric modulation can either be positive (increases the effect caused by agonist binding) or negative (decreases the effect caused by agonist binding).

There have been several allosteric ligands found that interact with the mAChRs but the most studied has been gallamine, which is a neuromuscular blocking agent (for a review see Tucek and Proska (1995)). Gallamine has been shown to act allosterically at all of the mAChRs, although it is most potent at the M_2 subtype (Ellis, *et al.*, 1991). Since gallamine can have its effect on intact cells, and cannot easily cross the lipid bilayer because it is a highly charged molecule, it was hypothesised that the interaction was at the extracellular side of the receptor. An investigation using site-directed mutagenesis on the extracellular loops and the extracellular ends of the TM domains gave a further insight in to where gallamine was interacting with the mAChR (Matsui, *et al.*, 1995). Alanine mutations of two tryptophan residues (Trp101 and Trp400 of the M_1 mAChR) in TMs 3 and 7, that are conserved among the mAChRs, reduced gallamine binding. These findings suggest that the gallamine binding site is located on the extracellular side of the agonist binding site. Therefore, gallamine may be having its effect by impeding agonist access to the binding domain, in addition to altering the structure of the agonist binding site.

As mentioned before, the effects of gallamine are most potent on the M_2 mAChR. A chimeric mutagenesis strategy was used to investigate the domain, in the M_2 mAChR, where gallamine had its effect (Ellis, *et al.*, 1993). This study, that used M_2/M_5 and M_2/M_3 chimeras, indicated that gallamine was interacting with TM 6 and the third extracellular loop. The M_2 mAChR containes a short sequence of acidic residues in the third extracellular loop (Glu-Asp-Gly-Glu) that is not found in the other mAChRs. Replacement of these acidic residues with the sequence found in the M_1 mAChR reduced the affinity of gallamine for the receptor by 8 fold, thus suggesting that the acidic residues are part of the allosteric binding domain (Leppik, *et al.*, 1994).

Whereas gallamine acts as a negative allosteric agent, particular brucine analogues seem to have a positive allosteric effect on the binding of ACh when they interact with particular subtypes of mAChRs (Lazareno, *et al.*, 1998). However, there is no direct indication, to date, that these ligands interact at the same binding domain as gallamine, although there are data which suggest that there might be a common allosteric site in M_2 mAChRs (Tränkle, *et al.*, 1998).

The studies mentioned above have given some information about the residues involved in the allosteric ligand binding domain, although more data are required to understand how and through which residues allosteric ligands exert their effect and whether there is just one or many allosteric binding domain(s).

1.4 Receptor-G protein coupling.

As already mentioned, GPCRs are involved in transferring an extracellular stimulus into an intracellular signal via their interaction with G proteins. Domains on the intracellular side of the receptor are involved in coupling with the G protein that once activated stimulate second messenger pathways. The family of G proteins that mainly interact with GPCRs are of the heterotrimeric type.

It is worth noting that recent results have suggested that rhodopsin-like receptors can also directly interact with small G proteins such as RhoA and ARF to activate phospholipase D (Mitchell, *et al.*, 1998), although more investigation is required to understand this process.

1.4.1 Heterotrimeric G proteins.

Heterotrimeric G proteins (and small G proteins) are members of the guanosine 5'-triphosphatase (GTPase) superfamily (which contain the small G proteins as a separate group) and as the name suggests are made up of three subunits: α, β and γ (for reviews see Hamm (1998); Sprang (1997)). There are at least 20 α, 6 β and 12 γ subunits produced so there is the possibility of an extremely large number of heterotrimeric G protein types. However, these types can be placed into four families: G_s, which activate adenylyl cyclase; G_i, which inhibit adenylyl cyclase; G_q, which activate phospholipase C; and G_{12} and G_{13}, of unknown function. G_t, the G protein associated with rhodopsin that mediates the stimulation of cyclic guanosine 5'-monophosphate (cGMP) phosphodiesterase, is part of the G_i family.

The M_1, M_3 and M_5 mAChRs primarily couple with the G_q family: G_q and G_{11} subtypes, that are pertussis toxin insensitive, whilst M_2 and M_4 subtypes tend to couple with proteins from the G_i family: G_i or G_o subtypes, that are pertussis toxin sensitive (Parker, *et al.*, 1991; Smrcka, *et al.*, 1991; Berstein, *et al.*, 1992).

Recently two heterotrimeric G proteins (G_{i1} and G_t, both members of the G_i family) have been crystallised, to yield both structural information and a better view of how they operate (Wall, *et al.*, 1995; Lambright, *et al.*, 1996). The α subunit contains one domain that is involved in the binding of guanosine 5'-triphosphate (GTP) and its subsequent hydrolysis, this domain consists of a central six-stranded β-sheet surrounded by α-helices and is structurally similar in all members of the GTPase superfamily (Kjeldgaard, *et al.*, 1996), and a helical domain that holds GTP/guanosine 5'-diphosphate (GDP) within its binding site (Noel, *et al.*, 1993; Coleman, *et al.*, 1994). The β subunit is made up of seven β sheets arranged in a propeller-like structure (Sondek, *et al.*, 1996) and the loops on opposite faces of the propeller either interact with the α or γ subunit (Bourne, 1997). The γ subunit contains two helical elements, with one at each end of the subunit and both interacting with the β subunit. The amino-terminal helical domain, of the γ subunit, makes contact with the helical element at the amino-terminal of the β subunit to form a 'coiled-coil,' whilst the carboxy-terminal helical domain, of the γ subunit, interacts with the β subunit propeller. There are extensive contacts between the β and γ subunits and they form a functional unit that does not dissociate. It has been shown that expressing the two subunits separately leads to unstable β subunits and unfolded γ subunits (Higgins and Casey, 1994). The γ subunit also has a prenylated cysteine residue at its carboxy-terminus that is hydrophobic and can associate with the lipid-bilayer. Prenylation involves the covalent modification of the cysteine residue by either a 20-carbon isoprenoid geranylgeranyl or 15-carbon isoprenoid farnesyl moiety (Clarke, 1992). It occurs on a CAAX motif (C = Cys; A = aliphatic residue; X = any amino-acid), at the carboxy-terminal, and is required for correct proteolytic processing of the γ subunit (removal of the three carboxy-terminal amino-acids) and for the βγ complex to interact with the α subunit, although it is not required for the βγ complex to form (Higgins and Casey, 1994; Rando, 1996). Prenylation of the γ subunit has also been shown to be important for stimulation of downstream processes, for example, phospholipase C (Dietrich, *et al.*, 1996), and suggested to play a role in efficient receptor-G protein coupling (Kisselev, *et al.*, 1995). The amino-terminus of the α subunit also contains lipophilic modifications: myristoylation and/or palmitoylation. Myristoylation is the linking of myristate, a 14-carbon saturated fatty acid, to a glycine

residue via an amide bond (Gordon, *et al.*, 1991), whereas palmitoylation attaches palmitate, a 16-carbon saturated fatty acid, to a cysteine residue via a thioester linkage (Schmidt, 1989). One of the roles of these lipid modifications is to locate the proteins close to the membrane. Analysis of crystallographic structures has indicated that the amino-terminus of the α subunit and the carboxy-terminus of the γ subunit locate close to one another on the lipid bilayer, suggesting that there is a single tether point for both subunits (Wall, *et al.*, 1995). It is worth noting that the process of palmitoylation is reversible, which can be used to regulate G protein activity (this will be discussed later). Lipid modification of G proteins is reviewed by: Casey (1994); Wedegaertner, *et al.*, (1995).

1.4.2 The receptor activation process.

The binding of agonists to GPCRs causes a conformational change which in turn stimulates G proteins on the intracellular side of the lipid bilayer. Investigations that have produced constitutively active receptors when specific residues are mutated have given an insight into the processes occurring during receptor activation (Scheer and Cotecchia, 1997). Site-directed mutagenesis carried out on Glu113 or Lys296 in TMs 3 and 7, respectively, of rhodopsin, produces a constitutively active mutant (Cohen, *et al.*, 1992; Robinson, *et al.*, 1992; Cohen, *et al.*, 1993). Analysis of these data suggest that a salt-bridge is formed between these residues to maintain the receptor in the inactive state. Mutating either of these residues prevents the salt-bridge from forming and allows receptor activation. Therefore, it can be hypothesised that activation of the wild-type receptor requires the salt-bridge to be broken. A similar hypothesis has been suggested from site-directed mutagenesis studies on the α_{1b}-adrenergic receptor (Porter, *et al.*, 1996). Studies carrying out mutagenesis on the M_5 mAChR that produced constitutively active mutants have suggested that the inactive receptor is sterically destabilised to become active (Spalding, *et al.*, 1995; Spalding, *et al.*, 1997). A similar observation has been made by mutating Leu116, in TM 3 of the M_1 mAChR (Hulme and Lu, 1998).

It is worth mentioning that, apart from giving information on receptor structure and function, constitutively active mutants can also have physiological consequences. For example, constitutively active rhodopsin can lead to autosomal dominant retinitis

pigmentosa and congenital night blindness (reviewed by Rao and Oprian (1996)). If the constitutively active mutants involved in the disease can be understood in more detail there is a better chance for a treatment to be developed.

An investigation using rhodopsin has shown that stimulation of the receptor leads to movement of the helices (Farrens, *et al.*, 1996). This study made double nitroxide spin labelled cysteine mutants with one mutant being in TM 3 and the other in TM 6 and showed that the cytoplasmic end of TM 6 rotated and moved outwards, relative to TM 3, when the receptor was activated. A similar observation, that TM 3 and TM 6 are close together and that movement of these helices relative to one another is required for receptor activation, was made by Sheikh, *et al.*, (1996). This study made histidine mutations at the cytoplasmic end of TMs 3 and 6 of rhodopsin and caused receptor activation to be blocked in the presence of metal ions, i.e., the histidines made a metal ion binding site which when occupied prevented helix movement. Results from the analysis of α_{1b}-adrenergic receptor mutants are also consistent with the idea that the helices move during receptor activation (Hwa, *et al.*, 1997). This helical movement could result in the salt-bridges, keeping the receptor in the inactive state, being broken, causing the receptor to become activated. A recent study combining the technology of nitroxide spin labelling and site-directed mutagenesis supports this hypothesis (Kim, *et al.*, 1997). This investigation showed that a glutamate residue in rhodopsin (Glu134), at the cytosolic side of TM 3, that is part of the 'E/DRY' motif which is conserved in the majority of rhodopsin-like GPCRs, caused TM domain movement when mutated to an uncharged residue (glutamine). Similar results, although the effect was smaller, were seen when the arginine of the 'E/DRY' motif was mutated to glutamine. The movement of the TM domains when these residues were mutated was not identical to normal receptor activation. Instead, it was more 'local' to the 'E/DRY' motif, suggesting that Glu134 and to some extent Arg135 play a role in maintaining receptor structure and the activation process. A site-directed mutation investigation on the 'E/DRY' motif in the M_1 mAChR is consistent with the idea that the aspartate (glutamate in rhodopsin) and possibly the tyrosine residues play a role in maintaining receptor structure, whilst the arginine is involved in either receptor activation or interacting with the G protein (Lu, *et al.*, 1997). Activation may involve the protonation of the aspartate residue, which then allows the arginine to

form interactions important for G protein coupling (Scheer, *et al.*, 1997; Scheer and Cotecchia, 1997; Ballesteros, *et al.*, 1998).

As mentioned above, the E/DRY motif is conserved in nearly all rhodopsin-like GPCRs. However, some variation does occur. For example, in the platelet activating receptor there is an asparagine instead of the glutamate/aspartate residue and a histidine in the P_2 purinergic receptors. These differences are probably present to give the respective receptor specific characteristics required for its activation.

1.4.3 Receptor/G protein interactions.

Extensive studies have investigated how GPCRs activate the G proteins associated with them. The majority of information has come from the use of molecular biology techniques. Initial studies carrying out deletion mutagenesis on the β-adrenergic receptor suggested that the third intracellular loop played a role in coupling to G_s (Dixon, *et al.*, 1987). Further studies using adrenergic receptor chimeras supported this observation as well as implicating the second intracellular domain and proximal end of the carboxy-terminal tail, in receptor/G protein coupling (Kobilka, *et al.*, 1988). Investigations carried out on the mAChRs have given similar results, showing that the third intracellular loop of the receptor plays an important role in coupling (Kubo, *et al.*, 1988). Computer models displaying a GPCR-G protein complex show that the third intracellular loop may fit into a cavity between the α and β subunits of the G protein (Bourne, 1997).

Detailed probing of the third intracellular loop of the mAChRs by deletion mutagenesis indicated that it was 8-12 residues at the amino- and carboxy-terminal ends of the loop that were necessary for interactions with G proteins (Shapiro and Nathanson, 1989; Arden, *et al.*, 1992; Kunkel and Peralta, 1993). Sequence analysis showed a small segment of residues at the amino-terminal end of the third intracellular loop, of the mAChRs, that was conserved depending on the G protein that the receptor coupled to, i.e., M_1, M_3 and M_5 mAChRs had a particular sequence of residues whilst the M_2 and M_4 subtypes had a different sequence. M_2/M_3 mAChR chimeras showed that it was indeed this amino-terminal sequence that conferred receptor/G protein coupling specificity (Wess, *et al.*, 1989; Lechleiter, *et al.*, 1990). Although the amino-terminal segment of the third intracellular loop was sufficient to

determine coupling selectivity, the chimeras produced responses that were reduced, compared to wild-type, and not always exclusive to a particular G protein effector pathway (Wess, *et al.*, 1990). These data would suggest that there is another domain that is also important for G protein coupling.

The amino-terminal domain of the third intracellular loop contains both charged and uncharged residues that seem to be in a pattern consistent with an amphiphilic α-helix. An investigation which inserted alanine residues into the domain gave results that agreed with this (Blüml, *et al.*, 1994a). Studies carrying out site directed mutagenesis, on M_1 and M_3 mAChRs, have shown that it is the uncharged residues, which when mutated to charged residues, seem to have the largest effect on G protein coupling (Moro, *et al.*, 1993; Blüml, *et al.*, 1994b; Blüml, *et al.*, 1994c; Högger, *et al.*, 1995). A similar conclusion was drawn for the β-adrenergic receptor (Cheung, *et al.*, 1992). There is a tyrosine residue that is conserved among the M_1, M_3 and M_5 mAChRs but which is not present in the M_2 and M_4 subtypes. When this residue (Tyr254 in the M_3 mAChR) was mutated to serine or alanine $G_{q/11}$ coupling was impaired (Blüml, *et al.*, 1994b; Blüml, *et al.*, 1994c). However, its replacement by other aromatic residues preserved efficient signalling, indicating that it is the aromatic properties of the tyrosine that are important for coupling (Blüml, *et al.*, 1994b). Similar results were found when the homologous tyrosine residue (Tyr217) was mutated in the M_5 mAChR (Burstein, *et al.*, 1996). However, substitution of the tyrosine residue into the homologous position of the M_2 mAChR did not cause coupling to $G_{q/11}$ (Blüml, *et al.*, 1994b). This further supports the evidence that there are other domains involved in G protein coupling specificity.

To try and find the other domains involved in receptor/G protein coupling M_2/M_3 mAChR chimeras were made (Blin, *et al.*, 1995). This study indicated that, for efficient coupling to $G_{q/11}$ by the M_3 mAChR, four residues in the second intracellular loop, four residues at the carboxy-terminal of the third intracellular loop and one or more residues in the amino-terminal domain of the third intracellular loop were required. The carboxy-terminal of the third intracellular loop was suggested, in the β-adrenergic receptor, to be α-helical, similar to the amino-terminal region (Strader, *et al.*, 1989). Mutagenesis data showed that it is an amphiphilic α-helix and that it is the non-charged side, displaying an AALS motif, in the M_3 mAChRs (Ala488-Ala489-

Leu492-Ser493), that interacts with $G_{q/11}$ (Blin, *et al.*, 1995). Similar observations have been obtained for the M_5 mAChR (Burstein, *et al.*, 1995). This AALS motif is conserved among M_1, M_3 and M_5 mAChR subtypes, suggesting it is required for $G_{q/11}$ coupling. In the M_2 and M_4 mAChRs the AALS residues are replaced by VTIL (M_2) or VTIF (M_4) motifs (Val-Thr-Ile-Leu/Phe). Okamoto and Nishimoto (1992) showed that a peptide corresponding to the carboxy-terminal of the third intracellular loop present in the M_4 mAChR subtype was sufficient to activate $G_{i/o}$. Further investigation revealed that replacement of the VTIL motif in the M_2 mAChR with AALS led to the abolition of G_i coupling (Liu, *et al.*, 1995). This study also looked at mutant G protein α subunits. It was shown that the M_2 mAChR could couple with the α subunit of G_q that had the last five residues of the carboxy-terminus mutated to those found in $G_{i/o}$, at the same position, but not with wild-type $G_{i/o}$. Interestingly, when the AALS motif found in the M_3 mAChR was mutated to VTIL, this hybrid receptor was unable to couple with wild-type G_q but was able to interact with G_q carboxy-tail mutants. Also the M_3-VTIL mutant gained the ability to couple with wild-type $G_{i/o}$, whilst showing significant diminished capacity to interact with wild-type $G_{q/11}$. These results indicated that the AALS or VTIL motifs probably interact with the carboxy-tail of the α subunit of G proteins and that the VTIL motif in the M_2 and M_4 mAChRs is necessary and sufficient for coupling with $G_{i/o}$, whilst, the AALS epitope, in the M_3 mAChR (also the M_1 and M_5 subtypes), is one of the interactions required for coupling with $G_{q/11}$, although on its own it does not give a full response (Figure 1.4)

Although hydrophobic residues have been shown to be important, some studies have indicated that there are also charged residues in the third intracellular loop of mAChRs which are important in G protein interactions (Kunkel and Peralta, 1993; Högger, *et al.*, 1995). Since TMs 5 and 6 are adjacent to each other it can be assumed that the amino- and carboxy-terminals of the third intracellular loop are in close proximity. A recent investigation carried out on the M_5 mAChR that made double mutants, with one mutation at each end of the loop, suggested that the third intracellular loop forms a G protein coupling pocket comprised of a positively charged edge with a hydrophobic core (Burstein, *et al.*, 1998).

As already mentioned, residues in the second intracellular loop are required for coupling between G_q and M_3 mAChR (Blin, *et al.*, 1995). This study indicated that

Figure 1.4: AALS and VTIL motifs.

A helical wheel representation of the intracellular end of TM 6/carboxyl-terminal end of third intracellular loop, of the rat M_1 mAChR (A) and human M_2 mAChR (B), showing the AALS and VTIL motifs, respectively. The residues making up the motifs are shown on red circles whilst residues conserved in all mAChR subtypes are shown in green and the asterisk on the arginine denotes that this residue is not conserved in all mAChR subtypes. The AALS and VTIL motifs have been shown to make specific interactions required for coupling with the carboxyl-terminal of the α subunit of $G_{q/11}$ and $G_{i/o}$, respectively (see text for details). This figure has been adapted from the work of Wess (1996).

A

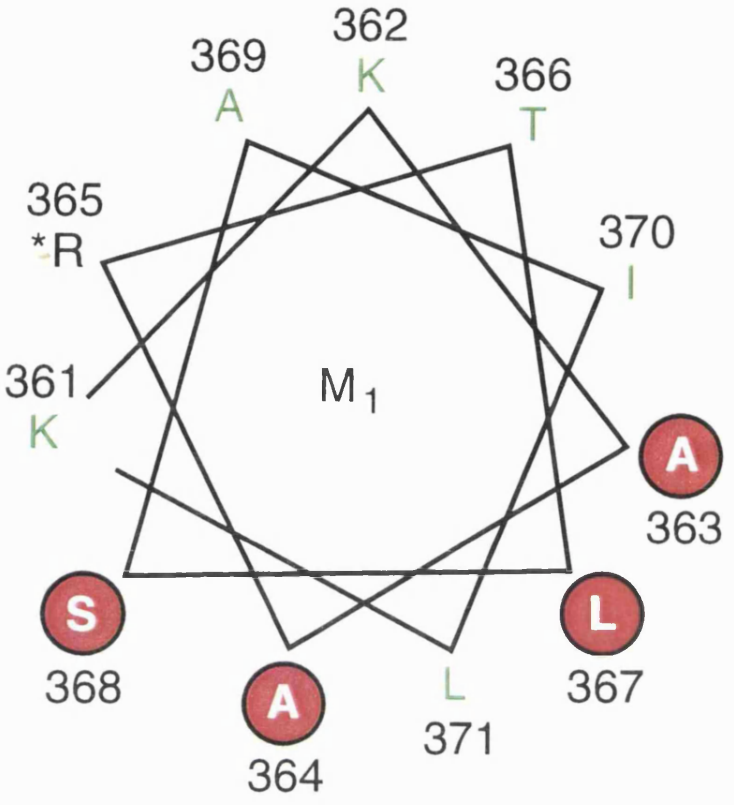
369
A
362
K
366
T
365
*R
370
I
361
K
M1
A
363
S
368
A
364
L
371
L
367

B

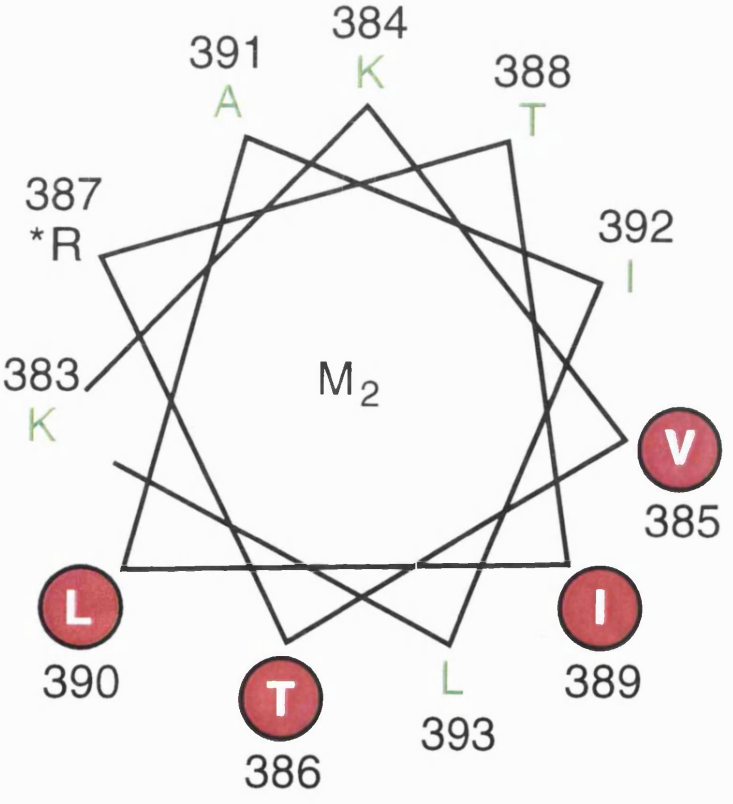
391
A
384
K
388
T
387
*R
392
I
383
K
M2
V
385
L
390
T
386
L
393
I
389

Figure 1.5: The receptor-G protein activation cycle.

This diagram briefly shows the events that occur during ligand binding and G protein activation. The heterotrimeric G protein is made up of the three subunits α, β and γ. The α-subunit binds guanine nucleotides whilst the β- and γ-subunits are always associated. In the inactive state of the G protein all three subunits are associated and GDP is bound to the α-subunit. Agonist binding to the receptor causes a conformational change which increases heterotrimeric G protein binding to the receptor. Once the G protein binds to the receptor-agonist complex this allows the exchange of GDP for GTP bound to the α-subunit which in turn allows the G protein to dissociate into the α- and βγ-subunits. These dissociated subunits are then free to activate effector molecules until the GTP is hydrolysed, by the GTPase activity of the α-subunit, which allows reassociation of the α- and βγ-subunits, and the cycle begins again.

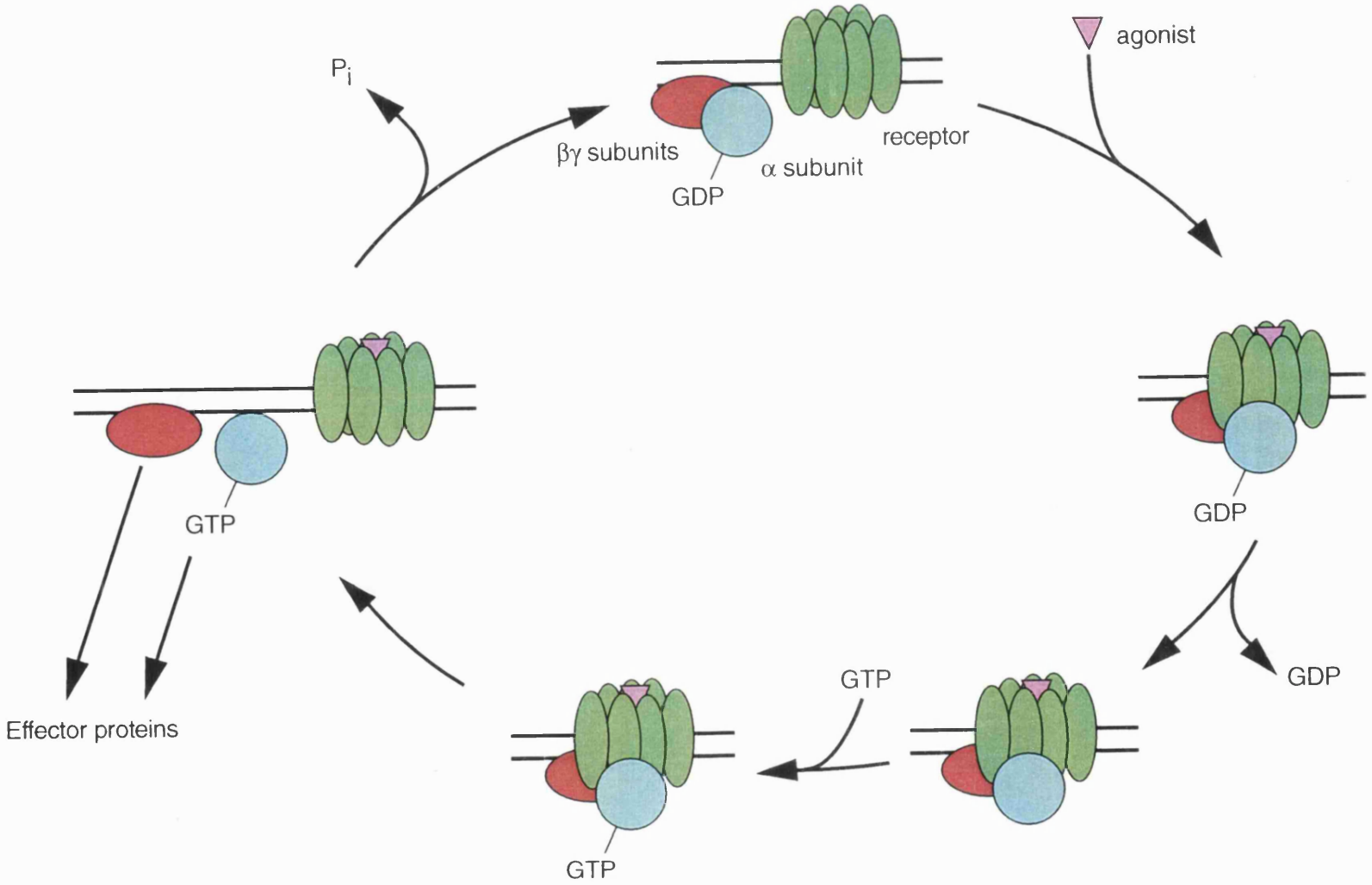
P_i
βγ subunits
α subunit
GDP
receptor
agonist
GDP
GDP
GTP
GTP
Effector proteins

three arginines and a serine residue (Ser168, Arg171, Arg176 and Arg183, in the M_3 mAChR), as well as residues in the third intracellular loop (previously discussed), were required for efficient coupling. Moro, *et al.*, (1993) showed that a hydrophobic residue in the middle of the second intracellular loop of the M_1 mAChR is required for G protein coupling. Data from alanine scanning mutagenesis carried out on the α subunit of G_t combined with G protein/receptor models showed that there were residues which were important for function close to the second intracellular loop of rhodopsin (Onrust, *et al.*, 1997). Therefore, the second intracellular loop of the M_1, M_3 and M_5 mAChRs may be important for interactions with the α subunit of $G_{q/11}$.

As mentioned above, there is an 'E/DRY' motif present at the cytosolic side of TM 3. Site-directed mutagenesis carried out on the M_1 and M_2 mAChRs has shown that the arginine residue is necessary for G protein coupling (Jones, *et al.*, 1995; Lu, *et al.*, 1997). It is the positive charge of the arginine that seems to be important for forming the agonist-receptor-G protein complex. On the other hand, the asparate and tyrosine residues seem to be important in maintaining proper receptor structure by forming intramolecular interactions, although the possibility of these residues making direct interactions with the G protein cannot be ruled out. More investigation is required.

1.4.4 The heterotrimeric G protein activation cycle.

The crystallographic structure of heterotrimeric G proteins has given some insight into the processes that are occurring during activation, although detailed information is limited. A cartoon displaying the activation cycle is shown in Figure 1.5. As previously mentioned, the binding of agonist to the receptor causes the receptor to undergo a conformational change. This change increases the affinity of the receptor for both agonist and G protein (reviewed by Strader, *et al.*, (1994)). The activated receptor then goes on to activate the bound G protein by stimulating GDP/GTP exchange at the α subunit.

In the inactivated state, the G protein has GDP bound to the α subunit and exists as a trimer that is able to interact with GPCRs. The GTP/GDP binding site is approximately 30 Å away from the receptor, therefore the receptor probably does not have a direct interaction in guanine nucleotide exchange (Bourne, 1997). There are three 'switch' regions in the α subunit that are flexible, and which undergo

conformational changes during activation: switch I, switch II and switch III (Lambright, *et al.*, 1994). The exact process by which the receptor causes a conformation change in the G protein is unknown, although a transition involving reciprocal order-disorder transitions of the carboxy-terminus and the binding site for the guanine ring has been proposed from a study using nuclear magnetic resonance (NMR) spectroscopy (Kisselev, *et al.*, 1998). For activation of $G_{q/11}$, tyrosine phosphorylation of the α subunit is said to be required (Umemori, *et al.*, 1997). This phosphorylation event seems to alter the interactions between the G protein and receptor.

Stimulation of the G protein by the activated receptor causes GDP release so that GTP can bind. The mechanisms by which this process operates are unknown, although the β subunit seems to be required (Hamm, 1998). Varying the magnesium ion concentration also affects the ability of mAChRs to activate G proteins, suggesting that magnesium ions are involved in formation of the ligand-receptor-G protein complex (Shiozaki and Haga, 1992). A magnesium ion is also involved in the binding of the phosphates present in GDP or GTP, in the GTPase domain (Kjeldgaard, *et al.*, 1996); however, it does not seem to play a role in GDP/GTP exchange per se (Lambright, *et al.*, 1994). During GDP/GTP exchange the three 'switch' regions, in the α subunit, have been shown to undergo a conformational change and become 'ordered' (Lambright, *et al.*, 1994). The conformational change in switch II causes a reduction of the affinity of the α subunit for the βγ subunits (Lambright, *et al.*, 1994; Lambright, *et al.*, 1996). Therefore, once GTP is bound, it causes the α subunit to dissociate from the βγ subunits of the G protein. This dissociation also has the effect of reducing the affinity of the G protein for the receptor and in turn allows the α and βγ subunits to dissociate from the receptor and activate second messenger pathways (reviewed by Sprang (1997) and Hamm (1998)). The release of the G protein also causes the receptor to revert to a low affinity for agonists (reviewed by Strader, *et al.*, (1994)).

The GTPase domain, in the α subunit, hydrolyses the bound GTP (Coleman, *et al.*, 1994). The hydrolysis of GTP to GDP causes the 'switch' regions to undergo conformational changes that allow them to become 'disordered' (Mixon, *et al.*, 1995).

This change in the α subunit, to the inactivated state, causes the affinity for the βγ subunits to increase. Therefore, the α and βγ subunits reassociate to form the trimer, that can then undergo the activation cycle again.

1.5 Regulation of receptor and G protein activity.

It is important to regulate the response of both receptors and G proteins since continuous activation could lead to undesirable consequences. Therefore, in most cases, the regulation processes acting on receptors and G proteins tend to be negative, i.e., are involved in 'turning off' the system and/or preventing further excessive stimulation.

1.5.1 Receptor regulation.

An agonist stimulating a GPCR has multiple effects. Firstly, the agonist causes receptor mediated processes to be activated. Then, after extensive agonist stimulation the receptor undergoes receptor desensitisation, and the receptor mediated events are attenuated. The process of receptor desensitisation (Figure 1.6) can be achieved in a number of ways (for a review of mAChR desensitisation see Wess (1996); for a general review on GPCR regulation see Böhm, *et al.*, (1997)).

The first phase of receptor desensitisation is 'uncoupling,' which occurs rapidly (seconds to minutes) after the initiation of agonist stimulation. This prevents the activated receptor from coupling with its G protein, and hence reduces excessive signalling. A receptor phosphorylation event, on the third intracellular loop (Pals-Rylaarsdam and Hosey, 1997) or carboxy-terminal domain (Haga, *et al.*, 1996), seems to be important in causing this desensitisation response. Receptor phosphorylation is described in more detail below.

Following 'uncoupling,' the GPCR then undergoes internalisation. This process occurs minutes after the commencement of agonist stimulation, and involves the removal of the receptor from the membrane. However, the receptor is not degraded and once the agonist is removed it is recycled to the membrane via endosomes. There are a number of mechanisms by which this process occurs (Koenig and Edwardson, 1997), although it seems that a receptor phosphorylation event and the third

Figure 1.6: Processes involved in receptor regulation.

The pathways in receptor desensitisation and resensitisation. After extensive agonist stimulation the receptor is phosphorylated by GPCR kinases (GRK) which allows arrestin to bind to the intracellular side of the receptor. This binding event seems to block G protein binding and hence attenuates receptor signalling. After uncoupling the receptor undergoes internalisation by being targeted to clathrin coated pits, although there may be other processes involved (see text). Once the receptor is internalised the receptor can either be recycled back to the membrane, after being dephosphorylated in a process stimulated by the high pH of the endosome, or degraded (down-regulated). The internalisation and down-regulation processes may be separate (see text). This figure was adapted from Böhm, *et al.*, (1997).

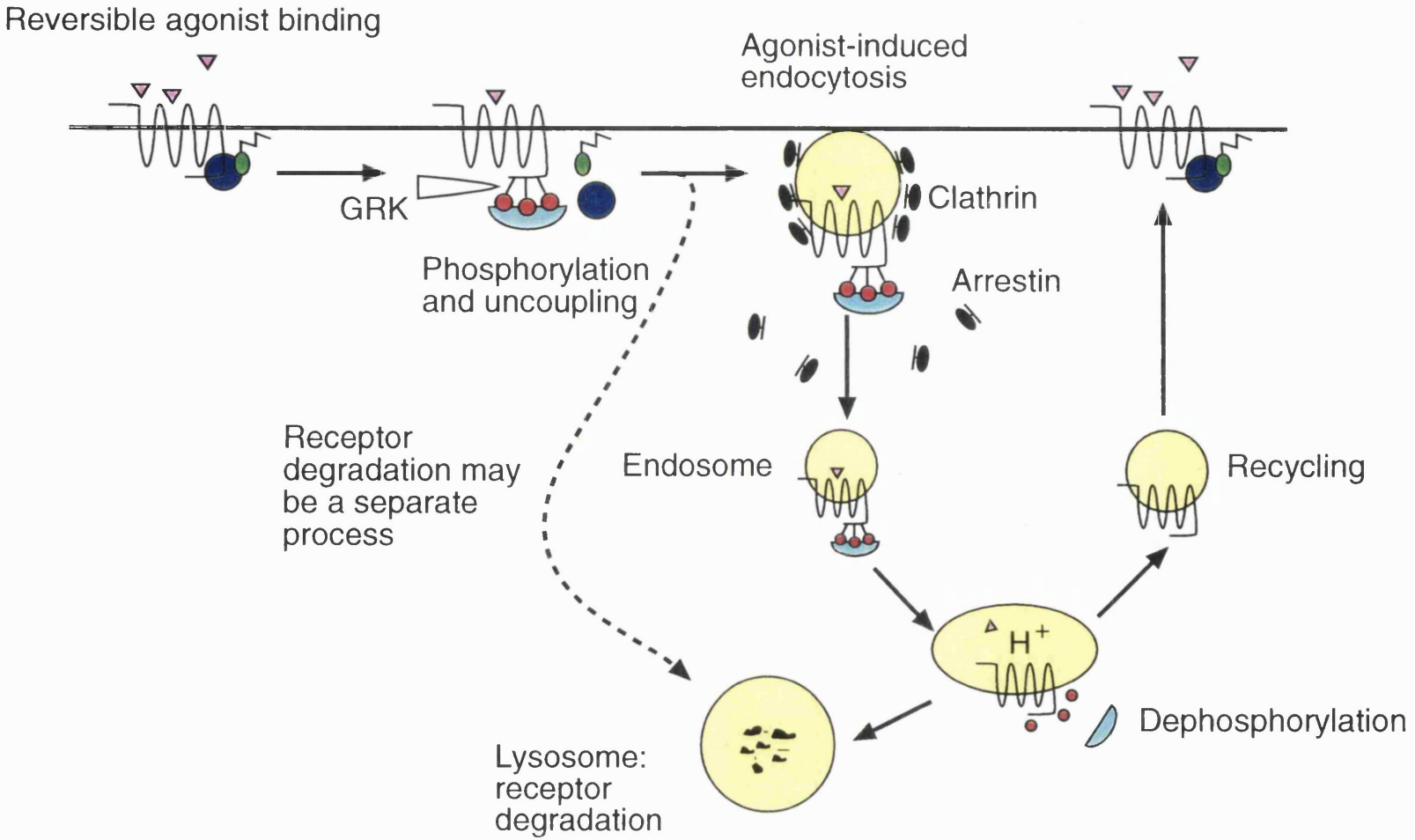
Reversible agonist binding
Agonist-induced endocytosis
GRK
Clathrin
Phosphorylation and uncoupling
Arrestin
Receptor degradation may be a separate process
Endosome
Recycling
H+
Dephosphorylation
Lysosome: receptor degradation

intracellular loop are required, for the internalisation to occur (Pals-Rylaarsdam and Hosey, 1997; Tsuga, *et al.*, 1998). There is evidence that phosphorylation of serine/threonine rich regions in the middle of the third intracellular loop have a direct effect on the internalisation process.

If agonist stimulation occurs for hours, the GPCRs may then undergo down-regulation that leads to a reduction in total receptor number, i.e., the receptors are degraded, and total receptor synthesis is required to reverse the process. It is unclear whether receptor internalisation is required to happen before down-regulation occurs. Studies on mAChRs have suggested that interalisation and down-regulation can be two separate processes (Shapiro and Nathanson, 1989; Goldman and Nathanson, 1994). Data have indicated that the process of down-regulation can be divided into two events. The first event is the increase in receptor degradation to reduce total receptor number (Klein, *et al.*, 1979; Doss, *et al.*, 1981), whilst further agonist exposure then leads to a decrease in receptor mRNA levels, therefore, decreasing new receptor synthesis (Lee, *et al.*, 1994).

Mutagenesis studies carried out on the mAChRs have indicated that the third intracellular loop may play a role in down-regulation (Shapiro and Nathanson, 1989; Lee and Fraser, 1993), although no specific amino-acids have been shown to be involved. However, a tyrosine residue in the carboxy-tail of the M_2 mAChR affects down-regulation, when mutated (Goldman and Nathanson, 1994). In the M_3 mAChR, there are three thronine residues in the carboxy-tail, whose mutation to alanine, affects down-regulation (Yang, *et al.*, 1993). Studies investigating the role of the decrease in mRNA expression in receptor down-regulation have indicated that this event may be regulated by second messengers (Lee, *et al.*, 1994).

Another structural feature that is present in the carboxy-tail of mAChRs and most rhodopsin-like receptors is one or two palmitoylated cysteine residues (Ovchinnikov, *et al.*, 1988). Palmitoylation is described in Section 1.4.1. As mentioned previously, palmitoylation is a reversible process and may, therefore, play a role in receptor regulation/function, although the exact purpose of this modification is unclear. Data have shown that palmitoylation may play a role in GPCR desensitisation (Bouvier, *et*

al., 1995). The palmitoylation of the vasopressin receptor seems to play a role in enhancing cell surface expression (Sadeghi, *et al.*, 1997).

1.5.1.1 Receptor phosphorylation.

As mentioned above, GPCRs have potential phosphorylation sites that when phosphorylated seem to play a role in receptor desensitisation. There are both second messenger dependent and specific kinases (GPCR kinases: GRKs) that are able to phosphorylate GPCRs (for reviews see Wess (1996); Hosey, *et al.*, (1995)).

The second messenger dependent kinases, for example, protein kinase A (PKA) and protein kinase C (PKC), tend to phosphorylate GPCRs in an agonist independent manner (Haga, *et al.*, 1993; Haga, *et al.*, 1996). This indicates that PKA and PKC may be involved in heterologous receptor desensitisation/regulation.

On the other hand the GRKs seem only to phosphorylate activated GPCRs (Premont, *et al.*, 1995; Hosey, *et al.*, 1995; Haga, *et al.*, 1996), therefore giving more specific receptor regulation. The GRKs are serine/threonine kinases and there are at least six subtypes (GRK 1-6). It has been shown that the free $\beta\gamma$ subunits of G proteins, that are produced after G protein activation, can stimulate phosphorylation of the M_2 mAChR by GRKs (Haga and Haga, 1992; Kameyama, *et al.*, 1993). This event may be part of a negative feedback control mechanism.

As mentioned above, receptor phosphorylation leads to a number of processes that regulate receptor activity. Investigations into receptor regulation, using the β_2-adrenergic receptor, have shown that a cytosolic protein, originally called β-arrestin and now called arrestin 2, interacts with the phosphorylated receptor to mediate receptor desensitisation (Lohse, *et al.*, 1990). Gurevich, *et al.*, (1997) proposed that these proteins bind to the phosphorylated receptor and block G protein binding, therefore reducing receptor signalling. Further investigation has also shown that arrestins are involved in targeting β_2-adrenergic receptors to clathrin-coated pits to undergo internalisation (Goodman, Jr., *et al.*, 1996; Ferguson, *et al.*, 1996).

However, it seems that the M_1, M_3 and M_4 mAChRs undergo desensitisation and internalisation via an arrestin-independent pathway (Lee, *et al.*, 1998). A similar observation has been made for M_2 mAChR, although if arrestins are over-expressed in

the cell expressing the M_2 subtype the receptor will desensitise and internalise via an arrestin-dependent pathway (Pals-Rylaarsdam, *et al.*, 1997). These data suggest that mAChRs are regulated by an arrestin-independent pathway but under certain circumstances an arrestin-dependent pathway can be used. Further investigation is required to fully understand the processes involved.

So that the phosphorylated receptors can be reactivated a dephosphorylation event must occur. It has been shown that protein phosphatase 2A is involved in dephosphorylating rhodopsin (Palczewski, *et al.*, 1989b) and that this process may be regulated by the dissociation of arrestin from the receptor (Palczewski, *et al.*, 1989a). Protein phosphatase 2A also seems to play a role in dephosphorylating the β-adrenergic receptor in bovine brain (Pitcher, *et al.*, 1995), whereas mAChRs expressed in *Xenopus* oocytes were reported to be dephosphorylated by protein phosphatase type 2B (Sakuta, *et al.*, 1991).

For dephosphorylation to occur, the receptor needs to be in the correct conformation. It seems that the acidic pH found in the endosomal vesicles, into which the receptor is internalised, causes the necessary conformational change to occur allowing phosphatase to bind (Kruegar, *et al.*, 1997). A study carried out on M_3 mAChRs expressed in SH-SY5Y human neuroblastoma cells suggests that internalisation of the receptor contributes to resensitisation, possibly by causing intracellular dephosphorylation (Szekeres, *et al.*, 1998). However, an investigation on M_4 mAChRs expressed in Chinese Hamster Ovary (CHO) cells showed that internalisation of these receptors strongly delays resensitisation (Bogatkewitsch, *et al.*, 1996). These differences observed between M_3 and M_4 mAChRs could either be due to the different cell types that the receptors are being expressed in or actual subtype differences. Further analysis is required to investigate this.

1.5.2 G protein regulation.

Similar to receptor regulation, there are a number of mechanisms that regulate G protein activity. In general, all tend to have a negative effect with the exception of the activated receptors that stimulate G protein activity.

As already mentioned, the α subunit of heterotrimeric G proteins can be palmitoylated (see Section 1.4.1.). It is thought that this lipid modification is involved in attaching the α subunit to the lipid-bilayer (Levis and Bourne, 1992). The activation of the G protein, i.e., GTP binding to the α subunit, leads to increased turnover of the palmitate attached to the α subunit (Degtyarev, *et al.*, 1993; Mumby, *et al.*, 1994). Since it has been shown that an unpalmitoylated G protein α subunit is unable to mediate signals from an activated receptor to its effector (Wedegaertner, *et al.*, 1993), depalmitoylation may play a role in reducing G protein activity (Wedegaertner, *et al.*, 1995). However, the mechanism by which this depalmitoylation occurs is not fully understood.

There is also a family of proteins that regulate heterotrimeric G protein activity which are called regulators of G protein signalling (RGS) proteins (reviewed by: Koelle (1997); Berman and Gilman (1998)). These proteins increase the GTPase activity of the α subunit of the heterotrimeric G protein and, therefore decrease G protein activation. However, the detailed mechanisms by which RGS proteins operate is poorly understood, although the structure of RGS4 bound to the AlF_4^- activated α subunit of G_i (Tesmer, *et al.*, 1997) should give insights into the mechanisms of RGS activation of the GTPase activity.

1.6 Second messengers and their effects.

The mAChRs are found in most organs and tissues (see Section 1.1.1) and they mediate a number of important functions, for example, contraction of many smooth muscles and involvement in depolarisation and hyperpolarisation response in neurones (for reviews see Caulfield (1993); Caulfield and Birdsall (1998)). As previously mentioned, M_1, M_3 and M_5 mAChRs couple with G_q and G_{11} heterotrimeric G proteins, whilst M_2 and M_4 subtypes couple with G_i or G_o. The difference between coupling of the 'odd' numbered subtypes and the 'even' numbered subtypes is shown in the downstream second messenger pathways activated. M_1, M_3 and M_5 subtypes cause the stimulation of phospholipase C(β) and the mobilisation of intracellular calcium, whilst M_2 and M_4 mAChR stimulation leads to the inhibition of adenylyl cyclase activity (see reviews by Caulfield (1993); Felder (1995)). There are a number of functional responses that are mediated by these major signalling pathways when

specific mAChRs are stimulated (Table 1.1). For example, the M_2 subtype, via the inhibition of adenylyl cyclase and possibly the stimulation of nitric oxide synthase, can inhibit voltage-gated calcium channels in the heart (see Mery, *et al.*, (1997) and references therein). The M_1 mAChR has been shown, by the production of mice lacking the M_1 subtype, to be solely involved in the inhibition of the M-current potassium channel activity in sympathetic ganglion neurones (Hamilton, *et al.*, 1997).

Stimulation of the mAChRs, in the brain, can initiate seizures (see Solberg and Belkin (1997) and references therein). Mice lacking the M_1 mAChR were resistant to seizures produced by the administration of pilocarpine, a mAChR agonist (Hamilton, *et al.*, 1997). These observations suggest that it is specifically the M_1 mAChR which is involved in seizure initiation and treatments (antagonists) targeting this subtype should be beneficial.

M_1 mAChR agonists can be used as therapeutic agents for the treatment of the cholinergic defect in Alzheimer's disease (Growdon, 1997). The receptor does not seem to be affected by the disease and therefore is a good target for treatment. The M_1 mAChR plays an important role in the function of the central nervous system.

There are also functional responses that can be caused by multiple mAChR subtypes. For example, there is the potential for all five mAChR subtypes to be involved in the inhibition of the L-type calcium channel (Pemberton and Jones, 1997). In smooth muscle, both M_2 and M_3 mAChRs are involved in causing contraction, although the M_2 subtype does this indirectly by inhibiting the β-adrenergic receptor relaxation response (Eglen, *et al.*, 1994). It is probably also worth noting that it has been shown by transfecting mAChRs in CHO cells that M_1 and M_3 subtypes can stimulate multiple types of G protein, i.e., cross-talk can occur (Lazareno, *et al.*, 1993).

Multiple mAChR subtypes can also cause pathological conditions. It has been shown that stimulation of M_1, M_3 and M_5 mAChRs can cause tumorigenesis. However, this may be a result of stimulation of phosphatidylinositol hydrolysis, because other receptors that stimulate this particular signalling pathway can cause tumorigenesis (Gutkind, *et al.*, 1991).

Table 1.1: The G protein, second messengers and functional responses affected by the activation of mAChR subtypes.

A table showing the major G protein subtypes and second messenger pathways that each mAChR couple with as well as the functional responses caused. Only the functional responses that have been clearly shown to be caused by stimulation of a particular subtype are shown. To date, the functional responses caused by the M_5 mAChR are unclear. The table is based on the one from Caulfield and Birdsall (1998).

mAChR subtype	M_1	M_2	M_3	M_4	M_5
G protein subtype	q/11	i/o	q/11	i/o	q/11
Second Messenger	Phospholipase C Inositol 1,4,5-trisphosphate Diacylglycerol Ca^{2+} Protein kinase C	Inhibition of adenylyl cyclase	Phospholipase C Inositol 1,4,5-trisphosphate Diacylglycerol Ca^{2+} Protein kinase C	Inhibition of adenylyl cyclase	Phospholipase C Inositol 1,4,5-trisphosphate Diacylglycerol Ca^{2+} Protein kinase C
Main Functional response	Inhibit M-current	Stimulate K^+ channels Inhibit Ca^{2+} channels Decrease heart rate and force Decrease presynaptic neurotransmitter release	Smooth muscle contraction Gland secretion Decrease presynaptic neurotransmitter release	Inhibit Ca^{2+} channels	

The majority of the responses described above involve the α subunit of the respective G protein, stimulating the second messenger event. There are also pathways that are activated by the βγ subunits of the G protein. Investigations have shown that the M_2 mAChR can stimulate cardiac inward rectifier K^+ channels via the direct interaction of the βγ subunits liberated by G protein activation (Krapivinsky, *et al.*, 1995). The M_2 and M_4 subtypes, when stimulated, also produce a small phospholipase C(β) response that has been shown to be caused by the βγ subunits of G_i (Katz, *et al.*, 1992). The mAChRs can also stimulate the activation of mitogen-activated protein kinases, via a ras-dependent pathway (Qian, *et al.*, 1995). It seems that the βγ subunits are involved in stimulating this pathway (Crespo, *et al.*, 1994; Koch, *et al.*, 1994). It has also been shown recently that tyrosine kinases and small G proteins may be involved in the supression of K^+ channels by mAChRs (Cachero, *et al.*, 1998).

1.7 Aims of the project.

The overall aim of the project was to determine the residues in the rat M_1 mAChR that play a role in receptor function and then to characterise the purpose of the residues found to be important. The rat M_1 mAChR was chosen because previous work carried out in the laboratory used this receptor (Jones, *et al.*, 1995; Page, *et al.*, 1995; Lu, *et al.*, 1997).

Since it would be impractical to characterise the whole receptor it was decided that the sequence from Tyr381 to Val387 in TM 6, in the rat M_1 mAChR, would be investigated. This set of residues were chosen because receptor models show that they lie in the same plane as Asp105, in TM 3, which has been shown to be crucial in both the agonist and the antagonist binding domains. To date a detailed study has not been carried out on TM 6 of the M_1 mAChR, although investigations on other monoamine GPCRs have shown that TM 6 plays an important role in receptor function (see previous sections).

Alanine scanning mutagenesis has been shown to be a powerful technique to efficiently analyse the role of residue side-chains in protein function (see Wells (1991) and Section 3). The alanine mutation deletes the residue's side-chain usually without disturbing the protein backbone, which reduces the chance of causing major

disturbance of the protein structure and/or function. This strategy was carried out on residues Tyr381 to Val387, and therefore each residue was sequentially mutated to alanine. The seven mutants were then characterised to measure the effects on ACh binding and the ability of ACh to produce a functional response by carrying out radioligand binding studies and phosphoinositide turnover experiments, respectively. These data gave information about the role of each residue's side-chain in receptor function.

The mutants that showed a significant effect on ACh (agonist) binding and its ability to cause a functional response were investigated further, although other residues that did not affect agonist interactions, but were found to be 'interesting,' were also looked at in more detail. This part of the study used series of agonists and antagonists that were structurally similar so that, in theory, a structure-activity relationship could be produced for the wild-type receptor and the effect of the alanine mutation on ligand binding could be compared.

There were three main groups of ligands. Firstly, compounds with a similar structure to ACh, although these compounds have been shown to have limited applicability (described in following sections). Therefore, a series of azanorbornane- and quinuclidine-based ligands that have higher binding affinities and tend to have a higher potency in the functional response than ACh analogues was used. Finally, a set of atropine-based ligands, that are antagonists, with high binding affinities, were used.

If the initial mutation produced from the alanine scanning mutagenesis showed altered ability to produce an ACh induced functional response, a subset of the agonists was used in functional assays. These data were combined with the binding data to measure the effects of the mutation on efficacy and hence give information on the function of the residue in receptor activation.

Apart from analysing the alanine mutants further, other mutations were made that tried to separate the functions of the constituent moieties of a particular residue further. These mutants were analysed with the same ligands, as described above.

Overall, it was hoped that data from this investigation would give a clearer view of the role of the residues in TM 6, of the rat M_1 mAChR in ligand binding and receptor function.

2. *Materials and methods.*

2.1 *Materials*

Tissue culture reagents were obtained from the Media Section, N.I.M.R. COS-7 cells (African Green Monkey kidney cells) were from E.C.A.C.C. The rat M_1 muscarinic acetylcholine receptor in a pCD expression vector was originally a gift from Dr. Noel Buckley (Bonner, *et al.*, 1987) and had undergone further modifications (Page, *et al.*, (1995); Curtis, C.A.M., unpublished data). The Chameleon™ double-stranded, site-directed mutagenesis kit, was bought from Stratagene. The Sequenase® Version 2.0 DNA Sequencing kit was obtained from US Biochemicals. Restriction endonucleases, T4 DNA Ligase and T4 Polynucleotide Kinase were obtained from Promega or Boehringer Mannheim. The Qiagen kits were obtained from Qiagen Ltd and the Geneclean® II kit from BIO 101. Dowex AG-1X8 resin (100-200 mesh size) and AG columns were from Bio-Rad. Liquiscint scintillation fluid was purchased from National Diagnostics. Immunoaffinity-purified rabbit antiserum raised against the C-terminal 13 amino acids of the M_1 mAChR was made by Dr. J. Pavia, at N.I.M.R., and the AP-conjugated goat-anti-rabbit IgG was from Promega. The compounds 3-(3-methyl-1,2,4-oxadiazol-5-yl)quinuclidine hydrochloride (L-658,903); 3-(2-methylfuran-4-yl)quinuclidine hydrochloride (L-661,326); 3-(4-methylfuran-2-yl)quinuclidine hydrochloride (L-661,319); (S)-3-(4-methyloxazol-2-yl)quinuclidine hydrochloride (L-683,355); (R)-3-(4-methyloxazol-2-yl)quinuclidine hydrochloride (L-683,356); 3-(3-pyridyl)quinuclidine hydrochloride (L-693,046); (R)-3-(3-methyl-1,2,4-oxadiazol-5-yl)-1-azabicyclo[2.2.1]heptane hydrochloride (L-698,583) were kindly provided by Dr. A. Fletcher, Merck Sharp and Dohme Research Laboratories. Phenylacetyltropine, diphenylacetyltropine, N,N-diethyl-N-methyl-aminoethyl acetate iodide (ACh-N$(Et)_2$), methylfurmethide, N-methylacetyltropine iodide and 3-acetoxy-N-methylquinuclidine iodide (Ac-N-Me-Quin) were a gift from Dr. R.B. Barlow. (–)[^{3}H]-*N*-methylscopolamine (85 Ci/mmol), (–)-[^{3}H]quinuclidinylbenzilate (48 Ci/mmol) and [^{3}H]-*myo*-D-inositol (80 Ci/mmol) were from Amersham International. Benzilylcholine iodide and methyl-(N,N-dimethyl-3-amino)propionate methiodide (ACh-reversed ester) were synthesised in the laboratory by Dr. E. C. Hulme and their

Figure 2.1: The pCD-rat M_1 mAChR construct.

The DNA sequence coding for the rat M_1 mAChR was in a pCD expression vector. The rat M_1 mAChR DNA sequence was modified to facilitate cloning procedures, but not the function of the protein, by removal of one Xma1 site and part of the 3' untranslated region (Page, *et al.*, 1995) and insertion of Nhe1 and EcoR1 sites (Curtis, C.A.M., unpublished data). The pCD plasmids contain a pBR322 origin of replication and an ampicillin resistance gene (Amp^R), so that replication and selection of the plasmid can occur in *E.coli*, respectively. The plasmid also contains a SV40 promoter that drives high levels of expression in COS-7 cells.

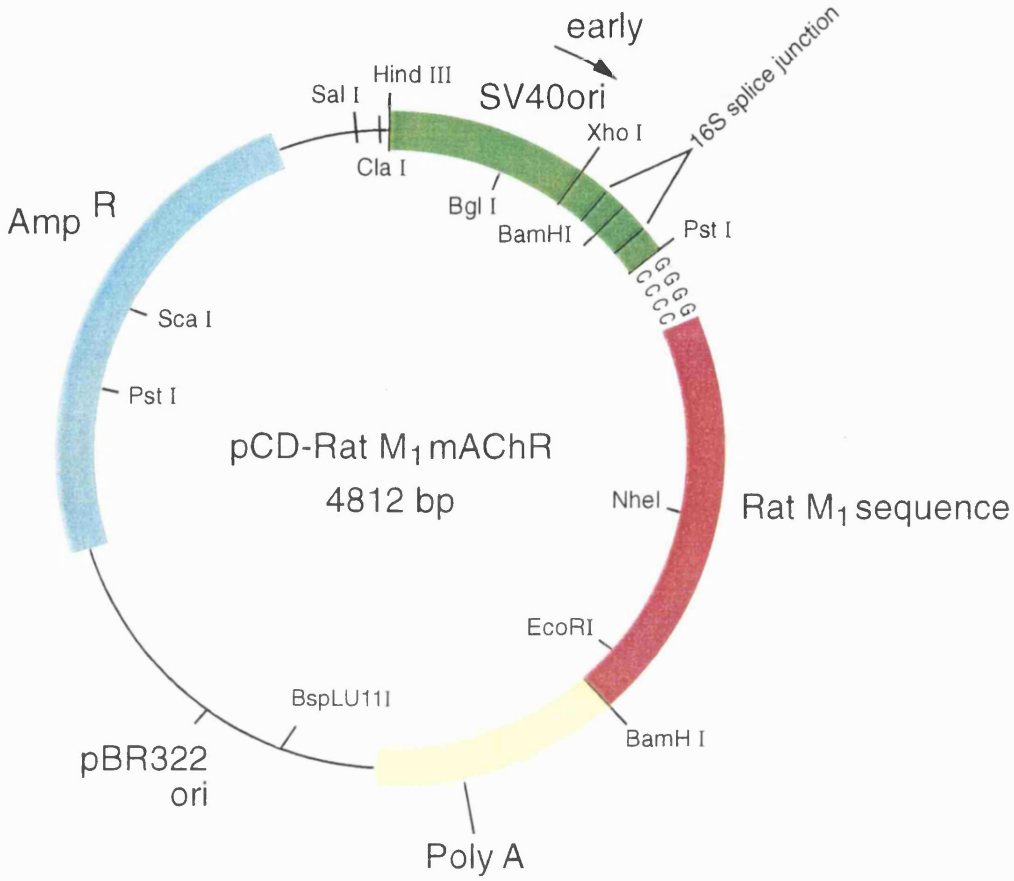
early
Hind III
Sal I
SV40ori
16S splice junction
Xho I
Cla I
Bgl I
BamHI
Pst I
Amp R
Sca I
Pst I
pCD-Rat M1 mAChR
4812 bp
NheI
Rat M1 sequence
EcoRI
BspLU11I
BamH I
pBR322
ori
Poly A

identity checked by NMR spectroscopy. All other compounds and materials used were obtained from Sigma, Research Biochemicals Inc. or Aldrich.

Other materials used were of the highest commercial grade available unless mentioned in the relevant methods section.

2.2 The pCD-rat M_1 mAChR construct.

As already mentioned, the DNA sequence coding for the rat M_1 mAChR was in a pCD expression vector (Figure 2.1). The pCD vectors are cloning and expression vectors designed to allow the cloning of the full-length mRNAs by reverse transciption 'in situ' and to select for large transcripts (Okayama and Berg, 1982; 1983). The vectors contain a Simian virus 40 (SV40) origin of replication, an SV40 promoter and an SV40 polyadenylation sequence. The binding of the SV40 large T-antigen to the SV40 promoter drives replication of the plasmid. Therefore, the pCD vector can replicate to high copy number in mammalian cell lines that constitutely express the SV40 large T-antigen. Therefore, the pCD vector produces high levels of transient expression of receptor genes in COS-7 cells, a line that has been SV40 transformed.

The pCD vector also contains a pBR322 origin of replication and an ampicillin-resistance gene. These two properties enable the propagation of the plasmid in *Escherichia coli* (*E.coli*) and selection of the plasmid by the presence of ampicillin.

The high levels of expression in COS-7 cells and the ability to grow the plasmid in *E.coli* make the pCD vector a good initial choice for manufacture and characterisation of receptor mutants.

2.3 Site-directed mutagenesis of M_1 mAChRs.

There are several site-directed mutagenesis techniques that can be used to obtain mutant receptors, although all the protocols have two main functions. Firstly, the manufacture of the required mutation within the DNA coding for the protein and secondly, a procedure to select for the mutated DNA.

The majority of receptor mutagenesis studies have used oligonucleotide-directed synthesis of the mutant coding sequence. This procedure requires an oligonucleotide encoding the required mutation to hybridise to the complementary single-stranded DNA sufficiently on either side of the site to be mutated. The oligonucleotide is then used to initiate the synthesis of the mutant strand *in vitro* forming a wild-type/mutant DNA double-strand hybrid. This DNA is then isolated and selection of the mutant strand carried out. A number of processes can used to obtain and select for the mutant DNA strand. Once selected, the mutant DNA strand can then be used to synthesise the complementary mutant DNA strand.

The first methods used to carry out this process used single-stranded DNA, i.e., the DNA needed to be cloned so that a single-stranded template was obtained, e.g., the method described by Kunkel (1998) involves the cloning of the DNA to be mutated into a M13 phage and then uracil enrichment of the template. The mutant strand is then made by oligonucleotide-directed synthesis and the uracil-enriched template degraded by transforming the phage into a uracil-N-glycosylase^{+} strain of *E.coli*. This leaves the mutant strand intact which can then be cloned (in a double-stranded form) into an expression vector if sufficient mutant DNA is produced. The main disadvantage to this procedure is that the DNA to be mutated needs to be cloned to produce a single-stranded template and then cloned into an expression vector once the mutant DNA has been produced.

Newer methods of site-directed mutagenesis use the polymerase chain reaction (PCR). These procedures tend to be more efficient and can be carried out on double-strand DNA, i.e., a single stranded template does not need to be made. One common method of oligonucleotide-directed synthesis using PCR is overlap extension (Ho, *et al.*, 1989). This process involves the production of the mutated sequence that is then cloned into the expression vector.

There are also unique site elimination strategies that can use double-stranded plasmid vectors as the starting point. These techniques link the production of the mutated sequence to either elimination or alteration of an unique restriction site (Deng and Nickoloff, 1992). Therefore, the mutated sequence can be selected for by the use of a restriction enzyme.

In this investigation, the Chameleon™ double-stranded, site-directed mutagenesis kit, was used to produce the mutant receptors. This kit works on the unique site elimination/alteration procedure described above and more details about the protocol used are shown below.

Oligonucleotides around 20-40 base pairs (bp) in length were designed (Table 2.1) so that they contained the sequence to code for the mutation of the required residue and were 5´ phosphorylated either during manufacture (carried out at N.I.M.R.) or by using T4 Polynucleotide Kinase (the oligonucleotides were incubated in the presence of T4 Polynucleotide Kinase, Kinase buffer and 1 mM ATP). Before use the oligonucleotides were purified by FPLC on a Resource™ Q column, from Pharmacia Biotech. The Chameleon™ kit also required a ScaI → MluI selection primer, obtained from Stratagene.

The method by which the Chameleon kit works is shown in Figure 2.2. Briefly, both the mutant and selection oligonucleotide primers are annealed to the wild-type plasmid and then an enzyme mix added, containing T7 DNA polymerase, to extend the oligonucleotide primers, and T4 DNA ligase to join the two new strands together to form a new plasmid sequence. A restriction enzyme, in this case ScaI, is then used to select the mutant plasmid by cleaving the wild-type plasmid before transformation into XL*mut*S competent cells which are grown overnight in 2YT medium at 37 °C with 300 rpm shaking. Plasmid DNA is extracted from the cells by the QIAprep Spin Miniprep kit and digested again with the selection enzyme. The plasmid DNA is transformed again but this time into Epicurian® Coli XL-1 Blue competent cells. The cells are plated out onto LB-agar containing 50 µg/ml ampicillin and grown overnight at 37 ° C.

A selection of the resulting colonies were grown up in 5 ml of LB-broth overnight at 37 ° C with 300 rpm shaking. The plasmid DNA was obtained from each culture by using the QIAprep Spin Miniprep kit. Dideoxynucleotide sequencing (Sanger, *et al.*, 1977) using the Sequenase® version 2.0 DNA sequencing kit and a 6 % (w/v) polyacrylamide gel was then used to determine whether the required mutated sequence was present.

Table 2.1: Oligonucleotides used to make the required rat M_1 mAChR mutants.

Oligonucleotides were manufactured so that they were around 20-40 bp in length and contained the required mutation (underlined nucleotides) to alter the receptor's amino-acid sequence. They were either 5' phosphorylated during manufacture or by using T4 Polynucleotide Kinase.

Mutant	Oligonucleotide sequence (5' → 3')
Tyr381Ala	GGA CAC CAG CTA ACA TCA TGG
Asn382Ala	GGA CAC CAT ATG CCA TCA TGG
Ile383Ala	CCA TAT AAC GCT ATG GTG CTG G
Met384Ala	CAT ATA ACA TCG CAG TGC TGG TA
Val385Ala	CAT CAT GGC TCT GGT ATC TAC
Leu386Ala	CAT CAT GGT GGC AGT ATC TAC C
Val387Ala	CAT GGT GCT GGC ATC TAC C
Tyr381Phe	CCT CAC CTG GAC ACC ATT TAA CAT CAT GGT GCT GGT ATC

Figure 2.2: The mutagenesis strategy using the Chameleon™ double-stranded, site-directed mutagenesis kit.

The mutagenesis strategy relies on a restriction site (ScaI → MluI) being altered in the ampicillin resistance gene at the same time as rat M_1 mAChR sequence is altered. Once the mutated plasmid has been produced, by using T7 DNA polymerase, it can be selected for by using ScaI restriction endonuclease. This procedure will linearise plasmids containing wild-type sequence and prevent subsequent transformation, i.e., only mutant plasmids will efficiently transform.

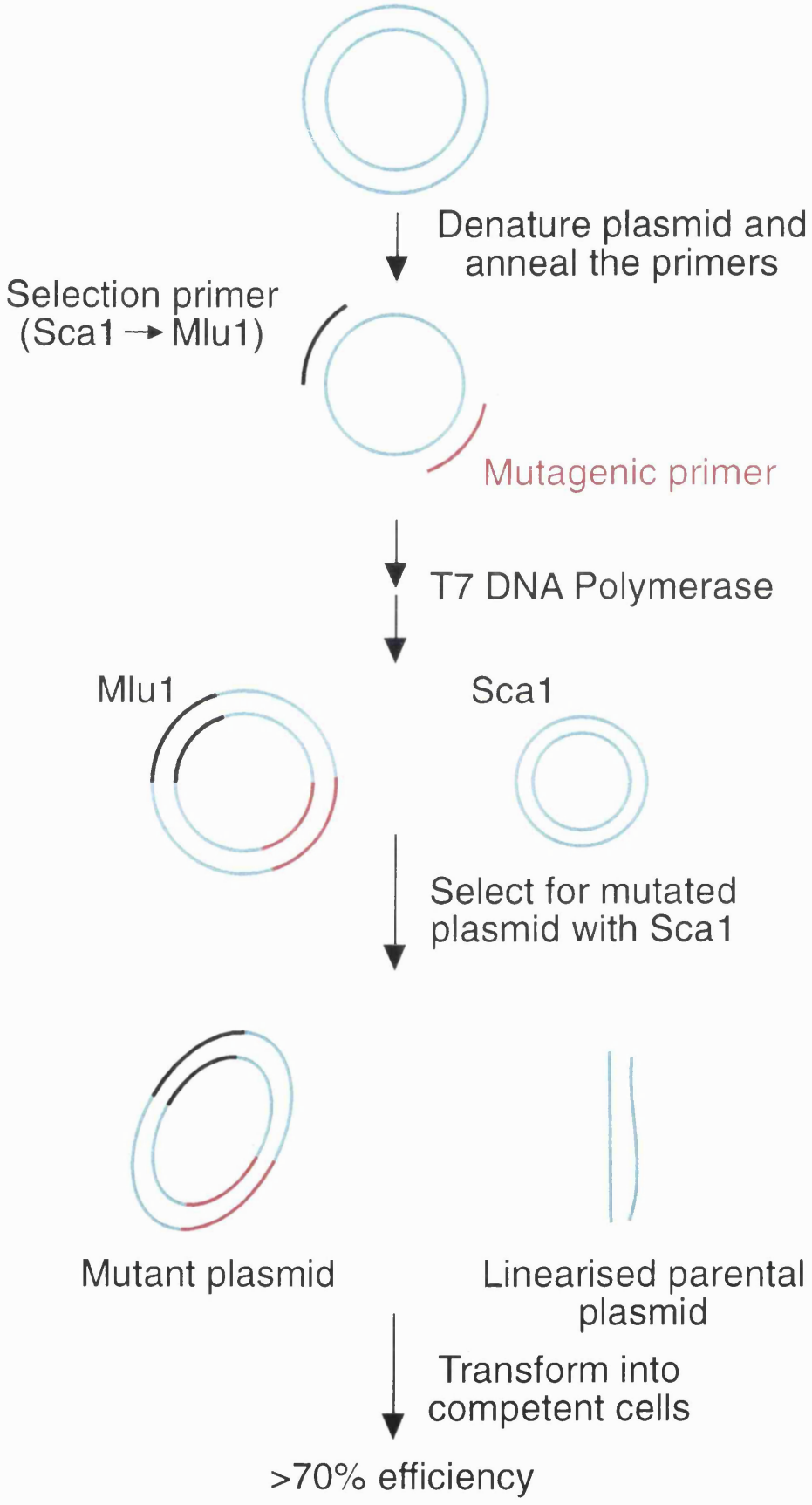
Denature plasmid and anneal the primers
Selection primer (Sca1 → Mlu1)
Mutagenic primer
T7 DNA Polymerase
Mlu1
Sca1
Select for mutated plasmid with Sca1
Mutant plasmid
Linearised parental plasmid
Transform into competent cells
>70% efficiency

So that the complete sequence coding for the mutated M_1 mAChR did not need to be sequenced to check that there were no other altered nucleotides, a subcloning procedure was then carried out. A 1.2 kbp fragment containing the mutated sequence was cleaved out of the mutated plasmid by using the Nhe1 and BspLU11I restriction endonucleases and purified on an 1 % (w/v) agarose/TAE gel. The Geneclean® II kit was used to extract the fragment from the gel which was then cloned back into the wild-type plasmid, which had the Nhe1-BspLU11I fragment removed, using T4 DNA ligase (the DNA strands were incubated with T4 DNA ligase, Ligase buffer, 10 μg acetylated bovine serum albumin and an additional 1 mM ATP).

After the sub-cloning procedure, the mutant plasmids were transformed into DH5α competent cells. The DH5α cells were thawed on ice before use (preparation of competent cells is described in Section 2.3.1). The plasmid DNA was added to the competent cells, in an 1.5 ml micro-centrifuge tube, that were then incubated on ice for 40 min. The DH5α/DNA mix was then given a heat-shock for 2 min at 42 °C, followed by 2 min on ice. 500 μl of SOC medium was added and the cells were then incubated at 37 °C for 30 min. 200 μl of the solution was plated onto LB-agar plates containing 50 μg/ml ampicillin that were then incubated at 37 °C overnight.

Colonies on the plate were then used to inoculate LB-broth and grown up so that plasmid DNA was produced that was then extracted. The procedures used were the same as for the Epicurian® Coli XL-1 Blue competent cells. Dideoxynucleotide sequencing, as described before, was then carried out on the plasmid DNA, to determine that the sequence which was transcribed down-stream of the Nhe1 site (~270 bp) only contained the mutation required.

2.3.1 Preparation of DH5α competent cells.

DH5α cells were streaked on a LB-agar plate that was incubated at 37 °C overnight. One colony was then picked off the plate to inoculate 100 ml LB-broth that was incubated at 37 °C, with 300 rpm shaking, until O.D., at 550 nm, was 0.25. The cells were placed on ice for 5 min before centrifuging at 3000 x *g* for 10 min, at 4 °C (using a Heraeus Megafuge 1.0R with rotor #7570 at 4,000 rpm). The supernatants were removed and the pellets resuspended in 40 ml of transformation buffer 1 (30 mM

potassium acetate, 100 mM $RbCl_2$, 10 mM $CaCl_2$, 50 mM $MnCl_2$, 15 % (v/v) glycerol, pH 5.8 (acetic acid), filter sterilised). The cells were then incubated on ice for 5 min and then centrifuged, same conditions used as described before. The pellets were then resuspended in 2 ml of ice cold transformation buffer 2 (10 mM MOPS, 75 mM $CaCl_2$, 10 mM $RbCl_2$, 15 % (v/v) glycerol, pH 6.5 (KOH), filter sterilised). The suspension was then placed on ice for 15 min, with gentle shaking every 5 min, before being aliquoted into 100 µl portions. The cells were then placed on dry ice for 15 min and then stored at -70 °C until required.

2.4 Production of the Asn382Ala-loop deletion construct.

The Asn382Ala-loop deletion construct (Asn382Ala-dLoop) was produced by combining the Asn382Ala mutant with the loop deletion construct (dLoop) that has residues 225-353 deleted from the third intracellular loop (Figure 2.3), a gift of Mrs. C.A.M. Curtis. NheI and HindIII restriction endonucleases were used to cleave a 3.1 kbp fragment out of the Asn382Ala mutant plasmid, The fragment was then purified on a 1 % (w/v) agarose/TAE gel before being ligated into dLoop, which had the NheI-HindIII fragment removed. The resulting plasmid was checked by dideoxynucleotide sequencing and size analysis on a 1 % (w/v) agarose/TAE gel. The dLoop construct is ~ 400 bp smaller than wild-type.

2.5 Preparation of plasmid DNA.

As already mentioned, during the mutagenesis procedure the QIAprep Spin Miniprep kit was used. Once the mutant plasmids were made, the Qiagen Plasmid Midi/Maxi kits was used to extract larger quantanties of DNA from growing transformed DH5α cells. The principle by which all these kits work is similar. Briefly, the bacteria are lysed in 0.2 M NaOH, 1 % (w/v) sodium dodecyl sulfate (SDS) in the presence of RNase A. The SDS causes the breakdown of cellular proteins whilst the NaOH denatures chromosomal and plasmid DNA. The alkali solution is then neutralised by the addition of 3 M potassium acetate (pH 5.5). The salt causes the chromosomal DNA to be precipitated with the bacterial cellular debris and SDS. The short plasmid DNA is left in solution that can be purified from the bacterial debris by passing it through a Qiagen Tip which is a cationic ion exchanger.

Figure 2.3: The rat M_1 mAChR loop deletion construct (dLoop).

The dLoop construct had residues 225-353 deleted from the third intracellular loop of the rat M_1 mAChR. This deletion of 129 amino-acids has been shown to increase expression levels of mutant M_1 mAChRs without affecting ligand binding affinities. A possible reason why dLoop causes increased receptor expression is that the deletion removes a PEST sequence (Rechsteiner and Rogers, 1996) and G protein-coupled receptor kinase (GRK) site (discussed in Section 1.5) which may be involved in reducing expression of the receptor at the membrane. Asp105, in TM3, is highlighted in green.

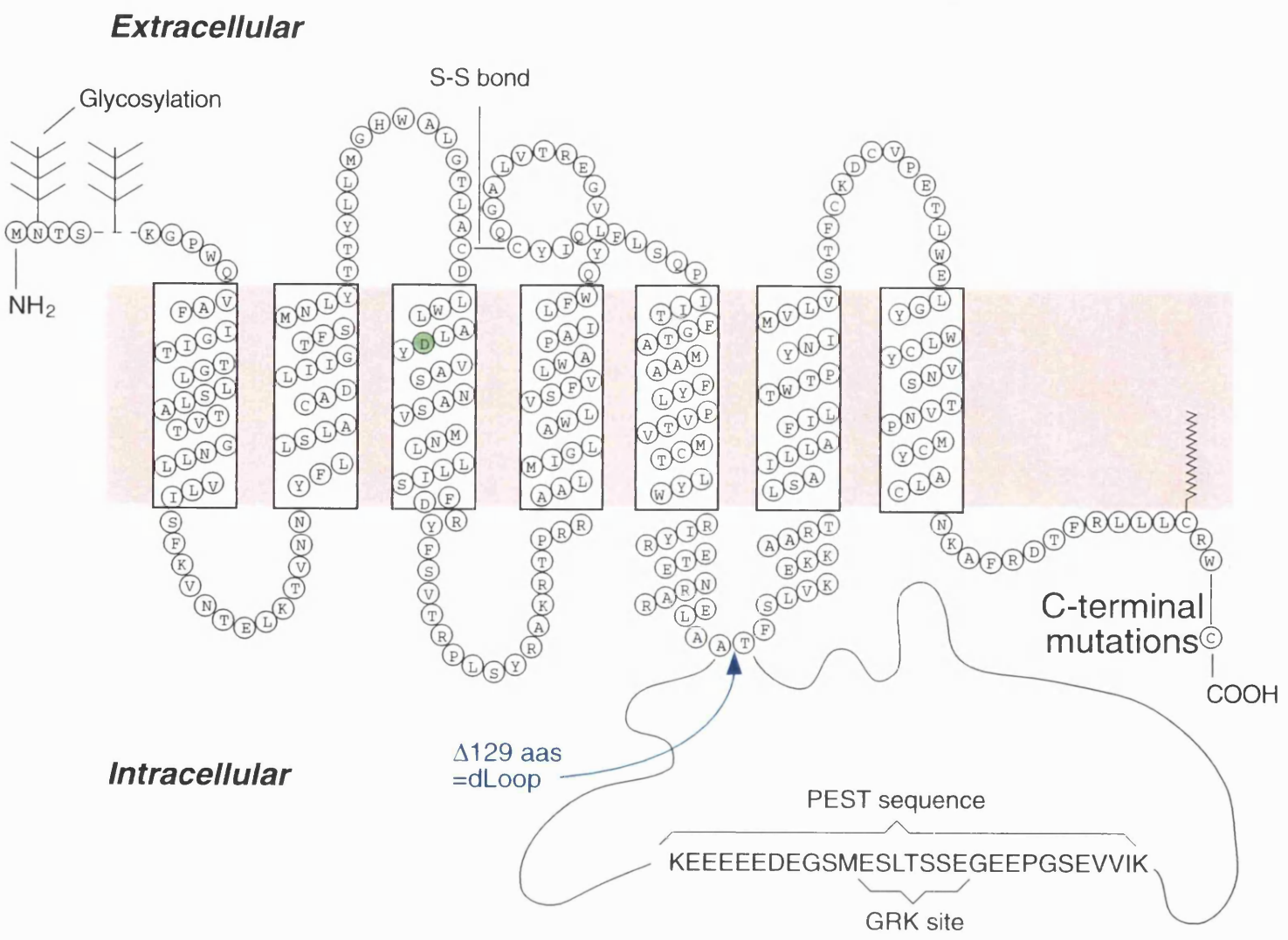
Extracellular
Glycosylation
S-S bond
NH2
C-terminal mutations
COOH
Intracellular
Δ129 aas
=dLoop
PEST sequence
KEEEEEDEGSMESLTSSEGEEPGSEVVIK
GRK site

2.6 Expression of M_1 mAChRs.

Wild-type and mutated receptors were transiently expressed in COS-7 cells. Wild-type and mutant receptor plasmid DNA was transfected into the COS-7 cells by electroporation. Growing cells, almost confluent, were washed twice with phosphate buffered saline and then removed from the surface of the flasks by adding 1 ml trypsin versene. The cells were resuspended in culture medium (α-minimal essential medium (α-MEM) supplemented with 10 % (v/v) new-born calf serum, antibiotics: penicillin and streptomycin, and 2 mM glutamine) and then spun gently (800 x *g* , 3 min, 10 °C) using a Heraeus Megafuge 1.0R with rotor #7570 at 2,000 rpm. The cells were washed with ice-cold α-MEM, re-spun and taken up in a volume (0.8 ml of ice-cold α-MEM/cuvette). 0.8 ml of cells ($4x10^7$ cells) were then placed in the electroporation cuvettes (0.4 cm electrode gap) containing 10 μg of DNA. The samples were electroporated with a single pulse of 180 volts, 960 microfarads, in a Bio Rad Gene Pulser™. The cells were left at room temperature (21 °C) for 10 min before being plated into tissue culture dishes and incubated at 37 °C, 5 % CO_2, in a humidified incubator.

2.7 Radioligand binding assays.

After 72 hrs, the transfected COS-7 cells were washed twice in phosphate buffered saline. Harvesting buffer (20 mM Na-HEPES, 10 mM EDTA, pH 7.5) was added to the cells which were then incubated at 4 °C for 15 min. The cells were scraped with a Teflon scraper before being homogenised with 20 strokes in a glass dounce homogeniser. The homogenised cells were centrifuged at 75,000 x *g*, 4 °C, for 30 min, using a Type 30 rotor in a Beckman L-70 Ultracentrifuge (29,000rpm). The pellets were resuspended in storage buffer (20 mM Na-HEPES, 1 mM EDTA, pH 7.5) and homogenised using a Polytron homogeniser. The membrane preparation was then aliquoted, frozen on dry-ice and placed at -70 °C until required.

The protein concentration of the membrane preparation was determined by the method of Lowry (Lowry, *et al.*, 1951), 10 % (w/v) trichloroacetic acid was used to precipitate the protein. In the radioligand binding assays the membrane preparations were diluted to give a final concentration of 10-15 μg protein/ml.

All binding assays were carried out in 20 mM Na-HEPES, 100 mM NaCl, 1 mM $MgCl_2$, pH 7.5. Saturation assays contained 0.01-3 nM (–)-[^{3}H]*N*-methylscopolamine ([^{3}H]-NMS) or 0.001-1 nM (–)-[^{3}H]quinuclidinylbenzilate ([^{3}H]-QNB), except for Asn382Ala-dLoop when 0.08-20 nM [^{3}H]-QNB was used, membrane preparation, and vehicle (0.3 % (v/v) DMSO in dH_2O) or 1 μM atropine (except for 100 μM benzilylcholine iodide for dLoop and Asn382Ala-dLoop) in vehicle (non-specific binding). Competition assays were carried out with 0.3 nM [^{3}H]-NMS or 90 pM (100 pM for Asn382Ala-dLoop) [^{3}H]-QNB, membrane preparation and competing ligand, vehicle or 1 μM atropine (100 μM benzilylcholine iodide for dLoop and Asn382Ala-dLoop) in vehicle. Assays, final volume 1 ml, were all performed in triplicate in polystyrene tubes and were incubated at 30 °C for 60 min ([^{3}H]-NMS) or 180 min ([^{3}H]-QNB). The assays were terminated by rapid vacuum filtration through GF/B glass fibre filters, pre-soaked in 0.15 % (w/v) polyethylene imine for 30 min, using a Brandel cell harvester. The filters were washed with 15 ml ice cold dH_2O. The radioactivity was extracted from the filters by 4.5 ml Liquiscint scintillation fluid and counted on a Wallac 1409 counter.

2.8 Phosphoinositide turnover assays.

Phosphoinositide (PI) turnover assays were performed by the method of Oldham (1990). Transfected cells were seeded into 12-well plates, and after 24 hrs labelled by adding 1 μCi/ml *myo*-D-[^{3}H]inositol to the culture medium. The cells were then incubated at 37 °C, 5 % CO_2, for a further 48 hrs. The medium, containing the inositol, was removed and replaced by Krebs-bicarbonate solution (120 mM NaCl, 3.1 mM KCl, 1.2 mM $MgSO_4$, 2.6 mM $CaCl_2$, 10 mM glucose and 25 mM $NaHCO_3$, pH 7.4) containing 10 mM LiCl (which inhibits the action of inositol monophosphatases (Berridge, *et al.*, 1982) and hence prevents the recycling of inositol (Figure 2.4)), for 30 min. Then agonists, and in some cases also antagonists, were added for a further incubation of 30 min at 37 °C, 5 % CO_2. The incubation time was shown to be within the linear period of the assay (Jones, *et al.*, 1995).

To terminate stimulation of PI hydrolysis, the medium was removed and 0.5 ml ice-cold 5 % (v/v) perchloric acid was added. The cells were incubated at 4 °C for 20 min

Figure 2.4: The phosphoinositide turnover cycle.

The phosphoinositide turnover experiment measures the accumulation of [^{3}H]-inositol phosphates within the cell. [^{3}H]-inositol that is added to the cells gets incorporated into the phosphatidylinositols, which are membrane phospholipids. Stimulation of the M_1 mAChR by agonist causes the activation of the G protein ($G_{q/11}$) that in turn causes the activation phospholipase C(β). The hydrolysing action of phospholipase C(β) on phosphatidylinositol-4,5-bisphosphate (pIns-4,5-P_2) produces diacylglycerol (DAG) and inositol-1,4,5-trisphosphate (Ins-1,4,5-P_3) that have second messenger roles. Phosphatases dephosphorylate Ins-1,4,5-P_3 to produce inositol which is then recycled to form pIns-4,5-P_2. In the phosphoinositide turnover experiments LiCl is added to the cells to block inositol monophosphatase and prevent the recycling of inositol. Therefore, when the system is stimulated this causes a build up of [^{3}H]-inositol phosphates that can be measured to indicate the functional response produced.

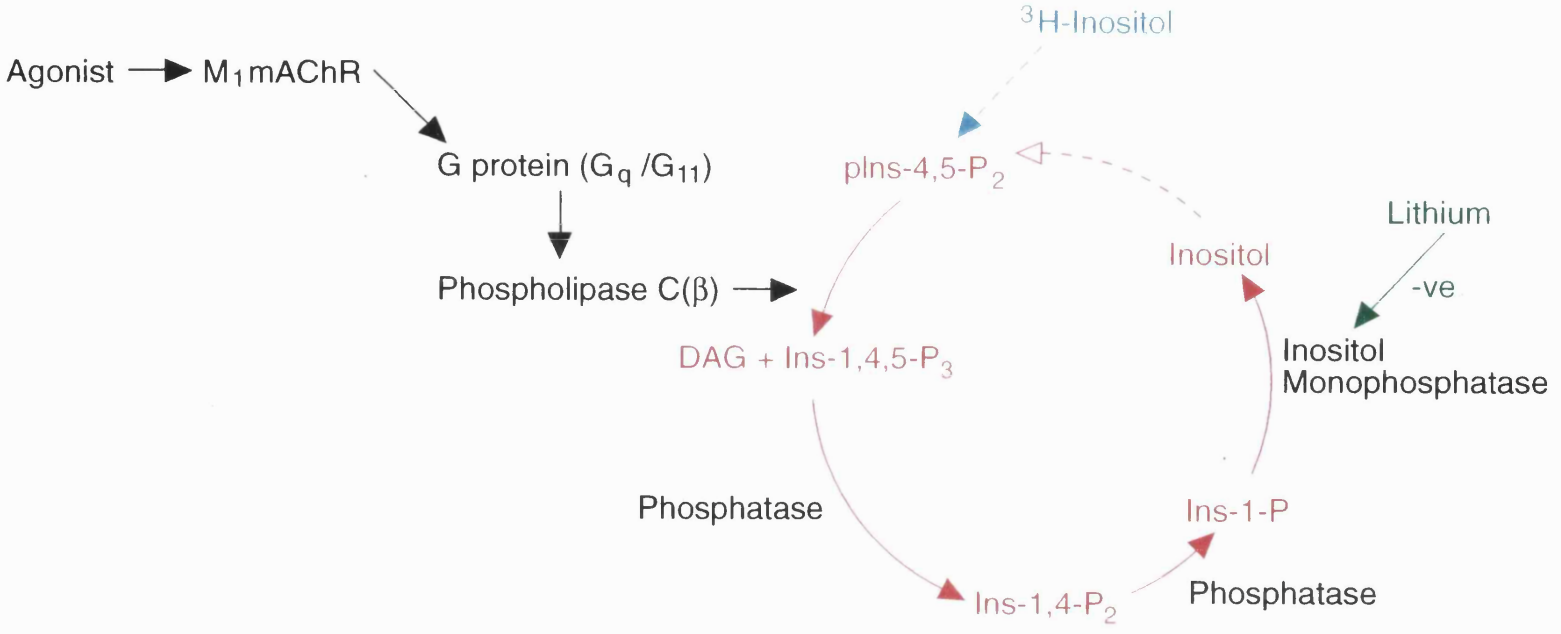
Agonist
M1mAChR
G protein (Gq /G11)
Phospholipase C(β)
DAG + Ins-1,4,5-P3
Phosphatase
Ins-1,4-P2
Ins-1-P
Phosphatase
Inositol
Inositol Monophosphatase
Lithium
-ve
pIns-4,5-P2
3H-Inositol

and then the lysate was added to 0.1 ml 10 mM EDTA, pH 8.0. The solution was neutralised by the addition of 0.5 ml 1:1 (v:v) tri-n-octylamine : 1,1,2-trichlorotrifluoroethane (Freon). After mixing the samples, they were centrifuged at 2,000 x *g* for 10 min in a Heraeus Megafuge 1.0R with rotor #7570 (3,000 rpm). 0.3 ml of the neutralised aqueous phase was added to columns containing 1 ml AG-1X8 resin (formate form, dry mesh size 100-200). The columns were washed with 10 ml dH_2O and then 10 ml 25 mM NH_4COOH before eluting [^{3}H]inositol phosphates with 10 ml 1 M NH_4COOH, 0.1 M HCOOH. 1 ml of the eluted sample was counted with 10 ml of Liquiscint scintillation fluid on a Wallac 1409 counter.

There are other methods of measuring the functional response caused by agonists binding to receptors. Probably, the most common alternative for measuring the functional response caused by the stimulation of M_1 mAChRs are ligand binding studies using [^{35}S]-guanosine 5'-O-(3-thiotriphosphate ([^{35}S]-GTPγS) (Northup, *et al.*, 1982). GTPγS is a non-hydrolysable analogue of GTP, therefore it essentially binds irreversibly to the agonist stimulated receptor. The binding of [^{35}S]-GTPγS can be analysed to give a measure of the functional response produced by the activated receptor. However, this technique has been found to be unsuitable for measuring a functional response produced by M_1 mAChRs expressed in COS-7 cells (Hulme, E.C., unpublished data).

2.9 Data analysis.

All data were analysed using SigmaPlot, version 4.00, for Windows (SPSS Inc.). So that the models described in the following text could be used to fit the data obtained, it was necessary to write them in terms of disintegrations per minute (dpm), taking into account the total and non-specific binding of the radioligand. Log concentrations of ligand were also used so that Log affinity constants could be obtained which had the advantage that a normal distribution of errors in the fitted parameters would result. For further details see: (Hulme and Birdsall, 1992). The rewriting of equations is not shown for every case, in the text, but the general trend was as follows:

If the equation was ([A] = competing ligand concentration; $[RL_{rad}]$ = concentration of radioligand-receptor complex in presence of competing ligand; $[RL_{radtotal}]$ = concentration of radioligand-receptor complex in the absence of competing ligand; K_{app} = apparent ligand affinity constant):

$$[RL_{rad}] = \frac{[RL_{radtotal}]}{1 + K_{app}[A]}$$

then it would be rewritten as:

$$dpm = \frac{dpm_{total} - nsb}{1 + 10^{(Log(Kapp) + Log([A]))}} + nsb$$

to take into account total amount of radioligand bound (dpm_{total}) and non-specific binding (nsb) as well as Log ligand concentrations and Log affinity constants.

The actual SigmaPlot models for each analysis are shown in the appendix (Section 8).

2.9.1 Analysis of saturation data: The one-site model of binding.

Saturation data (direct binding of [^{3}H]-NMS or [^{3}H]-QNB) were fitted to a one-site model of binding.

$$R + L_{rad} \underset{}{\overset{K}{\rightleftharpoons}} RL_{rad}$$

R = receptor; L_{rad} = radioligand; [Rt] = total receptor concentration; K = affinity constant.

$[RL_{rad}] = K[L_{rad}][R]$; where K is the affinity constant governing the binding of the ligand to the receptor.

The concentration of free receptor [R] may be calculated from the equation:

$$[Rt] = [R] + [RL_{rad}]$$

Rearrangement gives:

$$[R] = \frac{[Rt]}{1 + K[L_{rad}]}$$

and hence:

$$[RL_{rad}] = \frac{[Rt]K[L_{rad}]}{1 + K[L_{rad}]}$$

Fitting data to this model gives an affinity constant, K.

The computer programme used, fitted the specific and non-specific binding, as determined from the saturation experiments, simultaneously (described by Hulme and Birdsall, (1992)) as well as taking into account ligand depletion.

The effect of ligand depletion in saturation binding assays is to reduce the free radioligand concentration. This is potentially a serious problem when the total concentration of receptor binding sites is greater than 10 % of the K_D of the radioligand. To avoid ligand depletion either the total volume of the assay can be increased or the concentration of radioligand can be increased. By fitting the total and non-specific binding simultaneously the amount of free ligand can be modelled and the effects of ligand depletion can be compensated for (Hulme and Birdsall, 1992).

The one-site model of ligand binding was also used to fit data from competition studies using [^{3}H]-QNB and *N*-methylscopolamine binding to Tyr381Ala and Asn382Ala-dLoop mutant M_1 mAChRs. The affinity constant obtained was corrected with the Cheng-Prusoff correction factor which is explained in Section 2.9.2.

2.9.2 Analysis of competition assay data: The Hill equation.

Data from competition assays were fitted to a model using the Hill equation.

$$\frac{[RA]}{[Rt]} = \frac{(K[A])^{n_H}}{1 + (K[A])^{n_H}}$$

R = receptor; A = ligand; [Rt] = total receptor concentration; K = affinity constant if $n_H = 1$ otherwise it corresponds to $\frac{1}{IC_{50}}$; n_H = Hill coefficient.

The value of the Hill coefficient can indicates how the ligand binds to the receptor. If $n_H = 1$ then the ligand binds to a single, apparently homogeneous, class of binding sites. However, if $n_H > 1$ then there might be positive cooperativity in ligand binding

and if $n_H < 1$ then negative cooperativity might be occurring or the ligand is binding to a heterogeneous population of receptors.

The affinity constant obtained has to be corrected for the affinity of the radioligand for the receptor. This is done by using the Cheng-Prusoff correction (Cheng and Prusoff, 1973).

$$\text{Log}\, K_{cor} = \text{Log}\, K_{app} + \text{Log}(1 + K_{rad}[L_{rad}])$$

K_{cor} = affinity constant of competing ligand corrected with Cheng-Prusoff correction factor; K_{app} = measured affinity constant of competing ligand; K_{rad} = affinity constant of radioligand used; L_{rad} = concentration of radioligand used in the competition assay.

2.9.3 Analysis of competition assay data: The two-site model of binding.

In a number of cases it was necessary to analyse data from competition assays with a two-site model of binding. This model of binding was described by Hulme and Birdsall (1992). This model generates two fractions of binding sites, one having high affinity, the other having low affinity for the ligand.

$$[RL_{rad}] = K_{rad}[L_{rad}][Rt]\left(\frac{Fr_H}{1 + K_{rad}[L_{rad}] + K_H[A]} + \frac{Fr_L}{1 + K_{rad}[L_{rad}] + K_L[A]}\right)$$

Fr_H and Fr_L represent the fraction of high and low affinity states and K_H and K_L represent the high and low affinity constants. In the model used in fitting, the numerator and denominator were divided by $1 + K_{rad}[L_{rad}]$ (the Cheng-Prusoff shift) yielding apparent affinity constants and an estimation of specific binding. This was supplemented with the non-specific binding parameter (see Section 8.3). Thus, the high and low affinity constants obtained were corrected using the Cheng-Prusoff correction factor (see Section 2.9.2).

2.9.4 Analysis of phosphoinositide turnover data: Four parameter logistic function.

The PI data were analysed using a four parameter logistic function, based on the Hill equation, as described by Wells (1992). The data were fitted to the following equation:

$$dpm = (dpm_{total} - basal)\frac{(K[A])^{n_H}}{1+(K[A])^{n_H}} + basal$$

dpm_{total} = total dpm; basal = basal level of PI hydrolysis; K = apparent association constant; n_H = Hill coefficient.

2.9.4.1 Schild analysis.

In some of the PI assays competitive antagonists were present with the agonists. To determine the effect of the competitive antagonists on agonist stimulated activation of the receptor the data was fitted to the equation in Section 2.9.4. Then the binding affinity for the competitive antagonists (pK_B) was calculated according to the method of Arunlakshana and Schild (1959).

$$pK_B = \text{Log (conc.ratio)} - \text{Log } L_{antag}$$

L_{antag} = concentration of competitive antagonist in PI assay; conc.ratio = concentration ratio that can be determined by:

$$\text{conc.ratio} = \frac{EC_{50}(\text{agonist in presence of competitive antagonist})}{EC_{50}(\text{agonist without antagonist})}$$

2.9.5 Analysis to produce efficacy values.

Data from the analysis of ligand binding experiments and PI assays were used to calculate the effects of the mutations on efficacy. The model used, initially described by Hulme and Lu (1998), was based on the extended ternary complex model that was first used to analyse the properties of constitutively activated β-adrenergic receptors (Samama, *et al.*, 1993). A similar methodology was used to analyse the effects of β_2-adrenergic receptor expression on stimulation of adenylyl cyclase (Whaley, *et al.*, 1994).

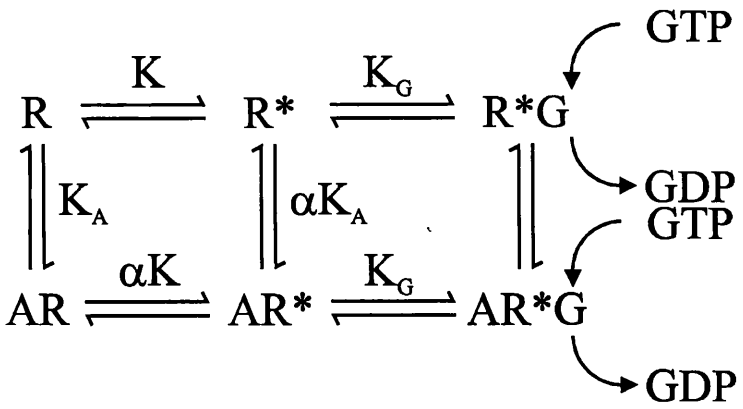

R = receptor (ground state); R* = receptor (activated state); A = agonist; G = G protein; [Rt] = total receptor concentration; [Gt] = total effector concentration.

In this model, either pre-existing (R*) or agonist-induced (AR*) activated receptor bind the G protein, leading to the formation of catalytically active R*G or AR*G complexes. These undergo GDP-GTP exchange that causes G protein activation. Agonists bind with higher affinity to the R* state than to R state.

In this model the following equilibria exist:

$[R^*] = K[R]$; this is a pre-existing equilibrium between the activated and ground state of the receptor defined by an equilibrium constant, K.

$[RA] = K_A[R][A]$; where the agonist binds to free receptor to give an agonist-receptor binary complex [AR]. This is governed by the equilibrium constant K_A.

$[R^*A] = K\alpha K_A[R][A]$; the formation of an activated receptor-agonist complex [R*A] is controlled by the equilibrium constants K and αK_A.

$[R^*G] = K_G[R^*]$; K_G is the affinity constant describing the affinity of activated receptor for the G protein.

In this model it is assumed that the receptor in its activated state acts like a ligand for the G protein and that the affinity constant K_G is the same for both R* and AR* binding to the G protein. This is a simplification of the model described by Samama, *et al.*, (1993) who found that in order to model some of their data it was preferable for

R* and AR* to have different affinities for the G protein. This may be because the study of Samama, *et al.*, investigated mutations within or close to the G protein binding domain. However, the simplifying assumption that K_G is constant seems to be adequate to model all the data from this laboratory (Hulme, E.C., personal communication).

It is also assumed, in the model described here, that the PI response is directly proportional to the ratio of the concentration of activated-receptor G protein complex to total G protein:

$$\frac{PI}{PI_{MAX}} = \frac{([AR*G]+[R*G])}{[Gt]} = \overline{[AR*G]}+\overline{[R*G]}$$

In the above equation and the following equations the line above symbols denotes normalisation either by the division by [Gt] for the concentrations of complexes involving receptor, or multiplication by [Gt] in the case of the affinity constant, K_G. In this derivation of the model it is assumed that [Rt] >> [Gt], i.e., there is more receptor than G protein.

$$G + R* \underset{}{\overset{K_G}{\rightleftharpoons}} R*G$$

where:

$$[Gt] = [G]+[R*G]$$

combining with the equilibrium equation defined above:

$$[Gt] = [G](1+K_G[R*])$$

rearrangement gives:

$$[R*G] = \frac{K_G[R*][Gt]}{1+K_G[R*]}$$

Therefore:

$$\overline{[R*G]} = \frac{\overline{K_G}\,\overline{[R*]}}{1+\overline{K_G}\,\overline{[R*]}}$$

This model also assumes that the receptor can exist in two states R and R* defined by the following equilibria:

$$R \underset{}{\overset{K}{\rightleftharpoons}} R^*$$

by using a similar procedure to that described above:

$$\overline{[R^*]} = \frac{K\overline{[Rt]}}{1+K}$$

Hence:

$$\overline{[R^*G]} = \frac{\overline{K_G}\,\frac{K\overline{[Rt]}}{1+K}}{1+\overline{K_G}\,\frac{K\overline{[Rt]}}{1+K}}$$

Since the receptor is normally in the ground state when no agonist is present, $K << 1$. Therefore:

$$\overline{[R^*G]} = \frac{\overline{K_G}K\overline{[Rt]}}{1+\overline{K_G}K\overline{[Rt]}}$$

(This equation represents the basal activity of the receptor-G protein complex.)

Agonist influences the R and R* equlibrium:

$$\begin{array}{ccc} R & \overset{K}{\rightleftharpoons} & R^* \\ \Big\| K_A & & \Big\| \alpha K_A \\ AR & \overset{\alpha K}{\rightleftharpoons} & AR^* \end{array}$$

The agonist binds with affinity K_A to the ground state of the receptor and with affinity αK_A to the activated receptor. The α component determines whether the ligand acts as an agonist ($\alpha > 1$), an inverse agonist ($\alpha < 1$) or a pure antagonist ($\alpha = 1$) of the R to R* conformational transistion.

The total amount of receptor is determined by:

$$[Rt] = [R] + [R^*] + [AR] + [AR^*]$$

Inserting the equilibria into the equation and then rearranging gives:

$$\overline{[R^*]} = \frac{K\overline{[Rt]}}{(1 + K + K_A[A] + K\alpha K_A[A])}$$

and

$$\overline{[AR^*]} = \frac{K\alpha K_A[A]\overline{[Rt]}}{(1 + K + K_A[A] + K\alpha K_A[A])}$$

Since it is assumed that the G protein binds to R* and AR* with the same affinity the two species can be summed:

$$\overline{[R^*]} + \overline{[AR^*]} = \frac{K\overline{[Rt]} + K\alpha K_A[A]\overline{[Rt]}}{(1 + K + K_A[A] + K\alpha K_A[A])}$$

combining the species able to activate G protein with the equation that defines G protein activation:

$$\overline{[R^*G]} = \frac{\overline{K_G}\,\overline{[R^*]}}{1 + \overline{K_G}\,\overline{[R^*]}}$$

gives:

$$\overline{[R^*G]} + \overline{[AR^*G]} = \frac{\dfrac{\overline{K_G}K\overline{[Rt]} + \overline{K_G}K\alpha K_A[A]\overline{[Rt]}}{1 + K + K_A[A] + K\alpha K_A[A]}}{1 + \dfrac{\overline{K_G}K\overline{[Rt]} + \overline{K_G}K\alpha K_A[A]\overline{[Rt]}}{1 + K + K_A[A] + K\alpha K_A[A]}}$$

It is assumed that in the absence of agonist the majority of the receptor remains in the inactive state, i.e., $K << 1$.

The agonist binding constant (K_{BIN}), as measured by the radioligand binding studies is defined by:

$$K_{BIN} = K_A(1 + \alpha K)$$

and other parameters are defined as:

$$P_2 = K\overline{K_G}$$

$$P_4 = K\overline{K_G}\alpha K_A$$

then:

$$\overline{[R*G]} + \overline{[AR*G]} = \frac{\frac{(P_2 + P_4[A])\overline{[Rt]}}{1 + K_{BIN}[A]}}{1 + \frac{(P_2 + P_4[A])\overline{[Rt]}}{1 + K_{BIN}[A]}}$$

this simplifies to (remembering that we assume the measured functional response is directly proportional to $\overline{[R*G]} + \overline{[AR*G]}$):

$$\frac{PI}{PI_{MAX}} = \overline{[R*G]} + \overline{[AR*G]} = \frac{P_2\overline{[Rt]} + P_4\overline{[Rt]}[A]}{1 + P_2\overline{[Rt]} + (K_{BIN} + P_4\overline{[Rt]})[A]}$$

The equation above is an extension of equation 22 of Black and Leff (1983). Black and Leff do not allow for pre-existing equilibrium, i.e., basal activity, which this model includes.

The following measurable parameters are defined by:

$$\text{Basal activity } ([A] = 0) = \frac{P_2\overline{[Rt]}}{1 + P_2\overline{[Rt]}}$$

$$K_{ACT} = \frac{1}{EC_{50}} = \frac{(K_{BIN} + P_4\overline{[Rt]})}{1 + P_2\overline{[Rt]}}$$

$$PI_{MAX}\ (A = \infty) = \frac{P_4\overline{[Rt]}}{K_{BIN} + P_4\overline{[Rt]}}$$

and during the modelling the parameters are determined by:

K_{BIN} determined by fitting data to the Hill equation (see Section 2.9.2).

$$P_2\overline{[Rt]} = \frac{\text{Basal activity}}{(1 - \text{Basal activiy})}$$

$$P_4[\overline{Rt}] = \frac{K_{ACT}}{(1 - \text{Basal actiity})} - K_{BIN} \qquad ; \text{if } K_{ACT} > K_{BIN}$$

$$P_4[\overline{Rt}] = K_{BIN}\frac{PI_{MAX}}{(1 - PI_{MAX})} \qquad ; \text{if } K_{ACT} \sim K_{BIN}$$

A value of $[\overline{Rt}] = 20$ for wild-type M_1 mAChR has been previously calculated (Lu, *et al.*, 1997). If the expression of the mutant is different then $[\overline{Rt}]$ is altered proportionally, i.e., 50 % of wild-type expression would have an $[\overline{Rt}] = 10$. Therefore, the parameters P_2, P_4 and K_{BIN} can be deduced, for the wild-type and mutant receptors, by fitting the data obtained.

Further analysis can then be carried out:

$\frac{P_4}{P_2} = \alpha K_A$; gives the affinity of the agonist for the R*G complex.

$\frac{P_4}{K_{BIN}} = \overline{K_G}\frac{\alpha K}{(1+\alpha K)}$; is a measure of the affinity of G protein for the ensemble of [AR] and [AR*].

This can be regarded as a measure of signalling efficacy of an agonist in the particular G protein linked pathway.

If a value of $\overline{K_G} = 14.1$ is used (Hulme and Lu, 1998), then αK can be determined allowing K_A to be deduced by the following equation:

$$K_A = \frac{K_{BIN}}{(1+\alpha K)}$$

K_A is a measure of the agonist's affinity for the receptor in its ground state and αK shows the ability of the agonist to induce the receptors activated state, i.e., it is a measure of the intrinsic efficacy of the agonist.

As already mentioned, the model described above assumes that [Rt] > [Gt]. When this is not the cases the following equations apply:

$$T_1^2[\overline{AR*G}]^2 - [\overline{AR*G}]T_2 + T_1(1+[\overline{Rt}]) + [\overline{Rt}] = 0$$

$$T_1 = 1 + \frac{P_2}{P_4[A]}$$

$$T_2 = \frac{K_{BIN}}{P_4} + \frac{1}{P_4[A]}\left(\frac{P_2}{K_G} + 1\right)$$

since it is assumed that $K << 1$ and $\frac{P_2}{K_G} = K$, then:

$$T_2 \sim \frac{K_{BIN}}{P_4} + \frac{1}{P_4[A]}$$

2.10 Immunocytochemistry.

This method was developed by Lu, *et al.*, (1997), for use with the wild-type and mutant rat M_1 mAChRs. COS-7 cells were transfected, using electroporation, as already mentioned in Section 2.6, and then plated onto coverslips previously exposed to 25 μg/ml fibronectin. After 72 hrs, the cells were washed three times with ice-cold phosphate buffered saline before being fixed with an ice-cold solution containing 4 % (w/v) paraformaldehyde in phosphate buffered saline, 0.05 % (v/v) Triton-X-100/NP40 (1:1 v/v) for 5 min. The cells were washed again and then blocked with 5 % (w/v) non-fat milk for 60 min, at 21 °C, before being washed and then incubated for 60 min, at 37 °C, with a 1:100 (v/v) dilution of an immunoaffinity-purified rabbit antiserum raised against the C-terminal 13 amino acids of the M_1 mAChR. Following washing, the cells were then incubated with a 1:5000 (v/v) dilution of a goat-anti-rabbit IgG-alkaline phosphatase conjugate. Tris-buffered saline was used to wash the cells before colour was developed by incubating with nitro blue tetrazolium/5-bromo-4-chloro-3-indolyl phosphate. The amount of staining was then determined by using a Molecular Dynamics laser scanning densitometer and Image-Quant software.

3. *Alanine scanning mutagenesis.*

3.1 Introduction.

Previous studies involving mutagenesis being carried out on the mAChRs have involved 'cherry picking' the residues to be mutated, i.e., looking at isolated residues that have properties which might be guessed to be important in binding. A less biased approach is to carry out a mutation study that looks at a series of residues to give details about amino-acids that are important in receptor function and those that are not. Therefore, to investigate the residues Tyr381 to Val387 in TM 6 of the rat M_1 mAChR, the alanine scanning mutagenesis technique was used. This strategy involves each residue in the series being individually mutated to alanine. The alanine mutants are then characterised to see the effects on ligand binding, activation of the receptor and receptor structure. The alanine residue is chosen, in this mutagenesis strategy, because it does not alter the hydrogen-bonding interactions formed by the protein backbone and does not have a sterically bulky or hydrophobic side-chain that may grossly alter the protein structure (Wells, 1991). Therefore, the effects caused by mutating the residue to alanine should, in principle, be due to the removal of the function or interaction of the amino-acid side-chain and not to disturbance of the protein backbone. The technique of alanine scanning mutagenesis has been used successfully to investigate the hormone binding domain of the human growth hormone receptor (Bass, *et al.*, 1991) as well as the platelet-activating factor receptor (Ishii, *et al.*, 1997) and is widely applied to studies on protein structure and function.

However, the amino-acid that the residues are sequentially mutated to, in scanning mutagenesis, does not necessarily have to be alanine. Probably the most common alternatives are histidine and cysteine because the mutated residue can then be investigated by a cation or a covalently binding ligand, respectively. Histidine mutations have been used to engineer a zinc binding site and give structural information about the tachykinin NK-1 receptor (Elling and Schwartz, 1996) and rhodopsin (Sheikh, *et al.*, 1996). The technique of cysteine substitution followed by chemical modification of the new sulfhydryls has been used in investigations on the nAChR (Akabas, *et al.*, 1992) and the aspartate receptor (Danielson, *et al.*, 1997).

This strategy has also been used to investigate the ligand binding domains of monoamine receptors (Javitch, *et al.*, 1995; Allman, *et al.*, 1997; Javitch, *et al.*, 1998).

In this investigation the alanine scanning mutagenesis strategy was used.

3.2 Results.

The seven alanine mutants and wild-type rat M_1 mAChRs were analysed primarily by using radioligand binding studies.

3.2.1 Antagonist binding.

Saturation binding assays showed that [^{3}H]-NMS and [^{3}H]-QNB affinity for the majority of the mutant receptors was unaffected, when compared to wild-type. The wild-type receptor had K_D values of 120-132 and 12-20 pM for [^{3}H]-NMS and [^{3}H]-QNB, respectively (Table 3.1). The expression levels of most of the mutants were also similar to wild-type ([^{3}H]-NMS: 0.84-1.28 pmol/mg protein; [^{3}H]-QNB: 0.88-1.60 pmol/mg protein) and the discrepancies seen were probably due to variability in the transfection procedure. However, there was no measurable binding of [^{3}H]-NMS to the Tyr381Ala mutant and both [^{3}H]-NMS and [^{3}H]-QNB failed to bind to Asn382Ala at the concentrations used. Relative to the wild-type, the Tyr381Ala mutant showed a 6 fold decrease in the number of receptors available to bind [^{3}H]-QNB, for equal amounts of DNA transfected, although the binding affinity was unchanged. Representative plots of [^{3}H]-NMS and [^{3}H]-QNB binding are shown in Figure 3.1.

Since [^{3}H]-QNB bound to the Tyr381Ala mutant, a competition assay was set up to determine the affinity of *N*-methylscopolamine (NMS). The data obtained were fitted to a one-site model of ligand binding. A representative plot is shown in Figure 3.2. This experiment showed that NMS affinity was reduced 660 fold, compared to wild-type. Thus, the [^{3}H]-NMS binding affinity was too low to allow direct binding to be measured.

3.2.2 Immunocytochemistry.

Immunocytochemistry, using an antibody that recognised the carboxy-tail of the receptor, was used to probe the expression of the total mutant M_1 mAChR protein. The experiments showed that the expression Tyr381Ala was reduced to 44 ± 7 %,

Table 3.1: The binding of [^{3}H]-NMS and [^{3}H]-QNB to alanine mutant and wild-type M_1 mAChRs.

Radioligand binding assays were carried out on COS-7 cells transiently expressing the wild-type and alanine mutant M_1 mAChRs. Assays were performed and direct binding of radioligands measured as described in "Materials and Methods." Results are shown as the mean ± S.E.M. of at least three experiments. The expression of the wild-type and mutant receptors is shown relative to wild-type control included in each transfection. Expression of the wild-type receptor is 1.06 ± 0.22 pmol/mg protein and 1.24 ± 0.36 pmol/mg protein when measured by [^{3}H]-NMS and [^{3}H]-QNB binding, respectively. There was no measurable binding (N.M.B.) of [^{3}H]-NMS to Tyr381Ala and Asn382Ala-dLoop and both [^{3}H]-NMS and [^{3}H]-QNB to Asn382Ala. [A] The data for [^{3}H]-NMS binding to dLoop was obtained from Lu, *et al.*, (1997). [B] pK_I value, corrected with the Cheng-Prusoff correction factor, obtained by carrying out a competition studies using [^{3}H]-QNB and NMS and fitting the data to a one-site model of ligand binding. t-test vs. wild-type value: ** $p < 0.01$; *** $p < 0.001$.

	[^{3}H]-NMS binding		[^{3}H]-QNB binding	
	Expression % Wild-type	pK_D -Log(M)	Expression % Wild-type	pK_D -Log(M)
Wild-type	(100)	9.90 ± 0.02	(100)	10.80 ± 0.11
Tyr381Ala	N.M.B.	7.08 ± 0.03 [B] ***	16 ± 2 ***	10.63 ± 0.15
Asn382Ala	N.M.B.		N.M.B.	
Ile383Ala	108 ± 7	9.96 ± 0.05	125 ± 11	10.89 ± 0.10
Met384Ala	75 ± 4 ***	10.03 ± 0.03	83 ± 10	10.83 ± 0.02
Val385Ala	104 ± 6	9.80 ± 0.02	96 ± 1	10.71 ± 0.03
Leu386Ala	121 ± 7 **	9.97 ± 0.03	109 ± 4	10.89 ± 0.01
Val387Ala	111 ± 6	9.95 ± 0.04	109 ± 9	10.95 ± 0.04
dLoop	170 ± 20 [A] **	10.00 ± 0.10 [A]	162 ± 10 **	10.85 ± 0.05
Asn382Ala-dLoop	N.M.B.	6.29 ± 0.12 [B] ***	128 ± 3 ***	8.86 ± 0.02 ***

Figure 3.1: The binding of [^{3}H]-NMS and [^{3}H]-QNB to wild-type and alanine mutant M_1 mAChRs.

This figure shows representative plots of [^{3}H]-NMS binding to the wild-type receptor (A) and [^{3}H]-QNB binding to wild-type (B), Tyr381Ala (C) and Asn382Ala-dLoop (D) M_1 mAChRs transiently expressed in COS-7 cells. Assays were performed and direct binding of radioligand measured as described in "Materials and Methods." The amount of radioligand bound is shown as pmol/mg protein (mean ± S.E.M., from three replicate values). In the case of [^{3}H]-QNB and [^{3}H]-NMS binding to wild-type M_1 mAChRs total binding (green), non-specific binding (black) and specific binding (red) of the radioligand are shown. Specific binding of [^{3}H]-QNB to Tyr381Ala and Asn382Ala-dLoop is shown (red). The calculated pK_D values are shown in Table 3.1. It is worth noting that the non-specific binding is linear.

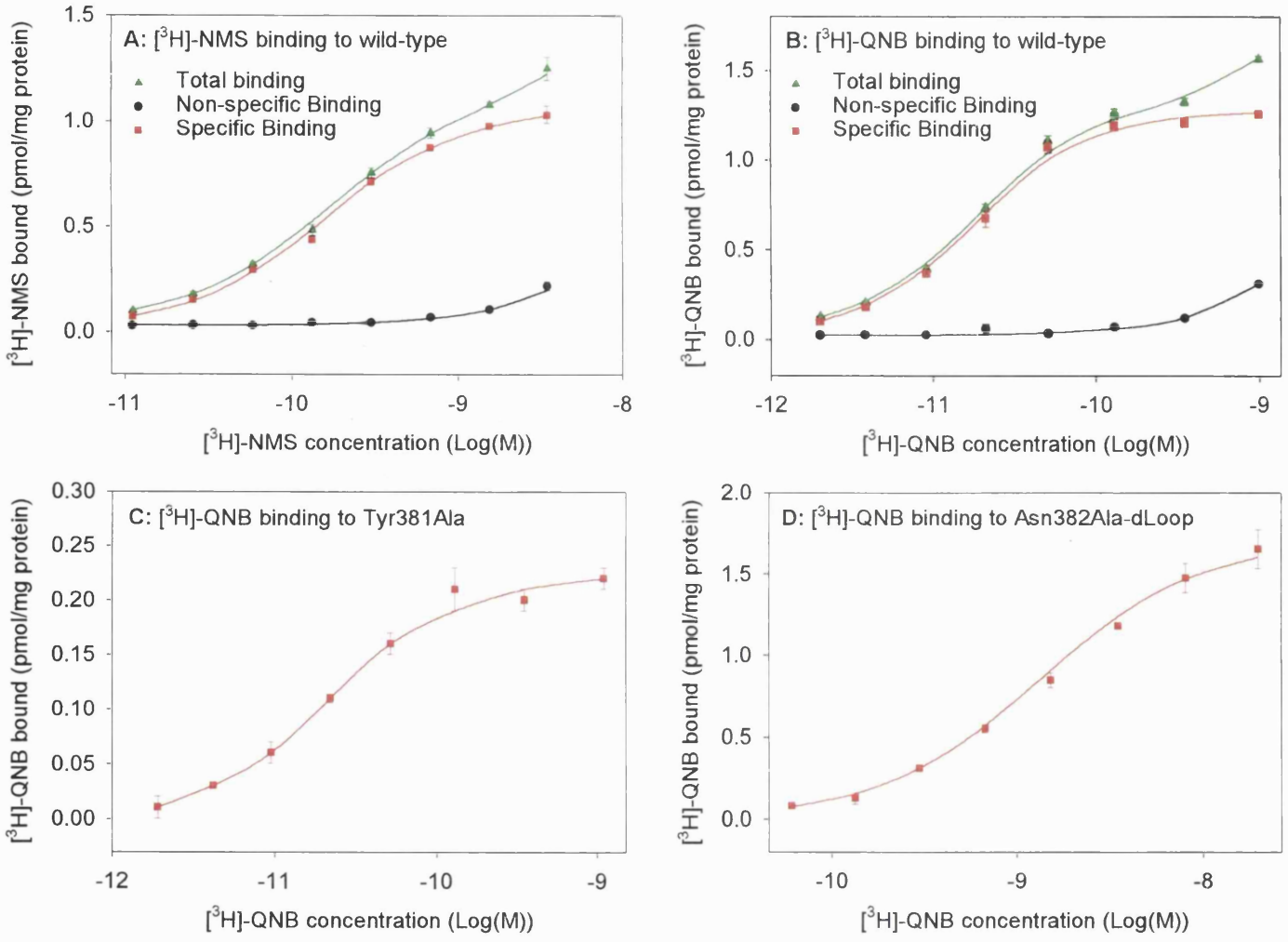
A: [3H]-NMS binding to wild-type
Total binding
Non-specific Binding
Specific Binding
[3H]-NMS bound (pmol/mg protein)
[3H]-NMS concentration (Log(M))
B: [3H]-QNB binding to wild-type
Total binding
Non-specific Binding
Specific Binding
[3H]-QNB bound (pmol/mg protein)
[3H]-QNB concentration (Log(M))
C: [3H]-QNB binding to Tyr381Ala
[3H]-QNB bound (pmol/mg protein)
[3H]-QNB concentration (Log(M))
D: [3H]-QNB binding to Asn382Ala-dLoop
[3H]-QNB bound (pmol/mg protein)
[3H]-QNB concentration (Log(M))

Figure 3.2: The inhibition of [^{3}H]-QNB binding to Tyr381Ala and Asn382Ala-dLoop by NMS.

Competition binding assays were carried out on COS-7 cells transiently expressing the Tyr381Ala (A) and Asn382Ala-dLoop (B) mutant receptors. Assays were performed as described in "Materials and Methods." The binding curves were analysed using a one-site model of binding. Data were plotted as a percentage of specific binding in the absence of competing ligand and have been corrected using the Cheng-Prusoff correction factor. Binding affinity constants are shown in Table 3.1. Data shown are from representative experiments and expressed as mean ± S.E.M. from three replicate values.

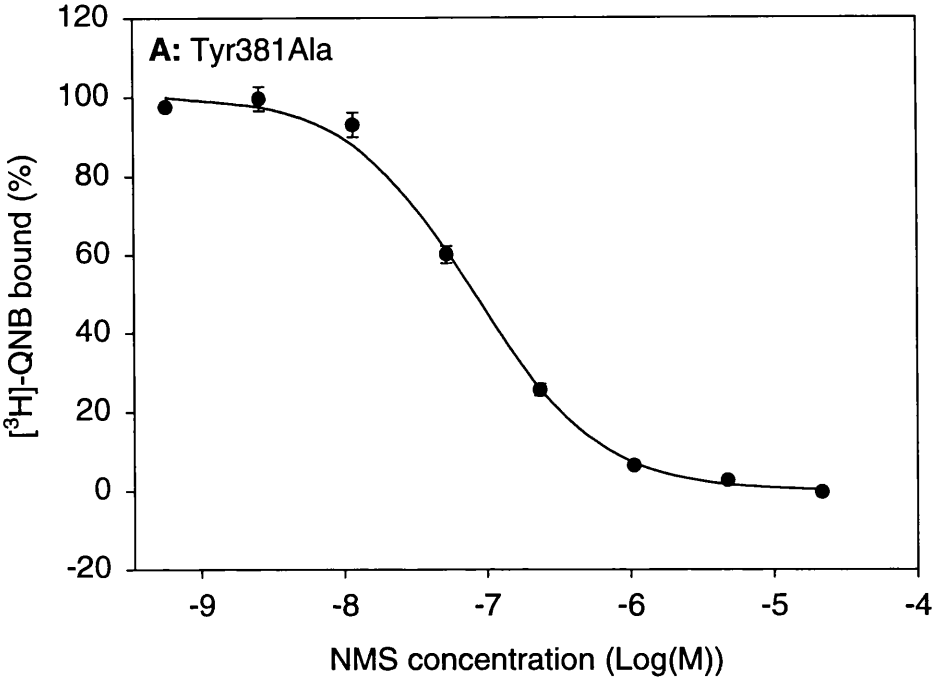
A: Tyr381Ala
120
100
80
60
40
20
0
-20
[3H]-QNB bound (%)
-9
-8
-7
-6
-5
-4
NMS concentration (Log(M))

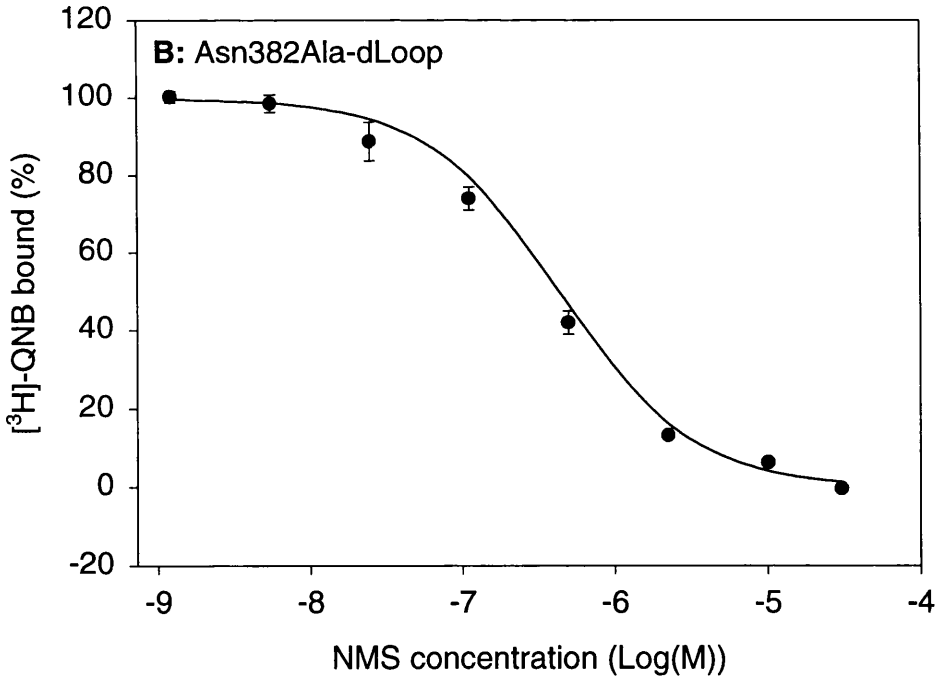
B: Asn382Ala-dLoop
120
100
80
60
40
20
0
-20
[3H]-QNB bound (%)
-9
-8
-7
-6
-5
-4
NMS concentration (Log(M))

Figure 3.3: Immunocytochemistry showing the expression of wild-type, Tyr381Ala and Asn382Ala M_1 mAChRs transiently expressed in COS-7 cells.

An antibody directed against a carboxyl-terminal epitope was used to probe the transient expression of wild-type (A), Tyr381Ala (B) and Asn382Ala (C) M_1 mAChRs in COS-7 cells. The procedure used is the same as described in "Materials and Methods." Magnification is 200 X. Analysis of the reaction product by using a Molecular Dynamics laser scanning densitometer and Image-Quant software revealed that Tyr381Ala and Asn382Ala expression was 44 ± 7 % and 24 ± 5 %, respectively, when compared to wild-type.

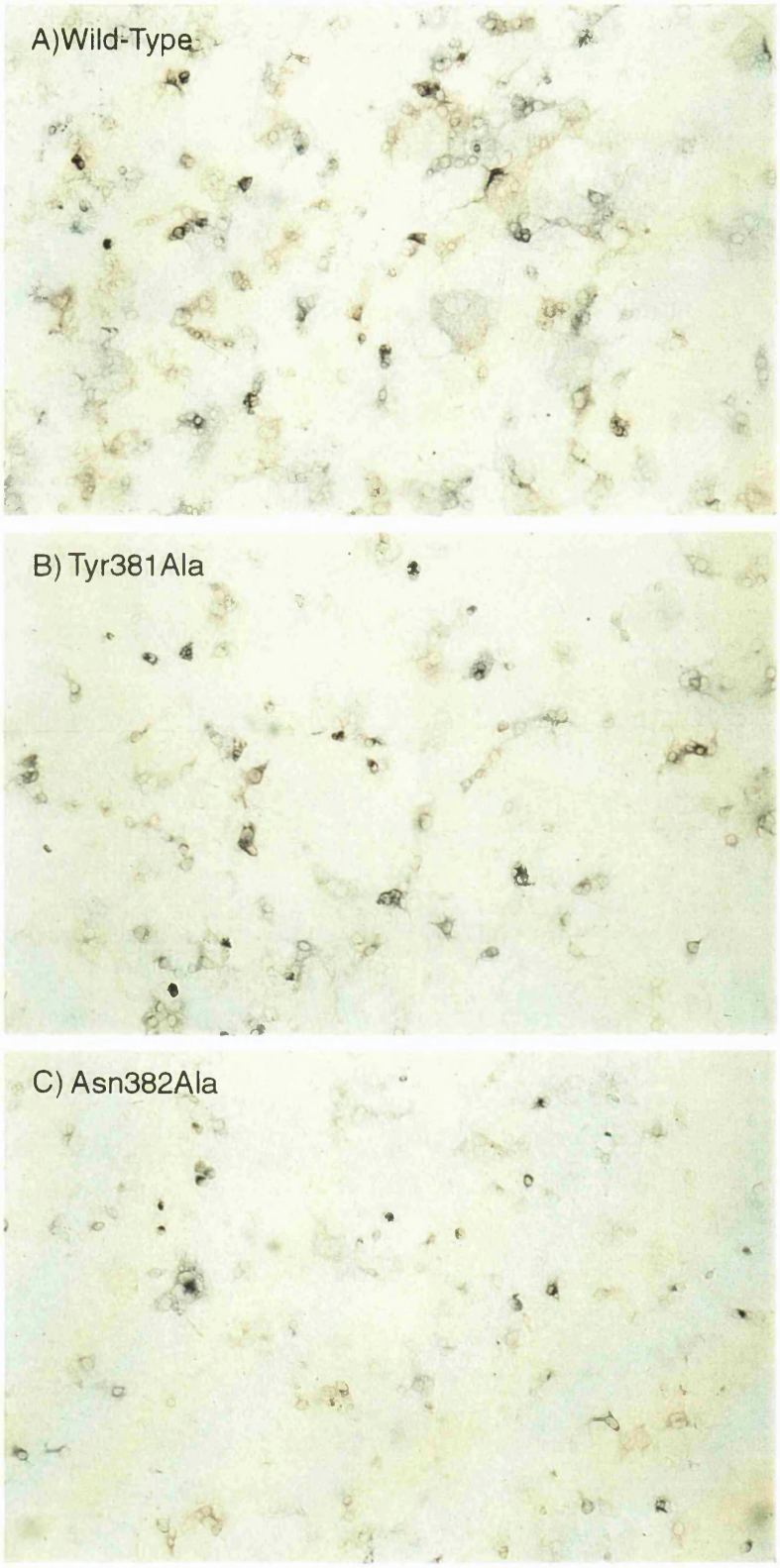
A)Wild-Type
B) Tyr381Ala
C) Asn382Ala

Figure 3.4: Immunocytochemistry showing the expression of wild-type, Asn382Ala, dLoop and Asn382Ala-dLoop M_1 mAChRs.

An antibody directed against a carboxyl-terminal epitope was used to probe the transient expression of wild-type (A), dLoop (B), Asn382Ala (C) and Asn382Ala-dLoop (D) M_1 mAChRs in COS-7 cells. The procedure used is the same as described in "Materials and Methods." Magnification is 200 X. Analysis of the reaction product by using a Molecular Dynamics laser scanning densitometer and Image-Quant software showed that the expression of the mutants, when compared to wild-type, was 125 ± 6 % (dLoop), 20 ± 1 % (Asn382Ala) and 80 ± 4 % (Asn382Ala-dLoop).

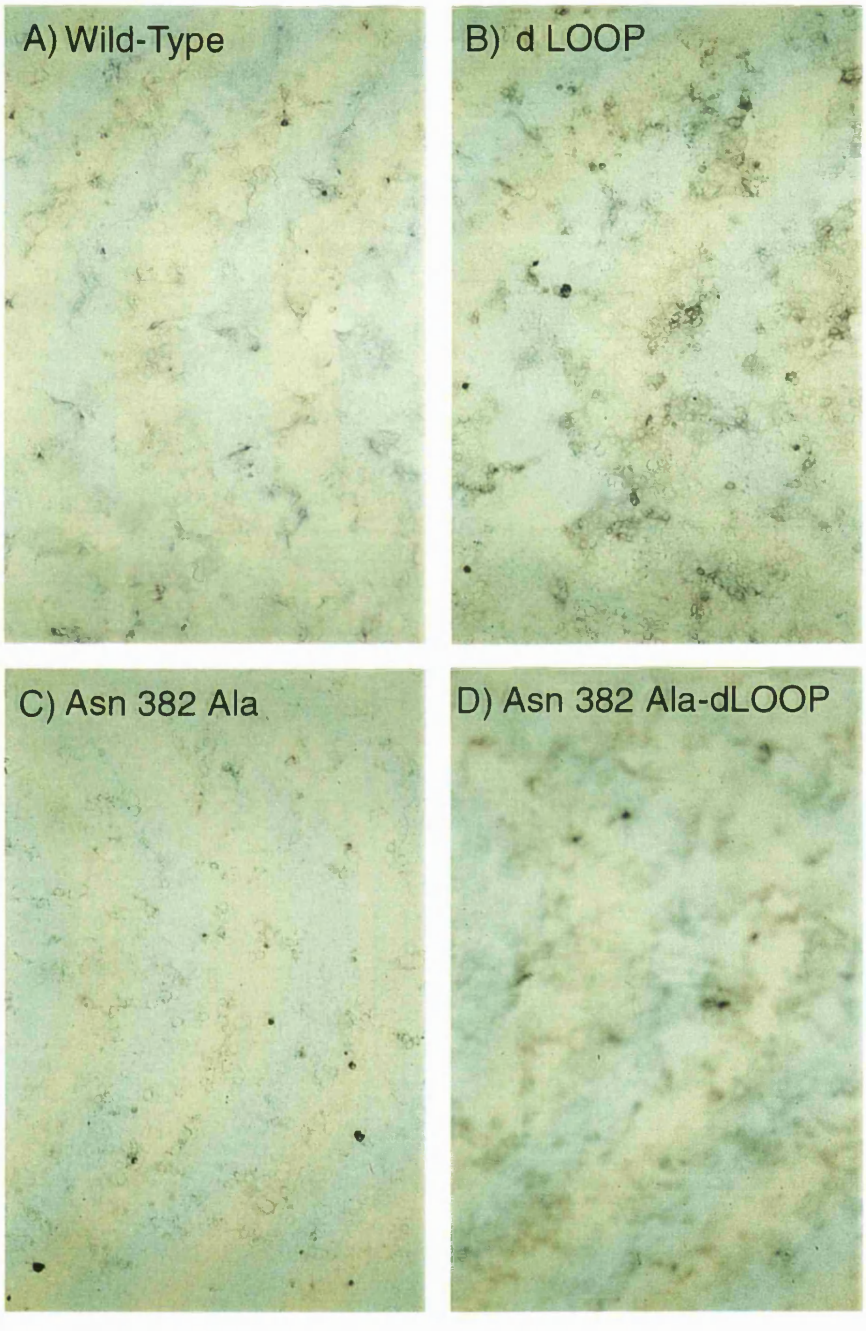
A) Wild-Type
B) d LOOP
C) Asn 382 Ala
D) Asn 382 Ala-dLOOP

when compared to wild-type, and Asn382Ala receptor expression was reduced further to 24 ± 5 % (Figure 3.3). These data gave higher apparent expression levels than the radioligand binding data. A possible reason for this is that the antibody interacts with both folded and unfolded receptors while the radioligands only interact with the receptors which are fully folded and properly processed and expressed. Therefore, the mutants that give low expression values by the use of radioligands may have a large component of unfolded receptors, which are not properly expressed. This results in a larger expression value being determined by the immunocytochemistry experiments. Another reason is the fact that the colour development, in the immunocytochemistry experiments, can become saturated. This effect is likely to occur at receptors with high expression, e.g., wild-type which could lead to the corrected values for the mutant receptors to be overestimated. However, this problem can be corrected for by carrying out a control experiment measuring the colour development for a variety of known expression levels.

Further investigation of the Asn382Ala mutant by radioligand binding studies was not possible since there was no measurable binding of either [^{3}H]-NMS or [^{3}H]-QNB. Therefore, an Asn382Ala-dLoop mutant was made that involves the deletion of residues 225-353 (dLoop), from the third intracellular loop of the receptor. This dLoop mutation has previously been shown to increase the expression of binding sites whilst having little effect on ligand binding affinities (see Table 3.1; Lu, *et al.*, 1997). The Asn382Ala-dLoop mutant was expressed at a similar level to the wild-type receptor, but showed an 90 fold reduction in [^{3}H]-QNB binding affinity. A representative binding curve is shown in Figure 3.1. However, there was no measurable binding of [^{3}H]-NMS to the Asn382Ala-dLoop M_1 mAChR. Data from immunocytochemistry analysis revealed an increase in the expression of the Asn382Ala mutant when combined with the dLoop mutation (Asn382Ala-dLoop) to 80 ± 4 % of wild-type (Figure 3.4).

A competition experiment was performed with [^{3}H]-QNB and NMS on Asn382Ala-dLoop. This assay showed that the binding affinity of NMS for Asn382Ala-dLoop was reduced 4070 fold, when compared to wild-type. A representative binding curve is shown in Figure 3.2.

3.2.3 ACh binding and ACh induced functional response.

Once saturation binding data was obtained for all the alanine mutant and wild-type M_1 mAChRs, ACh binding to each receptor was investigated. Competition binding assays used ACh and [^{3}H]-NMS in all cases except for Tyr381Ala, dLoop and Asn382Ala-dLoop where [^{3}H]-QNB was used. The data obtained are summarised in Table 3.2 and representative binding curves are shown in Figure 3.6.

As with the saturation binding studies, the majority of mutations did not affect the binding of ACh. The mutants that displayed a greater than 3 fold change in ACh binding affinity, when compared to wild-type M_1 mAChR (K_D = 13 μM) were Tyr381Ala (40 fold decrease), Leu386Ala (4 fold decrease) and Asn386Ala-dLoop (6 fold decrease). ACh binding to Asn382Ala could not be measured since no specific binding of radioligand could be detected.

The mean Hill coefficients measured for ACh binding to wild-type and alanine mutant M_1 mAChRs were slightly less than one, apart from Tyr381Ala. These data are consistent with the hypothesis that the receptor exists in several dynamic states with different agonist affinities depending on whether G protein is bound or not (Strader, *et al.*, 1994). However, studies carried out in this laboratory have shown that a measurable 'GTP-shift' does not occur with high levels of expression of the M_1 mAChR (Lu and Hulme, 1999). Therefore, other proteins may be interacting with the receptor to induce different receptor states. e.g., arrestins (Gurevich, *et al.*, 1997).

The ability of ACh to induce a functional response at wild-type and mutant M_1 mAChRs was measured using phosphoinositide turnover experiments (Table 3.3 and Figure 3.6). Tyr381Ala displayed the largest reduction in ACh potency with a 2750 fold decrease, when compared to wild-type. Interestingly, despite its low expression, Asn382Ala was able to produce as large a response as the wild-type receptor, although the ACh potency was reduced 40 fold. The response given by Asn382Ala-dLoop was compared to the dLoop construct, since deletion of residues from the third intracellular loop affects the potency of ACh in eliciting the functional response (Lu, *et al.*, 1997). In this case, 10 fold reduction in ACh potency resulted from the Asn382Ala mutation. The Leu386Ala mutant gave a 30 fold reduction in ACh potency relative to the wild-type receptor. Val387Ala and Ile383Ala produced 5 and 3

Table 3.2: Acetylcholine binding affinities for wild-type and mutant M_1 mAChRs.

Radioligand binding studies were performed on COS-7 cells transiently expressing wild-type and alanine mutant M_1 mAChRs. Using the assay procedure described in "Materials and Methods." Results are shown as the mean ± S.E.M. of at least three experiments. Acetylcholine binding affinity was determined by competition experiments using [^{3}H]-NMS in all cases except for Tyr381Ala, dLoop and Asn382Ala-dLoop when [^{3}H]-QNB was used as the radioligand (indicated with: ^{C}). pIC_{50} data have been corrected with the Cheng-Prusoff correction factor. t-test vs. wild-type value: ** $p < 0.01$; *** $p < 0.001$.

	pIC_{50} -Log(M)	n_H
Wild-type	4.89 ± 0.04	0.93 ± 0.04
Tyr381Ala	3.33 ± 0.18 [C] ***	1.11 ± 0.07
Asn382Ala		
Ile383Ala	4.63 ± 0.03 **	0.93 ± 0.03
Met384Ala	4.94 ± 0.05	0.88 ± 0.05
Val385Ala	4.55 ± 0.11	0.86 ± 0.03
Leu386Ala	4.30 ± 0.12 **	0.94 ± 0.05
Val387Ala	4.85 ± 0.06	0.92 ± 0.05
dLoop	4.85 ± 0.05 [C]	0.88 ± 0.01
Asn382Ala-dLoop	4.14 ± 0.05 [C] ***	0.97 ± 0.10

Figure 3.5: The inhibition of [^{3}H]-antagonist binding by ACh and the ACh induced phosphoinositide response at wild-type and alanine mutant M_1 mAChRs.

A) The figure shows representative plots of data obtained from competition binding experiments using [^{3}H]-antagonist (wild-type and Leu386Ala: [^{3}H]-NMS; Tyr381Ala and Asn382Ala-dLoop: [^{3}H]-QNB) and ACh binding to wild-type (black), Tyr381Ala (red), Asn382Ala-dLoop (green) and Leu386Ala (blue) M_1 mAChRs transiently expressed in COS-7 cells. The experimental procedures used are described in "Materials and Methods." The binding curves were fitted to the Hill equation and the corrected pIC_{50} values are shown in Table 3.2. Data were plotted as a percentage of specific [^{3}H]-antagonist binding in the absence of competing ligand and have been corrected using the Cheng-Prusoff correction factor. Each data point is the mean ± S.E.M. from three replicate values. The calculated pIC_{50} values are shown in Table 3.2.

B) Representative experiment showing the functional response stimulated by ACh binding at wild-type (black), Tyr381Ala (red), Asn382Ala (green) and Leu386Ala (blue) M_1 mAChRs transiently expressed in COS-7 cells. The data were obtained using procedures described in "Materials and Methods" and fitted to a four parameter logistic function. The PI response is shown as the dpm data (mean ± S.E.M., from three replicate values) obtained from the assay and have not been corrected. The measured pEC_{50} values are shown in Table 3.3.

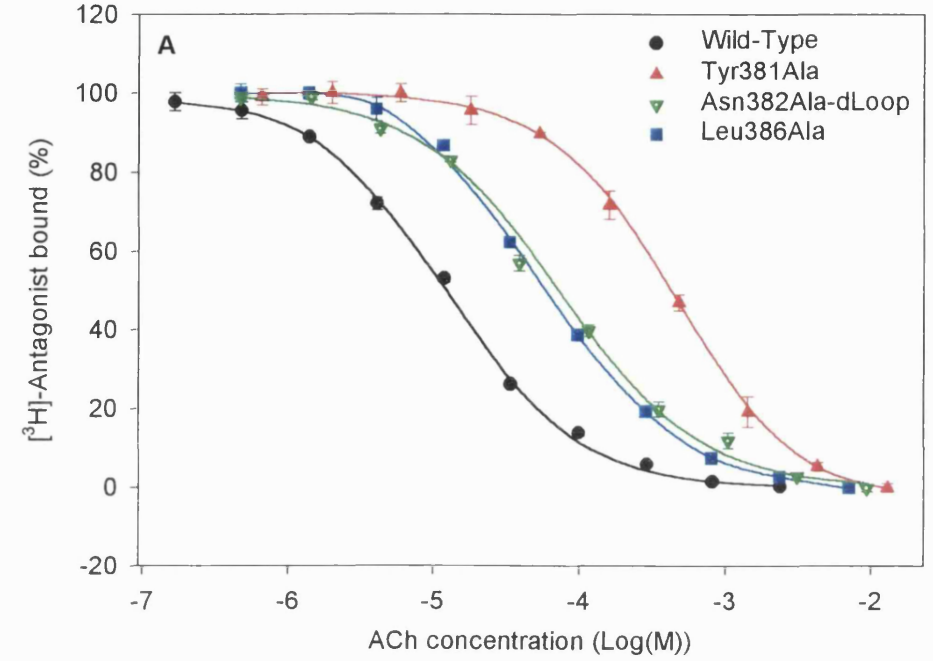
A
Wild-Type
Tyr381Ala
Asn382Ala-dLoop
Leu386Ala
[3H]-Antagonist bound (%)
120
100
80
60
40
20
0
-20
-7
-6
-5
-4
-3
-2
ACh concentration (Log(M))

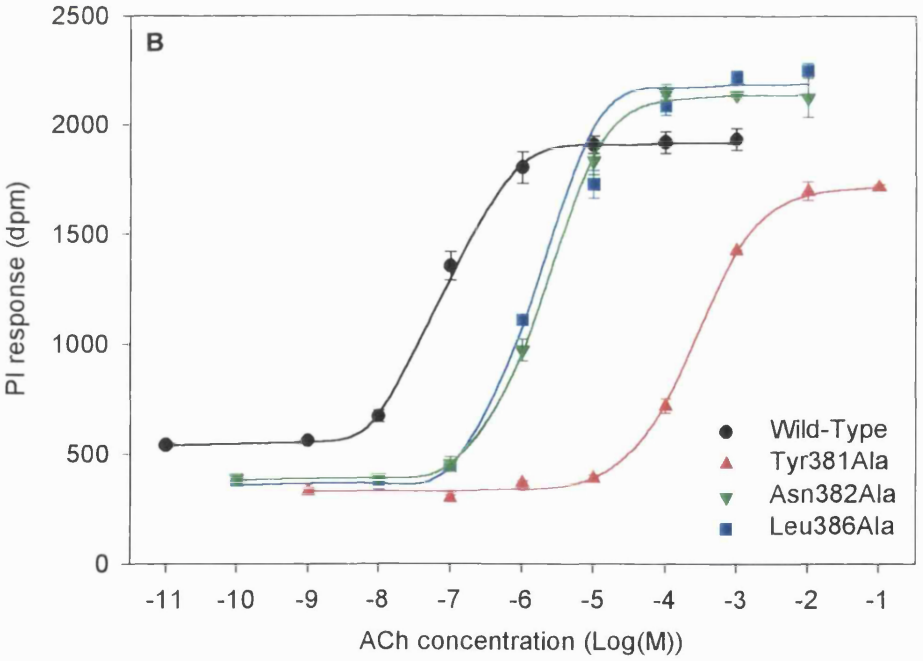
B
Wild-Type
Tyr381Ala
Asn382Ala
Leu386Ala
PI response (dpm)
2500
2000
1500
1000
500
0
-11
-10
-9
-8
-7
-6
-5
-4
-3
-2
-1
ACh concentration (Log(M))

Table 3.3: Acetylcholine induced phosphoinositide response for wild-type and alanine mutant M_1 mAChRs.

Phosphoinositide turnover assays were performed on COS-7 cells transiently expressing wild-type and alanine mutant M_1 mAChRs. Using the assay procedure described in "Materials and Methods." Results are shown as the mean ± S.E.M. of at least three experiments. Basal response, maximum response and maximum stimulated response are expressed as a % of the wild-type values: 457 ± 30 dpm, 4.4 ± 0.4 fold basal and 2050 ± 190 dpm, respectively. t-test vs. wild-type value: ** $p < 0.01$; *** $p < 0.001$.

	pEC_{50}: -Log(M) (n_H)	Basal response (% wild-type)	Maximum response (% wild-type fold basal)	Maximum stimulated response (% wild-type)
Wild-type	6.99 ± 0.08 (0.92 ± 0.04)	(100)	(100)	(100)
Tyr381Ala	3.55 ± 0.13 *** (0.91 ± 0.16)	73 ± 7	118 ± 7	85 ± 4
Asn382Ala	5.43 ± 0.11 *** (0.96 ± 0.08)	80 ± 2 ***	141 ± 8	112 ± 5
Ile383Ala	6.45 ± 0.00 ** (0.76 ± 0.05)	96 ± 5	128 ± 15	111 ± 12
Met384Ala	6.85 ± 0.05 (0.73 ± 0.09)	86 ± 3	113 ± 9	96 ± 5
Val385Ala	6.62 ± 0.05 (0.82 ± 0.04)	89 ± 20	124 ± 17	106 ± 8
Leu386Ala	5.53 ± 0.15 *** (0.97 ± 0.11)	74 ± 11	141 ± 7 **	103 ± 12
Val387Ala	6.31 ± 0.14 ** (0.87 ± 0.02)	78 ± 12	157 ± 2 ***	122 ± 17
dLoop	6.02 ± 0.06 *** (0.84 ± 0.10)	76 ± 3 **	79 ± 11	59 ± 5 **
Asn382Ala-dLoop	4.97 ± 0.05 *** (1.03 ± 0.06)	65 ± 1 ***	116 ± 4 **	76 ± 1 ***

Figure 3.6: Polar plots showing the effects on ACh binding and the ACh induced phosphoinositide response caused by alanine scanning mutagenesis of TM 6.

The effects of the alanine mutations on ACh binding affinity, A, and ACh induced phosphoinositide response, B, are displayed. The polar plots show the changes, measured on a logarithmic scale, in ACh binding affinity (pIC_{50}) and ACh induced phosphoinositide response (pEC_{50}). A positive value shown in the polar plot indicates a decrease in the affinity or response, compared to wild-type (value = 0). The length of the lines correspond to the magnitude of the change seen. The effects are also colour coded - red: > 10 fold decrease in IC_{50} or > 100 fold decrease in EC_{50}; blue: 3-10 fold decrease in IC_{50} or 10-100 fold decrease in EC_{50}; other residues are coloured green. The position of each residue around the polar plot is the position of the residue in TM 6 when looking along the helix. A value of 103 ° has been used for the angle between adjacent residues. Since the ACh binding affinity to the Asn382Ala mutant could not be determined due to no measurable radioligand binding, the binding affinity of ACh to Asn382Ala-dLoop was used instead.

A) Effects on ACh binding

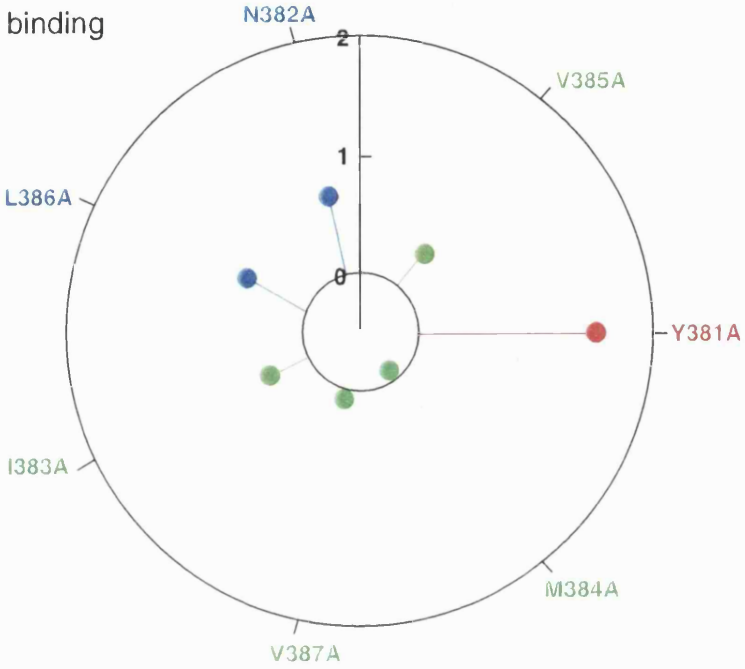

B) Effects on PI response

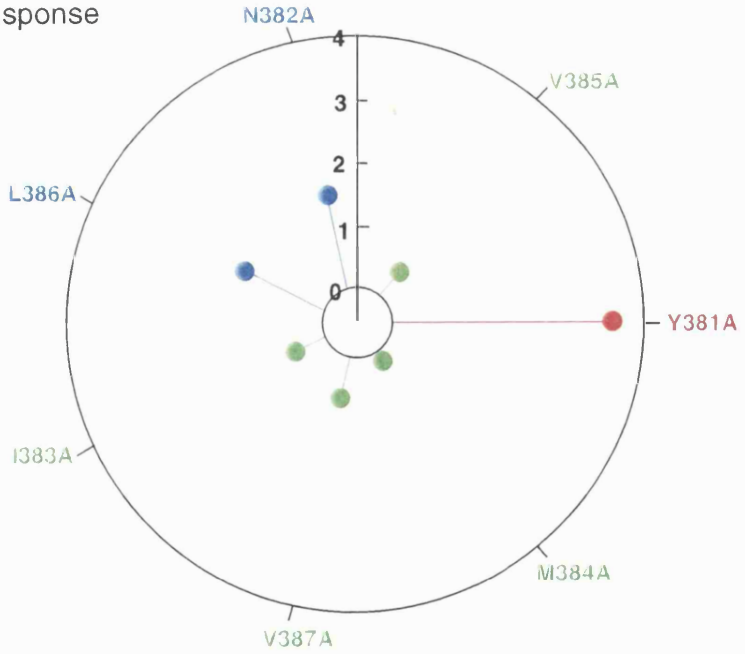

fold reductions in ACh potency to give a functional response, whilst Met384Ala and Val385Ala gave less than three fold changes.

The average basal response produced by the mutant receptors was less than wild-type in all cases and the average maximum responses, as measured as fold basal, tended to be higher than for the wild-type receptor. However, the maximum stimulated response produced by the majority of the mutant receptors was similar to wild-type. The only major exception to this observation, were the results obtained for dLoop and Asn382Ala-dLoop that showed that the maximum signal produced by ACh binding was reduced to 59 % and 76 %, respectively, when compared to wild-type.

3.2.4 Efficacy calculations.

Data for ACh binding and stimulated functional response, along with expression data, were combined and used in calculations to produce efficacy values for each mutant (see Section 2.9.5 for complete details and Table 3.4). This was done to try to analyse the effect of each mutation on the receptor activation step separately from the effects on the binding process.

The main assumption made in the calculation is that the un-activated and activated receptor is in equilibrium ($R \rightleftharpoons R^*$). The agonist binding induces an equilibrium ensemble of RA, R*A hence:

$$\frac{[R^*A]}{[RA]+[R^*A]} = \frac{\alpha K}{1+\alpha K}$$

Signalling efficacy can be measured by:

$$\frac{P_4}{K_{BIN}} = \overline{K_G}\frac{\alpha K}{(1+\alpha K)}$$

This then allows intrinsic efficacy (αK) to be calculated if $\overline{K_G}$ can be estimated. Once a value of αK is obtained the affinity of the agonist for the receptor in its ground state (K_A) can be determined. Therefore, the effects of mutations can be described in terms of binding to and activation of the receptor. However, this analysis does involve some assumptions (described above and in Section 2.9.5).

Table 3.4: The effect on ACh efficacy caused by the M_1 mAChR alanine mutations.

ACh efficacy was calculated for wild-type and alanine mutant M_1 mAChRs. The model used was based on the extended ternary complex model and is described in "Materials and Methods." ACh binding affinity, ACh potency in the functional response and receptor expression level data were used in the calculation to obtain: $\frac{P_4}{K_{BIN}}$; which is proportional to compound signalling efficacy. A value of $\overline{K_G} = 14.1$ was used (Hulme and Lu, 1998) to determine αK which is a true measure of compound intrinsic efficacy. [D] The ACh binding affinity for Asn382Ala-dLoop was used in the efficacy calculation for Asn382Ala since no ligand binding measurements were possible with this mutation. To show the effects of efficacy, when compared to wild-type ([E] dLoop and Asn382Ala-dLoop were compared to dLoop), the fold change in αK was determined for each receptor

	Signalling efficacy $\left(\frac{P_4}{K_{BIN}}\right)$	Intrinsic efficacy * (αK)	Fold change from wild-type αK: Decrease (Increase)
Wild-type	6.25	0.80	1
Tyr381Ala	0.21	0.015	52
Asn382Ala	8.5 [D]	1.54 [D]	(2)
Ile383Ala	2.6	0.22	4
Met384Ala	4.83	0.52	2
Val385Ala	6.06	0.75	1
Leu386Ala	0.73	0.05	16
Val387Ala	1.22	0.094	9
dLoop	0.41	0.029	1[E]
Asn382Ala-dLoop	0.23	0.017	2[E]

* Assuming that $\overline{K_G} = 14.1$

The ACh binding affinity for the Asn382Ala-dLoop mutant was used in the analysis of Asn382Ala, since the data obtained so far shows that the dLoop mutation does not seem to have a significant effect on the ligand binding affinities measured for either the wild-type or mutant M_1 mAChRs (Lu, *et al.*, 1997). Since no expression data for Asn382Ala, were obtained from [^{3}H]-NMS or [^{3}H]-QNB binding studies, it was treated as half of Tyr381Ala expression, as suggested by the immunocytochemistry data, i.e., 8 % of wild-type.

The majority of the alanine mutations affected ACh efficacy by less than 10 fold (increase or decrease), when compared to wild-type. The Tyr381Ala and Leu386Ala mutations reduced ACh efficacy by 50 and 20 fold, respectively, when compared to wild-type.

3.3 Discussion.

The results from the alanine scanning mutagenesis study carried out on residues Tyr381Ala to Val387Ala, in TM 6 of the rat M_1 mAChR, have shown that a number of these amino-acids play a role in rat M_1 mAChR function. These data are summarised in polar-plots shown in Figure 3.6. These plots represent the position of each residue, mutated in the alanine scanning mutagenesis study along an α-helix and show the effects that each alanine mutant had on ACh binding affinity and ACh potency in the functional response. Interestingly, the residues that have the greatest effects on receptor function (Tyr381, Asn382 and Leu386) are on one side of the α-helix and those that do not (with the exception of Val385) are on the other side. These observations support an α-helical conformation for this segment of TM 6.

Tyr381Ala showed the largest effects on both ACh binding affinity and functional response, as well as causing a decrease in receptor expression. The results showing the effect of the mutations on ACh efficacy also indicated that Tyr381Ala had the largest effect, out of the residues analysed. These data imply that the Tyr381 residue, which is conserved among all mAChRs, is important both in agonist binding and in receptor activation. This finding agrees with the investigation carried out by Wess, *et al.*, (1992) that shows Tyr506, the homologous residue to Tyr381 in the M_3 mAChR affects agonist-induced activation when mutated to phenylalanine. However, a study

carried out on the homologous tyrosine in the M_2 mAChR which mutated the residue to phenylalanine indicated that Tyr403 only plays a role in ACh binding and not in receptor activation (Vogel, *et al.*, 1997). However, these studies only investigated the tyrosine to phenylalanine mutant, in which the side-chain was partly deleted. The full effect of deleting the side-chain of residues homologous to Tyr381, in the M_2 and M_3 mAChRs has not been investigated.

The majority of the other monoamine receptors have a phenylalanine at the same position as Tyr381 (Probst, *et al.*, 1992). Studies have indicated that the phenylalanine in the β-adrenergic (Dixon, *et al.*, 1988) and D_2-dopamine (Cho, *et al.*, 1995) receptors may be important for the interactions with agonists. These data are consistent with the finding that Tyr381 is important for the interaction with ACh.

Apart from playing a role in ACh binding and receptor activation, Tyr381 is able to discriminate between antagonists. The Tyr381Ala mutation had no effect on [^{3}H]-QNB binding affinity whilst causing a significant reduction in [^{3}H]-NMS binding affinity. [^{3}H]-NMS and [^{3}H]-QNB may bind in different orientations, and/or make different interactions with Tyr381. Another possible role of Tyr381 may be to make an intra-molecular interaction, to stabilise receptor folding, since Tyr381Ala causes a reduction in receptor expression.

Asn382 also seems to play a role in receptor stabilisation, possibly by making an intra-molecular interaction, since the Asn382Ala mutation caused receptor expression to be reduced. Analysis based on the model by Baldwin, *et al.*, (1997) suggests that Asn382 faces towards TM 5 (Figure 3.7), indicating a potential helix-helix interaction. A similar observation has been made for Phe390 in the D_2-dopamine receptor, in that it seems to play a stabilisation role (Javitch, *et al.*, 1998).

The reduction in expression may be a contributing factor in preventing radioligand binding studies on this mutant, although the mutant is able to give a functional response. An explanation for this observation is that the PI assay is more sensitive than the radioligand binding study since the response is amplified through the signalling cascade.

Construction of the Asn382Ala-dLoop receptor enabled radioligand binding studies to be carried out because the dLoop mutation increased receptor expression to levels

Figure 3.7: A model displaying the positions of the residues shown to be involved in receptor function.

The model shows the positions of the residues that the data from the alanine scanning mutagenesis indicate as being important in receptor function. The positions of Tyr381 (red), Asn382 (blue), Leu386 (green) and Val387 (orange), in TM 6, and Asp105 (yellow), in TM 3, are shown. The model used is based on the one by Baldwin, *et al.*, (1997) and is viewed from the extracellular side of the membrane.

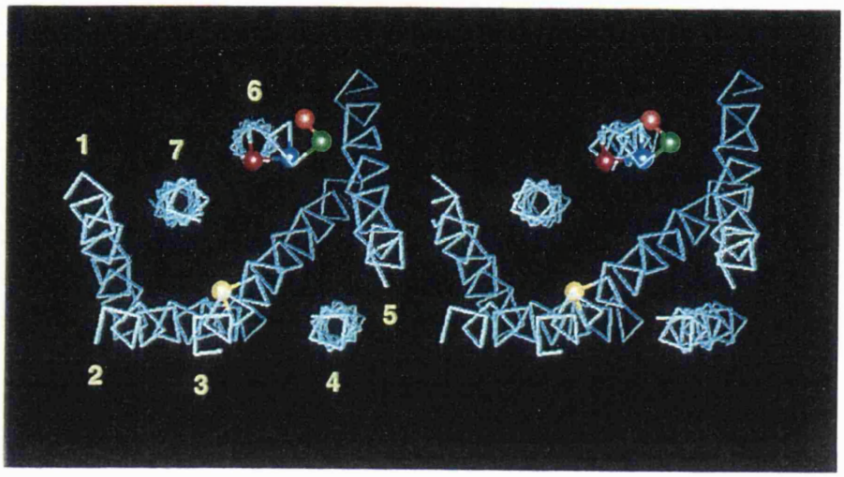
1
2
3
4
5
6
7

similar to those given by the wild-type M_1 mAChR. The results of this study and previous investigations (Lu, *et al.*, 1997) show that the dLoop mutation does not affect agonist (ACh) and antagonist ([^{3}H]-NMS and [^{3}H]-QNB) binding affinities, measured in the context of the wild-type receptor. From this it is assumed that the results obtained for Asn382Ala-dLoop are similar to those that would be obtained with Asn382Ala if radioligand binding studies were possible. The effects that Asn382Ala-dLoop (Asn382Ala) has on ligand binding affinities indicate that Asn382 probably plays more of a role in antagonist than in agonist binding. A similar observation was made when the homologous asparagine was mutated in the M_3 mAChR (Blüml, *et al.*, 1994), although the effect on [^{3}H]-QNB binding affinity of the asparginine to alanine mutant was greater in the M_1 mAChR (90 fold reduction) than the M_3 subtype (8 fold decrease).

These findings, that NMS and [^{3}H]-QNB binding affinities are reduced by Asn382Ala, combined with the reduction in expression, probably are the reason why radioligand binding studies are not feasible with the Asn382Ala mutation.

The functional response produced by ACh at the Asn382Ala mutant is similar to the maximum response given by the wild-type receptor, although the potency is reduced. The low expression of the Asn382Ala probably causes some of the reduction in potency. It has been shown by the use of propylbenzilylcholine mustard, which is an irreversible antagonist, that a decrease in the number of functional receptor binding sites leads to a reduction in the functional response potency, as measured by a PI assay (Lu, *et al.*, 1997). Similar behaviour is also suggested by the data obtained here. If the potency of ACh in the functional response is compared for Asn382Ala to wild-type and Asn382Ala-dLoop to dLoop (since the dLoop mutation has an effect on the functional response measured) it can be observed that the difference is smaller (about 10 fold compared to 40 fold) for the receptors that are both expressed at high levels, namely the dLoop mutations. The analysis carried out to determine efficacy takes into account both the low expression and reduction in potency of the functional response. Therefore, the calculated effect on ACh efficacy caused by the Asn382Ala mutation is only a nominal 2 fold increase. These results further suggest that Asn382 plays a major role in the binding of certain antagonists, but not ACh. The changes observed in ligand binding may possibly be due to deletion of an intra-molecular interaction and

may be indirect effects rather than direct residue-ligand interaction, although this is only a hypothesis.

In the other monoamine receptors there tends to be a phenylalanine instead of the asparagine found in the mAChRs. Studies have shown that when this phenylalanine in the β-adrenergic (Dixon, *et al.*, 1988), D_2-dopamine (Cho, *et al.*, 1995) and 5-HT_2 5-hydroxytrypamine (Choudhary, *et al.*, 1993) receptors is mutated, both agonist and antagonist binding are affected.

These data indicate that Tyr381 and Asn382, both conserved residues in the mAChRs, play roles that are specific to this type of receptor. In the other monoamine receptors these residues tend to be phenylalanines and mutating them leads to altered agonist and antagonist binding (especially the residue at the same position as Asn382). However, in the M_1 mAChR (and the other mAChRs) Tyr381 and Asn382 seem to have more specificity in the roles that they perform, i.e., one residue seems to be important for agonist binding and receptor activation whilst the other residue is important for antagonist binding and receptor stability and/or folding.

Leu386Ala affects ACh efficacy by greater than 10 fold. However, modelling (based on the model by Baldwin, *et al.*, (1997)) shows that Leu386 faces towards TM 5 (Figure 3.7). Therefore, this residue is probably making an intra-molecular interaction, although, unlike Asn382, this interaction does not seem to be important for receptor folding and stability. However, the Leu386Ala mutation does alter ACh binding and receptor activation. The effect on binding may be an indirect event, i.e., removal of the Leu386 interaction alters the association of ACh with another residue. However, the effect on the potency of the functional response may be due to a direct role in the activation process, i.e., Leu386 may have a role in the activation process, and in maintaining the receptor's activated state. There is a leucine residue at the same position as Leu386 in the V_2 vasopressin receptor, that has been shown to be mutated to proline in some patients with X-linked nephrogenic diabetes insipidus. A study analysing this mutation showed that it caused a decrease in cell surface expression and a functionally inactive receptor (Wenkert, *et al.*, 1996). These data further support the hypothesis that Leu386 may be involved in M_1 mAChR activation.

Val387 may also be involved in the M_1 mAChR activation process. The Val387Ala mutation does not affect the binding of ACh but causes a reduction in the potency of ACh in the functional response (hence a decrease in ACh efficacy). Modelling (Figure 3.7) suggests that Val387 is either facing the lipid-bilayer or TM 7. Therefore, Val387 may make an interaction that contributes to maintaining the receptors activated state. A study mutating residues in the intracellular portion of TM 3 of the gonadotropin-releasing hormone receptor suggest that there are residues involved in maintaining the activated state of the receptor (Ballesteros, *et al.*, 1998). Therefore, there are probably a number of residues that have the role of maintaining the receptor in the activated state, when the agonist binds.

The other residues in the alanine scanning mutagenesis (Ile383, Met384 and Val385) do not seem to play a major role in receptor function. These results agree with other studies with the exception of Val385. It has been shown that mutating residues in the same position as Val385 in other GPCRs affects ligand binding (van Rhee and Jacobson (1996), and references therein). The type of residue found at this position is also extremely variable (17 out of 20 amino-acids). Therefore, it has been hypothesised that one role of residues at this position is to differentiate between ligands, perhaps by making specific interactions between the receptor and its ligand. In the case of the mAChRs, where Val385 does not seem to play a role in receptor function, other residues such as Tyr381 may take over this role of being a 'specificity residue.'

Tyr381 is a good candidate for forming a specific interaction with ACh. Comparing the data obtained in this alanine scanning mutagenesis study on TM 6 to data obtained from alanine scanning mutagenesis studies on TMs 3 (Lu, Z.-L., personal communication) and 5 (Allman, K., personal communication), there are only two other residues which when mutated to alanine, affect ligand binding and the signal transduction process to a similar degree as Tyr381: Asp105 and Tyr106, in TM 3 of the M_1 mAChR. Therefore, Tyr381 almost certainly plays a important role, along with Asp105 and Tyr106, in M_1 mAChR function.

Since there has not been a similar study carried out on TM 6 of the other mAChR subtypes a direct comparison of the results obtained with the alanine mutants cannot

be performed. Perhaps the closest comparison that can be made is with a study probing the residues in TM 6 of the D_2 dopamine receptor that are accessible in the binding-site crevice (Javitch, *et al.*, 1998). This investigation used a cysteine scanning mutagenesis strategy followed by covalent modification by a ligand containing a sulfhydryl-reactive moiety. The pattern of residues able to be covalently modified, placing them in the binding-site crevice, is consistent with the results obtained from the M_1 mAChR. However, more residues in the D_2 dopamine receptor are shown to be important. One possible explanation for this observation is that the [^{3}H]-ligands used to probe the effects of the sulfhydryl-reagents are antagonists, and therefore may not have the same binding specificity as agonists. Interestingly, the residues in the D_2 dopamine receptor that are covalently modified to the greatest extent (Phe389 and Phe390) correspond to Tyr381 and Asn382, in the M_1 mAChR. These data further support the hypothesis that residues homologous to Tyr381 and Asn382 are in important positions on TM 6 for ligand binding. However, since no agonist binding was looked at in the D_2 dopamine study, no conclusions about the agonist binding domain can be made.

The data obtained in this study and the investigation carried out by Javitch, *et al.*, (1998) are also consistent with the hypothesis that TM 6 is an α-helix modified with a proline kink, i.e., when the residues are orientated in an α-helix, one face contains residues affected by covalently binding ligands and the proline kink allows more accessibility. A study on the B_2 bradykinin receptor, investigating ten TM 6 residues, also showed a similar pattern of residues that was consistent with an α-helix (Nardone and Hogan, 1994). This study indicated that Phe261, corresponding to Tyr381, in the M_1 mAChR, plays an important role in bradykinin (agonist) binding but only has a minor effect on antagonist binding. Gln262, that corresponds to Asn382 in the M_1 mAChR, seems to have a slightly greater involvement in antagonist than agonist binding. These conclusions are very similar to those suggested for Tyr381 and Asn382 by the alanine scanning mutagenesis study on the M_1 mAChR.

4. *The role of Tyr381 in M_1 mAChR function.*

4.1 Introduction.

The alanine scanning mutagenesis carried out on residues Tyr381 to Val387 indicated that mutation of Tyr381 had the largest effect on M_1 mAChR function. As already mentioned, this tyrosine is conserved within the mAChRs and analysis of the effect of the alanine mutations would suggest that Tyr381 may be playing a role particular to the mAChRs, i.e., it is involved in the specificity of ACh binding to these receptors.

A study of the M_3 mAChR suggested that Tyr506, which is the homologous residue to Tyr381 in the M_1 mAChR, interacts with the ester moiety of ACh and played an important role in receptor activation (Wess, *et al.*, 1992). A similar investigation of the M_2 mAChR indicated that the mutation of the homologous tyrosine (Tyr403) to phenylalanine affects ACh binding but not the activation of the receptor (Vogel, *et al.*, 1997). It has also been hypothesised that aromatic residues close to Asp105 in TM3, which include Tyr381, form a cage around the positively charged head-group of the agonist (the quaternary nitrogen of ACh) to stabilise the ion-ion interaction with the conserved asparate (Trumpp-Kallmeyer, *et al.*, 1992).

These studies and the alanine scanning mutagenesis data suggest that Tyr381 and the homologous tyrosines in the mAChRs play an important role in mAChR function. It was decided to investigate this residue further. The strategy used to carry out this study was twofold. Firstly, the Tyr381Phe mutation was made to dissect the function(s) of the tyrosine. Do the hydroxyl- and benzene-groups, that make up the tyrosine side-chain, have specific roles? None of the previous mutagenesis studies on this homologous tyrosine have used both the Tyr381Phe and Tyr381Ala mutations. Therefore, this strategy should give a more detailed picture. Secondly, the wild-type receptor and the Tyr381 mutants were probed with three types of ligand: two of which are agonists and the third antagonists (i) ACh derivatives, (ii) quinuclidine- and azanorbornane-based ligands and (iii) atropine analogues (Figure 4.1), to obtain structure-activity relationships so that the nature of the interactions occurring between the ligand and Tyr381 can be determined.

Figure 4.1: The structure of ACh and azanorbornane, quinuclidine and atropine-based ligands.

ACh analogues, quinuclidine- and azanorbornane-based ligands and atropine-like compounds were used to investigate Tyr381. The majority of ligands used had characteristics similar to ACh, i.e., a moiety able to form a cation-anion interaction (shown in red) and moieties able to form strong hydrogen-bonds (shown in blue).

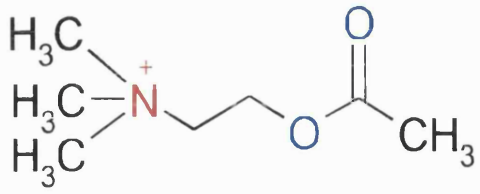

Acetylcholine

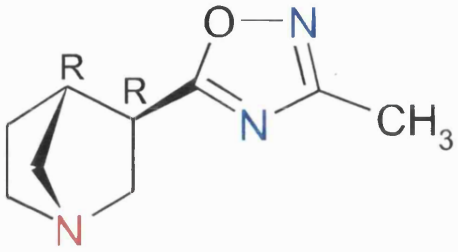

Azanorbornane based (L-698,583)

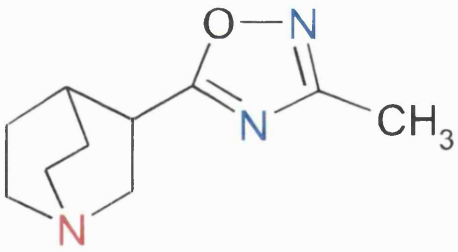

Quinuclidine based (L-658,903)

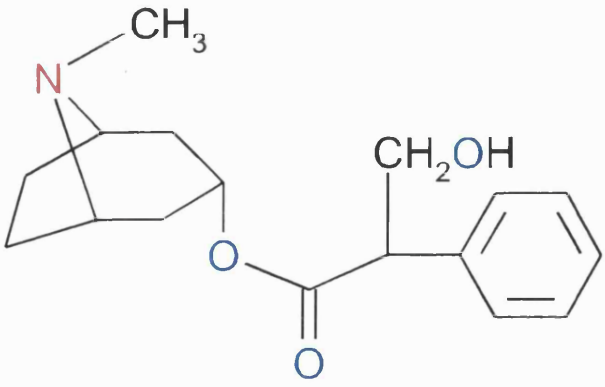

Atropine

The ACh derivatives were used to determine which moieties the Tyr381 residue interacts with: the head-group (quaternary nitrogen), or the side-chain (ester oxygens). One of the problems associated with trying to carry out structure-activity relationships with ACh and its analogues is that altering the structure of the ligand can have a drastic effect on the predominant mode of interaction within the binding site which undermines the analysis of structure-function relationships (Page, *et al.*, 1995). To attempt to overcome this, a series of quinuclidine- and azanorbornane-based agonists were used that have been produced with characteristics similar to ACh, i.e., a head-group able to form a anion-cation interaction and a side-chain that contains moieties able to form hydrogen-bonds, but which have increased binding affinities and efficacies for the M_1 mAChR (Freedman, *et al.*, 1990). These compounds were originally developed as potential therapeutic agents for the treatment of Alzheimer's disease. They contain a tertiary nitrogen, instead of the quaternary nitrogen found in ACh and are therefore able to cross the blood-brain barrier. This series of ligands potentially enabled two deductions to be made. Firstly, by comparing the quinuclidine and azanorbornane head-groups, it could be seen whether the extra methylene moiety present in the quinuclidine head-group makes an interaction with Tyr381, i.e., does the Tyr381 residue play a role in caging the head-group, as indicated by modelling studies? Secondly, the quinuclidine-based series of ligands, which had varying numbers of hydrogen-bond acceptors in the side-chain, could be used to see if Tyr381 interacted with the side-chain, as previously suggested (Wess, *et al.*, 1992).

The atropine analogues, which are antagonists, were used to probe the possible interactions of Tyr381 with the head-group and side-chain, particularly the basic nitrogen of the tropine ring and the side-chain of the tropic acid moiety, respectively. Like the azanorbornane- and quinuclidine-based ligands, these compounds have relatively high binding affinities for the M_1 mAChR allowing results to be obtained even if the mutation produces large reductions in ligand binding affinities. By comparing the effects of the Tyr381 mutations on the binding of the series of atropine analogues, a number of conclusions could be anticipated. The addition of a methyl group to the tropine ring nitrogen might give some indication about whether Tyr381 forms a head-group interaction, and by altering the position or removal of the hydroxyl group present on the tropic acid side-chain information about possible

hydrogen-bond interactions with Tyr381 may be obtained. The results from using these compounds could also give some indication why Tyr381 discriminates between QNB and NMS binding.

4.2 Results.

Firstly, the Tyr381 mutant M_1 mAChRs were analysed by measuring [^{3}H]-QNB binding. The data from the saturation radioligand binding studies are shown in Table 4.1 and representative plots in Figure 4.2. When compared to wild-type ([^{3}H]-QNB K_D of ~ 16 pM), the [^{3}H]-QNB binding affinity for the Tyr381Phe mutation was 2 fold higher ($p<0.05$), whereas the affinity for Tyr381Ala was unchanged. The Tyr381 mutants also affected the number of receptor ligand binding sites, i.e., expression level, with Tyr381Phe and Tyr381Ala producing 2 ($p<0.001$) and 6 ($p<0.001$) fold decreases, when compared to wild-type.

Competition radioligand binding assays, with [^{3}H]-QNB, were then carried out to see how the binding affinities of compounds were affected by the Tyr381 mutants. The results from these experiments are shown in Tables 4.2, 4.3, 4.4 and 4.5. To see whether differences in measured data of less than 10 fold were significant the t-test was used. The results of these statistical tests are shown in brackets after the specific comparison is mentioned in the following text, e.g., ($p<0.05$).

4.2.1 Binding of ACh analogues.

Tyr381Phe and Tyr381Ala both reduced ACh affinity by ~ 30 fold, when compared to wild-type, where ACh had a K_D of 17 μM. Representative binding curves are shown in Figure 4.3. The majority of ACh analogues showed a lower affinity than ACh at the wild-type receptor. However, the trends observed with the Tyr381Phe and Tyr381Ala mutations were similar in that both caused the affinities of carbachol, ACh-reversed ester and ACh-$N(Et)_2$ to be reduced by ~ 6 ($p<0.001$), ~ 6 ($p<0.001$) and ~ 5 ($p<0.01$) fold when compared to the wild-type receptor, respectively. In contrast, tetramethylammonium binding was affected by < 3 fold, when comparing the Tyr381Phe and Tyr381Ala mutant M_1 mAChRs to wild-type.

Table 4.1: The binding of [^{3}H]-QNB to wild-type and Tyr381 mutant M_1 mAChRs.

Radioligand binding assays were carried out on COS-7 cells transiently expressing the wild-type, Tyr381Phe and Tyr381Ala M_1 mAChRs. Assays were performed and direct binding of radioligands measured as described in "Materials and Methods." Results are shown as the mean ± S.E.M. of at least three experiments. The expression of the wild-type and mutant receptors are shown relative to wild-type control included in each transfection. Expression of the wild-type receptor was 1.24 ± 0.36 pmol/mg protein when measured by [^{3}H]-QNB binding. t-test vs. wild-type value: * $p < 0.05$; ** $p < 0.01$; *** $p < 0.001$.

Figure 4.2: The binding of [^{3}H]-QNB to wild-type and Tyr381 mutant M_1 mAChRs

The figure shows representative plots of specific binding of [^{3}H]-QNB to wild-type (black), Tyr381Phe (red) and Tyr381Ala (green) receptors transiently expressed in COS-7 cells. The assay procedures are described in "Materials and Methods." [^{3}H]-QNB binding is expressed as pmol/mg protein and data points are the mean ± S.E.M. of three replicate values. The calculated pK_D values are shown in Table 4.1.

	pK_D: -Log(M) (Expression: % wild-type)		
	Wild-type	Tyr381Phe	Tyr381Ala
[^{3}H]-Quinuclidinylbenzilate 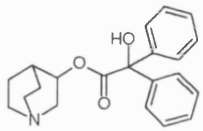	10.80 ± 0.11 (100)	11.19 ± 0.02 * (48 ± 3) ***	10.63 ± 0.15 (16 ± 2) ***

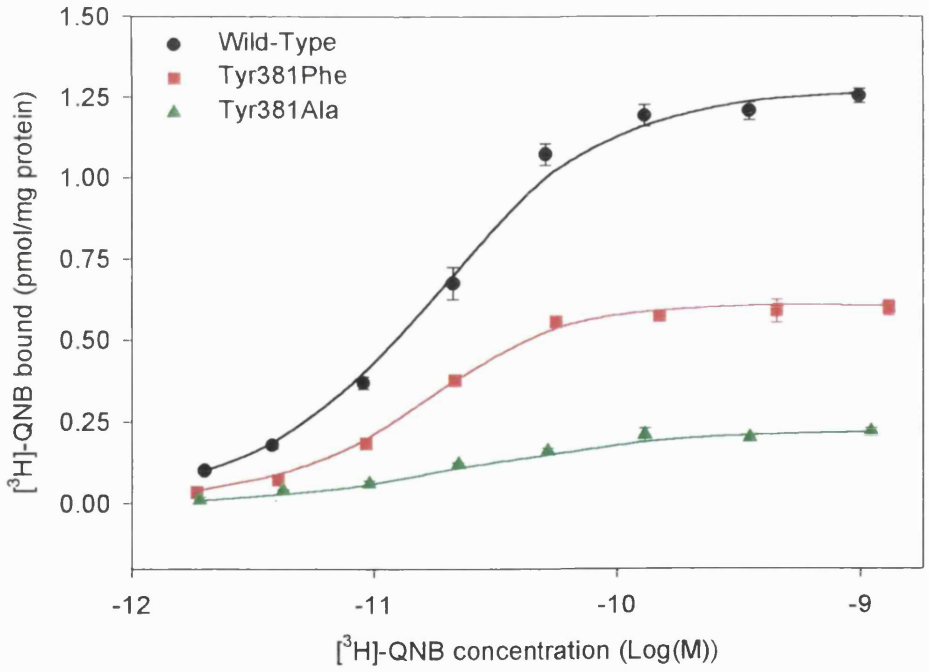

Table 4.2: Characterisation of the function of Tyr381 by measuring the binding of ACh analogues, oxotremorine-M and pilocarpine to Tyr381Phe and Tyr381Ala mutant and wild-type M_1 mAChRs.

Competition studies with [^{3}H]-QNB were performed on COS-7 cells transiently expressing wild-type, Tyr381Phe and Tyr381Ala M_1 mAChRs. The assay protocol was performed as described in "Materials and Methods." Data are given as pIC_{50} values obtained by using the Hill equation except for benzilylcholine (^{A}) data that are the high affinity constant from fitting with a two-site model of ligand binding due to the presence of occluded [^{3}H]-QNB binding sites (see Sections 4.2.1 and 4.2.4). pIC_{50} and affinity constant values have been corrected with the Cheng-Prusoff correction factor. The percentage of benzilylcholine high affinity sites compared to total number of binding sites were 87 ± 2 %, 82 ± 2 % and 86 ± 1% for wild-type, Tyr381Phe and Tyr381Ala, respectively. Affinity constants and pIC_{50} values (Hill coefficient: n_H, in brackets) are shown as mean ± S.E.M., from at least three separate experiments.

	Binding affinity: pIC_{50}: -Log(M) (n_H)		
	Wild-type	Tyr381Phe	Tyr381Ala
Acetylcholine	4.78 ± 0.04	3.26 ± 0.05	3.33 ± 0.18
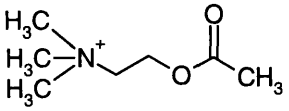	(0.85 ± 0.04)	(0.96 ± 0.10)	(1.11 ± 0.07)
ACh-reversed ester	3.92 ± 0.05	3.08 ± 0.02	3.22 ± 0.02
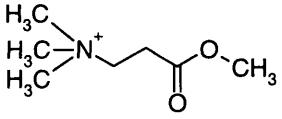	(0.91 ± 0.01)	(1.15 ± 0.03)	(1.09 ± 0.05)
ACh-$N(Et)_2$	4.37 ± 0.15	3.59 ± 0.09	3.96 ± 0.12
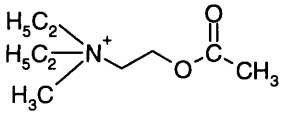	(0.88 ± 0.02)	(0.97 ± 0.12)	(1.07 ± 0.12)
Carbachol	3.87 ± 0.03	3.06 ± 0.07	3.11 ± 0.07
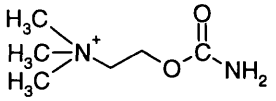	(0.85 ± 0.02)	(1.06 ± 0.05)	(1.03 ± 0.12)
Tetramethylammonium	2.90 ± 0.05	2.44 ± 0.01	2.68 ± 0.07
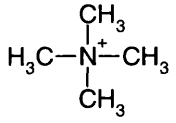	(0.98 ± 0.05)	(1.20 ± 0.19)	(0.93 ± 0.06)
Benzilylcholine	8.57 ± 0.05 [A]	8.89 ± 0.14 [A]	8.11 ± 0.02 [A]
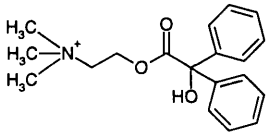			
Oxotremorine-M	4.88 ± 0.07	4.14 ± 0.03	3.76 ± 0.06
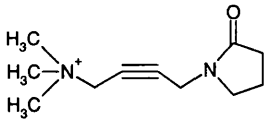	(0.84 ± 0.01)	(0.99 ± 0.05)	(1.04 ± 0.08)
Pilocarpine	5.18 ± 0.08	4.70 ± 0.01	4.07 ± 0.11
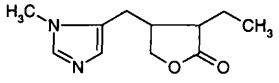	(0.96 ± 0.04)	(1.23 ± 0.06)	(1.15 ± 0.28)

Figure 4.3: The inhibition of [^{3}H]-QNB binding to wild-type and Tyr381 mutant M_1 mAChRs by ACh and benzilylcholine.

The figure shows representative plots of the inhibition of [^{3}H]-QNB binding by ACh (A) and benzilylcholine (B) to wild-type (black), Tyr381Phe (red) and Tyr381Ala (green) M_1 mAChRs transiently expressed in COS-7 cells. Assay procedures used are described in "Materials and Methods." Data are shown as mean ± S.E.M. from three replicate values. The ACh binding curves were fitted to the Hill equation whereas a two-site model of ligand binding was used for the benzilylcholine data since there seemed to be some occluded binding sites present (see Sections 4.2.1 and 4.2.4). The amount of [^{3}H]-QNB bound is expressed as a percentage of specific binding in the absence of competing ligand and has been corrected with the Cheng-Prusoff correction factor. The calculated pIC_{50} values for ACh and the high affinity constants for benzilylcholine are shown in Table 4.2.

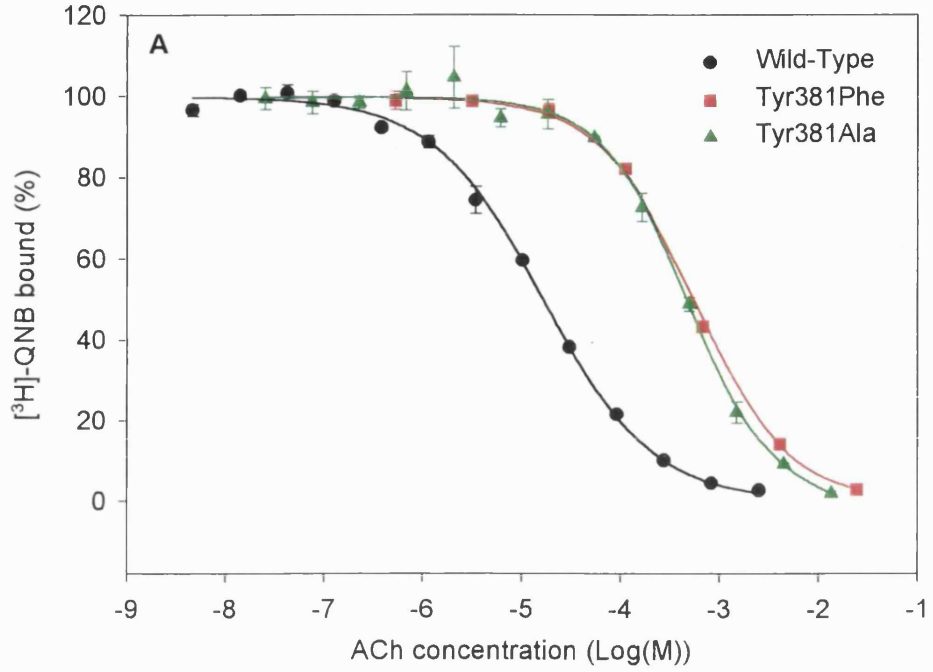
A
Wild-Type
Tyr381Phe
Tyr381Ala
[3H]-QNB bound (%)
ACh concentration (Log(M))
120
100
80
60
40
20
0
-9
-8
-7
-6
-5
-4
-3
-2
-1

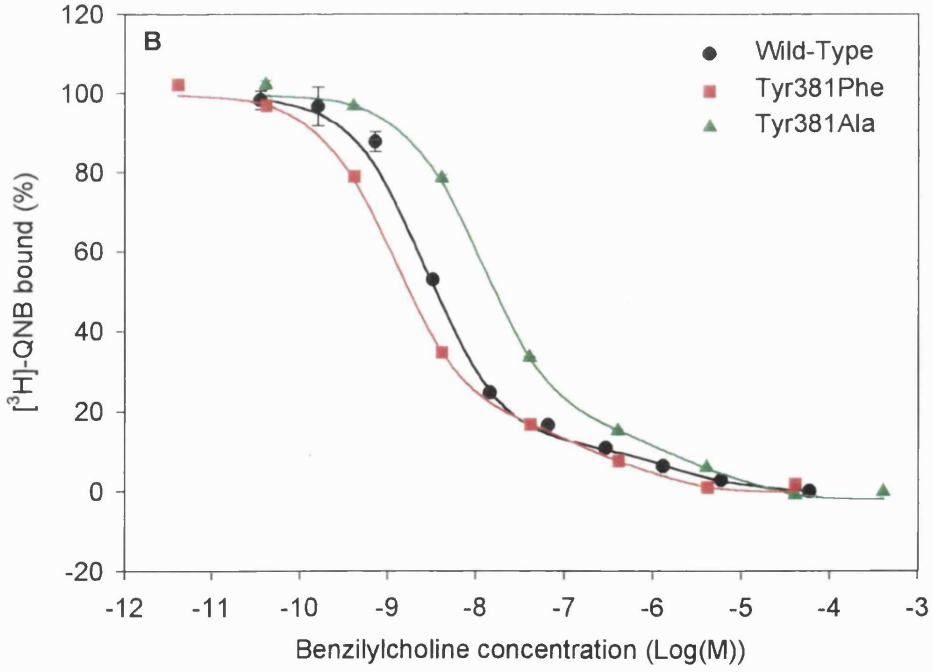
B
Wild-Type
Tyr381Phe
Tyr381Ala
[3H]-QNB bound (%)
Benzilylcholine concentration (Log(M))
120
100
80
60
40
20
0
-20
-12
-11
-10
-9
-8
-7
-6
-5
-4
-3

Initial fitting of the benzilylcholine binding data to the Hill equation gave a Hill coefficient of less than 0.8 for wild-type and both Tyr381 mutations. As already mentioned Hill coefficients of less than one are expected for agonists (see Section 3.2.3). However, benzilylcholine is an antagonist (Barlow, 1964). Inspection of the binding curves revealed two clear populations of binding site (Figure 4.3). From analysis of NMS and (-)scopolamine binding data it seemed that the low affinity population might be caused by the presence of occluded binding sites (see Section 4.2.4). Therefore, the high affinity site was used to analyse the effects of the Tyr381 mutations on benzilylcholine binding. Interestingly, the binding affinity of the antagonist benzilylcholine was increased by 2 fold ($p<0.05$) at the Tyr381Phe mutant and decreased by 3 fold ($p<0.01$) at the Tyr381Ala receptor, when compared to wild-type.

4.2.2 Binding of oxotremorine-M and pilocarpine.

The binding affinities of oxotremorine-M and pilocarpine to Tyr381Phe showed a 5 ($p<0.001$) and 3 ($p<0.05$) fold decrease, respectively, when compared to wild-type. A 10 fold reduction in their affinities, when compared to wild-type, was observed for both compounds at the Tyr381Ala mutant.

4.2.3 Binding of azanorbornane- and quinuclidine-based ligands.

The azanorbornane- and quinuclidine-based compounds (Table 4.3) generally had higher binding affinities than ACh for the wild-type M_1 mAChR. The only exception to this observation was Ac-N-Me-Quin which had a binding affinity similar to that of ACh. This compound also gave a similar response to the Tyr381 mutations, both of which reduced its affinity by ~ 4 fold ($p<0.05$ for both comparisons), when compared to the wild-type M_1 mAChR. Representative binding curves are shown in Figure 4.4.

4.2.3.1 Head-group comparisons.

The azanorbornane-based compound (L-698,583) had a 2 fold higher ($p<0.01$) binding affinity, for wild-type M_1 mAChR, when compared to the quinuclidine-based ligand with the same side-chain (L-658,903). However, the binding affinities of the two compounds were similar for the Tyr381Phe mutant (K_D ~ 1.5 μM),

Table 4.3: The binding of azanorbornane- and quinuclidine-based ligands to wild-type and Tyr381 mutant M_1 mAChRs.

Competition studies with [^{3}H]-QNB were performed on COS-7 cells transiently expressing wild-type, Tyr381Phe and Tyr381Ala M_1 mAChRs. The assay protocol is described in "Materials and Methods." Data are given as pIC_{50} values obtained by using the Hill equation, and corrected with the Cheng-Prusoff correction factor. pIC_{50} (and Hill coefficient: n_H, in brackets) are shown as mean ± S.E.M., from at least three separate experiments.

	Binding affinity: pIC_{50}: -Log(M) (n_H)		
	Wild-type	Tyr381Phe	Tyr381Ala
L-698,583 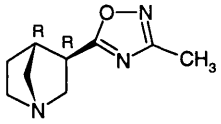	6.80 ± 0.04 (0.93 ± 0.03)	5.85 ± 0.08 (1.08 ± 0.02)	4.82 ± 0.05 (1.12 ± 0.07)
L-658,903 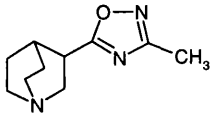	6.46 ± 0.03 (1.05 ± 0.01)	5.81 ± 0.09 (1.07 ± 0.07)	5.01 ± 0.04 (1.28 ± 0.17)
L-683,355 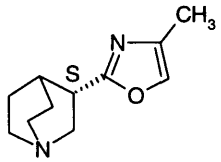	6.24 ± 0.02 (1.11 ± 0.07)	5.87 ± 0.04 (1.20 ± 0.04)	5.75 ± 0.12 (1.23 ± 0.19)
L-683,356 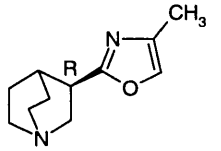	6.52 ± 0.02 (1.09 ± 0.03)	6.02 ± 0.02 (1.33 ± 0.11)	5.91 ± 0.08 (1.17 ± 0.06)
L-661,326 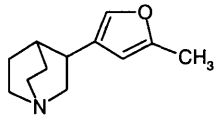	5.98 ± 0.04 (1.14 ± 0.05)	5.67 ± 0.07 (0.95 ± 0.08)	6.31 ± 0.01 (1.41 ± 0.11)
L-661,319 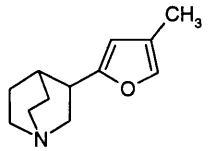	6.37 ± 0.02 (1.18 ± 0.04)	6.26 ± 0.02 (1.15 ± 0.10)	6.78 ± 0.03 (1.29 ± 0.09)
L-693,046 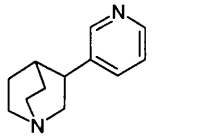	6.08 ± 0.02 (1.05 ± 0.02)	5.46 ± 0.09 (0.99 ± 0.13)	5.27 ± 0.07 (1.17 ± 0.21)
Ac-N-Me-Quin 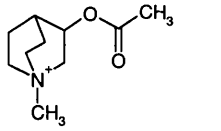	4.35 ± 0.12 (0.91 ± 0.01)	3.69 ± 0.06 (1.05 ± 0.04)	3.71 ± 0.01 (0.96 ± 0.12)

Figure 4.4: The inhibition of [^{3}H]-QNB binding to wild-type and Tyr381 mutant M_1 mAChRs by L-698,583.

The figure shows a representative plot of the inhibition of [^{3}H]-QNB binding by L-698,583 to wild-type (black), Tyr381Phe (red) and Tyr381Ala (green) M_1 mAChRs transiently expressed in COS-7 cells. Assay procedures used are described in "Materials and Methods." Data are shown as mean ± S.E.M. from three replicate values. The binding curves were fitted to the Hill equation and the corrected pIC_{50} values are shown in Table 4.3. The data is expressed as a percentage of specific [^{3}H]-QNB binding in the absence of competing ligand and has been corrected using the Cheng-Prusoff correction factor.

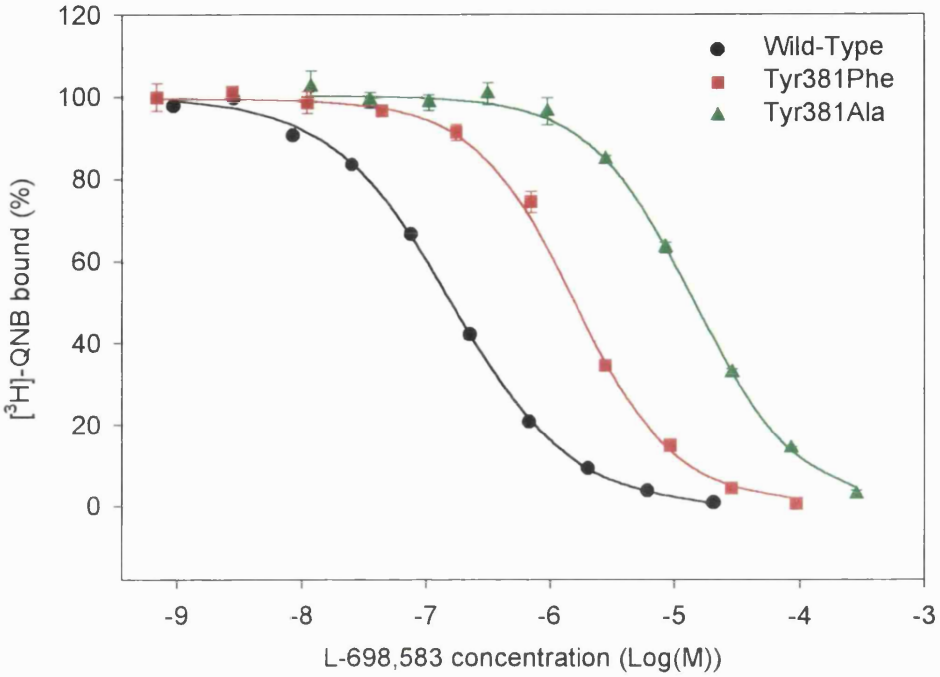
120
100
80
60
40
20
0
[3H]-QNB bound (%)
-9
-8
-7
-6
-5
-4
-3
L-698,583 concentration (Log(M))
Wild-Type
Tyr381Phe
Tyr381Ala

Figure 4.5: The effect of the Tyr381 mutations on the binding of quinuclidine-based ligands.

The figure shows the effects on the binding affinities of quinuclidine-based ligands when the Tyr381 hydroxyl group (Tyr381Phe compared to wild-type shown in red) and benzene ring (Tyr381Ala compared to Tyr381Phe shown in green) are deleted relative to the number of nitrogen atoms present in the ligand's side-chain. These results were obtained using assay procedures described in "Materials and Methods." The decrease in binding affinity was calculated from the mean pIC_{50} values obtained from at least three separate experiments and corrected with the Cheng-Prusoff correction factor.

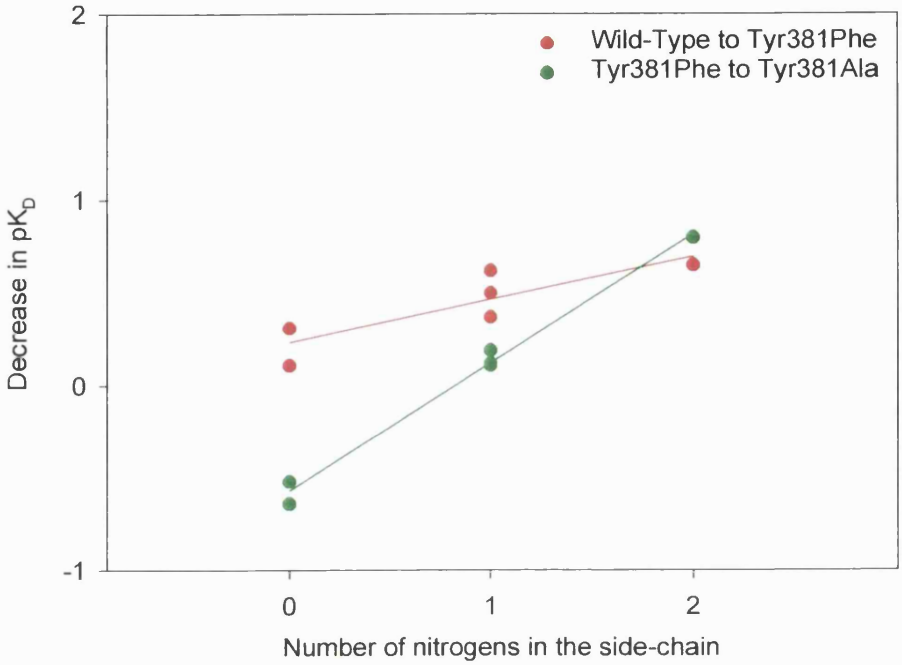
Wild-Type to Tyr381Phe
Tyr381Phe to Tyr381Ala
Decrease in pK$_D$
2
1
0
-1
0
1
2
Number of nitrogens in the side-chain

whereas L-658,903 had almost a 2 fold higher ($p<0.05$) binding affinity, when compared to L-698,583, for the Tyr381Ala mutant M_1 mAChR.

4.2.3.2 Side-chain comparisons.

If the quinuclidine-based ligands, that have varying numbers of nitrogens in the side-chain are compared, it can be seen that as the number of nitrogens decreases there is little systematic effect on the binding affinity at the wild-type receptor. The binding affinities of the compounds are all similar for the Tyr381Phe mutation (K_D ~ 1.4 μM) except for L-661,319 and L-693,046, that either have ~ 3 fold increase ($p<0.001$ for both comparisons) or ~ 2 fold decrease ($p<0.01$ for both comparisons) in binding affinity, when compared to L658,903 binding to Tyr381Phe, respectively. By comparing the binding affinities of these compounds for wild-type and Tyr381Phe receptors, i.e., the consequences of removal of Tyr381 hydroxyl group, it can be seen that there is a trend related to the number of nitrogens in the side-chain, although the effect is not large (Figure 4.5).

The ligands binding to Tyr381Ala do show a trend according to the number of nitrogens in their side-chain. As the number of nitrogens in the side-chain decreases the binding affinity of the compounds increases. If the effects of removing the benzene ring are compared by measuring the change in binding affinity between Tyr381Phe and Tyr381Ala it can be seen that the number of nitrogens in the side-chain has a major effect on the reduction measured (Figure 4.5).

The quinuclidine-based ligands with one nitrogen in the side-chain (L-683,355, L-683,356 and L-693,046) all show similar results to those obtained for ACh, i.e., the removal of the hydroxyl group (wild-type to Tyr381Phe) affects the ligand binding affinity by causing a 2 ($p<0.01$), 3 ($p<0.001$) and 4 ($p<0.01$) fold decrease, respectively, whilst removal of the benzene ring (Tyr381Phe to Tyr381Ala) does not significantly alter the ligand binding affinity.

4.2.4 Binding of atropine analogues.

The atropine-based ligands (Tables 4.4 and 4.5) allowed a number of comparisons to be made and the data obtained from analysing the binding affinity of these compounds for wild-type and Tyr381 mutant M_1 mAChRs enabled a structure-activity relationship

to be built up. Representative binding curves are shown in Figure 4.6. NMS, out of all the atropine-based compounds looked at, has the highest binding affinity for the wild-type receptor (K_D = 130 pM) and it can be seen that altering moieties in both the tropine ring and side-chain reduced this ligand binding affinity. The Tyr381 mutations also affected the binding affinities of these compounds, although a general observation can be made: the change in binding affinity observed between the wild-type and Tyr381Phe mutant, for the atropine-based ligands, tends to be smaller than the change measured between Tyr381Phe and Tyr381Ala.

Analysis of the NMS binding data by the Hill equation gave a Hill coefficient of less than 0.8 for wild-type and Tyr381Phe mutant M_1 mAChRs. Inspection of these particular binding curves revealed two populations of binding site (Figure 4.6). However, this was not observed with (-)scopolamine (the difference between the two compounds being an extra methyl group attached to the tropine-ring nitrogen causing the nitrogen to become positively charged). [^{3}H]-QNB can either be charged or uncharged depending on the protonation state of the quinuclidine nitrogen. These data suggest that there may be a population of binding sites occluded within sealed vessicles that [^{3}H]-QNB can label but NMS cannot easily access because it is incapable of existing in an uncharged state. Therefore, the NMS data was analysed using a two-site model of ligand binding (Tyr381Ala was included so that direct comparisons could be made) and the high affinity site, which accounted for at least 80 % of the total number of binding sites, used in subsequent analysis.

The benzilyltropine binding curves showed the same phenomeon so data obtained using this compound was also analysed using a two-site model of ligand binding and the high affinity constant used in data analysis. Since benzilyltropine is not constantly protonated this suggests that other structural moieties may be responsible for preventing this compound reaching the occluded binding sites.

4.2.4.1 Head-group comparisons.

Addition of the epoxide oxygen to the tropine ring enhances binding affinity at the wild-type receptor (Figure 4.7). Comparing the binding affinities of NMS to N-methylatropine, and (-)scopolamine to atropine, there is a 2 fold ratio for both cases (NMS to N-methylatropine: $p<0.05$; (-)scopolamine to atropine: $p<0.01$).

Table 4.4. The binding of atropine analogues with a quaternary nitrogen to wild-type and Tyr381 mutant M_1 mAChRs.

Competition studies with [^{3}H]-QNB were performed on COS-7 cells transiently expressing wild-type, Tyr381Phe and Tyr381Ala M_1 mAChRs. The assay was performed as described in "Materials and Methods." Data are given as pIC_{50} values obtained by using the Hill equation except for NMS (^{B}) data that are the high affinity constant from fitting with a two-site model of ligand binding due to the presence of occluded [^{3}H]-QNB binding sites (see Section 4.2.4). pIC_{50} and affinity constant values have been corrected with the Cheng-Prusoff correction factor. The percentage of NMS high affinity sites compared to total number of binding sites were 80 ± 2 %, 83 ± 2 % and 80 ± 9 % for wild-type, Tyr381Phe and Tyr381Ala, respectively. Affinity constants and pIC_{50} values (Hill coefficient: n_H, in brackets) are shown as mean ± S.E.M., from at least three separate experiments.

	Binding affinity: pIC_{50}: -Log(M) (n_H)		
	Wild-type	Tyr381Phe	Tyr381Ala
(-)*N*-Methylscopolamine 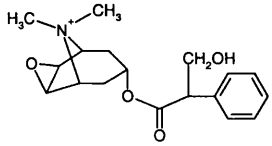	9.89 ± 0.08 [B]	9.16 ± 0.02 [B]	7.06 ± 0.12 [B]
N-Methylatropine 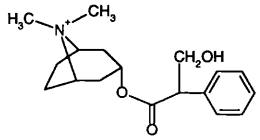	9.56 ± 0.10 (0.79 ± 0.06)	8.74 ± 0.08 (0.93 ± 0.08)	7.17 ± 0.08 (0.79 ± 0.02)
N-Methylhomatropine 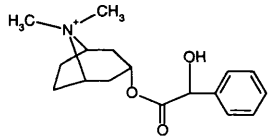	7.61 ± 0.04 (0.86 ± 0.05)	7.07 ± 0.02 (0.94 ± 0.04)	6.26 ± 0.04 (0.90 ± 0.01)
N-Methylacetyltropine 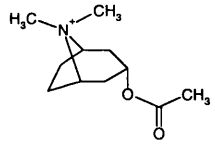	5.44 ± 0.07 (0.89 ± 0.06)	4.77 ± 0.01 (0.99 ± 0.03)	4.49 ± 0.02 (0.85 ± 0.04)

Table 4.5: The binding of atropine analogues with a tertiary nitrogen to wild-type and Tyr381 mutant M_1 mAChRs.

Competition studies with [^{3}H]-QNB were performed on COS-7 cells transiently expressing wild-type, Tyr381Phe and Tyr381Ala M_1 mAChRs. The assay protocol is described in "Materials and Methods." Data are given as pIC_{50} values obtained by using the Hill equation except for benzilyltropine (^{C}) data that are the high affinity constant from fitting with a two-site model of ligand binding due to the presence of occluded [^{3}H]-QNB binding sites (see Section 4.2.4). pIC_{50} and affinity constant values have been corrected with the Cheng-Prusoff correction factor. The percentage of benzilyltropine high affinity sites compared to total number of binding sites were 93 ± 3 %, 95 ± 4 % and 80 ± 1 % for wild-type, Tyr381Phe and Tyr381Ala, respectively. Affinity constants and pIC_{50} values (Hill coefficient: n_H, in brackets) are shown as mean ± S.E.M., from at least three separate experiments.

	Binding affinity: pIC_{50}: -Log(M) (n_H)		
	Wild-type	Tyr381Phe	Tyr381Ala
(-)Scopolamine 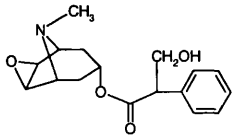	9.51 ± 0.04 (1.00 ± 0.02)	8.85 ± 0.01 (1.11 ± 0.01)	7.22 ± 0.05 (1.00 ± 0.21)
Atropine 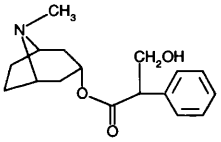	9.19 ± 0.04 (1.02 ± 0.03)	8.49 ± 0.01 (1.10 ± 0.02)	7.12 ± 0.03 (1.01 ± 0.02)
DL-Homatropine 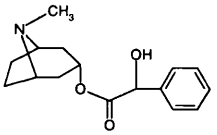	7.37 ± 0.03 (1.03 ± 0.01)	7.06 ± 0.03 (1.15 ± 0.04)	6.38 ± 0.12 (1.21 ± 0.15)
Phenylacetyltropine 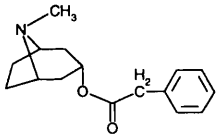	6.64 ± 0.03 (1.02 ± 0.01)	6.48 ± 0.01 (1.07 ± 0.02)	6.18 ± 0.10 (0.86 ± 0.16)
Diphenylacetyltropine 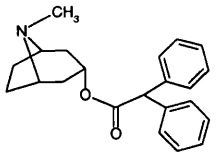	8.12 ± 0.01 (1.02 ± 0.01)	8.46 ± 0.03 (0.98 ± 0.05)	7.05 ± 0.09 (0.95 ± 0.01)
Benzilyltropine 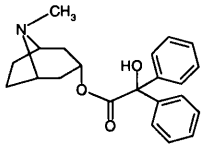	9.75 ± 0.10 [c]	10.24 ± 0.19 [c]	9.47 ± 0.13 [c]
Benztropine 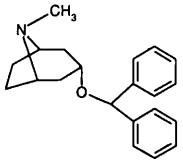	9.45 ± 0.03 (0.99 ± 0.00)	9.32 ± 0.06 (1.16 ± 0.06)	8.62 ± 0.02 (1.04 ± 0.10)

Figure 4.6: The inhibition of [^{3}H]-QNB binding to wild-type and Tyr381 mutant M_1 mAChRs by NMS and (-)scopolamine.

The figure shows representative plots of the inhibition of [^{3}H]-QNB binding by NMS (A) and (-)scopolamine (B) to wild-type (black), Tyr381Phe (red) and Tyr381Ala (green) M_1 mAChRs transiently expressed in COS-7 cells. The assay procedures used are described in "Materials and Methods." Data shown are mean ± S.E.M. from three replicate values. The NMS data were fitted to a two-site model of ligand binding and the (-)scopolamine data were fitted to the Hill equation. The bound [^{3}H]-QNB is expressed as a percentage of the specific bound [^{3}H]-QNB in the absence of a competing ligand. The data has also been corrected using the Cheng-Prusoff correction factor. The calculated pIC_{50} and affinity constants are shown in Tables 4.4 and 4.5.

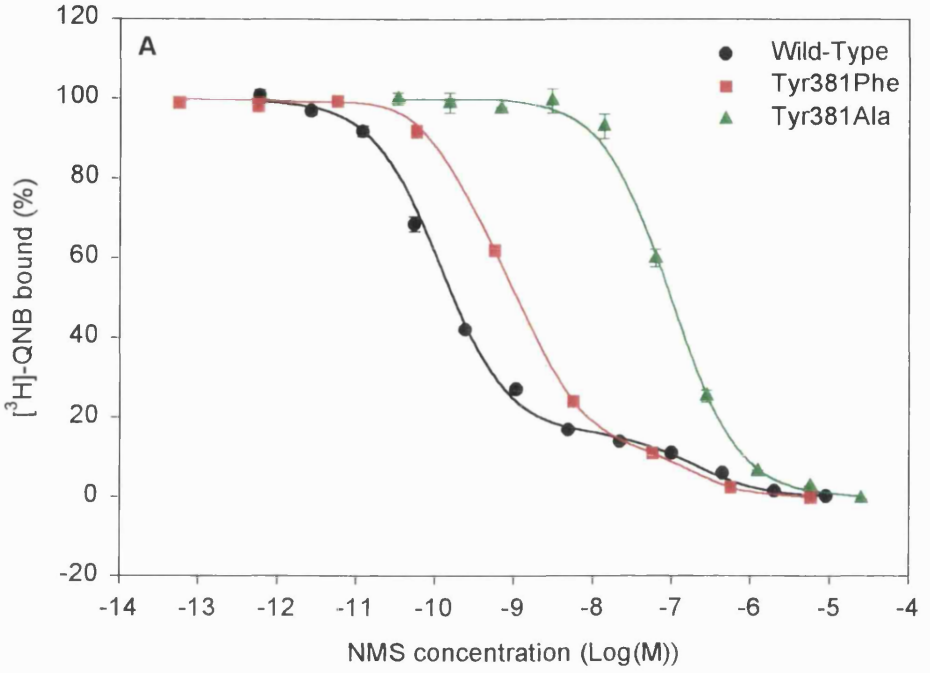
A
Wild-Type
Tyr381Phe
Tyr381Ala
[3H]-QNB bound (%)
120
100
80
60
40
20
0
-20
-14
-13
-12
-11
-10
-9
-8
-7
-6
-5
-4
NMS concentration (Log(M))

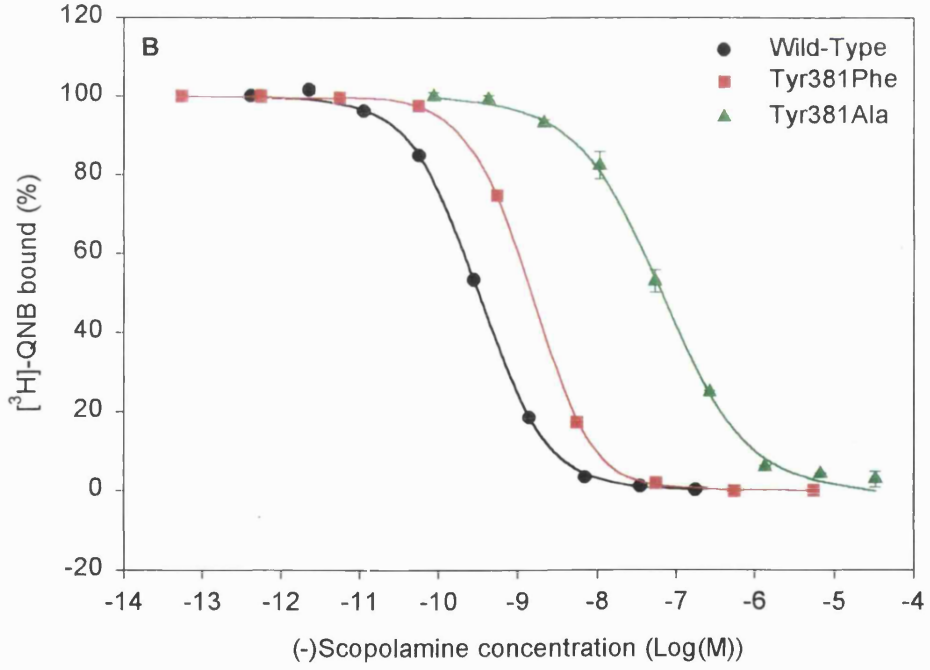
B
Wild-Type
Tyr381Phe
Tyr381Ala
[3H]-QNB bound (%)
120
100
80
60
40
20
0
-20
-14
-13
-12
-11
-10
-9
-8
-7
-6
-5
-4
(-)Scopolamine concentration (Log(M))

Figure 4.7: The effects on atropine analogues binding to wild-type and Tyr381 mutant receptors when the epoxide oxygen is removed.

The figure shows the mean binding affinities (with error bars displaying S.E.M.) of NMS and N-methylatropine (A) or (-)scopolamine and atropine (B) for wild-type, Tyr381Phe and Tyr381Ala M_1 mAChRs, from at least two separate experiments. By comparing these two sets of compounds the effect of an epoxide oxygen being present in the head-group of atropine analogues on binding to Tyr381 mutant receptors can be analysed. The assay procedure used is described in "Materials and Methods." The binding affinity data obtained were corrected with the Cheng-Prusoff correction factor.

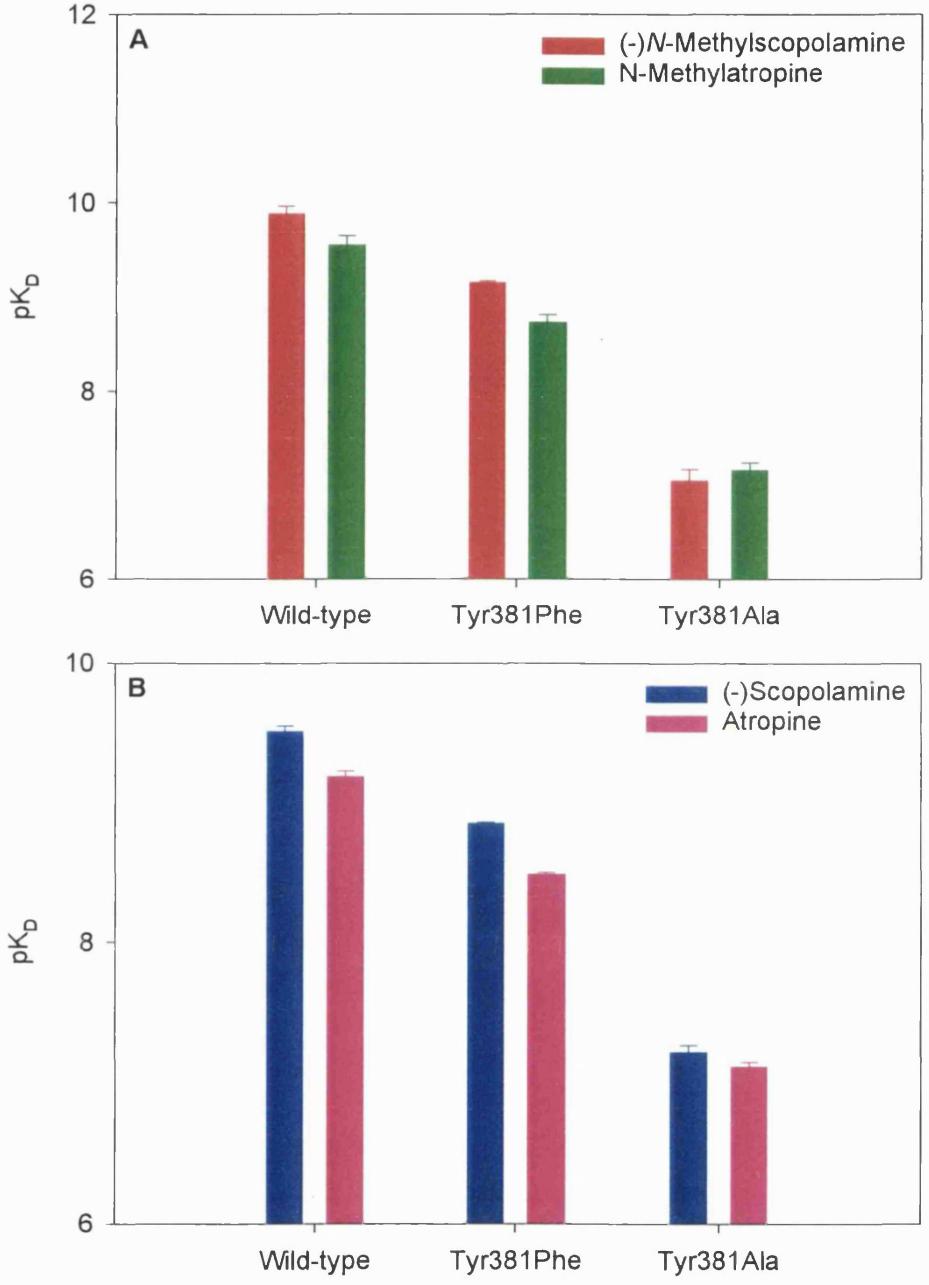
A
(-)N-Methylscopolamine
N-Methylatropine
12
10
8
6
pK_D
Wild-type
Tyr381Phe
Tyr381Ala
B
(-)Scopolamine
Atropine
10
8
6
pK_D
Wild-type
Tyr381Phe
Tyr381Ala

These two pairs of compounds also showed different affinities for the Tyr381Phe mutant receptor, although the affinity ratio was slightly reduced (NMS to N-methylatropine: $p<0.01$; (-)scopolamine to atropine: $p<0.001$). In contrast, the binding affinities of all four compounds for the Tyr381Ala M_1 mAChR are all described by a K_D of ~ 68 nM, i.e., the presence or absence of the epoxide oxygen in this subset of compounds did not affect their binding to Tyr381Ala.

The atropine-based ligands also allowed investigation of differences between the binding of antagonists containing a quaternary or a tertiary nitrogen (Figure 4.8). If the binding affinity of NMS is compared to that obtained for (-)scopolamine (both compounds containing an epoxide oxygen) it can be seen that removal of a methyl group attached to the nitrogen (quaternary to tertiary) results in a 2 fold decrease ($p<0.05$) in binding affinity for the wild-type receptor. Similar results were obtained for the comparisons between N-methylatropine and atropine ($p<0.05$), and N-methylhomatropine and homatropine ($p<0.01$), with both pairs of compounds displaying a 2 fold decrease in binding affinity for the wild-type M_1 mAChR. At the Tyr381Phe mutation, the higher affinities of the quaternary analogues were preserved in the case of atropine ($p<0.05$) and (-)scopolamine ($p<0.001$), but not homatropine. These differences were abolished by the Tyr381Ala mutation, whereas a substantial difference in binding affinity between the atropine and homatropine analogues was maintained by the Tyr381Ala mutant.

4.2.4.2 Side-chain comparisons (hydroxyl group).

The hydroxylmethyl group found on the tropic acid side-chain of NMS and other atropine-based ligands is also important for binding. If the binding of N-methylatropine is compared to N-methylhomatropine and atropine to homatropine it can be seen that the binding affinity for the wild-type receptor is reduced 89 and 66 fold (Figure 4.9), respectively, when the methylene group is removed, shortening the side-chain bearing the hydroxyl group. The Tyr381Phe mutant causes a slightly smaller change to be observed, with the change from N-methylatropine to N-methylhomatropine giving a 47 fold decrease in binding affinity and from atropine to homatropine giving a 27 fold reduction in binding affinity, when the methylene group is removed from the side-chain containing the hydroxyl group. The Tyr381Ala

Figure 4.8: The effect of a quaternary or a tertiary nitrogen present in the head-group of atropine analogues on the binding to wild-type and Tyr381 mutant receptors.

The figure shows the mean binding affinities (with error bars displaying S.E.M.) of NMS and (-)scopolamine (A), N-methylatropine and atropine (B) or N-methylhomatropine and DL-homatropine (C) for wild-type, Tyr381Phe and Tyr381Ala M_1 mAChRs, from at least two separate experiments. By comparing these three sets of compounds the effect of a tertiary or quaternary nitrogen being present in the head-group of atropine analogues on binding to Tyr381 mutant receptors can be analysed. The assay procedure used is described in "Materials and Methods." The binding affinity data obtained were corrected with the Cheng-Prusoff correction factor.

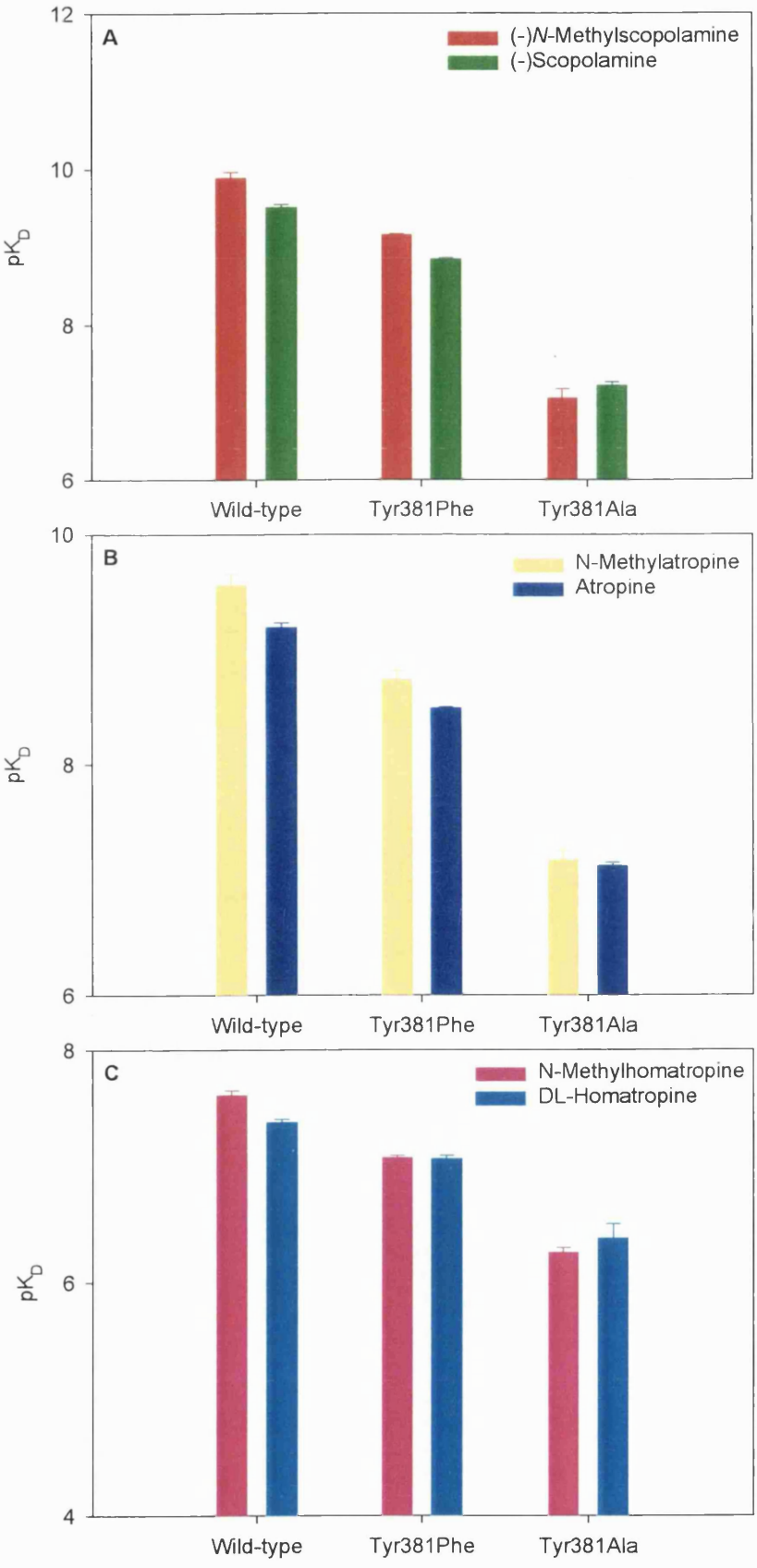
A
(-)N-Methylscopolamine
(-)Scopolamine
12
10
8
6
pK_D
Wild-type
Tyr381Phe
Tyr381Ala
B
N-Methylatropine
Atropine
10
8
6
pK_D
Wild-type
Tyr381Phe
Tyr381Ala
C
N-Methylhomatropine
DL-Homatropine
8
6
4
pK_D
Wild-type
Tyr381Phe
Tyr381Ala

Figure 4.9: The effects of altering the position/presence of the hydroxyl group present in the side-chain of atropine analogues on binding to wild-type and Tyr381 mutant receptors.

The figure shows the mean binding affinities (with error bars displaying S.E.M.) of N-methylatropine and N-methylhomatropine (A) or atropine, homatropine and phenylacetyltropine (B) for wild-type, Tyr381Phe and Tyr381Ala M_1 mAChRs, from at least two separate experiments. By comparing these two sets of compounds the effect of the presence and position of a hydroxyl group in the side-chain of atropine analogues on binding to Tyr381 mutant receptors can be analysed. The assay procedure used is described in "Materials and Methods." The binding affinity data obtained were corrected with the Cheng-Prusoff correction factor.

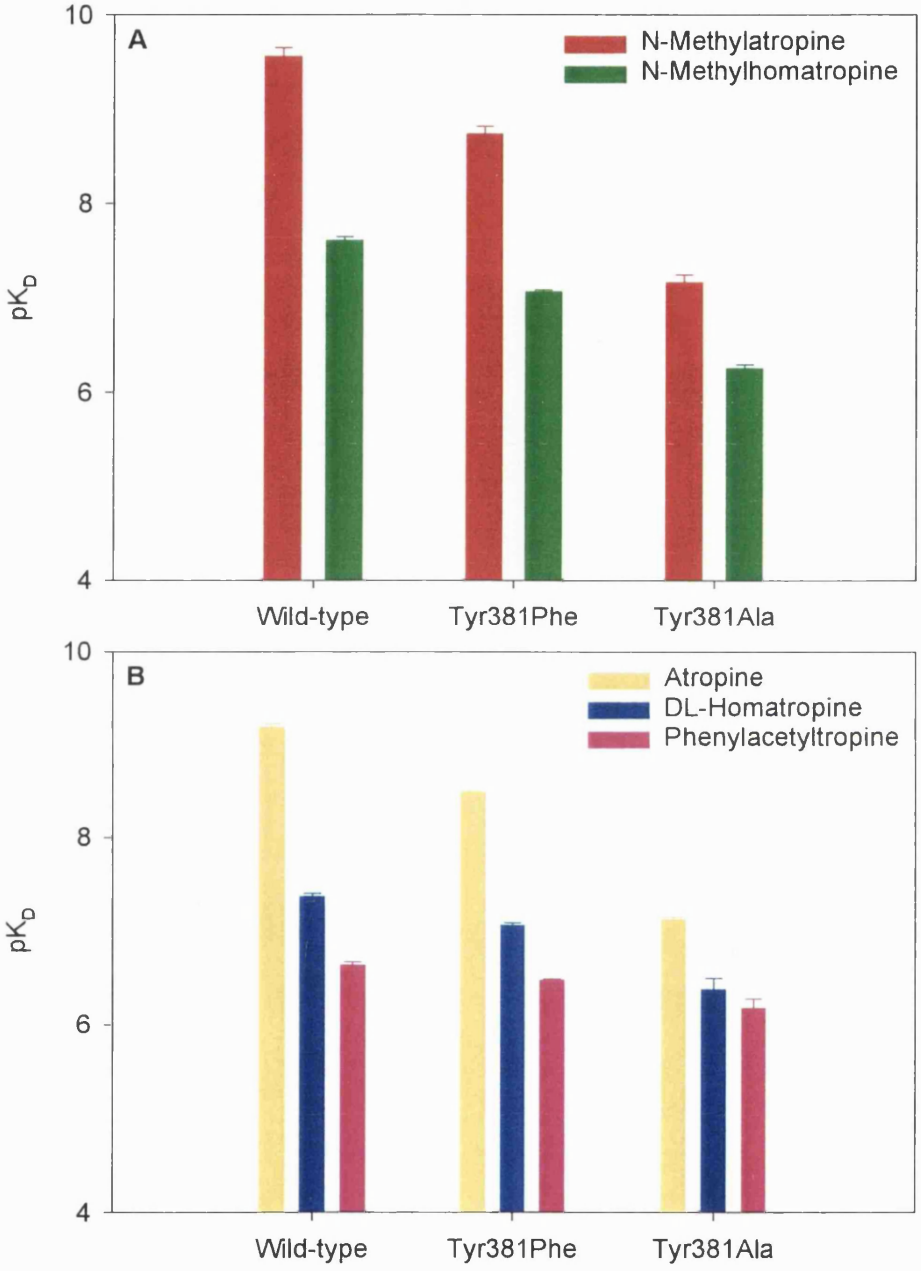
A
N-Methylatropine
N-Methylhomatropine
pK$_D$
10
8
6
4
Wild-type
Tyr381Phe
Tyr381Ala
B
Atropine
DL-Homatropine
Phenylacetyltropine
pK$_D$
10
8
6
4
Wild-type
Tyr381Phe
Tyr381Ala

receptor produces similar results, in that the differences are still seen, with N-methylatropine to N-methylhomatropine and atropine to homatropine giving a 8 ($p<0.001$) and 5 ($p<0.01$) fold reduction in binding affinity, respectively. These differences, although reduced, are still significant.

The comparison of either atropine and phenylacetyltropine or homatropine and phenylacetyltropine gives some information about what happens when the hydroxyl group is completely removed. The latter pair will be considered since in the first pair the methylene group is removed as well. At the wild-type receptor removing the hydroxyl group causes a 5 fold reduction ($p<0.001$) in the binding affinity (homatropine to phenylacetyltropine). This difference is almost identical at the Tyr381Phe mutant (4 fold; $p<0.001$) but isnot significant when binding to the Tyr381Ala M_1 mAChR.

4.2.4.3 Side-chain comparisons (benzene ring).

The presence of the benzene ring at the end of the tropic acid side-chain is necessary for high-affinity binding by atropine-based compounds. The effect of the removal of the ring, approximated by comparing the binding of phenylacetyltropine and N-methylacetyltropine (Figure 4.10), reveals a 20 fold decrease in the ligand binding affinity at the wild-type receptor. This change increased to 50 fold at both the Tyr381Phe and Tyr381Ala mutant M_1 mAChRs. In contrast, the addition of a benzene ring to the side-chain, increases ligand binding affinities (Figure 4.11). If diphenylacetyltropine is compared to phenylacetyltropine and benzilyltropine to homatropine it can be seen that the addition of an extra benzene ring increased the ligand binding affinities to the wild-type receptor by 30 and 240 fold, respectively. The Tyr381Phe mutation enlarges the differences observed between the two pairs of compounds to 100 and 1510 fold increase, whilst at the Tyr381Ala receptor, there is a 10 and 1230 fold increase.

The absolute binding affinity of diphenylacetyltropine increased by 2 fold ($p<0.01$) and decreased by 10 fold at the Tyr381Phe and Tyr381Ala M_1 mAChRs, when compared to the wild-type value (K_D of 8 nM). In contrast, benzilyltropine binding was not significantly affected by the Tyr381 mutations (wild-type and Tyr381 mutant K_Ds ~ 150 pM). The results obtained for benztropine, which has

Figure 4.10: The effects of atropine analogues binding to wild-type and Tyr381 mutant M_1 mAChRs when the side-chain benzene ring is removed.

The figure shows the mean binding affinities (with error bars displaying S.E.M.) of phenylacetyltropine and N-methylacetyltropine for wild-type, Tyr381Phe and Tyr381Ala M_1 mAChRs, from at least two separate experiments. By comparing these compounds the effect of removing the benzene ring at the terminus of the side-chain of atropine analogues on binding to Tyr381 mutant receptors can be analysed. The assay procedure used is described in "Materials and Methods." The binding affinity data obtained were corrected with the Cheng-Prusoff correction factor.

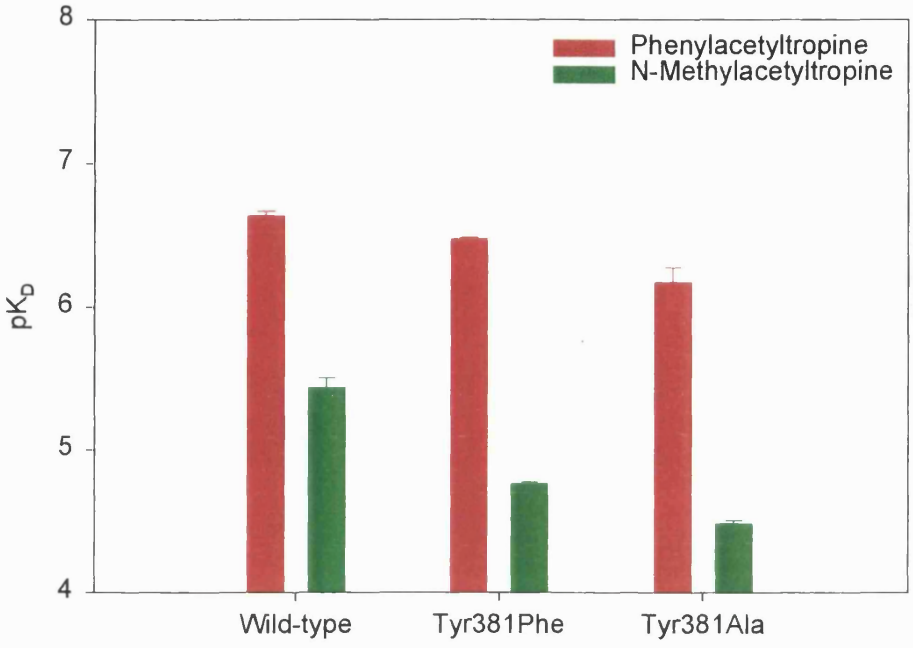
8
7
6
5
4
pK$_D$
Phenylacetyltropine
N-Methylacetyltropine
Wild-type
Tyr381Phe
Tyr381Ala

Figure 4.11: The effects on atropine analogue binding to wild-type and Tyr381 mutant M_1 mAChRs when there is an additional benzene ring attached to the side-chain.

The figure shows the mean binding affinities (with error bars displaying S.E.M.) of phenylacetyltropine and diphenylacetyltropine (A) or DL-homatropine and benzilyltropine (B) for wild-type, Tyr381Phe and Tyr381Ala M_1 mAChRs, from at least two separate experiments. By comparing these two sets of compounds the effect of adding an extra benzene ring to the side-chain of atropine analogues on binding to Tyr381 mutant receptors can be analysed. The assay procedure used is described in "Materials and Methods." The binding affinity data obtained were corrected with the Cheng-Prusoff correction factor.

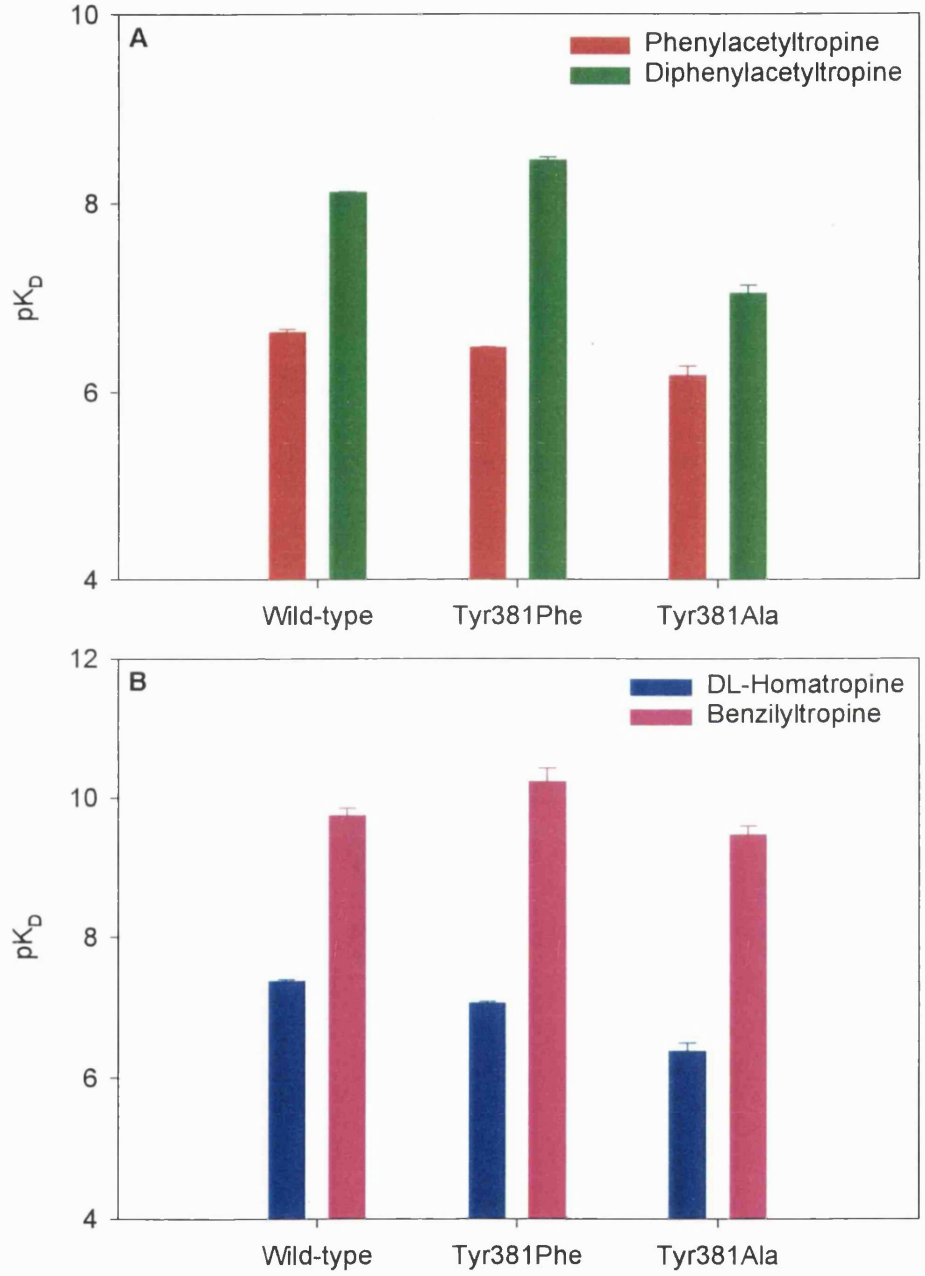
A
Phenylacetyltropine
Diphenylacetyltropine
pK$_D$
10
8
6
4
Wild-type
Tyr381Phe
Tyr381Ala
B
DL-Homatropine
Benzilyltropine
pK$_D$
12
10
8
6
4
Wild-type
Tyr381Phe
Tyr381Ala

the two benzene rings attached to the tropine ring via an ether linkage with no hydroxyl group, show that its binding affinities for wild-type and Tyr381Phe receptors are similar (K_Ds ~ 412 pM), while at the Tyr381Ala M_1 mAChR, its binding affinity is reduced 7 ($p<0.001$) fold, when compared to wild-type.

This observation of increased or unchanged affinities for binding to the Tyr381Phe mutant does not represent the general trend, i.e, the Tyr381Phe mutation causes a decrease in the binding affinity of most ligands, when compared to the binding affinity for the wild-type receptor.

4.2.5 Functional response induced by ACh analogues.

To try to get information about the role of Tyr381 in receptor activation a selection of the agonists used in the radioligand binding studies, described above, were used in phosphoinositide turnover assays. The results from these experiments are shown in Table 4.6 and Figure 4.12. Tyr381Phe and Tyr381Ala caused a 70 and 2750 fold reduction in ACh potency in the functional response, respectively, when compared to the wild-type response (EC_{50} = 102 nM), whilst both Tyr381 mutations produced a slight increase in the maximum response, measured as fold basal (Tyr381Phe: 5.5 ± 0.3 and Tyr381Ala: 5.2 ± 0.6), when compared to wild-type (4.4 ± 0.4), although, the basal measurements for each mutant were reduced (Tyr381Phe: 379 ± 30 dpm and Tyr382Ala: 332 ± 32 dpm), when compared to wild-type (475 ± 32 dpm). However, apart from Tyr381Ala basal which was significantly lower than wild-type ($p<0.05$), the basal and maximum responses caused by the Tyr381 mutant M_1 mAChRs were not statistically different from wild-type. Further analysis of these results showed that the increase in response from basal to maximum, i.e., change in dpm measured, for both Tyr381 mutations (Tyr381Phe: 1711 ± 198 dpm and Tyr381Ala: 1365 ± 78 dpm) was similar to that observed for the wild-type receptor (1593 ± 177 dpm).

The ability of two other ACh analogues (ACh-reversed ester and tetramethylammonium) to produce a function response at the wild-type and Tyr381 mutant receptor was measured. The data showed that altering the ACh structure had significant effects on the functional response produced by the wild-type receptor. ACh-reversed ester and tetramethylammonium had a 50 and 1320 fold reduction in

Table 4.6: Functional response, as measured by the phosphoinositide turnover assays, caused by ligand binding to wild-type and Tyr381 mutant M_1 mAChRs.

Phosphoinositide turnover assays were performed on COS-7 cells transiently expressing wild-type, Tyr381Phe and Tyr381Ala M_1 mAChRs. The assay procedure is described in "Materials and Methods." Results are shown as the mean ± S.E.M. of at least three experiments. [F] The response has been measured as a % of the fold basal response produced by acetylcholine at the wild-type M_1 mAChR. The maximum response produced by acetylcholine binding as measured by fold basal (and basal response) at wild-type, Tyr381Phe and Tyr381Ala were 4.4 ± 0.4 (475 ± 32 dpm), 5.5 ± 0.3 (379 ± 30 dpm) and 5.2 ± 0.6 (332 ± 32 dpm), respectively.

	Wild-type		Tyr381Phe		Tyr381Ala	
	pEC_{50}: -Log(M) (n_H)	Response [F] % ACh response	pEC_{50} (n_H)	Response [F] % ACh response	pEC_{50} (n_H)	Response [F] % ACh response
Acetylcholine	6.99 ± 0.08 (0.92 ± 0.04)	(100)	5.17 ± 0.04 (0.98 ± 0.04)	125 ± 5	3.55 ± 0.13 (0.91 ± 0.16)	118 ± 10
ACh-reversed ester	5.32 ± 0.05 (0.55 ± 0.04)	83 ± 3	3.99 ± 0.04 (0.97 ± 0.19)	86 ± 9	3.03 ± 0.02 (0.51 ± 0.02)	35 ± 0
Tetramethylammonium	3.87 ± 0.06 (1.04 ± 0.02)	85 ± 5	3.05 ± 0.02 (1.25 ± 0.26)	49 ± 6	No Measurable Response	
L-698,583	9.09 ± 0.14 (0.78 ± 0.03)	102 ± 2	7.12 ± 0.03 (1.02 ± 0.04)	126 ± 1	5.08 ± 0.06 (1.17 ± 0.10)	118 ± 1
L-658,903	7.75 ± 0.10 (0.88 ± 0.05)	89 ± 7	6.34 ± 0.05 (1.06 ± 0.19)	91 ± 15	4.32 ± 0.30 (0.98 ± 0.02)	46 ± 5

Figure 4.12: The PI response measured when ACh and L-698,583 bound to wild-type and Tyr381 mutant M_1 mAChRs.

The figure shows representative dose response curves for the functional response stimulated by ACh (A) and L-698,583 (B) binding at wild-type (black), Tyr381Phe (red) and Tyr381Ala (green) M_1 mAChRs. The data were obtained using procedures described in "Materials and Methods." The data were fitted to a four paramter logistic function. The measured pEC_{50} values are shown in Table 4.6. The PI response is shown as the dpm data (mean ± S.E.M., from three replicate values) obtained from the assay and have not been corrected.

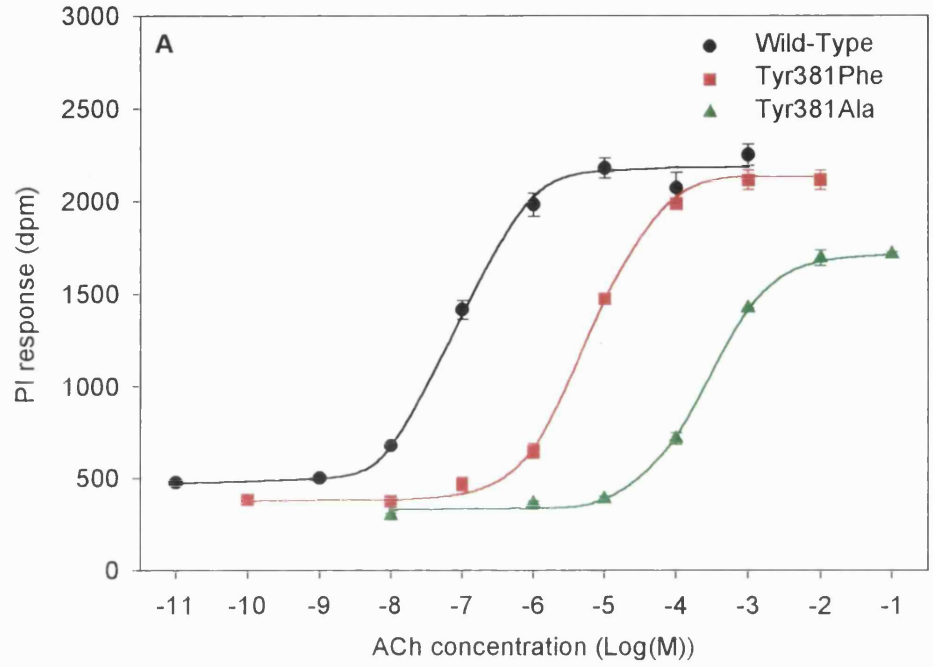
A
Wild-Type
Tyr381Phe
Tyr381Ala
PI response (dpm)
3000
2500
2000
1500
1000
500
0
-11
-10
-9
-8
-7
-6
-5
-4
-3
-2
-1
ACh concentration (Log(M))

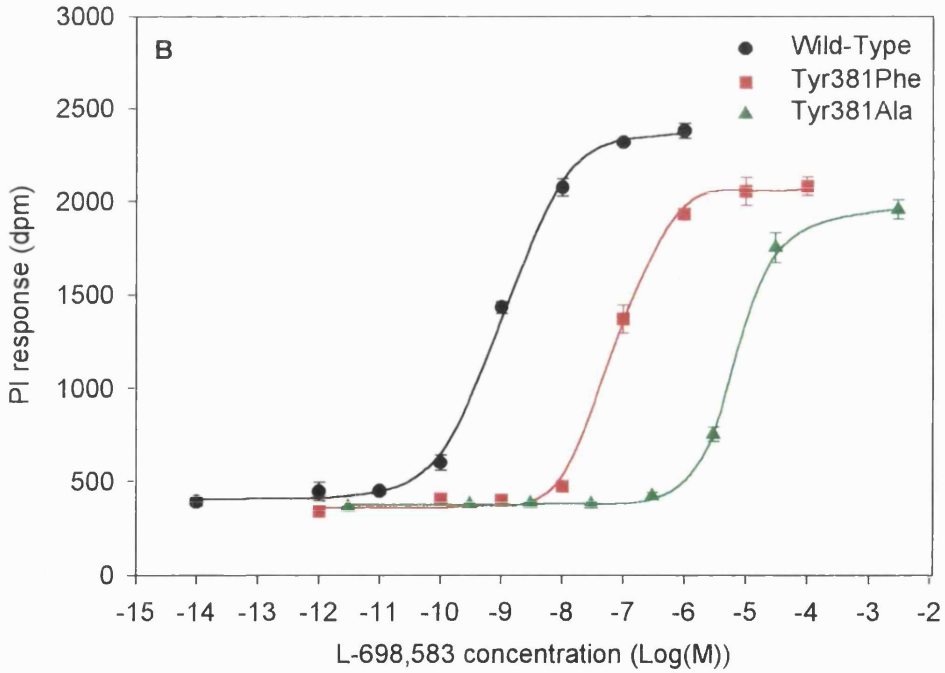
B
Wild-Type
Tyr381Phe
Tyr381Ala
PI response (dpm)
3000
2500
2000
1500
1000
500
0
-15
-14
-13
-12
-11
-10
-9
-8
-7
-6
-5
-4
-3
-2
L-698,583 concentration (Log(M))

potency and both compounds only gave maximum response of ~ 84 %, when compared to the data for ACh.

The effect of the Tyr381Phe mutation on the functional response caused by binding of ACh-reversed ester and tetramethylammonium was to produce a 20 and 7 ($p<0.001$) fold reduction in potency, when compared to wild-type. Whilst the maximum response produced by ACh-reversed ester binding to Tyr381Phe was similar to its wild-type response, tetramethylammonium showed almost a 2 fold decrease ($p<0.01$) in the maximum response produced by binding to Tyr381Phe, when compared to the wild-type receptor. A 2 fold decrease ($p<0.05$) in maximum response and 200 fold decrease in potency was observed for ACh-reversed ester activation of Tyr381Ala, when compared to the wild-type response. However, no measurable functional response was evoked by tetramethylammonium binding to the Tyr381Ala M_1 mAChR.

The Hill coefficients measured for the PI response caused by ACh-reversed ester binding to wild-type and Tyr381Ala were low (~ 0.5). The exact meaning of these values is unclear. Further investigation would be required to substantiate this phenomenon.

4.2.6 Functional response induced by azanorbornane- and quinuclidine-based ligands.

The azanorbornane-based ligand, L-698,583, and quinuclidine-based ligand, L-658,903, were also used in functional studies. L-698,583 and L-658,903, binding to the wild-type M_1 mAChR, both showed increased potencies in the functional response (130 and 6 ($p<0.001$) fold, respectively) and similar maximal responses when compared to ACh. The Tyr381Phe mutation reduced the potency of the functional response produced by L-698,583 and L-658,903 by 90 and 30 fold, respectively, although both compounds still gave a similar maximal response to that evoked by ACh binding to wild-type. The Tyr381Ala mutation had an effect on the maximal response produced by L-658,903 (reducing it to 50 % of the wild-type response), whilst L-698,583 was able to give a larger maximal response equivalent to 118 % of the wild-type ACh response ($p<0.001$). However, the potencies of L-698,583 and

Figure 4.13: The potency in the function response and efficacy of quinuclidine-based ligands at the wild-type M_1 mAChR.

The figure shows the potency in the functional response (A) and the calculated intrinsic efficacy (B) of the quinuclidine-based compounds (L-658,903; L-683,355; L-683,356; L-661,326; L-693,046) interacting with the wild-type M_1 mAChR relative to the number of nitrogen atoms present in the ligand's side-chain. The assay procedure and efficacy calculations were performed as described in "Materials and Methods." The potency in the function response is shown as pEC_{50} (linear scale) and the efficacy is shown as αK (logarithmic scale). L-661,319 did not produce a functional response, therefore the data are not shown.

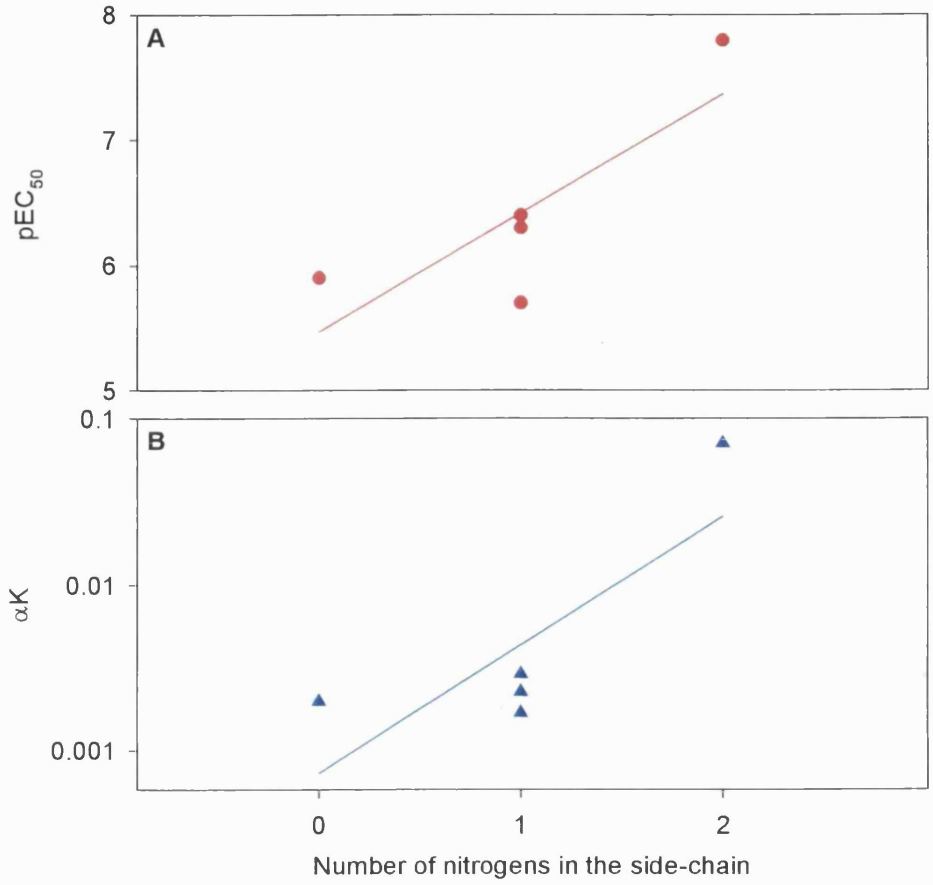
A
B
8
7
6
5
pEC50
0.1
0.01
0.001
αK
0
1
2
Number of nitrogens in the side-chain

Table 4.7: Effects on compound efficacy caused by Tyr381 mutant M_1 mAChRs.

Compound efficacy was calculated for wild-type, Tyr381Phe and Tyr381Ala M_1 mAChRs. The model used was based on the extended ternary complex model and is described in "Materials and Methods." Compound binding affinity, compound potency in the functional response and receptor expression level data were used in the calculation to obtain: $\frac{P_4}{K_{BIN}}$, which is proportional to compound signalling efficacy. A value of $\overline{K_G} = 14.1$ was used (Hulme and Lu, 1998) to estimate αK which is a true measure of compound intrinsic efficacy. The fold change decrease in compound intrinsic efficacy (αK) caused by the Tyr381 mutants, when compared to wild-type, was also calculated. Tetramethylammonium efficacy when interacting with the Tyr381Ala mutant M_1 mAChR was estimated by modelling the highest value that produced no measurable response, since no data was obtained from the phosphoinositide turnover assay.

	Signalling efficacy $\left(\frac{P_4}{K_{BIN}}\right)$			Intrinsic efficacy * (αK) (Fold change decrease from wild-type)		
	Wild-type	Tyr381Phe	Tyr381Ala	Wild-type	Tyr381Phe	Tyr381Ala
Acetylcholine	8.10	8.00	0.20	1.35	1.30 (1)	0.015 (90)
ACh-reversed ester	1.20	0.71	0.10	0.09	0.053 (2)	0.006 (15)
Tetramethylammonium	0.42	0.31	< 0.013	0.031	0.022 (1)	< 0.001 (> 31)
L-698,583	9.70	1.76	0.25	2.02	0.14 (14)	0.018 (112)
L-658,903	0.93	0.24	0.032	0.071	0.017 (4)	0.0023 (31)

* Assuming that $\overline{K_G} = 14.1$

L-658,903 were reduced by the Tyr381Ala mutation 10200 and 2700 fold, respectively, when compared to the response at the wild-type receptor.

The potency of L-658,903 in the functional response when binding to Tyr381Ala appears to be 5 fold lower than the binding affinity. This finding indicates that the results for L-658,903 may not be accurate. One possible explanation for this is that the concentrations of L-658,903 used in the phosphoinositide turnover assay were at the feasible limits. Therefore, the analysis may have given a pEC_{50} that is lower than the actual value.

Experiments (n = 1; recorded data are not shown) were carried out to measure the functional response produced by the other quinuclidine-based ligands at the wild-type receptor (L-683,355; L-683,356; L-661,326; L-661,319; L-693,046). A correlation was observed between the number of nitrogen atoms present in the ligand side-chain and potency in the functional response (Figure 4.13). All these compounds also displayed greatly reduced maximal responses (fold basal < 2), compared to the majority of the other agonists used in this study. Therefore, the ability of these compounds to be good probes for the functional response was limited so it was decided to not carry out detailed investigations on their ability to activate the Tyr381 mutants.

4.2.7 Efficacy calculations.

The data obtained from the phosphoinositide turnover experiments using wild-type and Tyr381 mutant receptors were combined with the binding affinity data to produce efficacy values. These results are shown in Table 4.7. It can be seen that both the ACh analogues and the quinuclidine, L-658,930, have lower efficacy (ACh-reversed ester: 15 fold, tetramethylammonium: 44 fold and L-658,903: 19 fold) than ACh, at the wild-type receptor. However, the azanorbornane, L-698,583, has efficacy at the wild-type receptor which is comparable to that of ACh. The other observation which can be made is that the Tyr381Ala mutation affects compound efficacy to a larger extent (> 10 fold) than Tyr381Phe, when compared to the wild-type receptor.

4.3 Discussion.

Probing the effect of mutating Tyr381 to either phenylalanine or alanine by the use of various compounds, with different structures and characteristics, has given a considerable amount of information about the role of Tyr381 in M_1 mAChR function and probably the role of the homologous tyrosine residue in the other mAChR subtypes, as well.

However, the interpretation of results from mutagenesis studies can be complicated (Shortle, 1992). Altering a residue's side-chain may have both direct effects, e.g., through altering ligand binding, and indirect effects, such as structural and/or conformational changes that may in turn cause other changes. These possibilities cannot readily be differentiated. Therefore, conclusions drawn about the role of a particular residue in protein function should be regarded as provisional, and require independent confirmation.

In this investigation, the extended ternary complex model has been used to attempt to get a better insight into the indirect effects caused by the mutations and whether they are real or not (Hulme and Lu, 1998). This model takes into account all the parameters measured for each mutation (ligand binding affinity, potency in functional response and receptor expression) to give an efficacy value. This value can be compared to the efficacy of the compound at the wild-type receptor and therefore, can be used to give a measure of the effect of the mutation on the energetics of the receptor activation process.

The process of ligand binding is also complex (Strange, 1996). Another factor that needs to be considered is that fact that protein mutations may affect the mode of interaction by ligands, i.e., if a residue involved in ligand binding is altered, this may completely rearrange the other interactions that the ligand makes (Figure 4.14). This phenomenon can limit the change in the ligand binding affinity observed, making the interpretation of the results more difficult.

The data show that Tyr381 is involved in both the stabilisation of receptor structure and in ligand binding.

Figure 4.14: Rearrangement of ligand interactions caused by receptor mutations.

A cartoon showing the potential effects of receptor mutations on the binding of ligands. When a ligand binds to the wild-type receptor specific interactions are formed and it is the nature of these interactions that are normally being investigated in mutagenesis studies. However, when the receptor is mutated and a key interaction is removed there is the possibility that the ligand can alter its mode of binding and at the extreme can form interactions with residues that do not play a key role in the binding of ligands to the wild-type receptor. Therefore, there is a possibility that incorrect conclusions will be made.

A) Wild-Type Receptor

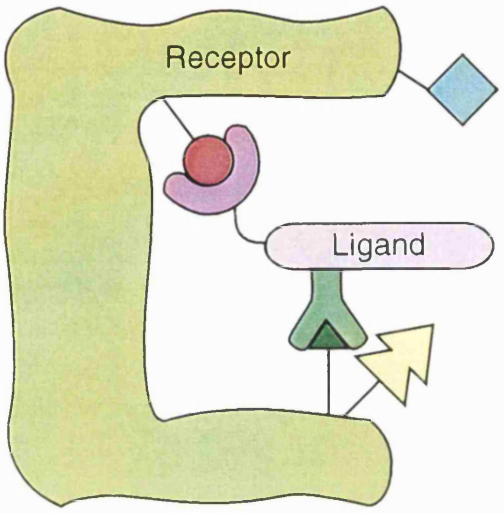

B) Mutant Receptor

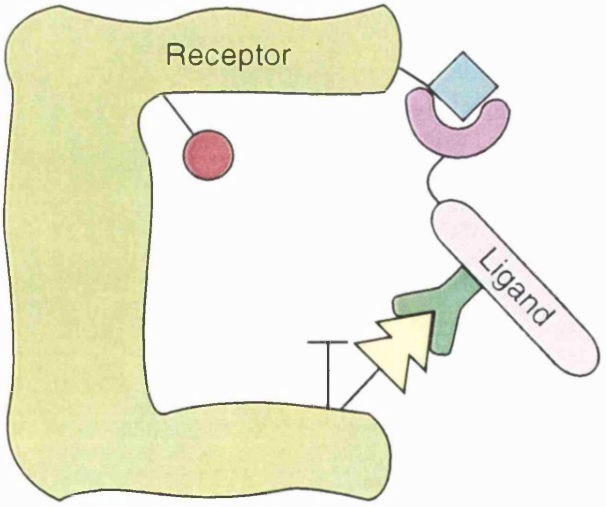

4.3.1 The role of Tyr381 in receptor structure.

The [^{3}H]-QNB binding data support the idea that Tyr381 might be making an intra-molecular interaction that is required to stabilise the receptor. The Tyr381Phe mutant causes the number of receptors able to bind [^{3}H]-QNB to decrease by half, when compared to wild-type expression. The Tyr381Ala causes a further reduction in ligand binding sites. These data indicate that apart from playing a important role in ligand binding, the Tyr381 residue may be making intra-molecular interactions to stabilise the receptor. Such intra-molecular interactions may be broken when ligands bind, although there are no data directly to support this hypothesis.

4.3.2 Interactions made by ACh and ACh analogues.

The radioligand binding experiments using ACh indicate that removal of the hydroxyl group from Tyr381 (comparison between wild-type and Tyr381Phe) has a significant effect on ACh binding in the ground state of the receptor. In contrast, the Tyr381 hydroxyl group does not affect ACh efficacy, i.e., removal of the hydroxyl group does not affect the formation of the agonist-receptor-G protein complex relative to the agonist-receptor complex alone. This implies that ACh remains in its original binding mode, and that its ability to activate the receptor is not altered by the Tyr381Phe mutation.

However, deletion of the benzene ring of Tyr381 (by comparing Tyr381Phe to Tyr381Ala) seems to cause the opposite effects when compared to removal of the hydroxyl group. The binding affinity of ACh to both Tyr381 mutants is similar whilst the ability of ACh to activate the M_1 mAChR is severely impaired by Tyr381Ala. These data support the hypothesis that the benzene ring of Tyr381 is not involved in strong binding to ACh in the ground state but does play a role in the receptor's activation process. A function of the benzene ring may be to interact with ACh and stabilise the receptor in the activated state.

Therefore, the simplest hypothesis describing a dual role carried out by the Tyr381 residues can be formulated as follows. The hydroxyl group of Tyr381 is involved in binding to ACh but does not make a further contribution to receptor activation. In contrast, the benzene ring, which is the other component making-up the tyrosine

residue side-chain, does not make a contribution to the receptor's ground state, but is critical for formation of the activated state. This hypothesis, describing how Tyr381 interacts with ACh, is supported by the other ACh analogues that also give further indications about the exact nature of interactions the Tyr381 residue is making.

ACh-reversed ester, which has the relative positions of the carbonyl- and ether-oxygens interchanged, showed reduced binding affinity, when compared to ACh at the wild-type receptor. This would suggest that residues within the M_1 mAChR make contacts with the oxygen atoms of ACh that cannot be completely satisfied by the ACh-reversed ester.

Relative to the data obtained with the wild-type M_1 mAChR, removal of the Tyr381 hydroxyl group (Tyr381Phe) decreases the binding affinity of ACh-reversed ester, although subsequent deletion of the benzene ring (Tyr381Ala) has no further effect. These data, along with the data for ACh, are consistent with the hypothesis that, in the receptor's ground state, the hydroxyl group of Tyr381 may form a hydrogen-bond interaction with one or both of the oxygens present in the ACh side-chain.

The effects of the Tyr381 mutants on ACh-reversed ester efficacy are similar to those observed for ACh, i.e., deletion of the hydroxyl group of Tyr381 has no significant effect on compound efficacy, but removal of the benzene ring does, therefore further suggesting that the benzene ring makes an interaction that is important in stabilising the receptor in its activated state.

Carbachol, which has an amide group instead of a methyl group present at the end of the side-chain, has a significantly lower affinity for the wild-type receptor, when compared to ACh. This indicates that the methyl group of ACh is probably making interaction(s) with residue(s) in the receptor's ground state. Data obtained from this laboratory have led to the proposal that the side-chain methyl group of ACh probably makes a contact with Thr192, present in TM 5 of the M_1 mAChR (Allman, *et al.*, 1997). In fact, Tyr381Phe and Tyr381Ala mutations have similar binding affinities for carbachol which are also comparable to the results obtained for ACh and ACh-reversed ester binding to the Tyr381 mutants. These data may suggest that while the hydroxyl group of Tyr381 may be involved in the orientation of the side-chain so that the methyl group of ACh can form its binding interaction, equally, that the methyl

group of ACh is important in orientating the ester function to interact with the Tyr381 hydroxyl group. Thus, the two interactions are likely to be co-operative.

Tetramethylammonium, which is the simplest ligand to activate mAChRs, was affected by the Tyr381 mutations, as measured by the radioligand binding assays, although the changes were relatively small (< 3 fold decrease when compared to wild-type). These results indicate that in the receptor's ground state, neither the hydroxyl group nor benzene ring are forming strong selective interactions with tetramethylammonium. Since tetramethylammonium lacks a side-chain with moieties able to hydrogen-bond, this observation would be expected if the Tyr381 residue interacted with the ACh side-chain, as previously described. However, since tetramethylammonium is a small ligand, it is probably able to alter its mode of interaction with the receptor. Therefore, the changes observed may not be a true reflection of how the ligand interacts with the wild-type receptor and further analysis is required with other compounds that remain in the same mode of interaction when the receptor is mutated.

The best insight obtained from the use of tetramethylammonium was to give an indication of what the benzene ring of Tyr381 may be doing. Whilst the Tyr381Phe mutant, when compared to wild-type, had little effect on tetramethylammonium efficacy the Tyr381Ala mutant reduced it greatly so that no PI response was observed. A possible explanation is that the benzene ring of Tyr381 interacts with the quaternary nitrogen of tetramethylammonium in the receptor's activated state. If so, the benzene ring may be interacting with the quaternary nitrogen found in ACh, in the M_1 mAChR's activated state. Tyrosine residues are known to be able to form cation-π interactions (Scrutton and Raine, 1996; Dougherty, 1996; Ma and Dougherty, 1997), suggesting a possible mechanism by which this interaction takes place.

The results would also suggest that there is another interaction with ACh important for formation and/or stabilisation of the receptor's activated state. This conclusion is suggested from comparing the efficacy data for ACh and ACh-reversed ester. At wild-type and both Tyr381 mutants there are differences between the efficacy values measured for the two ligands. This suggests that even the Tyr381Ala mutant is able to distinguish between the two compounds in the receptor's activated state.

Figure 4.15: Models of the interactions made between Tyr381 and ligands.

Cartoons showing the interactions Tyr381 makes with ACh and bulkier and/or more complex ligands, e.g., L-658,903, in the receptor's ground and activated state. Apart from Tyr381 residue side-chain, the conserved aspartate (Asp105) in TM 3, that has been shown to play an important role in ligand binding, is also displayed, as well as a residue, labelled X, which has been implicated by this study to play a significant function in ligand binding, although its location and type are unknown. In the receptor's ground state ACh (A) seems to form a hydrogen-bond interaction with the hydroxyl group of Tyr381 via the ester moiety present in its side-chain and there is an interaction formed between Asp105 and the positively charged head-group. In the receptor's activated state (B) these interactions are preserved and there are additional interactions formed between the benzene ring of Tyr381 and the head-group of ACh and the ester moiety and an 'unknown' residue: X. In the case of L-658,903 (C), both the Tyr381 hydroxyl group and benzene ring as well as Asp105 and residue X make interactions with the ligand in both the receptor's ground and activated states.

A) ACh: Ground State

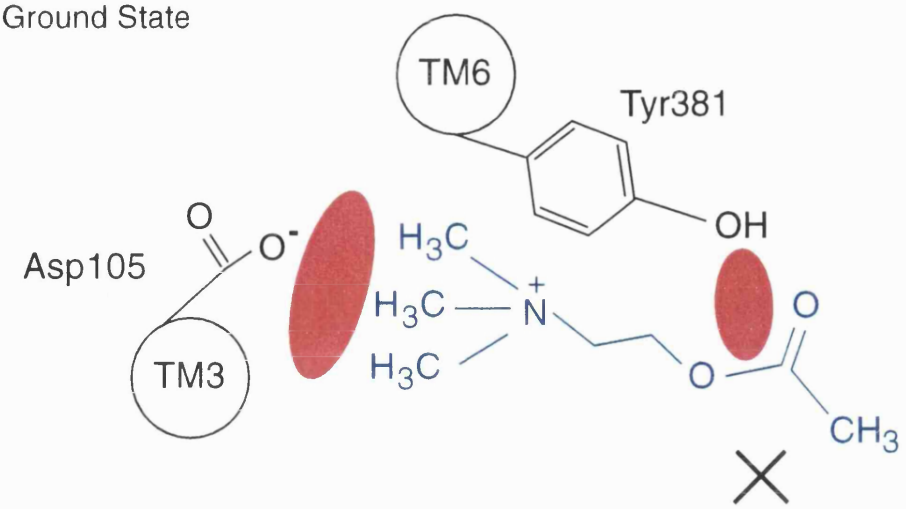

B) ACh: Activated State

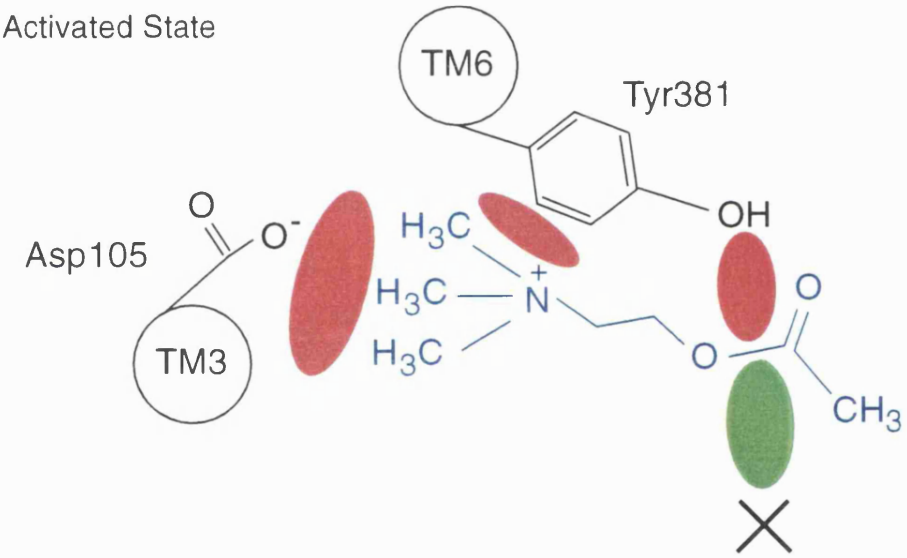

C) L-658,903:Ground and Activated State

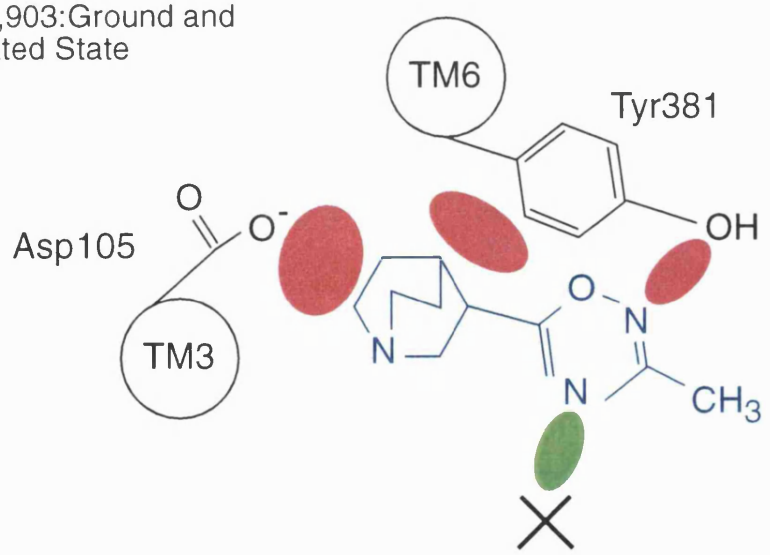

Therefore, there is probably another interaction being formed with the ester-moiety, but not with Tyr381, in the receptor's activated state, although the exact residue involved is unknown. However, this interaction does not seem to be necessary in the receptor's ground state since both ACh and ACh-reversed ester have similar binding affinities at both Tyr381 mutants.

These observations can be contrasted to data obtained with carbachol. If the efficacy values obtained for ACh and carbachol at the wild-type receptor are compared it can be seen that partial disruption of the side-chain methyl interaction does not affect the activation mechanism (Page, *et al.*, 1995). If there is a second interaction with ACh required for forming and/or stabilising the receptor's activated state it is likely to be with the ester moiety, not the terminal methyl group.

These data, obtained from the use of ACh analogues suggest a hypothesis about the function of Tyr381 (Figure 4.15). The hydroxyl group of Tyr381 may be involved in forming hydrogen-bonds with the oxygen atoms present in the ACh side-chain, in the receptor's ground state. This interaction does not seem to be essential for the actual process of receptor activation by ACh. However, the benzene ring of Tyr381 may play a role in stabilising the receptor in its activated state by forming an interaction (possibly a cation-π interaction) with the head-group (quaternary nitrogen) of ACh and also, perhaps, by helping to rearrange the three-dimensional structure of the receptor. There also seems to be another unknown interaction formed with the ester moiety, present in these ligands, in the receptor's activated state.

Benzilylcholine has a higher binding affinity for the Tyr381Phe mutant, when compared to binding to the wild-type receptor. This suggests that deletion of the Tyr381 hydroxyl group removes a constraint that then allows benzilylcholine to make a better interaction with the M_1 mAChR, i.e., benzilylcholine's mode of binding is changed. The removal of the Tyr381 benzene ring causes a decrease in benzilylcholine's binding affinity. These data suggest that benzilylcholine is interacting with the benzene ring present in the Tyr381Phe mutation, although this interaction may not occur with the wild-type receptor, i.e., the presence of the hydroxyl group may restrict the access of benzilylcholine, with its bulky side-chain, to the Tyr381 benzene ring.

The problem with the data obtained in this study from using ACh analogues, is that when the structure of ACh is altered, in most cases, the binding affinity and functional response potency are severely affected. Mutating the receptor or altering the ligand normally leads to a further decrease in affinities that can result in the ligand forming different modes of binding which can lead to problems in the analysis of the data. This phenomenon has also been noted before by this laboratory (Page, *et al.*, 1995).

To try to overcome this problem, it was decided to use ligands that have higher binding affinities than ACh to probe the Tyr381 mutants. This strategy was used to attempt to support the suggestions about the function of Tyr381 arising from the use of ACh and ACh analogues.

4.3.3 Interactions made by azanorbornane- and quinuclidine-based ligands.

The azanorbornane- and quinuclidine-based ligands show increased binding affinities and functional response potency, with respect to ACh. These compounds have greater conformational restrictions than ACh that may result in smaller unfavourable entropy/enthalpy changes when they bind to the receptor (Strange, 1996). This may be the reason for the azanorbornane- and quinuclidine-based ligand's higher affinities. The data obtained from using these ligands also gives information about the role of Tyr381 in ligand binding, although the interactions made are not completely identical to the ones made by ACh.

The azanorbornane- and quinuclidine-based ligands were designed to emulate ACh, with a head-group with a nitrogen which is able to become positively charged as a result of protonation, a side-chain with moieties able to form hydrogen-bonds, and a methyl group at its terminus. It can been seen that the ligands with one nitrogen in the side-chain, which is a good hydrogen bond acceptor, (L-683,355 and L-683,356) interact with Tyr381 in a similar way to ACh, i.e., the hydroxyl group of Tyr381 seems to interact with the ligand in the binding complex, but removal of the benzene ring has little further effect. Similar observations can be made for Ac-N-Me-Quin and L-693,046 that have quinuclidine head-groups with either a simple side-chain able to hydrogen-bond or a pyridyl ring that has one good hydrogen-bond acceptor. These data support the conclusions describing ACh binding to the M_1 mAChR in the binary complex.

The compounds that have either two nitrogens in the side-chain or none (the nitrogen atoms are strong hydrogen-bond acceptors whilst the ring oxygens are weaker) seem to display a slightly different mode of interaction. Removal of both the hydroxyl group and benzene ring of Tyr381 affects ligand binding by these compounds. However, a number of the ligands all have similar binding affinities to the Tyr381Phe M_1 mAChR (L-698,583, L-658,903, L-683,355, L-683,356 and L-661,326). If the quinuclidine-based ligands, out of this sub-series, are compared it can been seen that there is a weak correlation between the number of good hydrogen-bond acceptors in the side-chain and the difference in binding affinities between wild-type and Tyr381Phe receptors. These data suggest that the hydroxyl group of the Tyr381 residue may be forming hydrogen-bonds with the side-chain of the quinuclidine-based (and probably azanorbornane-based) ligands, although if L-698,583 is compared to L-658,903 it can be seen that the extra methylene group in the head-group also decreases the interaction made by the hydroxyl group of Tyr381.

It seems unlikely that the head-group of the quinuclidine- and azanorbornane-based ligands interact directly with the hydroxyl group of Tyr381. Instead the modified head-group interaction probably indirectly affects the contact that the hydroxyl group is making.

In contrast to ACh and its analogues, the Tyr381 benzene ring plays a significant part in the binding of the azanorbornane- and quinuclidine-based ligands, particularly the more efficacious azanorbornane derivative (L-698,583). This interaction is likely to be with the head-group. Adding a methylene moiety to the azanorbornane head-group reduces the changes in affinity when the Tyr381 benzene ring is removed.

When one of the nitrogens in the quinuclidine side-chain is removed, this results in the Tyr381 benzene ring having no net binding role in the receptor's ground state. However, complete removal of nitrogens from the ligand's side-chain results in an increase in binding affinity when the Tyr381 benzene ring is deleted, i.e., the removal now seems to take a constraint on ligand binding away.

The ligands with no nitrogens in their side-chains have greater potential to make non-polar interactions. The data so far seems to suggest that Tyr381 plays an important role in the polar binding domain. Therefore, deletion of the Tyr381 side-chain may

allow ligands that have non-polar characteristics, better access to a non-polar binding domain.

The binding affinity of [^{3}H]-QNB (which has a similar side-chain to benzilylcholine) for the Tyr381Phe mutation is increased, compared to wild-type, and for the Tyr381Ala mutation it is statistically unchanged. These data suggest that increasing the bulk and/or aromaticity of the side-chain alters the mode of binding. Removal of the Tyr381 hydroxyl group increases binding affinity, which indicates that a constraint is removed. This may allow the benzene ring to make a stronger interaction with [^{3}H]-QNB than would normally take place. Therefore, [^{3}H]-QNB does not interact with Tyr381 in the wild-type receptor. These conclusions are similar to those made for benzilylcholine binding and further support the hypothesis that moieties within the side-chain modulate Tyr381 interactions.

L-698,583 and L-658,903 were also analysed for their ability to produce a functional response. The efficacy data show, when compared to ACh efficacy at the wild-type receptor, that L-698,583 is a full agonist, whilst L-658,903 is a partial agonist. The Tyr381 mutants have slightly different effects on efficacy to the other compounds analysed, i.e., the Tyr381Phe mutant has a significant effect (< 10 fold decrease) on L-698,583 efficacy suggesting that the hydroxyl group of the Tyr381 residue does play a role in receptor activation by this compound, perhaps by orientating the compound so that it can make a stronger interaction to cause receptor activation more efficiently. Removal of the Tyr381 benzene ring has a large effect on ligand efficacy, therefore suggesting that this residue moiety is still important for receptor activation by these compounds. The effects measured for L-658,903 interacting with the Tyr381 mutants are smaller than for L-698,583. These data suggest that the extra methylene group reduces the efficiency of the receptor activation mechanism.

The two nitrogens present in the side-chain of L-698,583 and L-658,903 seem to be important for the production of a functional response since removal of either one or both nitrogens greatly reduces the functional response measured at the wild-type receptor. As mentioned before, one of the nitrogens may be interacting with the hydroxyl group of Tyr381 and it seems that the presence of two nitrogens in the side-chain is important for mediating the interaction of the ligand with the benzene ring of

Tyr381. This is especially seen with L-698,583 which has a smaller head-group than L-658,903 and may be able to gain better access to the binding domain. One hypothesis is that the second nitrogen must be making an important interaction with another 'unknown' residue to aid ligand binding and receptor activation, although the data does not suggest which nitrogen is involved in which particular interaction.

In summary, the data obtained for the azanorbornane- and quinuclidine-based ligands suggest that Tyr381 plays an important role in the binding of and subsequent receptor activation by these compounds. The results also indicate that the complete Tyr381 residue (hydroxyl group and benzene ring) plays a role in forming interactions in both the ground and activated states of the receptor. The hydroxyl group of Tyr381 seems to be forming hydrogen-bond interactions with the side-chain of these ligands and the benzene ring may be involved in forming an interaction with the ligand's head-group in the receptor's activated state. It appears that the side-chain interaction is also important for determining the nature of the head-group interaction made, and that a second side-chain interaction with an 'unknown' residue is required for efficient ligand binding and receptor activation.

4.3.4 Interactions made by oxotremorine-M and pilocarpine.

Similarly to the azanorbornane- and quinuclidine-based ligands, both the hydroxyl group and benzene ring of Tyr381 seem to make interactions with oxotremorine-M and pilocarpine in the receptor's ground state. The structures of these ligands have more binding moieties than ACh and this situation may result in these ligands having different modes of binding to that of ACh.

This illustrates one of the problems, already mentioned, that may occur when analysing data from mutagenesis studies using a variety of ligands. Different ligands may have different modes of binding depending on their structural features, therefore, a mutation in the receptor could differentially affect the binding of ligands depending on their structure. Hence the data obtained from experiments in which a range of ligands were used, may not be totally comparable.

4.3.5 Interactions made by the atropine analogues.

Since the removal of the benzene ring of Tyr381 has more effect on the binding affinities of the atropine analogues than the removal of the hydroxyl group, the benzene ring must play an important role in the binding of these compounds. Further analysis suggests that the benzene ring may form interactions with the tropine ring. Comparing compounds with different moieties attached to the tropine ring, e.g., an epoxide oxygen or a quaternary/tertiary nitrogen, there are differences in binding affinities at the wild-type receptor that are still present (to a degree) at the Tyr381Phe mutant, although, there are no differences in binding affinity measured at the Tyr381Ala mutant receptor. Therefore, the benzene ring is probably interacting close to these moieties in the tropine ring so that the differences in binding are seen. The data do not rule out the possibility of a cation-π interaction taking place between the benzene ring of Tyr381 and the nitrogen of the atropine analogues which is in the protonated form when it binds to the receptor.

However, the removal of the hydroxyl group reduces the differences observed between compounds with different head-group structures, although this mutation does not prevent the differences being seen. The hydroxyl group of Tyr381 makes an interaction that is probably not with the head-group of the atropine-based ligands. When the hydroxyl group is deleted it allows the compounds to adopt a slightly different mode of interaction which reduces the differences in ligand binding affinities measured.

Inspecting the structure of the atropine-based compounds suggests a number of potential moieties able to form hydrogen-bond interactions with the hydroxyl group of Tyr381, e.g., the hydroxymethyl group or the carbonyl- and ether-oxygens. Analysing the effect of moving the position of the hydroxyl group indicate that Tyr381 is probably not making an interaction with this moiety. The differences observed in ligand binding affinity between compounds where the hydroxyl group position has been altered still remain when binding to both Tyr381 mutant M_1 mAChRs. However, there is a change in ligand binding affinity as the position of this hydroxyl group on the side tropic acid side-chain is altered. These results suggest that the hydroxymethyl

group is interacting with a residue other than Tyr381, in the M_1 mAChR, and that this interaction is important for orientating the ligand so that it interacts with Tyr381.

Where does the hydroxyl group of Tyr381 form its interaction? From analysis of the data obtained by using N-methylacetyltropine, which simply has an acetyl group attached to the tropine ring, it can be seen that removal of the hydroxyl group has a significant effect on ligand binding. This may indicate that the hydroxyl group of Tyr381 interacts with the carbonyl- or ether-oxygen of the atropine-based ligands. However, this hypothesis requires further investigation.

The 'unknown' residue that the hydroxylmethyl group of the atropine analogues is postulated to interact with may be the same as residue X that has been proposed to be involved in the binding of the side-chains of the azanorbornane- and quinuclidine-based ligands and ACh analogues. The atropine analogues used in this part of the study may be good probes to find the extra interaction hypothesised. This will be discussed in Section 6.

In parallel to observations made with benzilylcholine and [^{3}H]-QNB, if two benzene rings are attached to the side-chain of the atropine analogues the binding affinities either increase or remain constant for the Tyr381Phe mutation, compared to wild-type. Therefore, it appears that these compounds do not make particularly strong interactions with Tyr381 in the wild-type receptor. This suggests that Tyr381 does not interact with the benzene ring(s) present in the side-chain of atropine analogues. However, removal of the Tyr381 hydroxyl group may allow the benzene ring of Tyr381 to make an interaction with these compounds, indicating that the phenyl moiety may become less constrained.

4.3.6 Summary.

This investigation has given information about the role of the Tyr381 residue in M_1 mAChR function (Figure 4.15). When binding ACh, the M_1 mAChR's natural ligand, the hydroxyl group probably forms a hydrogen-bond with the ester linkage oxygens, in the receptor's ground state. This conclusion agrees with previous investigations in which the homologous tyrosine in the M_2 and M_3 mAChRs were mutated to phenylalanine (Wess, *et al.*, 1992; Vogel, *et al.*, 1997).

In contrast, the benzene ring of Tyr381 may make contact with the head-group quaternary nitrogen of ACh, possibly by a cation-π interaction, to stabilise the receptor's activated state. This finding agrees with the modelling which suggests that the Tyr381 is involved in caging the head-group whilst it interacts with Asp105 (Trumpp-Kallmeyer, *et al.*, 1992). More complex ligands seem to bind to both the hydroxyl group and the benzene ring of Tyr381, in the receptor's ground state, and both interactions are strengthened in the receptor's activated state. However, the extra methylene group present in the quinuclidine-based ligands, when compared to the azanorbornane-based ligands, does not seem to form an interaction with Tyr381. This moiety seems to form an interaction with a residue, that is important for altering the functional response produced, whose structure and position are unknown.

Tyr381 seems to play a role in the selection of mAChR ligands to specifically bind the M_1 mAChR. As mentioned before, this tyrosine is conserved in the mAChRs whereas in other monoamine receptors the residue at the same position as Tyr381 tends to be a phenylalanine. The data would indicate that the hydroxyl group is required to specifically bind ACh through formation of a hydrogen-bond with its side-chain. In fact, the removal of Tyr381 hydroxyl group has a greater effect on ACh binding than on the binding of any other ligand used in this study.

Apart from being involved in ligand binding, Tyr381 may also make an intra-molecular interaction that stabilises the ground state structure of the receptor. This interaction is probably present even when no ligand is bound to the receptor. It may be broken during ligand binding allowing the receptor-ligand complex to form a different receptor state or conformation.

Overall, this study has given data that may also apply to the other mAChRs, although further investigations should be carried out to confirm this. Previous studies have been limited by the fact that the tyrosine has only been mutated to phenylalanine (Wess, *et al.*, 1992; Vogel, *et al.*, 1997). Therefore, only the effects of removing the hydroxyl group have been seen. This investigation has gone further by analysing the effects of mutating the tyrosine to alanine, i.e., complete removal of the functional part of the residue's side-chain. It has been shown that the conserved tyrosine residues in the

mAChRs, homologous to Tyr381 in the M_1 mAChR, play crucial roles in receptor function.

5. *The role of Asn382 in M_1 mAChR function.*

5.1 Introduction.

The data from the alanine scanning mutagenesis study, carried out on residues Tyr381 to Val387, indicated that the Asn382 residue plays a significant role in antagonist (NMS and [^{3}H]-QNB) binding and receptor stability and/or folding. Similarly to Tyr381, the asparagine is conserved in the mAChR subtypes while in the other monoamine receptors this residue tends to be a phenylalanine. Therefore, the asparagine (Asn382 in the M_1 mAChR) might be playing a role specific to the mAChRs. It was modelled as playing a key role in hydrogen-bonding to the side-chain of ACh (Hibert, *et al.*, 1991). However, the alanine scanning mutagenesis study suggested that Asn382 was not making a key interaction with ACh, nor involved in stabilising the receptor's activated state.

A study carried out on the M_3 mAChR that analysed the effect of mutating Asn507, the homologous residue to Asn382 in the M_1 mAChR, to alanine, aspartate and serine concluded that this residue is primarily involved in the binding of certain subclasses of muscarinic antagonists: 'atropine-like agents and pirenzepine' (Blüml, *et al.*, 1994). These results agree with the results of the alanine scanning mutagenesis study.

Since neither the alanine scanning mutagenesis study nor the investigation carried out on Asn507, in the M_3 mAChR, allowed any conclusions regarding the exact role of this conserved asparagine in M_1 mAChR function, it was decided to probe the Asn382 mutant with an array of ligands to try to obtain more information.

As in the Tyr381 investigation, the ligands used to probe Asn382 could be divided into three categories: ACh analogues, azanorbornane- and quinuclidine-based ligands and atropine-based compounds. The latter series was of particular interest since the data described above had suggested that the conserved asparagine had a specific role in the interaction between the receptor and the atropine-based compounds.

As previously mentioned, the Asn382Ala mutation affected both receptor expression and the binding affinities of certain ligands, which included [^{3}H]-QNB and [^{3}H]-NMS. This prevented radioligand binding experiments from being carried out.

Therefore, the Asn382Ala mutation was combined with the third intracellular loop deletion mutation (dLoop) to try to increase the expression of this mutant and enable radioligand binding experiments to be performed. The data from the alanine scanning mutagenesis study showed that the dLoop mutation did increase receptor expression and that this allowed radioligand binding experiments to be carried out.

An investigation that has used the dLoop mutant has shown that this mutation does not affect ligand binding affinities but does cause a reduction in the functional potency of agonists (Lu, *et al.*, 1997). Since the Asn382Ala-dLoop M_1 mAChR was used instead of Asn382Ala to perform binding experiments, functional studies were also performed to ensure that the dLoop mutation did not affect the affinity of atropine for the Asn382Ala mutant.

5.2 Results.

This investigation into the role of Asn382 is at a preliminary stage. Most of the data are from an initial screen using a variety of ligands and the majority of the results are from each ligand being used in one experiment only. Therefore, the analysis should be viewed with this in mind and any observations or conclusions need to be confirmed by further experimentation.

Since the majority of the results obtained for the binding affinities of ligands for dLoop were each obtained from one experiment, a comparison between ligand binding affinities for dLoop and wild-type was carried out. The majority of wild-type data were obtained during the Tyr381 study and each ligand binding affinity was determined from at least two separate experiments. The only exception to this rule was methylfurmethide, where the ligand binding affinities for wild-type, dLoop and Asn382Ala-dLoop were obtained from one experiment for each receptor. The results showed that the binding affinities obtained by using the dLoop M_1 mAChR are similar, if not identical, to the binding affinities of each ligand for the wild-type receptor (Tables 5.1, 5.2, 5.3, 5.4 and 5.5). Representative plots are shown in Figures 5.1, 5.2, 5.3 and 5.4.

Table 5.1: The binding of [^{3}H]-QNB to wild-type, dLoop and Asn382Ala-dLoop M_1 mAChRs.

Radioligand binding assays were carried out on COS-7 cells transiently expressing the wild-type, dLoop and Asn382Ala-dLoop M_1 mAChRs. Assays were performed and direct binding of [^{3}H]-QNB measured as described in "Materials and Methods." Results are shown as the mean ± S.E.M. of at least three experiments. The expression levels of the wild-type and mutant receptors are shown relative to a wild-type control included in each transfection. Expression of the wild-type receptor is 1.24 ± 0.36 pmol/mg protein when measured by [^{3}H]-QNB binding. The decrease in pK_D between dLoop and the Asn382Ala-dLoop mutation is also shown. t-test vs. wild-type value: ** $p < 0.01$; *** $p < 0.001$.

Figure 5.1: The binding of [^{3}H]-QNB to wild-type, dLoop and Asn382Ala-dLoop M_1 mAChRs.

The figure shows representative plots of specific binding of [^{3}H]-QNB to wild-type (black), dLoop (red) and Asn382Ala-dLoop (green) receptors transiently expressed in COS-7 cells. The assay procedures are described in "Materials and Methods." [^{3}H]-QNB binding is expressed as pmol/mg protein and data points are the mean ± S.E.M. of three replicate values. The calculated pK_D values are shown in Table 5.1.

	pK$_D$: -Log(M) (Expression: % wild-type)			
	Wild-type	dLoop	Asn382Ala-dLoop	ΔpK$_D$ decrease
[^{3}H]-Quinuclidinylbenzilate 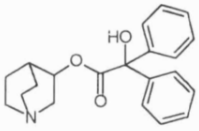	10.80 ± 0.11 (100)	10.85 ± 0.05 (162 ± 10)**	8.86 ± 0.02 *** (128 ± 3)***	1.99

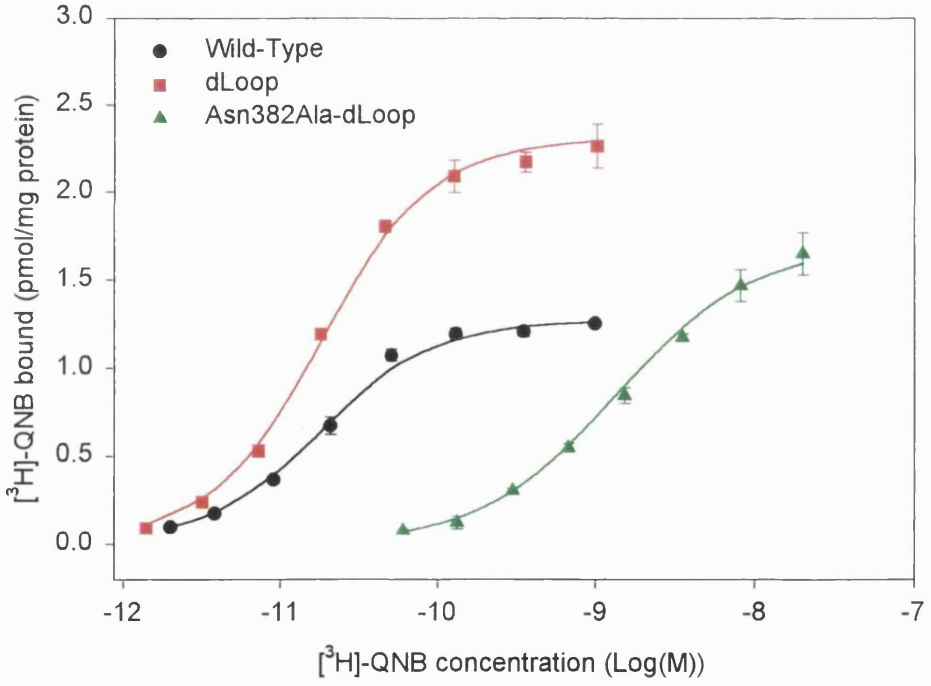

Table 5.2: Characterisation of Asn382 by measuring the binding of ACh analogues and other ligands to Asn382Ala-dLoop, dLoop and wild-type M_1 mAChRs.

Competition studies with [^{3}H]-QNB were performed on COS-7 cells transiently expressing wild-type, dLoop and Asn382Ala-dLoop M_1 mAChRs. The assay protocol is described in "Materials and Methods." Data are expressed as pIC_{50} values obtained by using the Hill equation except for benzilylcholine (^{A}) data for wild-type and dLoop M_1 mAChRs that are the high affinity constant from fitting with a two-site model of ligand binding due to the presence of occluded [^{3}H]-QNB binding sites (see Sections 4.2.1 and 4.2.4). pIC_{50} and affinity constant values have been corrected with the Cheng-Prusoff correction factor. The percentage of benzilylcholine high affinity sites compared to the total number of binding sites were 87 ± 2 % and 85 % for wild-type and dLoop, respectively. Affinity constants and pIC_{50} values (and Hill coefficient: n_H, in brackets) are shown as mean ± S.E.M. (when more than two experiments were carried out). The data obtained using wild-type M_1 mAChR are from at least three experiments (except for methylfurmethide which was only used once). The results measuring ligand binding to dLoop and Asn382Ala-dLoop are from single experiments with the exception of the ACh binding data that are from at least three separate experiments. The decrease in pIC_{50} between dLoop and Asn382Ala-dLoop is also shown.

	Binding affinity: pIC_{50}: -Log(M) (n_H)			
	Wild-type	dLoop	Asn382Ala-dLoop	ΔpIC_{50} decrease
Acetylcholine 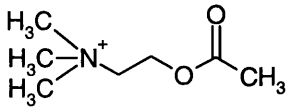	4.78 ± 0.04 (0.85 ± 0.04)	4.85 ± 0.05 (0.88 ± 0.01)	4.14 ± 0.05 (0.97 ± 0.10)	0.71
ACh-reversed ester 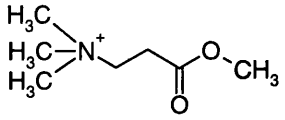	3.92 ± 0.05 (0.91 ± 0.01)	4.09 (0.97)	2.81 (0.82)	1.28
Carbachol 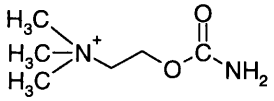	3.87 ± 0.03 (0.85 ± 0.02)	4.12 (0.81)	3.59 (1.42)	0.53
Tetramethylammonium 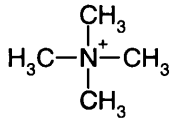	2.90 ± 0.05 (0.98 ± 0.05)	2.89 (1.05)	2.09 (1.35)	0.80
Benzilylcholine 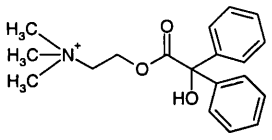	8.57 ± 0.05 [A]	8.45 [A]	7.35 (0.66)	1.10
Oxotremorine-M 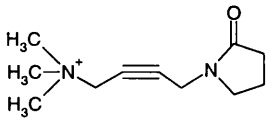	4.88 ± 0.07 (0.84 ± 0.01)	5.16 (0.95)	2.40 (0.45)	2.76
Methylfurmethide 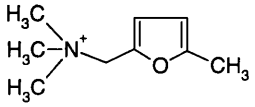	4.93 (0.93)	4.96 (0.96)	4.00 (1.29)	0.96
Pilocarpine 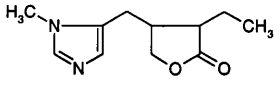	5.18 ± 0.08 (0.96 ± 0.04)	5.39 (1.03)	3.69 (0.61)	1.70

Figure 5.2: The inhibition of [^{3}H]-QNB binding to dLoop and Asn382Ala-dLoop M_1 mAChRs by ACh and pilocarpine.

The figure shows representative plots of the inhibition of [^{3}H]-QNB binding by ACh (A) and pilocarpine (B) at the dLoop (black) and Asn382Ala-dLoop (red) receptors transiently expressed in COS-7 cells. The assay procedures used are described in "Materials and Methods." The data are expressed as mean ± S.E.M. of three replicate values and are expressed as a percentage of [^{3}H]-QNB specific binding in the absence of competing ligand. The data have also been corrected with the Cheng-Prusoff correction factor. The corrected pIC_{50} values are shown in Table 5.2.

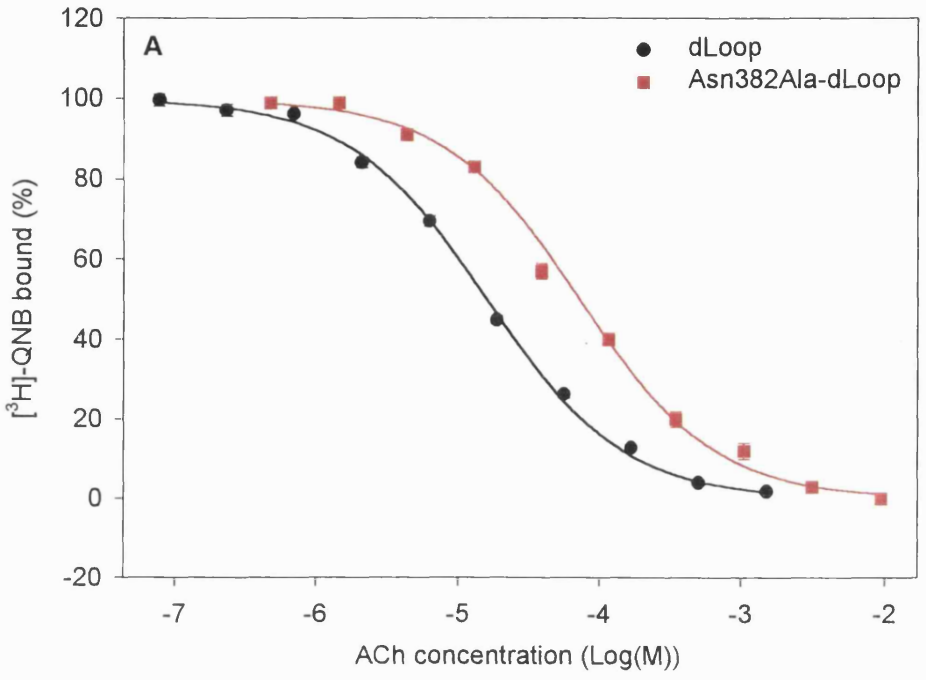
A
dLoop
Asn382Ala-dLoop
120
100
80
60
40
20
0
-20
[3H]-QNB bound (%)
-7
-6
-5
-4
-3
-2
ACh concentration (Log(M))

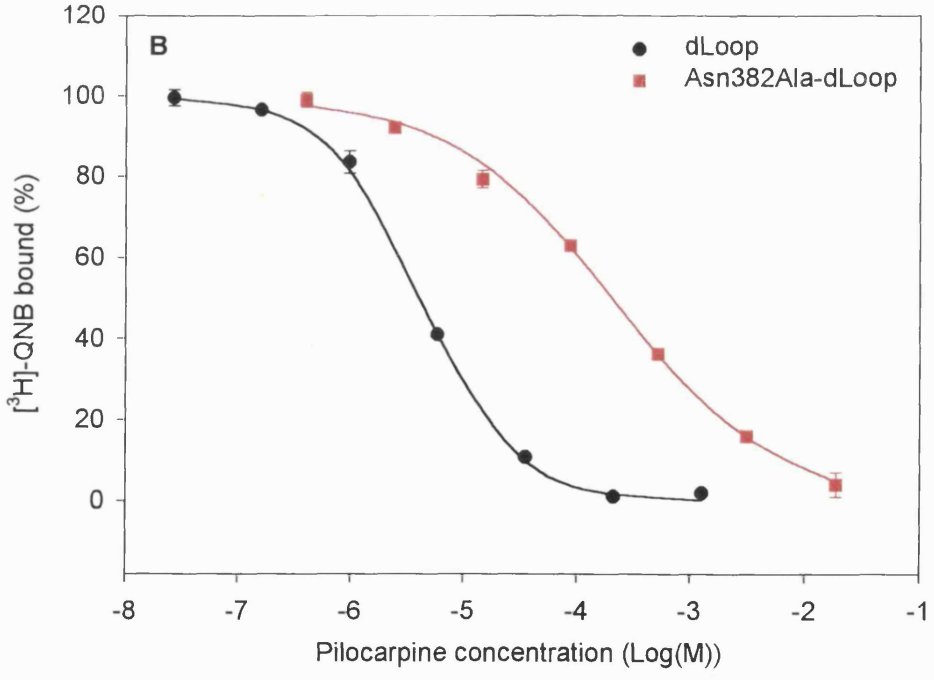
B
dLoop
Asn382Ala-dLoop
120
100
80
60
40
20
0
[3H]-QNB bound (%)
-8
-7
-6
-5
-4
-3
-2
-1
Pilocarpine concentration (Log(M))

5.2.1 Binding of ACh analogues.

The effects of the Asn382Ala-dLoop mutant on the binding of ACh-like compounds was measured (Table 5.2). Representative binding curves are shown in Figure 5.2. As already discussed, the Asn382Ala-dLoop mutant had a 5 fold affect on the binding affinity of ACh, when compared to dLoop (see Section 3). Similar decreases, caused by the Asn382Ala-dLoop mutant when compared to dLoop, were observed for carbachol and tetramethylammonium binding affinities (3 and 6 fold reductions, respectively). However, ACh-reversed ester binding affinity was affected 20 fold by the Asn382Ala-dLoop mutant, when compared to dLoop M_1 mAChR.

ACh-reversed ester, carbachol and tetramethylammonium all had lower binding affinities than ACh for dLoop (6 fold, 5 fold and 90 fold, respectively). Other ligands (methylfurmethide, oxotremorine-M and pilocarpine) had similar binding affinities to ACh for dLoop (K_D ~ 10 μM). In the dLoop background, the Asn382Ala mutation caused the binding affinities of these compounds to be decreased by 10, 580 and 50 fold, respectively. The binding affinity of benzilylcholine was 3980 fold higher than that of ACh but was only reduced 10 fold by the Asn382Ala mutation.

Interestingly, if the binding affinities of the compounds with a quaternary nitrogen moiety are ranked it can be seen that the order of potency at the Asn382Ala-dLoop (benzilylcholine > ACh ~ methylfurmethide > carbachol > ACh-reversed ester > oxotremorine-M > tetramethammonium) is similar to that at the dLoop mutant (benzilylcholine > oxotremorine-M ~ methylfurmethide ~ ACh > carbachol ~ ACh-reversed ester > tetramethylammonium), with the single exception of oxotremorine-M which undergoes a very large decrease in affinity.

5.2.2 Binding of azanorbornane- and quinuclidine-based ligands.

The azanorbornane- and quinuclidine-based compounds (Table 5.3) had higher binding affinities than ACh for the dLoop M_1 mAChR (L-698,583: 120 fold; L-658,903: 30 fold; L-661,319: 30 fold). However, the Asn382Ala-dLoop mutation, when compared to binding to dLoop, had little or no effect on ligand binding affinities (the binding affinity of L-661,319 was affected by a 2 fold reduction). However, the

Table 5.3: The binding of azanorbornane- and quinuclidine-based ligands to wild-type, dLoop and Asn382Ala-dLoop M_1 mAChRs.

Competition studies with [^{3}H]-QNB were performed on COS-7 cells transiently expressing wild-type, dLoop and Asn382Ala-dLoop M_1 mAChRs. The assay protocol is described in "Materials and Methods." The data are expressed as pIC_{50} values obtained by using the Hill equation and corrected with the Cheng-Prusoff correction factor. pIC_{50} (and Hill coefficient: n_H, in brackets) are shown as mean ± S.E.M. (when more than two experiments were carried out). The data obtained for ligand binding to wild-type M_1 mAChR are from at least three experiments, whilst the results for ligands binding to dLoop and Asn382Ala-dLoop are from single experiments. The decrease in pIC_{50} between dLoop and Asn382Ala-dLoop is also shown.

	Binding affinity: pIC_{50}: -Log(M) (n_H)			
	Wild-type	dLoop	Asn382Ala-dLoop	ΔpIC_{50} decrease
L-698,583 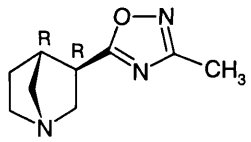	6.80 ± 0.04 (0.93 ± 0.03)	6.94 (0.91)	7.01 (0.78)	-0.07
L-658,903 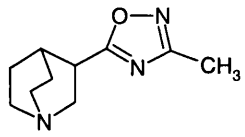	6.46 ± 0.03 (1.05 ± 0.01)	6.38 (1.06)	6.47 (0.71)	-0.09
L-661,319 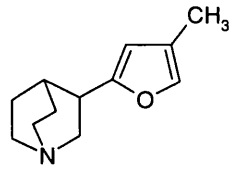	6.37 ± 0.02 (1.18 ± 0.04)	6.24 (1.17)	6.02 (1.49)	0.22

binding affinity of [^{3}H]-QNB, which is also a quinuclidine-based compound, was reduced 100 fold by the Asn382Ala-dLoop mutant (Table 5.1).

5.2.3 Binding of atropine analogues.

The atropine analogues, had higher binding affinities than ACh for dLoop (Tables 5.4 and 5.5). However, these compounds were all significantly affected by the Asn382Ala-dLoop mutation. All compounds showed a > 160 fold reduction. If the ligands were placed in rank order of their binding affinities it can be seen that Asn382Ala-dLoop mutant, when compared to dLoop, changed the relative positions of benztropine and diphenylacetyltropine (dLoop: benzilyltropine ~ NMS > N-methylatropine ~ (-)scopolamine ~ benztropine > atropine > diphenylacetyltropine > N-methylhomatropine > homatropine > phenylacetyltropine > N-methylacetyltropine; Asn382Ala-dLoop: benzilyltropine > NMS ~ atropine ~ N-methylatropine ~ (-)scopolamine > benztropine > N-methylhomatropine ~ homatropine > diphenylacetyltropine > phenylacetyltropine).

Apart from making comparisons involving all the ligands, like the Tyr381 investigation, a number of specific comparisons can be made with the atropine-like ligands. Representative binding curves are shown in Figure 5.3.

5.2.3.1 Head-group comparisons.

In general the changes in antagonist affinities caused by alterations in head-group structure are relatively small. The Asn382Ala data are not complete enough to allow the detection of subtle changes. However, there are no strong indications of a change in the head-group structure-activity-relationship of the atropine analogues.

5.2.3.2 Side-chain comparisons (hydroxyl group).

The position and presence of the hydroxyl group present on the tropic acid side-chain was also shown to important for binding of the atropine-like ligands to the M_1 mAChR. Manipulating the ligand's side-chain hydroxyl group causes larger affinity changes. Comparing the binding affinities of either N-methylatropine and N-methylhomatropine or atropine and homatropine it could be seen that shortening the

Table 5.4. The binding of atropine analogues with a quaternary nitrogen to wild-type, dLoop and Asn382Ala-dLoop M_1 mAChRs.

Competition studies with [^{3}H]-QNB were performed on COS-7 cells transiently expressing wild-type, dLoop and Asn382Ala-dLoop M_1 mAChRs. The assay protocol is described in "Materials and Methods." The data are expressed as pIC_{50} values that were obtained by using the Hill equation except for NMS (^{B}) data for wild-type and dLoop M_1 mAChRs that are the high affinity constant from fitting with a two-site model of ligand binding due to the presence of occluded [^{3}H]-QNB binding sites (see Section 4.2.4). pIC_{50} and affinity constant values have been corrected with the Cheng-Prusoff correction factor. The percentage of NMS high affinity sites compared to the total number of binding sites were 80 ± 2 % and 84 ± 1 % for wild-type and dLoop, respectively. Affinity constants and pIC_{50} (and Hill coefficient: n_H, in brackets) are shown as mean ± S.E.M. for ligand binding to wild-type M_1 mAChR and NMS binding to dLoop and Asn382Ala-dLoop, from at least three separate experiments. Other ligand binding data are shown as mean ± range, from two separate experiments (except N-methylacetyltropine binding to dLoop and Asn382Ala-dLoop that was only measured once). There was no measurable binding (N.M.B.) of N-methylacetyltropine to Asn382Ala-dLoop. The decrease in pIC_{50} between dLoop and Asn382Ala-dLoop is also shown (except for N-methylacetyltropine where a value could not be calculated).

	Binding affinity: pIC_{50}: -Log(M) (n_H)			
	Wild-type	dLoop	Asn382Ala-dLoop	ΔpIC_{50} decrease
(-)*N*-Methylscopolamine 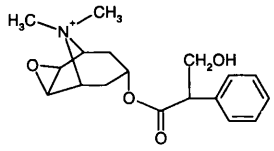	9.89 ± 0.08 [B]	9.90 ± 0.01 [B]	6.56 ± 0.12 (0.63 ± 0.01)	3.34
N-Methylatropine 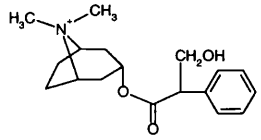	9.56 ± 0.15 (0.79 ± 0.06)	9.53 ± 0.06 (0.92 ± 0.02)	6.21 ± 0.26 (0.45 ± 0.09)	3.32
N-Methylhomatropine 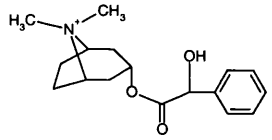	7.61 ± 0.04 (0.86 ± 0.05)	7.49 ± 0.02 (0.93 ± 0.03)	5.20 ± 0.02 (0.44 ± 0.11)	2.29
N-Methylacetyltropine 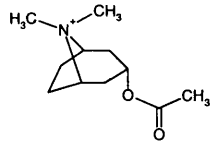	5.44 ± 0.07 (0.89 ± 0.06)	5.30 (1.08)	N.M.B.	—

Table 5.5: The binding of atropine analogues with a tertiary nitrogen to wild-type, dLoop and Asn382Ala-dLoop M_1 mAChRs.

Competition studies with [^{3}H]-QNB were performed on COS-7 cells transiently expressing wild-type, dLoop and Asn382Ala-dLoop M_1 mAChRs. The assay protocol is described in "Materials and Methods." Data are expressed as pIC_{50} values obtained by using the Hill equation except for benzilyltropine (^{C}) data for wild-type and dLoop M_1 mAChRs that are the high affinity constant from fitting with a two-site model of ligand binding due to the presence of occluded [^{3}H]-QNB binding sites (see Section 4.2.4). pIC_{50} and affinity constant values have been corrected with the Cheng-Prusoff correction factor. The percentage of benzilyltropine high affinity sites compared to the total number of binding sites were 93 ± 3 % and 77 % for wild-type and dLoop, respectively. Affinity constants and pIC_{50} (and Hill coefficient: n_H, in brackets) are shown as mean ± S.E.M. (when more than two experiments were carried out). The data obtained for ligand binding to wild-type M_1 mAChR was determined from at least three separate experiments, whilst the results showing ligand binding to dLoop and Asn382Ala-dLoop was measured by single experiments (except benztropine binding which was determined by two separate assays and are shown as mean ± range). The decrease in pIC_{50} between dLoop and Asn382Ala-dLoop is also shown.

	Binding affinity: pIC_{50}: -Log(M) (n_H)			
	Wild-type	dLoop	Asn382Ala-dLoop	ΔpIC_{50} decrease
(-)Scopolamine 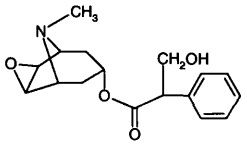	9.51 ± 0.04 (1.00 ± 0.02)	9.48 (1.03)	6.13 (0.73)	3.35
Atropine 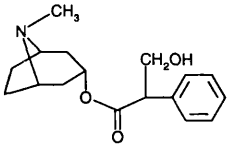	9.19 ± 0.04 (1.02 ± 0.03)	9.19 (0.93)	6.56 (0.62)	2.63
DL-Homatropine 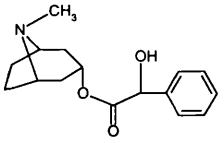	7.37 ± 0.03 (1.03 ± 0.01)	7.27 (1.12)	5.04 (0.49)	2.23
Phenylacetyltropine 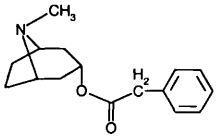	6.64 ± 0.03 (1.02 ± 0.01)	6.66 (0.91)	4.47 (0.77)	2.19
Diphenylacetyltropine 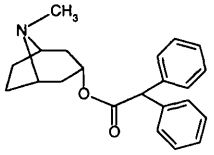	8.12 ± 0.01 (1.02 ± 0.01)	8.50 (0.98)	4.80 (0.30)	3.70
Benzilyltropine 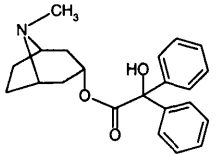	9.75 ± 0.10 [C]	9.50 [C]	7.67 (0.58)	1.83
Benztropine 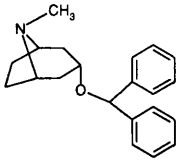	9.45 ± 0.03 (0.99 ± 0.00)	9.45 ± 0.01 (0.96 ± 0.03)	5.80 ± 0.05 (1.07 ± 0.07)	3.65

Figure 5.3: The inhibition of [^{3}H]-QNB binding to dLoop and Asn382Ala-dLoop M_1 mAChRs by N-methylatropine and atropine.

The figure shows representative plots of N-methylatropine (A) and atropine (B) inhibiting [^{3}H]-QNB binding at dLoop (black) and Asn382Ala-dLoop (red) M_1 mAChRs transiently expressed in COS-7 cells. The assay procedures used are described in "Materials and Methods." The data (mean ± S.E.M., from three replicate values) were fitted to the Hill equation except for the inhibition of [^{3}H]-QNB binding by NMS at the Asn382Ala-dLoop receptor. The data are expressed as a percentage of specific [^{3}H]-QNB binding in the absence of a competing ligand and have been corrected with the Cheng-Prussof correction factor. The corrected pIC_{50} and affinity constants are shown in Tables 5.4 and 5.5.

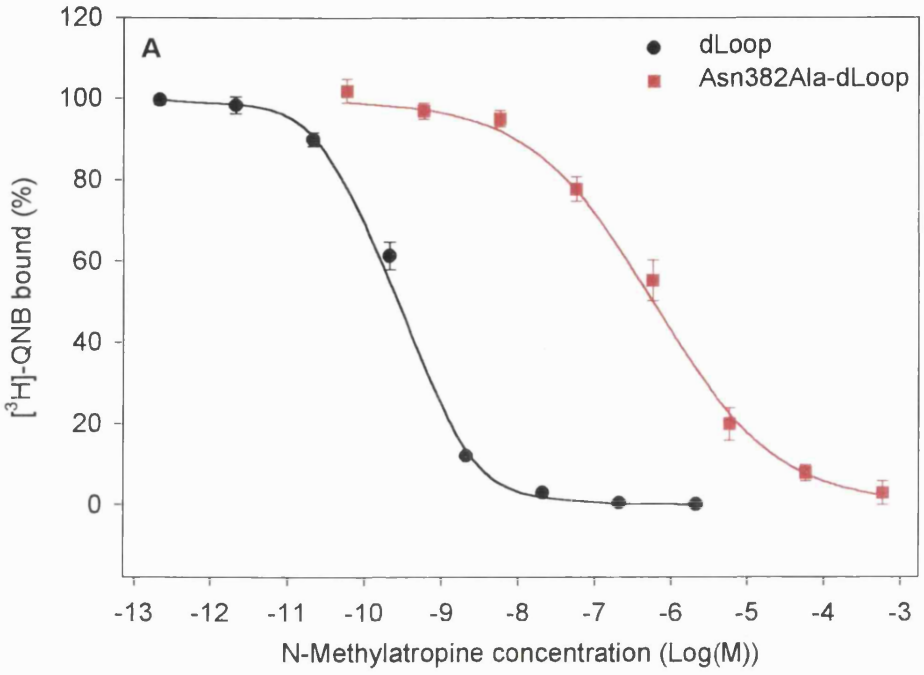
A
dLoop
Asn382Ala-dLoop
[3H]-QNB bound (%)
120
100
80
60
40
20
0
-13
-12
-11
-10
-9
-8
-7
-6
-5
-4
-3
N-Methylatropine concentration (Log(M))

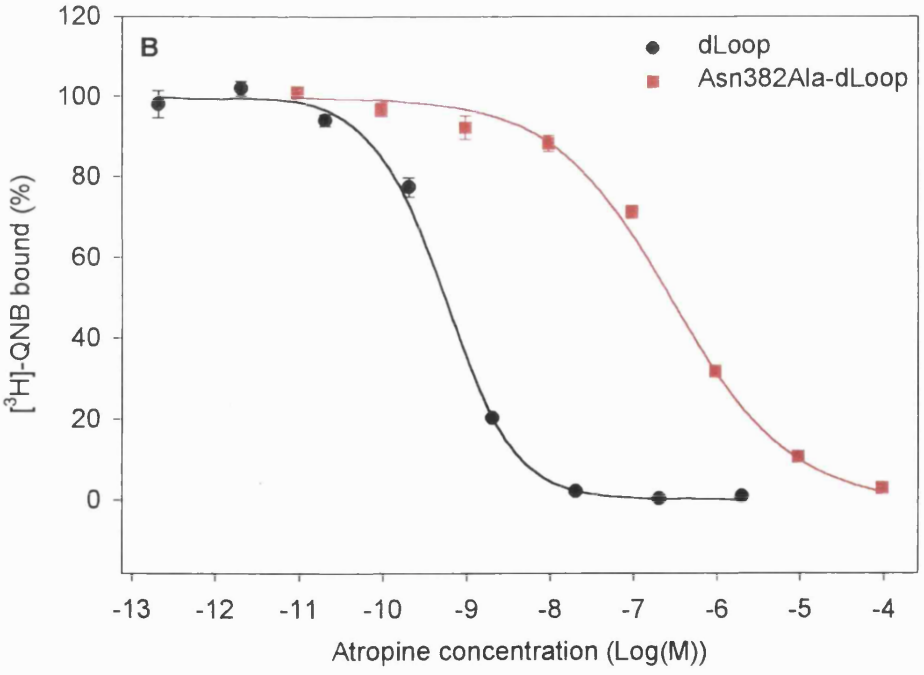
B
dLoop
Asn382Ala-dLoop
[3H]-QNB bound (%)
120
100
80
60
40
20
0
-13
-12
-11
-10
-9
-8
-7
-6
-5
-4
Atropine concentration (Log(M))

hydroxyl side-chain by removing a methylene group reduced the ligand binding affinity for dLoop by ~ 100 fold. When bound to the Asn382Ala-dLoop mutant there was still a 10 (N-methylatropine and N-methylhomatropine) and 30 (atropine and homatropine) fold reduction in ligand binding affinities when the methylene group is removed. Subsequent removal of the hydroxyl group, by comparing the binding of homatropine and phenylacetyltropine, caused a 4 fold decrease in ligand binding affinity at both the dLoop and Asn382Ala-dLoop M_1 mAChRs.

5.2.3.3 Side-chain comparisons (benzene ring).

Attaching an extra benzene ring to the tropic acid side-chain increased binding affinities. The ligand binding affinity of diphenylacetyltropine for dLoop was increased by 70 fold, when compared to phenylacetyltropine, although, there was only a 2 fold increase in the ligand binding affinity, when comparing the same compounds interacting with Asn382Ala-dLoop.

Analysis of the ligand binding affinities of homatropine and benzilyltropine showed that the extra benzene ring caused a larger increase in binding affinity at the Asn382Ala-dLoop M_1 mAChR (430 fold), when compared to dLoop (170 fold).

Removal of the benzene ring and hydroxyl group present on the tropic acid side-chain reduced ligand binding affinities. N-methylacetyltropine binding affinity for dLoop was 160 fold less than the binding affinity of N-methylhomatropine for dLoop. Interestingly, N-methylacetyltropine was unable to inhibit the binding of [^{3}H]-QNB to the Asn382Ala-dLoop mutant.

5.2.4 Other observations/comparisons.

A general observation is that the Hill coefficients measured for each ligand used are generally lower for the Asn382Ala-dLoop mutant, when compared to the respective values obtained using the dLoop M_1 mAChR. A possible explanation is that the Asn382Ala-dLoop mutation may allow the ligands to adopt a non-competitive as well as a competitive mode of binding, so that multiple ligand binding modes may become possible. It is worth noting that if all of the modes are competitive and reach equilibrium a Hill coefficient equal to 1.0 would be expected.

Figure 5.4: Schild analysis to determine the binding of atropine to wild-type, dLoop, Asn382Ala and Asn382Ala-dLoop M_1 mAChRs.

PI turnover experiments were carried out on COS-7 cells transiently expressing wild-type (A), dLoop (B), Asn382Ala (C) and Asn382Ala-dLoop (D) M_1 mAChRs. The assay protocol is described in "Materials and Methods." Cells were stimulated with ACh in the presence and absence of fixed concentrations of atropine. The final concentrations of atropine used were: 10 nM = red, 100 nM = green, 3 μM = blue, 30 μM = magenta and none = black/yellow. Data are shown as mean ± S.E.M. from three replicate values. PI response for each M_1 mAChR type has been corrected so that the maximum and minimum stimulation by ACh in the absence of atropine equals 100 % and 0 %, respectively.

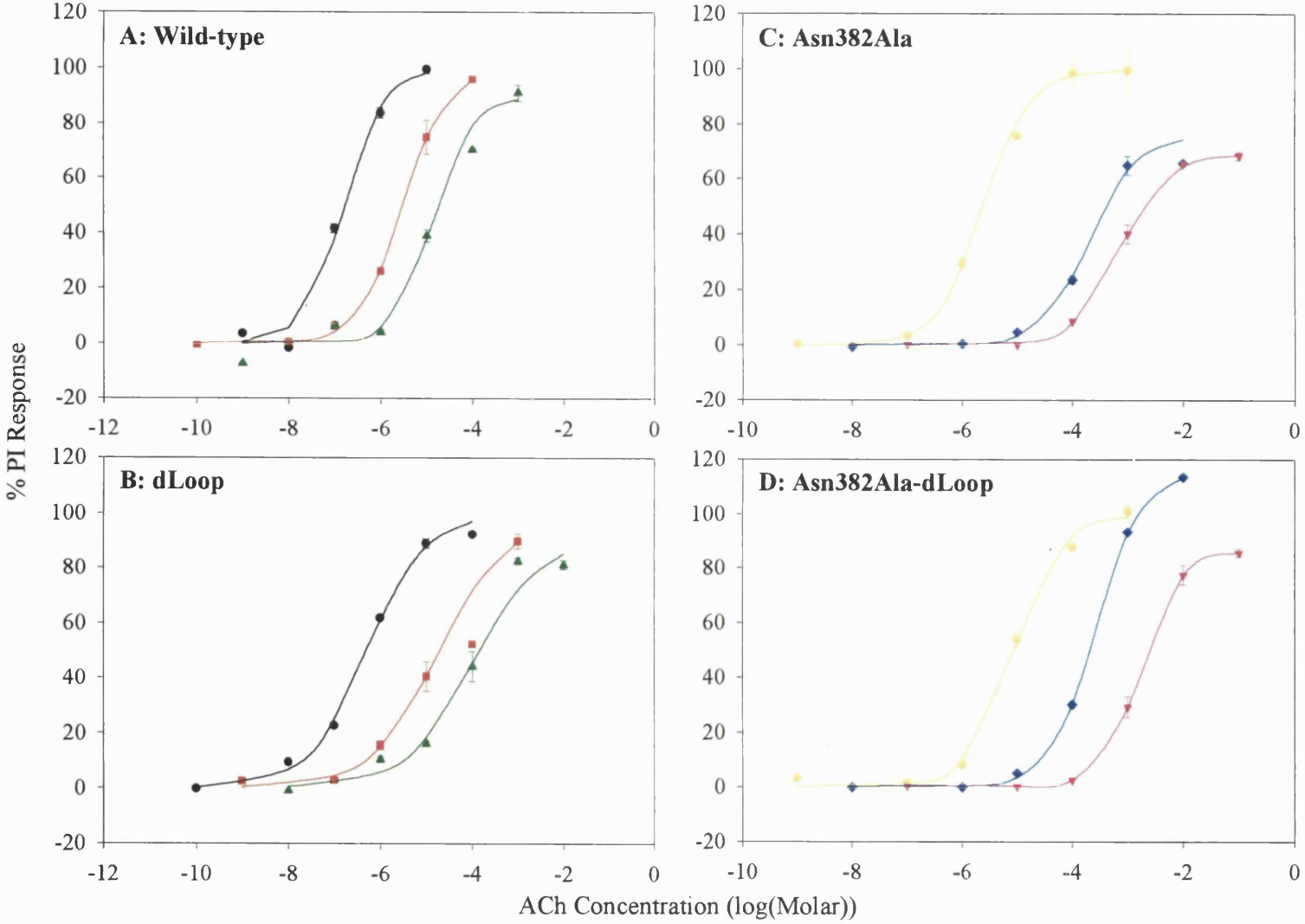
A: Wild-type
B: dLoop
C: Asn382Ala
D: Asn382Ala-dLoop
% PI Response
ACh Concentration (log(Molar))
120
100
80
60
40
20
0
-20
-12
-10
-8
-6
-4
-2
0

To try to ensure that the ligand binding data obtained by using the Asn382Ala-dLoop mutant was the same as could have been obtained for Asn382Ala, if radioligand binding studies had been possible, antagonism of the functional response was studied. Varying concentrations of ACh were used to stimulate wild-type, dLoop, Asn382Ala and Asn382Ala-dLoop in the presence and absence of fixed concentrations of atropine (Figure 5.4). Schild analysis was then used to calculate the pK_B for atropine binding to the wild-type and the mutant receptors. The pK_B values obtained were, wild-type: 9.08 ± 0.16; dLoop: 9.42 ± 0.12; Asn382Ala: 7.22 ± 0.22; Asn382Ala-dLoop: 6.90 ± 0.09. These data are similar to the pK_D values obtained for atropine binding to the respective receptor (except for the Asn382Ala mutation where the measurement was not possible).

As previously mentioned, the expression of the Asn382Ala mutant is significantly reduced, when compared to wild-type. A similar conclusion can be drawn when the expression of Asn382Ala-dLoop receptor binding sites, determined by the binding of [^{3}H]-QNB, is compared to the value obtained for dLoop (Table 5.1). However, the expression of Asn382Ala-dLoop mutant relative to dLoop is 79 %, whereas Asn382Ala expression relative to wild-type M_1 mAChR is ~ 8 %.

5.3 Discussion.

The data obtained in this investigation gives some indication about the role that Asn382 plays in M_1 mAChR function. The results clearly show that out of all the compounds looked at, the Asn382Ala-dLoop mutant affects the binding of the atropine-like ligands to the greatest extent. This observation agrees with the results from the study carried out on the asparagine residue homologous to Asn382, in the M_3 mAChR (Blüml, *et al.*, 1994).

The binding affinities of the majority of the ACh analogues are affected to similar degrees by the Asn382Ala-dLoop mutant, when compared to their binding affinities for dLoop. Oxotremorine-M binding affinity is significantly affected by the Asn382Ala-dLoop mutation but the effects on the binding of the other ACh analogues are small. These data suggest that Asn382 does not make a major interaction with the ACh analogues, apart from oxotremorine-M.

Tetramethylammonium binding is affected by the Asn382Ala-dLoop mutant. Since there are no moieties on Asn382 for tetramethylammonium to make a strong interaction with, this may be due to a secondary effect caused by the Asn382Ala-dLoop mutation.

Modelling based on the model by Baldwin, *et al.*, (1997) suggests that Asn382 faces towards TM 5. The decrease in receptor expression level, which results from the Asn382Ala and Asn382Ala-dLoop mutants, may be due to the deletion of an intra-molecular interaction. This may cause incorrect receptor folding which can have two main effects. Firstly, an increase in receptor degradation, giving rise to low expression, and secondly, improper formation of the ligand binding pocket, i.e., residues not in the correct orientation for binding. However, it is worth mentioning that the receptor activation mechanism is unaffected by the Asn382Ala mutations since the efficacy of ACh remains at the wild-type level. Therefore, Asn382 might not make contact directly with tetramethylammonium but could be involved in orientating a residue so that it can make a strong interaction with this ligand.

An alternative explanation is that Asn382 is involved in the ligand binding process, but in ligand docking rather than the final binding equilibrium. Ligand binding is probably not a simple binary mechanism, with the ligand either being unbound or fully bound. The actual process may involve the 'funnelling' of the ligand, via a number of intermediate steps, into its binding domain. This concept has been modelled in terms of electrostatic interactions (Wade, *et al.*, 1998), although other types of interactions, e.g., aromatic, probably take place to guide the ligand into the binding pocket.

The idea of ligands being guided into the binding domain has been suggested for acetylcholinesterase (Ripoll, *et al.*, 1993; Axelsen, *et al.*, 1994). These studies suggest that it is the quaternary nitrogen of ACh that is guided into the binding domain by an electrostatic field and that aromatic residues aid the process. Electrostatic steering may also occur in the mAChRs and other cationic amine receptors.

The effects on the binding affinities of ACh, carbachol and methylfurmethide caused by the Asn382Ala-dLoop mutation, relative to dLoop, were all similar to that observed for tetramethylammonium. Therefore, the effects seen may be due to

incorrect binding pocket formation and/or improper 'funnelling' of the ligand into the binding domain. These mutations could exert a differential effect on the forward and reverse rate constraints of the ligand binding process.

The ligand binding affinities of benzilylcholine, ACh-reversed ester and oxotremorine-M are all affected to a larger extent than that of ACh by the Asn382Ala-dLoop mutation. The magnitude of the changes in the affinities of these compounds suggests that they could make an interaction with Asn382. ACh-reversed ester, which has the position of the ether- and carbonyl-oxygens of ACh reversed, would suggest that altering the side-chain structure allows an interaction to take place between Asn382 and one of the oxygens. Therefore, the mode of interaction between Asn382 and these ligands is probably via a hydrogen-bond.

Combining data from both the Tyr381 and Asn382 investigations suggest that the Asn382 interaction with ACh-reversed ester may be caused by a 'knock-on effect.' The data suggest that the ester-oxygens of ACh interact more strongly with Tyr381 than with Asn382 in the fully bound state. If the ester-oxygens are swapped as in ACh-reversed ester, this leads to an altered mode of binding that may involve weakened binding to Tyr381 and strengthened binding to Asn382.

Benzilylcholine and oxotremorine-M have hydrogen-bonding moieties that are further away from the quaternary nitrogen than the oxygens present in ACh. These ligands also have a more bulky structure than ACh which may prevent them gaining full access to the ACh binding pocket. If the 'funnelling' hypothesis is true, these compounds may make the intermediate contact, like ACh, with Asn382 but cannot move further into the ACh binding domain (Figure 5.5). Therefore, the ligands remain in the intermediate binding stage. In this context, it is notable that the binding of oxotremorine-M is less sensitive to modifications of Asp105 than is the binding of ACh (Page, *et al.*, 1995). The observations made for pilocarpine also agree with these hypotheses.

The binding affinities of the azanorbornane- and quinuclidine-based ligands were scarcely affected by the Asn392Ala-dLoop mutant. These data suggest that Asn382

Figure 5.5: A possible mechanism of Asn382 in ligand docking.

There are probably intermediate stages in ACh binding. Asn382 may play a role in these events (A). Asn382 could form a hydrogen-bond interaction with the ester-oxygens present in the ACh side-chain. As the electrostatic interaction between the quaternary nitrogen of ACh and Asp105, in TM 3, is formed and the ligand moves into the agonist binding domain the side-chain hydrogen-bond interaction is then formed with Tyr381 (B). Ligands like oxotremorine-M, that are larger than ACh and have hydrogen-bonding moieties further away from the quaternary nitrogen may only make the intermediate interaction (C) because they cannot get fully into the ACh binding domain. Therefore, the interaction with Asn382 is preserved.

A) ACh: Docking Interactions

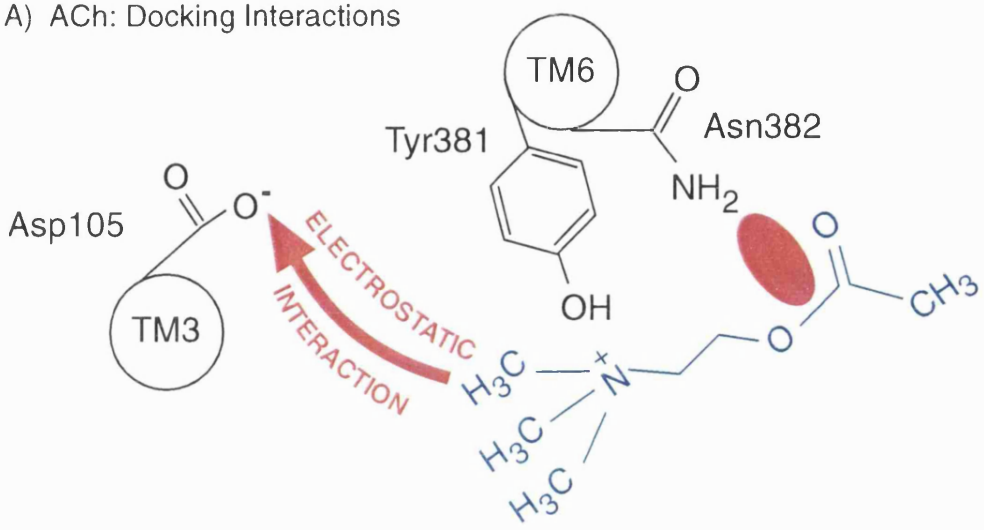

B) ACh: Binding-Site Interactions

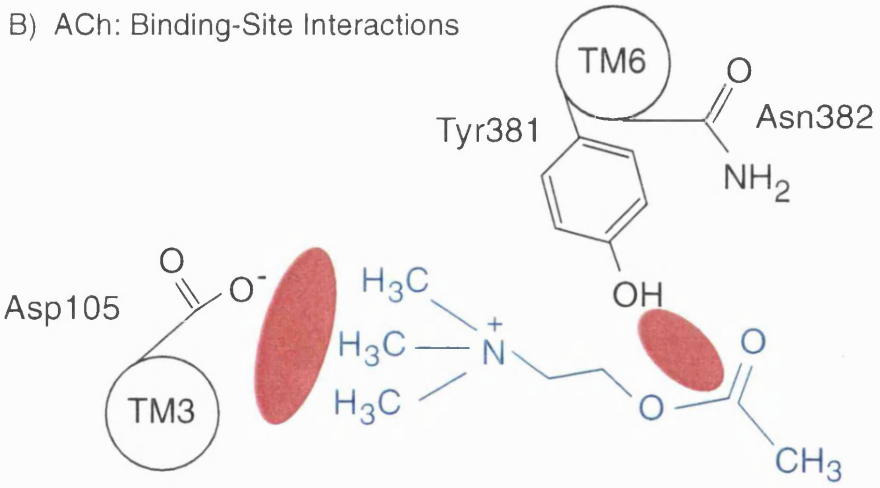

C) Oxotremorine-M : Binding-Site Interactions

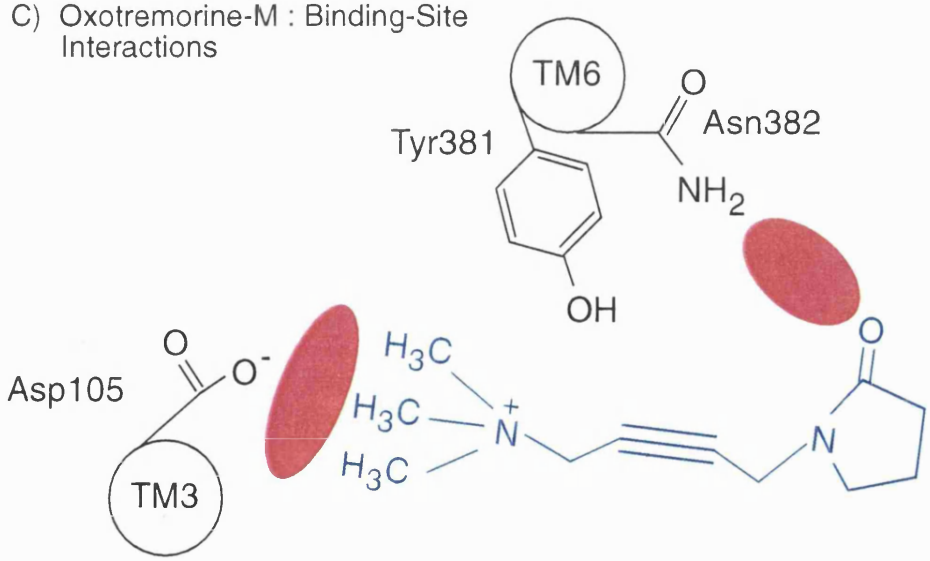

is not involved in forming interactions which contribute to the equilibrium binding of this type of ligand. However, further kinetic analysis would be required to fully investigate whether Asn382 is making an intermediate docking interaction or not (this will be explained further in Section 6).

Therefore, the azanorbornane- and quinuclidine-based ligands must be interacting with other residues. Data from these investigations suggest that Tyr381 interacts with the side-chain of these ligands when there are good hydrogen-bond acceptors present and suggest that there is another 'unknown' residue making a side-chain contact. However, this 'unknown' residue does not seem to be Asn382.

As already mentioned, Asn382Ala-dLoop has its largest effect on the binding of atropine-like compounds. The data give some indication about which moieties Asn382 may be interacting with, although, most of the analysis gives details about the moieties that do not interact with Asn382. That there is little change in the rank order of ligand binding affinities suggests that, in the majority of ligands, no moieties involved in making direct interactions with Asn382 are removed.

Comparing atropine-like compounds with different structural features on the tropine ring, i.e., an epoxide oxygen or quaternary/tertiary nitrogen, binding to dLoop and Asn382Ala-dLoop, it can be concluded that Asn382 probably does not make strong contacts with these head-group moieties since differences in ligand binding affinities are generally similar at both M_1 mAChR constructs.

If the effects of the Asn382Ala-dLoop mutation on the binding of benzilyltropine, benzilylcholine and [^{3}H]-QNB, i.e., compounds with the same side-chain and different head-groups, are compared, it can be seen that benzilyltropine and [^{3}H]-QNB are affected by a ~ 100 fold decrease, whilst benzilylcholine is only affected by ~ 10 fold decrease. These results suggest that a tropine or quinuclidine head-group positions the side-chain to make an optimum interaction with Asn382.

The hydroxyl group on the tropic acid side-chain also does not seem to have an interaction with Asn382, for reasons similar to those described above, although, the magnitude of the changes in ligand binding affinity between compounds with altered hydroxyl group position is reduced at the Asn382Ala-dLoop mutant, when compared to dLoop. These data suggest that the hydroxyl group may be important for making an

interaction with an 'unknown' residue which is involved in orientating atropine-like ligands in the binding domain and allowing Asn382 to make its interaction. This 'unknown' residue may or may not be the same one as the 'unknown' residue suggested by the Tyr381 investigation.

The results obtained are compatible with the hypothesis that Asn382 is involved in an intermediate contact as ligands dock into the agonist binding domain. Compounds with bulky and/or high aromatic side-chains probably cannot dock into the agonist binding domain but can get into an intermediate stage which involves Asn382. This hypothesis also explains why these compounds act as antagonists, i.e., there is a overlap of binding sites and they interact with a residue that is involved in the agonist binding mechanism, and this blocks subsequent agonist binding.

The data from the use of N-methylacetyltropine gives an indication about the moiety that the Asn382 interacts with. There is no detectable binding of this 'relatively simple' atropine-like compound to the Asn382Ala-dLoop mutant. This suggests that Asn382 is making an important contact with a moiety present in N-methylacetyltropine. From data described above we can conclude that Asn382 probably does not interact with the tropine ring. Therefore, the most likely moieties to interact with Asn382 are the carbonyl- and ether-oxygens present in the acetyl group.

Asn382Ala-dLoop has a large affect on benztropine binding This suggests that Asn382 may make an interaction with the ether-oxygen. It is worth noting that removal of the Tyr381 side-chain (Tyr381Ala) only resulted in a 7 fold decrease in benztropine binding affinity, whereas removal of the Asn382 side-chain caused a 4470 fold reduction.

The separation of the ether-oxygen of the atropine analogues from the nitrogen present in the tropine ring is greater than the distance between the ether-oxygen and the nitrogen in ACh (Figure 5.6). This is also true of the ether-oxygen in ACh-reversed ester. Increasing the distance between the head-group interaction and a moiety in the side-chain able to form hydrogen-bonds may increase the possibility that an interaction with Asn382 will take place.

Figure 5.6: Distance between head-group nitrogen and side-chain oxygen.

The structures of ACh, ACh-reversed ester and atropine are shown. For each ligand the number of atoms from the head-group nitrogen to the first side-chain oygen(s) are shown (in red). It can be seen that ACh-reversed ester and atropine have one more atom between these two moieties than ACh. This characteristic may contribute to the greater interaction made with Asn382 by ACh-reversed ester and atropine, when compared to ACh.

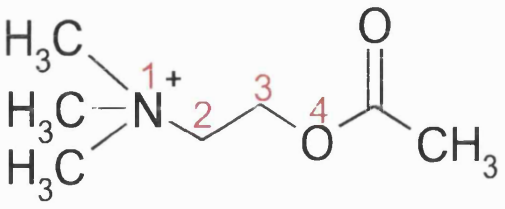

Acetylcholine

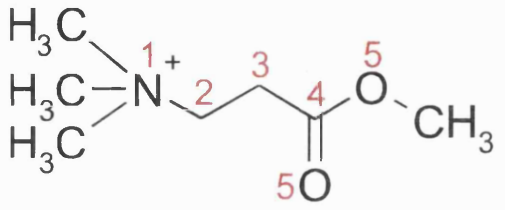

Acetylcholine-reversed ester

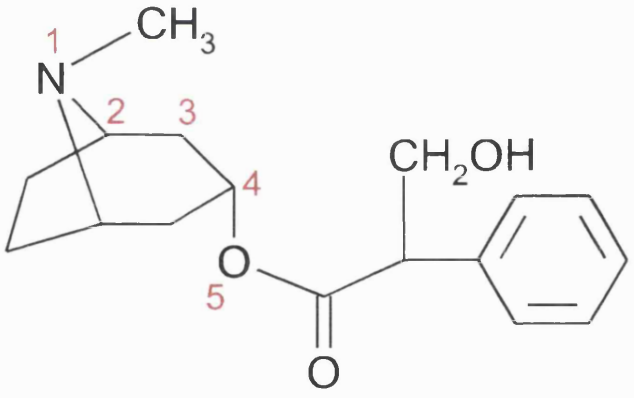

Atropine

As well as suggesting ligand moieties which are candidates for interactions with Asn382, the results also support the methodology used. The analysis of the binding of ligands to dLoop agrees with the data obtained for wild-type M_1 mAChR. This suggests that the dLoop mutation does not affect ligand binding affinities and agrees with previous investigations (Lu, *et al.*, 1997). The pK_B data for atropine obtained from a functional assay agreed with the data obtained from radioligand binding studies. This further supports the conclusion that the dLoop construct does not affect ligand binding affinities and that the results obtained for Asn382Ala-dLoop would resemble those obtained for Asn382 if it were possible to carry out radioligand binding studies on this mutant.

In summary the Asn382 residue, in the M_1 mAChR, plays a number of roles. Firstly, it appears to form an important intra-molecular contact. If this interaction is broken, improper receptor folding occurs. Secondly, Asn382 plays a role in the binding of ligands, especially atropine-like ligands, by forming a hydrogen-bond with the ligand's side-chain. A similar finding is that His265 in the NK-1 receptor, which is at the same position as Asn382 in TM 6, seems to be involved in the binding of antagonists via a hydrogen-bond (Fong, *et al.*, 1994).

The Asn382 residue may also play a role in the binding of most ligands by being involved in an intermediate event, specifically the residue may be involved in channelling ligands, especially agonists, into the agonist binding domain. Antagonists tend to be larger molecules and have more potential binding moieties than agonists (Barlow, 1964). These compounds can bind to Asn382 but cannot complete the agonist binding process because they may not be able to gain access to the agonist binding domain. Therefore they may act by blocking subsequent agonist binding. The results described only suggest that this 'funnelling' mechanism may be occurring and further investigation of this hypothesis is required.

However, some of the interpretation in this investigation disagrees with a recently published study by Spalding, *et al.*, (1998). The Spalding, *et al.*, study uses a random mutagenesis strategy followed by receptor selection and amplification technology, that measures the functional response produced by the mutant receptor (the protocol outlining the procedure is described in Burstein, *et al.*, (1995)). This study suggests

that Asn459, in TM 6 of the M_5 mAChR, which is homologous to Asn382, plays an important role in the binding of mAChR agonists and the subsequent activation of the receptor. These observations by Spalding, *et al.*, (1998) disagree with the interpretation of the data obtained in this investigation, although the two studies do agree on the possible interactions that Asn382 makes with ligands, i.e., hydrogen bonding to the ester moiety present in the side-chain of ligands.

The techniques used in the Spalding, *et al.*, investigation are probably the cause of the different results. Firstly, the majority of the data obtained are functional response measurements and do not take into account the possibility that mutations can cause low receptor expression. It is known a decrease in receptor expression will cause an altered functional response (Lu, *et al.*, 1997). The set of ligands used to stimulate the functional response was also limited. If as suggested by the M_1 mAChR study, Asn382 and homologous residues are primarily involved in a binding interaction rather than the activation process it is probably better to perform studies that measure binding affinities directly. These binding affinity data are limited in the Spalding, *et al.*, study, reducing the scope of the investigation and the conclusions that can be drawn from it. On the other hand, the effects on functional response caused by Asn382 mutations should be looked at in more detail.

6. *Summary.*

The aim of this investigation was to study the role of residues Tyr381 to Val387 in rat M_1 mAChR function. Alanine scanning mutagenesis was used to obtain information about which of the seven residues play the most important role in receptor function.

The data from the alanine scanning mutagenesis showed that a number of the residues participate in receptor function. The residue that caused the largest effects, when mutated to alanine, was Tyr381. The results suggested that this residue plays a greater part in ACh (agonist) than antagonist binding and has an important function in the receptor activation mechanism. The Asn382 residue located next on the helix after Tyr381 tended to have the opposite effects on receptor properties when it was mutated to alanine, i.e., Asn382 seems to play a significant role in antagonist but not agonist binding and is not involved in the receptor activation process. However, both Tyr381 and Asn382 may be required to make intra-molecular interactions to stabilise receptor folding, since both alanine mutants caused significant decreases in receptor expression. These intra-molecular contacts may be modified when a ligand binds.

The alanine scanning mutagenesis also suggested that Leu386 and Val387 may play a role in M_1 mAChR activation mechanism but not in agonist binding since both alanine mutations caused a decrease in ACh efficacy but only a minor reduction in ACh binding and the model by Baldwin, *et al.*, (1997) indicates that they do not face towards the proposed agonist binding domain. The other residues (Ile383, Met384, Val385) analysed in the alanine scanning mutagenesis strategy did not seem to play roles in M_1 mAChR function.

The residues determined by the alanine scanning mutagenesis investigation to have the greatest effect on receptor function (Tyr381 and Asn382) are conserved in all of the mAChRs, whereas in the other monoamine receptors phenylalanine residues usually occupy at both positions (Probst, *et al.*, 1992). Therefore, the structural information combined with the mutagenesis data would indicate that the Tyr381 and Asn382 in the M_1 mAChR, as well as the homologous residues present in the other subtypes, are playing specific roles characteristic of the mAChRs.

The role of Tyr381 (primarily because it had the greatest effect on agonist binding when mutated to alanine) and Asn382 was further analysed by using a greater number of ligands to build up a view of the structure-activity relationships. However, the Asn382 study needs further experimentation to complete the data set.

The Tyr381 residue was also mutated to phenylalanine so that results from the use of this mutant combined with the data for wild-type and Tyr381Ala could be used to investigate whether the components that make up the tyrosine residue (the hydroxyl group and the benzene ring) have specific roles in receptor function.

6.1 Interactions made by Tyr381 and Asn382 in the receptor's ground state.

The results indicated that, in the receptor's ground state, both Tyr381 and Asn382 are involved in forming interactions with the side-chain of mAChR ligands via the formation of hydrogen-bonds. The position of the hydrogen-bonding moieties on the ligand's side-chain, relative to the polar head-group, appear to determine with which residues an interaction is formed.

In the receptor's ground state, ACh, which is the receptor's natural agonist, forms a major hydrogen-bond interaction with the hydroxyl group of Tyr381 and a second minor interaction may also occur between Asn382 and the side-chain of ACh via a hydrogen-bond. These findings could be interpreted to indicate that mutating Tyr381 or Asn382 has a 'knock-on' effect on the interaction made by the other residue, i.e., Tyr381mutants may affect Asn382 interactions and vice versa, since they are at adjacent positions on TM 6. Alternatively, Asn382 may be involved in the docking of ligands into the agonist binding domain.

Asn382 seems to make stronger interactions than Tyr381 with agonists that have hydrogen-bonding moieties further away from the polar head-group, e.g., oxotremorine-M. The probable reason for this is that the hydrogen-bonding moieties are positioned better for an interaction with Asn382 than Tyr381, therefore the hydrogen-bonding interaction is not fully switched to Tyr381 as the ligand enters the agonist binding domain.

The results obtained with the azanorbornane- and quinuclidine-based ligands suggest that if there is a strong hydrogen-bond acceptor in the side-chain of these ligands then an interaction is formed with the hydroxyl-group of Tyr381. A cation-π interaction may be formed between the azanorbornane or quinuclidine head-group and the benzene ring of Tyr381 when there are two hydrogen-bond acceptors in the ligand's side-chain. However, the extra methylene moiety in the head-group of quinuclidine-based ligands does seem to form a direct interaction with Tyr381. These experiments suggested that another residue may be involved in binding to the side-chain of this type of ligand and orientating it to make a strong interaction with the Tyr381 benzene ring. This residue is probably not Asn382, since mutating it had no major effect on the binding of these ligands (with the exception of [^{3}H]-QNB). Therefore, the position and type of this 'unknown' residue remains to be established. In addition, there are also likely to be residue(s) that interact with the extra methylene moiety in the quinuclidine-based ligands but these have not yet been investigated.

Surprisingly, [^{3}H]-QNB binding is affected by the Asn382Ala mutant but not by Tyr381Ala. The binding properties of the other quinuclidine-based ligands are not affected by the Asn382Ala mutation suggesting that there is a characteristic specific to [^{3}H]-QNB that causes it to have an interaction with Asn382. [^{3}H]-QNB has a different side-chain when compared to the other quinuclidine-based ligands used in this study. This side-chain probably has moieties that interact with Asn382 but not Tyr381. Benzilylcholine and benzilyltropine have the same side-chains as [^{3}H]-QNB and their binding is affected in a similar way. All these compounds appear to make a stronger interaction with Asn382 than with Tyr381. However, the results obtained also show that removing the hydroxyl group of Tyr381 allows these compounds to alter their mode of binding and bind more tightly. This observation suggests that the interaction of these antagonists with Asn382 in the binding domain may be constrained by Tyr381.

The atropine-analogues also appear to make hydrogen-bond interactions with Tyr381 and Asn382 via the ester-link in their side-chains. Asn382 seems to play a bigger role in forming this interaction. The role that Tyr381 plays seems to be modulated by the head-group interaction, i.e., a quaternary nitrogen leads to the hydroxyl-group of Tyr381 forming a stronger interaction than to the compounds with a tertiary nitrogen.

The data suggested that Asn382 may form an interaction with the ether-oxygen moiety in the atropine-analogues, although this may not be the case if Tyr381 also forms a strong hydrogen-bond interaction with these compounds.

It appears that it is the benzene ring rather than the hydroxyl group of Tyr381 which forms the primary interaction with the atropine-analogues, perhaps by forming a cation-π interaction with their head-group. It may be the case that the head-group interaction determines the role that Tyr381 and Asn382 play in hydrogen-bonding to these ligands. Another moiety that may determine the interactions made is the hydroxyl group present in the majority of atropine-analogues used in this study. The results suggest that this moiety does not interact with either Tyr381 and Asn382 but makes a key interaction with another 'unknown' residue that helps to orientate the ligand in the binding domain. This 'unknown' residue may be the same residue that interacts with the second hydrogen-bond acceptor present in some of the azanorbornane- and quinuclidine-based ligands but this hypothesis needs further investigation (see Section 6.4).

6.2 Interactions made by Tyr381 and Asn382 in the receptor's activated state.

The results obtained indicate that the interactions made by Tyr381 hydroxyl group and by Asn382 in the receptor's ground state are maintained in the receptor's activated state. However, it seems that Tyr381 plays a much bigger role than Asn382 in forming and/or stabilising the receptor's activated state, either through the modification of intra-molecular contacts or by binding to the agonist. It should be noted that the data relevant to analysing the role of Asn382 in the receptor's activated state is currently limited.

The benzene ring of Tyr381 appears to be involved in the receptor's activation process, possibly by forming a cation-π interaction with the quaternary nitrogen head-group present in ACh and ACh analogues. A similar mechanism appears to hold for the other agonists. For example, an interaction between the head-group of azanorbornane- or quinuclidine-based ligands and the benzene ring of Tyr381 is important for receptor activation. For the azanorbornane-based ligand, L-698,583, it

appears that an interaction made by the hydroxyl-group of Tyr381 is also required for efficient receptor activation. Removal of a methylene moiety in the head-group of the ligand (when compared to L-658,903) may allow the ligand better access to the ligand binding domain, although, as observed in the ground state of the receptor, this altered head-group does not affect the interaction that Tyr381 is making.

In summary, these data can be interpreted in terms of a four-point model of ligand binding and receptor activation (Figure 4.15).

6.3 Conclusions.

The findings presented in this thesis have given some clear information about the role (and possible role) of residues Tyr381 to Val387, in TM 6, of the rat M_1 mAChR. In general the results agree with and build on conclusions made by previous investigations (see previous sections) and suggest the role of residues specific for mAChRs. The summary of the conclusions, in terms of ACh (the receptor's natural agonist) binding, are as follows:

- Alanine scanning mutagenesis of residues Tyr381 to Val387 showed that Tyr381 is the most important residue for agonist binding and subsequent M_1 mAChR activation.

- Further analysis of Tyr381 indicated that the two functional parts of the residue (the hydroxyl group and the benzene ring) have different roles in the receptor's function.

- The hydroxyl group of Tyr381, in the receptor's ground state, forms hydrogen-bond interactions with the ester-linkage present in the side-chain of ACh.

- The benzene ring of Tyr381 plays an important role in forming an interaction with the positively charged head-group of ACh to stabilise and/or form the receptor's activated state.

- Tyr381 may also form intra-molecular contacts to stabilise the receptor's structure when no ligand is bound.

- Asn382 was also shown to play important roles in receptor function, although not in ACh binding and receptor activation.
- Asn382 is necessary to form intra-molecular contacts to stabilise the receptor's structure.
- The hydrogen-bonding properties of Asn382 are important for the binding of antagonists (especially atropine analogues via their ester-link).
- Leu386 and Val387 seem to play a role in the receptor activation mechanism.

These conclusions are subject to the reservations about the interpretation of mutagenesis studies as described by Shortle (Shortle, 1992). Protein mutations can have both direct and direct effects. Similar ambiguities may arise as compound structures are altered (Strange, 1996). The greatest problems associated with this study is that some of the compounds adopted different binding modes at the mutant receptors, when compared to wild-type. Moreover, alteration of the compound structures also resulted in changed binding characteristics in some cases. These problems made analysis of certain results difficult and caution should be exercised in their interpretation. However, as previously mentioned, useful information was obtained.

The results obtained agree with the fact that residues in TM 6 of GPCRs play important roles in the binding of ligands to their respective receptors. As described in previous sections the data presented here are consistent with the majority of the published data on the role of these residues in the mAChRs. A recent modelling study on the rhodopsin photoreceptor, which has a tyrosine residue at the same position as Tyr381 in the M_1 mAChR shows that in rhodopsin this tyrosine plays a role informing a contact with the β-ionone ring of retinal (Pogozheva, *et al.*, 1997).

In the monoamine receptors the phenylalanine residue at the same positions as Tyr381 in both the β-adrenergic (Dixon, *et al.*, 1988) and D_2-dopamine (Cho, *et al.*, 1995) receptors have been shown to be important for agonist binding. The phenylalanine residues at the same position as Asn382 are involved in both agonist and antagonist binding. Clearly, TM 6 plays a significant role in both agonist and antagonist binding in a range of receptors.

Non-peptide antagonists also bind to resides in the NK-1 (substance P) receptor that are at the same position as Tyr381 and Asn382 (Turcatti, *et al.*, 1997). Therefore, the homologous region in a number of other types of receptor is extremely important for the binding of ligands and activating or inhibiting receptor function.

The conclusions drawn from this study also support previous investigations which have suggested that TM 6 is involved in the receptor activation mechanism (see Section 1.4.2). Combined with data obtained in this study, it is reasonable to propose that the interaction of the positively charged head-group of muscarinic agonists with the benzene ring of Tyr381 is part of the primary trigger mechanism involved in receptor activation.

In addition, the results obtained here are consistent with the new generation of GPCR models. Tyr381 is in an ideal position to make important interactions with ligands. These findings help to reassure us that the model of the M_1 mAChR based on the work of Baldwin, *et al.*, (1997), is essentially correct. Hypotheses derived from this model should provide a good basis for future investigations (see below).

6.4 Future directions.

The results obtained suggest a number of experiments that could be performed to try to obtain more information regarding the role of residues Tyr381 to Val387 in rat M_1 mAChR function.

Even though the study on Tyr381 was quite extensive it would be beneficial to probe the effects on ligand binding further. Since it has been suggested that Tyr381 forms a hydrogen-bond with the ester moiety of ACh, ACh analogues and atropine analogues it would be useful to obtain compounds with both the position and presence of the ester moiety altered to test this hypothesis. However, the synthesis of these compounds may be complicated and further investigation will be required to determine whether this approach is feasible. A similar strategy could also be used for Asn382 since it is also thought to form a hydrogen-bond with the side-chain ester moiety.

Apart from using additional compounds, production of other Tyr381 and Asn382 mutations and the analysis of the effects on ligand binding and the functional response

would also give further information that would hopefully support the current hypothesis. In theory, the Tyr381Gln mutation would produce a receptor that had little effect on the binding of ligands, especially ACh and ACh analogues, in the receptor's ground state, i.e., a hydrogen-bond could be formed with the ligand's side-chain, but activation of the receptor should be impaired.

In the case of Asn382, the serine and valine mutations might be useful to see whether a hydrogen-bonding moiety or side-chain size is important for receptor function, respectively. As mentioned above (Section 5.3), further investigation into the effects caused by the Asn382 mutants on receptor activation process may be beneficial in understanding the mechanisms occurring and the data could be compared to that obtained by Spalding, *et al.*, (1998). The data obtained could also be compared to the results for the Asn507Ser and Asn507Asp mutations in the M_3 mAChR (Blüml, *et al.*, 1994).

Another mutagenesis approach is to make double mutants. These mutations could give information about whether there is a 'knock-on' effect when Tyr381 is mutated, i.e., does Asn382 take over some of the hydrogen-bonding potential of Tyr381? If the Tyr381Phe and Asn382Ala double mutation were made, it could give some information that would answer this question. However, the likely problem with this double mutant would be extremely low expression and the dLoop construct would have to be used. This mutation may also give some indication whether a hydrogen-bond formed by either Tyr381 or Asn382 is necessary for activation.

Double cysteine mutagenesis followed by disulfide bond formation could give structural information. This strategy has been used to determine residues that are close together and which may form an intra-molecular interaction, e.g., between helices (Yu, *et al.*, 1995). This strategy has been recently used on the M_3 mAChR (Zeng and Wess, 1999). This type of investigation is also useful because it helps to deduce whether modelling information is correct or not, i.e., are the residues which are adjacent in the model actually close together in the receptor?

It is hypothesised that Asn382 (and Tyr381) may make intra-molecular interactions since mutation of these residues affects receptor expression. Modelling studies suggest that Asn382 faces TM 5, in the vicinity of Phe197, and that any intra-molecular

contact is likely to be between TMs 5 and 6 (Figure 6.1). The potential intra-molecular contact made by Tyr381 is less clear, although it is in close proximity to Tyr106 and Asn110 in TM 3 of the receptor (Figure 6.1). These residues may interact with each other when no ligand is bound, with the interaction being modified upon ligand binding. Data, from this laboratory, shows that Tyr106Ala has similar effects to the Tyr381Ala mutation on receptor function, i.e., it has a significant effect on ACh binding and receptor activation, as well as, affecting NMS binding (Hulme and Lu, 1998). These results further support the hypothesis described above, that the residues work together to stabilise the receptor when no ligand is present and that both are involved in binding the ligand.

If Asn382 was mutated to cysteine this disulfide bond forming strategy could be attempted with the cysteine mutations of residues in TM 5, already made in this laboratory (Allman, *et al.*, 1997), to test the intra-molecular interaction theory. A similar procedure could be used to see if Tyr106 and Tyr381 are in close proximity and can potentially form an intra-molecular interaction.

A problem with this technique is that native cysteine residues in the receptor might have to be mutated so that false positive results are not obtained because a disulfide bond has formed somewhere other than the region targeted. These extra mutations may disrupt normal receptor activation. Therefore, careful analysis of the mutant receptor's ligand binding and functional response characteristics would be required before definitive conclusions could be drawn.

The results obtained in this investigation did not clearly show the effects of the M_1 mAChR mutations, especially Tyr381Phe/Ala and Asn382Ala on the basal functional response. A possible reason for this is that the $G_{q/11}$ G protein subtype is not expressed at high levels in COS-7. As a consequence small reductions in basal receptor activity may be undetectable (Hulme, E.C., unpublished data). Increased G protein expression by carrying out a receptor/G protein co-transfection could overcome this problem. Recent results from this laboratory have shown that this strategy can work and that effects on the basal functional response can be measured (Lu, Z.-L., unpublished data).

Figure 6.1: A model showing possible intra-molecular interactions.

The data suggest that there are intra-molecular interaction between Asn382 and Leu386 in TM 6 and residues in TM 5. This stereo view, that is based on the one produced by Baldwin, *et al.*, (1997), indicates that Asn382 and Leu386 are close to Phe197 and Tyr198, in TM 5, respectively. The other possible intra-molecular interaction suggested by the model is between Tyr381, in TM 6, and Tyr106 and/or Asn110, in TM 5. The model is viewed from the extracellular side of the membrane.

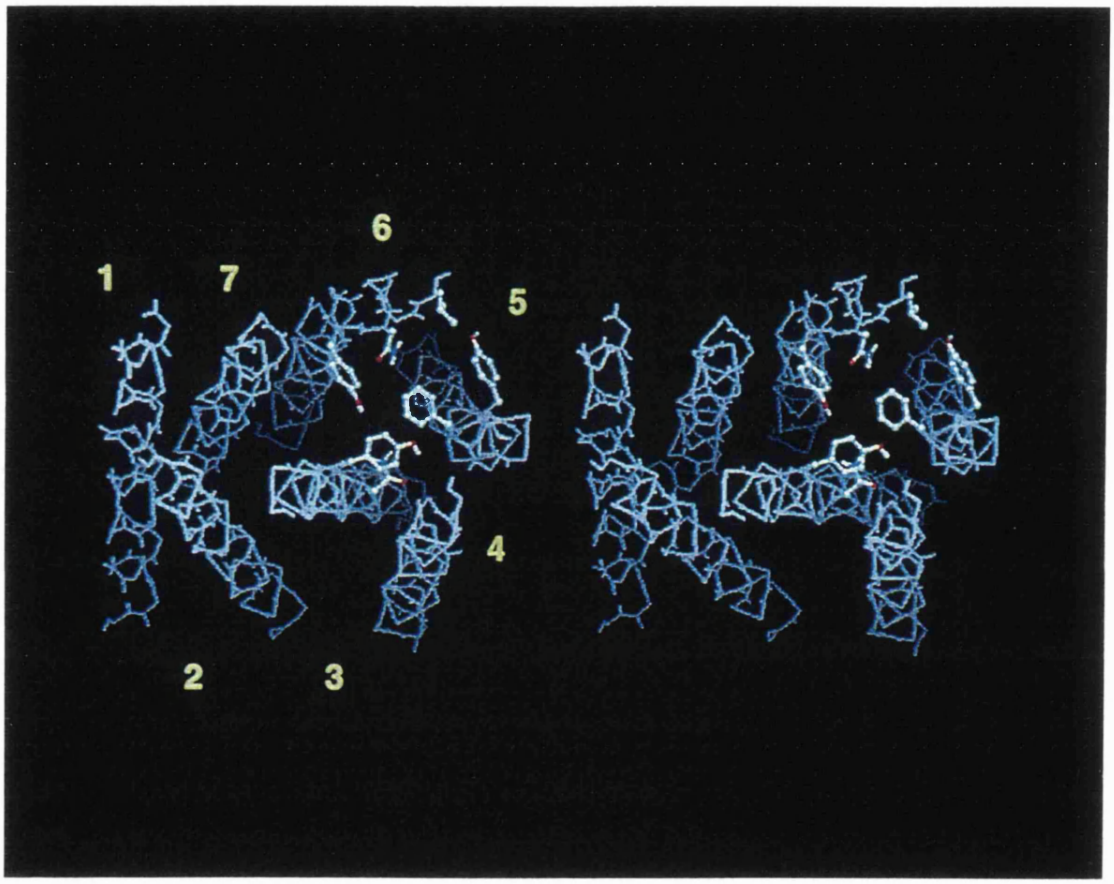
6
1
7
5
4
2
3

A system that combined increased G protein expression with high levels of receptor expression (Hulme and Curtis, 1998) might also be useful for investigating whether Asn382 plays a role in ligand docking, by providing a large number of high affinity receptor-G protein complexes. These conditions could then be used to measure the effects of mutations, especially Asn382Ala, on the kinetics of ligand binding by measuring [^{3}H]-agonist binding. A similar procedure was used to measure the kinetics of binding to mAChRs (primarily M_2 subtype) in rat myocardium (Berrie, *et al.*, 1984).

[^{3}H]-ACh, or better still [^{3}H]-L-698,583, could be used as a ligand since Asn382Ala only has a relatively small effect on the binding of these compounds. However, a better approach may be to use an alternative technique such as fluorescence spectroscopy. Labelling the β_2-adrenergic receptor with fluorescent probes allows ligand-induced conformational changes to be measured (Kobilka and Gether, 1998). If this methodology could be applied to the mAChRs it might give information about the effects of Asn382Ala on ligand docking, allowing one to ask whether the rate of ligand binding is affected by the mutation.

The techniques described above could also be used further to investigate the roles of Leu386 and Val387, since the alanine scanning investigation indicated that both residues play a part in receptor activation. Similar to Asn382, Leu386 faces towards TM 5 and is suggested, by models, to be close to Tyr198 (Figure 6.1). Therefore, double cysteine mutagenesis followed by disulfide bond formation could be a useful tool to see exactly which residues are in close proximity. Further mutagenesis of the residues and subsequent analysis of the effects could then be used to try to determine the exact function of Leu386. A similar approach could be used for Val387, although, from the models, it is difficult to predict what this residue is involved in since it seems to point into the lipid bilayer.

Apart from suggesting further analysis of the residues from Tyr381 to Val387, this study indicated that there were other 'unknown' residues in the M_1 mAChR which played a role in forming interaction(s) with quinuclidine- and azanorbornane-based ligands that contain two nitrogen atoms in their side-chains, i.e., L-698,583 and L-658,903, and with the hydroxyl group in the side-chain of atropine analogues. The

same residue(s) may also contribute extra binding energy to ACh in the activated state of the receptor. It is not known whether one or more residues are involved in forming these predicted interactions with the ligands described.

Model analysis indicates that the hydrogen-bonding moieties that are interacting with 'unknown' residues could be close to Tyr106, Ser109 and Asn110 in TM 3, when docked into the receptor (Figure 6.2). In the case of L-658,903 it seems that Ser109, in TM 3, is close to the second nitrogen in the side-chain and may be forming a hydrogen-bond, if the first nitrogen is interacting with Tyr381. However, Asn110 appears closer than Ser109 to the hydroxyl group present in the side-chain of atropine and may be forming the 'unknown' interaction with these ligands. If ACh is forming an extra interaction it seems that Asn110 will also be a prime candidate for carrying out this role by forming a hydrogen-bond interaction with the carbonyl-oxygen. Interestingly, Tyr106 seems to act as a 'lid' when all of these ligands are docked into the receptor. This observation may explain why Tyr106 appears to play such an important role in receptor function.

The models are not clear on which residue(s) the extra methylene group, present in the head-group of quinuclidine-based ligands, may form interaction(s) with (model not shown). However, this extra moiety seems to be pointing away from TM 6 and this agrees with a previous modelling study (Nordvall and Hacksell, 1993). Similar observations can be made for the atropine analogues with a quaternary nitrogen in their head-group.

A study carried out in this laboratory shows that Tyr106, Ser109 and Asn110, in TM 3 of the M_1 mAChR, are all important for receptor function (Hulme and Lu, 1998). The Tyr106Ala and Ser109Ala mutations affect ACh binding and ACh efficacy and Tyr106Ala also affects NMS binding. The Asn110Ala mutant affects ACh and NMS binding but not ACh efficacy. These data support the hypothesis that ACh and atropine analogues (that include NMS) form a binding interaction with Asn110 and Tyr106. The results also suggest that Ser109 may form an interaction with the azanorbornane- and quinuclidine-based ligands, although this interaction does not seem to be a major one made by ACh.

Figure 6.2: The possible 'unknown' residues that are required for ligand interactions.

These stereo views, based on the one produced by Baldwin, *et al.*, (1997), suggest that the moieties interacting with 'unknown' residues may be close to Tyr106, Ser109 and Asn110, in TM 3. The carbonyl-oxygen present in the side-chain of ACh (A) and the hydroxyl group in the side-chain of atropine (C) are positioned close to Asn110. However, the second nitrogen present in the side-chain of L-658,903 (B) is close to Ser109. Therefore, there may be hydrogen-bond interactions formed between these side-chain moieties and residues in TM 3. In all three cases Tyr106 seems to act as a 'lid' on the side-chains of these ligands. All the models are viewed from the extracellular side of the membrane.

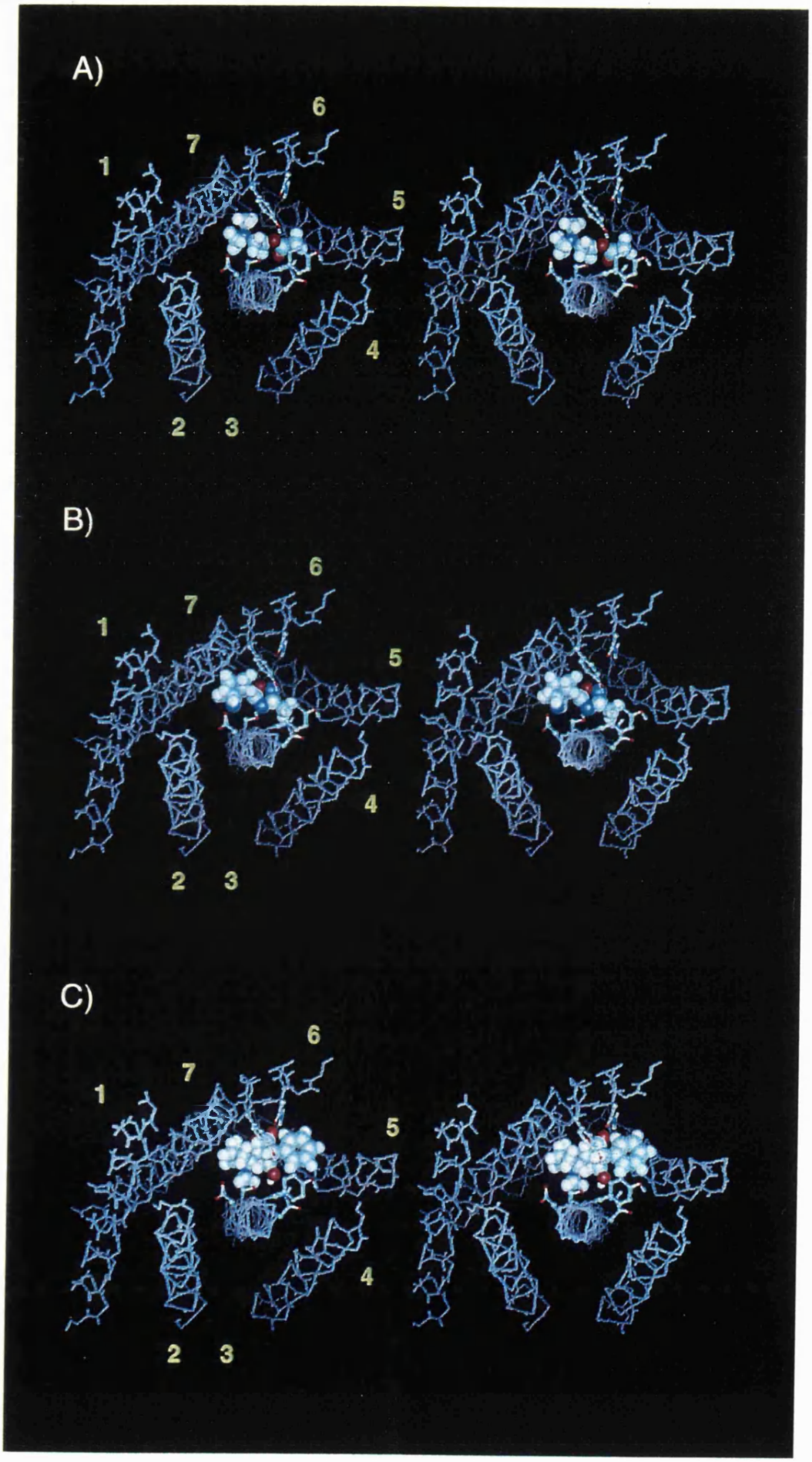
A)
6
7
1
5
4
2
3
B)
6
7
1
5
4
2
3
C)
6
7
1
5
4
2
3

However, the exact functions of Tyr106, Ser109 and Asn110 are still to be deduced and a similar investigation to the one performed on Tyr381 is required, namely, the production of other mutants, especially Tyr106Phe, and subsequent analysis of the effects of this mutation on ligand binding and receptor response. Since modelling suggests that these residues in TM 3 may be involved in the binding of L-698,583, L-658,903 and atropine analogues these would be good ligands to use as initial probes in these studies.

In summary, the investigation carried out on the sequence between Tyr381 and Val387 have clarified several issues, and have provided many potential directions for future research!

7. References.

Adem, A. and Karlsson, E. (1997) Muscarinic receptor subtype selective toxins. *Life Sci.* **60**, 1069-1076.

Akabas, M.H., Stauffer, D.A., Xu, M. and Karlin, A. (1992) Acetylcholine receptor channel structure probed in cysteine-substitution mutants. *Science* **258**, 307-310.

Alexander, S.P.H. and Peters, J.A. (1998) 1998 receptor and ion channel nomenclature supplement. *Trends Pharmacol. Sci.*

Allman, K., Page, K.M. and Hulme, E.C. (1997) Cysteine scanning mutagenesis of transmembrane domain V of the M1 muscarinic receptor. *Life Sci.* **60**, 1177.

Arden, J.R., Nagata, O., Shockley, M.S., Philip, M., Lameh, J. and Sadée, W. (1992) Mutational analysis of third cytoplasmic loop domains in G-protein coupling of the HM1 muscarinic receptor. *Biochem. Biophys. Res. Commun.* **188**, 1111-1115.

Arunlakshana, O. and Schild, H.O. (1959) Some quantitative uses of drug antagonists. *Br. J. Pharmacol.* **14**, 48-58.

Axelsen, P.H., Harel, M., Silman, I. and Sussman, J.L. (1994) Structure and dynamics of the active site gorge of acetylcholinesterase: synergistic use of molecular dynamics simulation and X-ray crystallography. *Protein Sci.* **3**, 188-197.

Baldwin, J.M., Schertler, G.F.X. and Unger, V.M. (1997) An alpha-carbon template for the transmembrane helices in the rhodopsin family of G-protein-coupled receptors. *J. Mol. Biol.* **272**, 144-164.

Ballesteros, J., Kitanovic, S., Guarnier, F., Davies, P., Fromme, B.J., Konvicka, K., Chi, L., Millar, R.P., Davidson, J.S., Weinstein, H. and Sealfon, S.C. (1998) Functional microdomains in G-protein-coupled receptors. *J. Biol. Chem.* **273**, 10445-10453.

Barlow, R.B. (1964) *Introduction to chemical pharmacology*, 2nd edn. London: Methuen & Co. Ltd.

Bass, S.H., Mulkerrin, M.G. and Wells, J.A. (1991) A systematic mutational analysis of hormone-binding determinants in the human growth hormone receptor. *Proc. Natl. Acad. Sci. USA* **88**, 4498-4502.

Beck-Sickinger, A.G. (1996) Structural characterization and binding sites of G-protein-coupled receptors. *Drug Discovery Today* **1**, 502-513.

Berman, D.M. and Gilman, A.G. (1998) Mammalian RGS proteins: barbarians at the gate. *J. Biol. Chem.* **273**, 1269-1272.

Berridge, M.J., Downes, C.P. and Hanley, M.R. (1982) Lithium amplifies agonist-dependent phosphatidylinositol responses in brain and salivary glands. *Biochem. J.* **206**, 587-595.

Berrie, C.P., Birdsall, N.J.M., Hulme, E.C., Keen, M. and Stockton, J.M. (1984) Solubilization and characterisation of guanine nucleotide-sensitive muscarinic agonist binding sites from rat myocardium. *Br. J. Pharmacol.* **82**, 853-861.

Berstein, G., Blank, J.L., Smrcka, A.V., Higashijima, T., Sternweis, P.C., Exton, J.H. and Ross, E.M. (1992) Reconstitution of agonist-stimulated phosphatidylinositol 4,5-bisphosphate hydrolysis using purified m1 muscarinic receptor, $G_{q/11}$, and phospholipase C-β1. *J. Biol. Chem.* **267**, 8081-8088.

Black, J.W. and Leff, P. (1983) Operational models of pharmacological agonism. *Proc. R. Soc. Lond. B.* **220**, 141-162.

Blin, N., Yun, J. and Wess, J. (1995) Mapping of single amino acid residues required for selective activation of $G_{q/11}$ by the m3 muscarinic acetylcholine receptor. *J. Biol. Chem.* **270**, 17741-17748.

Blüml, K., Mutschler, E. and Wess, J. (1994) Functional role in ligand binding and receptor activation of an asparagine residue present in the sixth transmembrane domain of all muscarinic acetylcholine receptors. *J. Biol. Chem.* **269**, 18870-18876.

Blüml, K., Mutschler, E. and Wess, J. (1994b) Functional role of a cytoplasmic aromatic amino acid in muscarinic receptor-mediated activation of phospholipase C. *J. Biol. Chem.* **269**, 11537-11541.

Blüml, K., Mutschler, E. and Wess, J. (1994c) Identification of an intracellular tyrosine residue critical for muscarinic receptor-mediated stimulation of phosphatidylinositol hydrolysis. *J. Biol. Chem.* **269**, 402-405.

Blüml, K., Mutschler, E. and Wess, J. (1994a) Insertion mutagenesis as a tool to predict the secondary structure of a muscarinic receptor domain determining specificity of G-protein coupling. *Proc. Natl. Acad. Sci. USA* **91**, 7980-7984.

Bogatkewitsch, G.S., Lenz, W., Jakobs, K.H. and Van Koppen.C.J. (1996) Receptor internalization delays m4 muscarinic acetylcholine receptor resensitization at the plasma membrane. *Mol. Pharmacol.* **50**, 424-429.

Bonner, T.I., Buckley, N.J., Young, A.C. and Brann, M.R. (1987) Identification of a family of muscarinic acetylcholine receptor genes [published erratum appears in *Science* (1987) **237:** 1556]. *Science* **237**, 527-532.

Bonner, T.I., Young, A.C., Brann, M.R. and Buckley, N.J. (1988) Cloning and expression of the human and rat m5 muscarinic acetylcholine receptor genes. *Neuron* **1**, 403-410.

Borjigin, J. and Nathans, J. (1994) Insertional mutagenesis as a probe of rhodopsin's topography, stability, and activity. *J. Biol. Chem.* **269**, 14715-14722.

Bourne, H.R. (1997) How receptors talk to trimeric G proteins. *Curr. Opin. Cell Biol.* **9**, 134-142.

Bouvier, M., Loisel, T.P. and Hebert, T. (1995) Dynamic regulation of G-protein coupled receptor palmitoylation: potential role in receptor function. *Biochem. Soc. Trans.* **23**, 577-581.

Böhm, S.K., Grady, E.F. and Bunnett, N.W. (1997) Regulatory mechanisms that modulate signalling by G-protein-coupled receptors. *Biochem. J.* **322**, 1-18.

Burstein, E.S., Spalding, T.A. and Brann, M.R. (1996) Amino acid side chains that define muscarinic receptor/G-protein coupling. *J. Biol. Chem.* **271**, 2882-2885.

Burstein, E.S., Spalding, T.A. and Brann, M.R. (1998) Structure/function relationships of a G-protein coupling pocket formed by the third intracellular loop of the m5 muscarinic receptor. *Biochemistry* **37**, 4052-4058.

Burstein, E.S., Spalding, T.A., Hill-Eubanks, D. and Brann, M.R. (1995) Structure-function of muscarinic receptor coupling to G proteins. *J. Biol. Chem.* **270**, 3141-3146.

Cachero, T.G., Morielli, A.D. and Peralta, E. (1998) The small GTP-binding protein RhoA regulates a delayed rectifier potassium channel. *Cell* **93**, 1077-1085.

Candell, L.M., Yun, S.H., Tran, L.L. and Ehlert, F.J. (1990) Differential coupling of subtypes of the muscarinic receptor to adenylate cyclase and phosphoinositide hydrolysis in the longitudinal muscle of the rat ileum. *Mol. Pharmacol.* **38**, 689-697.

Casey, P.J. (1994) Lipid modifications of G proteins. *Curr. Opin. Cell Biol.* **6**, 219-225.

Caulfield, M.P. (1993) Muscarinic receptors - characterization, coupling and function. *Pharmacol. Ther.* **58**, 319-379.

Caulfield, M.P. and Birdsall, N.J.M. (1998) International union of pharmacology. XVII. Classification of muscarinic acetylcholine receptors. *Pharmacol. Rev.* **50**, 279-290.

Cervantes-Olivier, P., Delavier-Klutchko, C., Durieu-Trautmann, O., Kaveri, S., Desmandril, M. and Strosberg, A.D. (1988) The β_2-adrenergic receptors of human epidermoid carcinoma cells bear two different types of oligosaccharides which influence expression on the cell surface. *Biochem. J.* **250**, 133-143.

Cheng, Y. and Prusoff, W.H. (1973) Relationship between the inhibition constant (K_I) and the concentration of inhibitor which causes 50 per cent inhibition (I_{50}) of an enzymatic reaction. *Biochem. Pharmacol.* **22**, 3099-3108.

Cheung, A.H., Huang, R.C. and Strader, C.D. (1992) Involvement of specific hydrophobic, but not hydrophilic, amino acids in the third intracellular loop of the β-adrenergic receptor in the activation of G_s. *Mol. Pharmacol.* **41**, 1061-1065.

Cho, W., Taylor, L.P., Mansour, A. and Akil, H. (1995) Hydrophobic residues of the D_2 dopamine receptor are important for binding and signal transduction. *J. Neurochem.* **65**, 2105-2115.

Choudhary, M.S., Craigo, S. and Roth, B.L. (1993) A single point mutation (Phe^{340} to Leu^{340}) of a conserved phenylalanine abolishes 4-[^{125}I]iodo-(2,5-dimethoxy)phenylisopropylamine and [^{3}H]mesulergine but not [^{3}H]ketanserin binding to 5-hydroxytryptamine$_2$ receptors. *Mol. Pharmacol.* **43**, 755-761.

Clarke, S. (1992) Protein isoprenylation and methylation at carboxyl-terminal cysteine residues. *Annu. Rev. Biochem.* **61**, 355-386.

Cohen, G.B., Oprian, D.D. and Robinson, P.R. (1992) Mechanism of activation and inactivation of opsin: role of Glu^{113} and Lys^{296}. *Biochemistry* **31**, 12592-12601.

Cohen, G.B., Yang, T., Robinson, P.R. and Oprian, D.D. (1993) Constitutive activation of opsin: influence of charge at position 134 and size at position 296. *Biochemistry* **32**, 6111-6115.

Coleman, D.E., Berghuis, A.M., Lee, E., Linder, M.E., Gilman, A.G. and Sprang, S.R. (1994) Structures of active conformations of $G_{i\alpha 1}$ and the mechanism of GTP hydrolysis. *Science* **265**, 1405-1412.

Crespo, P., Xu, N., Simonds, W.F. and Gutkind, J.S. (1994) Ras-dependent activation of MAP kinase pathway mediated by G-protein $\beta\gamma$ subunits. *Nature* **369**, 418-420.

Curtis, C.A., Wheatley, M., Bansal, S., Birdsall, N.J.M., Eveleigh, P., Pedder, E.K., Poyner, D. and Hulme, E.C. (1989) Propylbenzilylcholine mustard labels an acidic residue in transmembrane helix 3 of the muscarinic receptor. *J. Biol. Chem.* **264**, 489-495.

Dale, H.H. (1914) The action of certain esters and ethers of choline, and their relation to muscarine. *J. Pharmacol. Exp. Ther.* **6**, 147-190.

Danielson, M.A., Bass, R.B. and Falke, J.J. (1997) Cysteine and disulfide scanning revels a regulatory α-helix in the cytoplasmic domain of the aspartate receptor. *J. Biol. Chem.* **272**, 32878-32888.

Davidson, F.F., Loewen, P.C. and Khorana, H.G. (1994) Structure and function in rhodopsin: replacement by alanine of cysteine residues 110 and 187, components of a conserved disulfide bond in rhodopsin, affects the light-activated metarhodopsin II state. *Proc. Natl. Acad. Sci. USA* **91**, 4029-4033.

Degtyarev, M.Y., Spiegel, A.M. and Jones, T.L. (1993) Increased palmitoylation of the Gs protein alpha subunit after activation by the beta-adrenergic receptor or cholera toxin. *J. Biol. Chem.* **268**, 23769-23772.

Deng, W.P. and Nickoloff, J.A. (1992) Site-directed mutagenesis of virtually any plasmid by eliminating a unique site. *Anal. Biochem.* **200**, 81-88.

Dietrich, A., Brazil, D., Jensen, O.N., Meister, M., Schrader, M., Moomaw, J.F., Mann, M., Illenberger, D. and Gierschik, P. (1996) Isoprenylation of the G protein gamma subunit is both necessary and sufficient for beta gamma dimer-mediated stimulation of phospholipase C. *Biochemistry* **35**, 15174-15182.

Dixon, R.A.F., Hill, W.S., Candelore, M.R., Rands, E., Diehl, R.E., Marshall, M.S., Sigal, I.S. and Strader, C.D. (1989) Genetic analysis of the molecular basis for β-adrenergic receptor subtype specificity. *Proteins* **6**, 267-274.

Dixon, R.A.F., Sigal, I.S., Rands, E., Register, R.B., Candelore, M.R., Blake, A.D. and Strader, C.D. (1987) Ligand binding to the β-adrenergic receptor involves its rhodopsin-like core. *Nature* **326**, 73-77.

Dixon, R.A.F., Sigal, I.S. and Strader, C.D. (1988) Structure-function analysis of the β-adrenergic receptor. *Cold Spring Harb. Symp. Quant. Biol.* **53**, 487-497.

Donnelly, D., Overington, J.P., Ruffle, S.V., Nugent, J.H.A. and Blundell, T.L. (1993) Modeling α-helical transmembrane domains: the calculation and use of substitution tables for lipid-facing residues. *Protein Sci.* **2**, 55-70.

Doss, R.C., Perkins, J.P. and Harden, T.K. (1981) Recovery of beta-adrenergic receptors following long term exposure of astrocytoma cells to catecholamine. Role of protein synthesis. *J. Biol. Chem.* **256**, 12281-12286.

Dougherty, D.A. (1996) Cation-π interactions in chemistry and biology: a new view of benzene, Phe, Tyr, and Trp. *Science* **271**, 163-168.

Doyle, D.A., Cabral, J.M., Pfuetzner, R.A., Kuo, A., Gulbis, J.M., Cohen, S.L., Chait, B.T. and MacKinnon, R. (1998) The structure of the potassium channel: molecular basis of K^+ conduction and selectivity. *Science* **280**, 69-77.

Dörje, F., Levey, A.I. and Brann, M.R. (1991) Immunological detection of muscarinic receptor subtype proteins (m1-m5) in rabbit peripheral tissues. *Mol. Pharmacol.* **40**, 459-462.

Eglen, R.M., Reddy, H., Watson, N. and Challiss, R.A.J. (1994) Muscarinic acetylcholine receptor subtypes in smooth muscle. *Trends Pharmacol. Sci.* **15**, 114-119.

Elling, C.E. and Schwartz, T.W. (1996) Connectivity and orientation of the seven helical bundle in the tachykinin NK-1 receptor probed by zinc site engineering. *EMBO J.* **15**, 6213-6219.

Ellis, J., Huyler, J. and Brann, M.R. (1991) Allosteric regulation of cloned m1-m5 muscarinic receptor subtypes. *Biochem. Pharmacol.* **42**, 1927-1932.

Ellis, J., Seidenberg, M. and Brann, M.R. (1993) Use of chimeric muscarinic receptors to investigate epitopes involved in allosteric interactions. *Mol. Pharmacol.* **44**, 583-588.

Farrens, D.L., Altenbach, C., Yang, K., Hubbell, W.L. and Khorana, H.G. (1996) Requirement of rigid-body motion of transmembrane helices for light activation of rhodopsin. *Science* **274**, 768-770.

Felder, C.C. (1995) Muscarinic acetylcholine receptors: signal transduction through multiple effectors. *FASEB J.* **9**, 619-625.

Ferguson, S.S.G., Downey, W.E.I., Colapietro, A.-M., Barak, L.S., Caron, M.G. and Caron (1996) Role of β-arrestin in mediating agonist-promoted G protein-coupled receptor internalization. *Science* **271**, 363-366.

Fong, T.M., Yu, H., Cascieri, M.A., Underwood, D., Swain, C.J. and Strader, C.D. (1994) The role of histidine 265 in antagonist binding to the neurokinin-1 receptor. *J. Biol. Chem.* **269**, 2728-2732.

Fraser, C.M., Wang, C.-D., Robinson, D.A., Gocayne, J.D. and Venter, J.C. (1989) Site-directed mutagenesis of m_1 muscarinic acetylcholine receptors: conserved aspartic acids play important roles in receptor function. *Mol. Pharmacol.* **36** , 840-847.

Freedman, S.B., Harley, E.A., Patel, S., Newberry, N.R., Gilbert, M.J., McKnight, A.T., Tang, J.K., Maguire, J.J., Mudunkotuwa, N.T., Baker, R., Street, L.J., MacLeod, A.M., Saunders, J. and Iversen, L.L. (1990) A novel series of non-quaternary oxadiazoles acting as full agonists at muscarinic receptors. *Br. J. Pharmacol.* **101**, 575-580.

Frielle, T., Daniel, K.W., Caron, M.G. and Lefkowitz, R.J. (1988) Structural basis of β-adrenergic receptor subtype specificity studied with chimeric β_1/β_2-adrenergic receptors. *Proc. Natl. Acad. Sci. USA* **85**, 9494-9498.

Gadbut, A.P. and Galper, J.B. (1994) A novel M_3 muscarinic acetylcholine receptor is expressed in chick atrium and ventricle. *J. Biol. Chem.* **269**, 25823-25829.

George, S.T., Ruoho, A.E. and Malbon, C.C. (1986) N-glycosylation in expression and function of β-adrenergic receptors. *J. Biol. Chem.* **261**, 16559-16564.

Goldman, P.S. and Nathanson, N.M. (1994) Differential role of the carboxyl-terminal tyrosine in down- regulation and sequestration of the m2 muscarinic acetylcholine receptor. *J. Biol. Chem.* **269**, 15640-15645.

Goodman, O.B., Jr., Krupnick, J.G., Santini, F., Gurevich, V.V., Penn, R.B., Gagnon, A.W., Keen, J.H. and Benovic, J.L. (1996) β-Arrestin acts as a clathrin adaptor in endocytosis of the β_2-adrenergic receptor. *Nature* **383**, 447-450.

Gordon, J.I., Duronio, R.J., Rudnick, D.A., Adams, S.P. and Gokel, G.W. (1991) Protein N-myristoylation. *J. Biol. Chem.* **266**, 8647-8650.

Growdon, J.H. (1997) Muscarinic agonists in Alzheimer's disease. *Life Sci.* **60**, 993-998.

Gurevich, V.V., Pals-Rylaarsdam, R., Benovic, J.L., Hosey, M.M. and Onorato, J.J. (1997) Agonist-receptor-arrestin, an alternative ternary complex with high affinity. *J. Biol. Chem.* **272**, 28849-28852.

Gutkind, J.S., Novotny, E.A., Brann, M.R. and Robbins, K.C. (1991) Muscarinic acetylcholine receptor subtypes as agonist-dependent oncogenes. *Proc. Natl. Acad. Sci. USA* **88**, 4703-4707.

Haga, K. and Haga, T. (1992) Activation by G protein beta gamma subunits of agonist- or light-dependent phosphorylation of muscarinic acetylcholine receptors and rhodopsin. *J. Biol. Chem.* **267**, 2222-2227.

Haga, K., Kameyama, K., Haga, T., Kikkawa, U., Shiozaki, K. and Uchiyama, H. (1996) Phosphorylation of human m1 muscarinic acetylcholine receptors by G protein-coupled receptor kinase 2 and protein kinase C. *J. Biol. Chem.* **271**, 2776-2782.

Haga, T., Haga, K., Kameyama, K. and Nakata, H. (1993) Phosphorylation of muscarinic receptors: regulation by G proteins. *Life Sci.* **52**, 421-428.

Hamilton, S.E., Loose, M.D., Qi, M., Levey, A.I., Hille, B., McKnight, G.S., Idzerda, R.L. and Nathanson, N.M. (1997) Disruption of the m1 receptor gene ablates muscarinic receptor-dependent M current regulation and seizure activity in mice. *Proc. Natl. Acad. Sci. USA* **94**, 13311-13316.

Hamm, H.E. (1998) The many faces of G protein signalling. *J. Biol. Chem.* **273**, 669-672.

Herrera, L., Carvallo, P., Antonelli, M. and Olate, J. (1994) Cloning of a *Xenopus laevis* muscarinic receptor encoded by an intronless gene. *FEBS Lett.* **352**, 175-179.

Hersch, S.M., Gutekunst, C.A., Rees, H.D., Heilman, C.J. and Levey, A.I. (1994) Distribution of m1-m4 muscarinic receptor proteins in the rat striatum: light and electron microscopic immunocytochemistry using subtype-specific antibodies. *J. Neurosci.* **14**, 3351-3363.

Hibert, M., Trumpp-Kallmeyer, S., Bruinvels, A. and Hoflack, J. (1991) Three-dimensional models of neurotransmitter G-binding protein-coupled receptors. *Mol. Pharmacol.* **40**, 8-15.

Higgins, J.B. and Casey, P.J. (1994) In vitro processing of recombinant G protein γ subunits. Requirements for assembly of an active βγ complex. *J. Biol. Chem.* **269**, 9067-9073.

Ho, B.Y., Karschin, A., Branchek, T., Davidson, N. and Lester, H.A. (1992) The role of conserved aspartate and serine residues in ligand binding and in function of the 5-HT_{1A} receptor: a site-directed mutation study. *FEBS Lett.* **312**, 259-262.

Ho, S.N., Hunt, H.D., Horton, R.M., Pullen, J.K. and Pease, L.R. (1989) Site-directed mutagenesis by overlap extension using the polymerase chain reaction. *Gene* **77**, 51-59.

Horn, F., Weare, J., Beukers, M.W., Horsh, S., Bairoch, A., Chen, W., Edvardsen, Ø., Campagne, F. and Vriend, G. (1998) GPCRDB: an information system for G protein-coupled receptors. *Nucleic Acids Res.* **26**, 275-279.

Hosey, M.M., Benovic, J.L., DebBurman, S.K. and Richardson, R.M. (1995) Multiple mechanisms involving protein phosphorylation are linked to desensitization of muscarinic receptors. *Life Sci.* **56**, 951-955.

Högger, P., Shockley, M.S., Lameh, J. and Sadée, W. (1995) Activating and inactivating mutations in N- and C-terminal i3 loop junctions of muscarinic acetylcholine Hm1 receptors. *J. Biol. Chem.* **270**, 7405-7410.

Hulme, E.C. and Birdsall, N.J.M. (1992) Strategy and tactics in receptor-binding studies. In: Hulme, E.C., (Ed.) *Receptor-ligand interactions - a practical approach*, pp. 63-176. Oxford: IRL Press.

Hulme, E.C., Curtis, C.A., Page, K.M. and Jones, P.G. (1995) The role of charge interactions in muscarinic agonist binding, and receptor-response coupling. *Life Sci.* **56**, 891-898.

Hulme, E.C. and Curtis, C.A.M. (1998) Purification of recombinant M1 muscarinic acetylcholine receptor. *Biochem. Soc. Trans.* **26**, S361.

Hulme, E.C. and Lu, Z.-L. (1998) Scanning mutagenesis of transmembrane domain 3 of the M1 muscarinic acetylcholine receptor. *J. Physiol. Paris* **92**, 269-274.

Hwa, J., Gaivin, R., Porter, J.E. and Perez, D.M. (1997) Synergism of constitutive activity in α_1-adrenergic receptor activation. *Biochemistry* **36**, 633-639.

Ishii, I., Izumi, T., Tsukamoto, H., Umeyama, H., Ui, M. and Shimizu, T. (1997) Alanine exchanges of polar amino acids in the transmembrane domains of a platelet-activating factor receptor generate both constitutively active and inactive mutants. *J. Biol. Chem.* **272**, 7846-7854.

Javitch, J.A., Ballesteros, J.A., Weinstein, H. and Chen, J. (1998) A cluster of aromatic residues in the sixth membrane-spanning segment of the dopamine D2 receptor is accessible in the binding-site crevice. *Biochemistry* **37**, 998-1006.

Javitch, J.A., Fu, D., Chen, J. and Karlin, A. (1995) Mapping the binding-site crevice of the dopamine D2 receptor by the substituted-cysteine accessibility method. *Neuron* **14**, 825-831.

Jenkinson, D.H., Barnard, E.A., Hoyer, D., Humphrey, P.P.A., Leff, P. and Shankley, N.P. (1998) Terms and symbols in quantitative pharmacology. In: *The IUPHAR compendium of receptor characterization and classification*, 1st edn. pp. 6-20. London: IUPHAR Media.

Jones, P.G., Curtis, C.A.M. and Hulme, E.C. (1995) The function of a highly-conserved arginine residue in activation of the muscarinic M_1 receptor. *Eur. J. Pharmacol. - Mol. Pharmacol. Sect.* **288**, 251-257.

Kameyama, K., Haga, K., Haga, T., Kontani, K., Katada, T. and Fukada, Y. (1993) Activation by G protein $\beta\gamma$ subunits of β-adrenergic and muscarinic receptor kinase. *J. Biol. Chem.* **268**, 7753-7758.

Karnik, S.S. and Khorana, H.G. (1990) Assembly of functional rhodopsin requires a disulfide bond between cysteine residues 110 and 187. *J. Biol. Chem.* **265**, 17520-17524.

Katz, A., Wu, D. and Simon, M.I. (1992) Subunits $\beta\gamma$ of heterotrimeric G protein activate β2 isoform of phospholipase C. *Nature* **360**, 686-689.

Kaushal, S., Ridge, K.D. and Khorana, H.G. (1994) Structure and function in rhodopsin: the role of asparagine-linked glycosylation. *Proc. Natl. Acad. Sci. USA* **91**, 4024-4028.

Kim, J.-M., Altenbach, C., Thurmond, R.L., Khorana, H.G. and Hubbell, W.L. (1997) Structure and function in rhodopsin: rhodopsin mutants with a neutral amino acid at E134 have a partially activated conformation in the dark state. *Proc. Natl. Acad. Sci. USA* **94**, 14273-14278.

Kisselev, O., Ermolaeva, M. and Gautam, N. (1995) Efficient interaction with a receptor requires a specific type of prenyl group on the G protein γ subunit. *J. Biol. Chem.* **270**, 25356-25358.

Kisselev, O.G., Kao, J., Ponder, J.W., Fann, Y.C., Gautam, N. and Marshall, G.R. (1998) Light-activated rhodopsin induces structural binding motif in G protein α subunit. *Proc. Natl. Acad. Sci. USA* **95**, 4270-4275.

Kjeldgaard, M., Nyborg, J. and Clark, B.F.C. (1996) The GTP binding motif: variations on a theme. *FASEB J.* **10**, 1347-1368.

Klein, W.L., Nathanson, N. and Nirenberg, M. (1979) Muscarinic acetylcholine receptor regulation by accelerated rate of receptor loss. *Biochem. Biophys. Res. Commun.* **90**, 506-512.

Kobilka, B.K. and Gether, U. (1998) Examination of ligand-induced conformational changes in the β_2-adrenergic receptor by fluorescence spectroscopy. *Adv. Pharmacol.* **42**, 470-473.

Kobilka, B.K., Kobilka, T.S., Daniel, K., Regan, J.W., Caron, M.G. and Lefkowitz, R.J. (1988) Chimeric α_2-,β_2-adrenergic receptors: delineation of domains involved in effector coupling and ligand binding specificity. *Science* **240**, 1310-1316.

Koch, W.J., Hawes, B.E., Allen, L.F. and Lefkowitz, R.J. (1994) Direct evidence that G_i-coupled receptor stimulation of mitogen-activated protein kinase is mediated by $G_{\beta\gamma}$ activation of $p21^{ras}$. *Proc. Natl. Acad. Sci. USA* **91**, 12706-12710.

Koelle, M.R. (1997) A new family of G-protein regulators - the RGS proteins. *Curr. Opin. Cell Biol.* **9**, 143-147.

Koenig, J.A. and Edwardson, J.M. (1997) Endocytosis and recycling of G protein-coupled receptors. *Trends Pharmacol. Sci.* **18**, 276-287.

Kornfeld, R. and Kornfeld, S. (1985) Assembly of asparagine-linked oligosaccharides. *Annu. Rev. Biochem.* **54**, 631-664.

Krapivinsky, G., Krapivinsky, L., Wickman, K. and Clapham, D.E. (1995) $G_{\beta\gamma}$ binds directly to the G protein-gated K^+ channel, I_{KACh}. *J. Biol. Chem.* **270**, 29059-29062.

Kruegar, K.M., Daaka, Y., Pitcher, J.A. and Lefkowitz, R.J. (1997) The role of sequestration in G protein-coupled receptor resensitization. Regulation of β_2-adrenergic receptor dephosphorylation by vesicular acidification. *J. Biol. Chem.* **272**, 5-8.

Kubo, T., Bujo, H., Akiba, I., Nakai, J., Mishina, M. and Numa, S. (1988) Location of a region of the muscarinic acetylcholine receptor involved in selective effector coupling. *FEBS Lett.* **241**, 119-125.

Kubo, T., Fukuda, K., Mikami, A., Maeda, A., Takahashi, H., Mishina, M., Haga, T., Haga, K., Ichiyama, A., Kangawa, K., Kojima, M., Matsuo, H., Hirose, T. and Numa, S. (1986a) Cloning, sequencing and expression of complementary DNA encoding the muscarinic acetylcholine receptor. *Nature* **323**, 411-416.

Kubo, T., Maeda, A., Sugimoto, K., Akiba, I., Mikami, A., Takahashi, H., Haga, T., Haga, K., Ichiyama, A., Kangawa, K., Matsuo, H., Hirose, T. and Numa, S. (1986b) Primary structure of procine cardiac muscarinic acetylcholine receptor deduced from the cDNA sequence. *FEBS Lett.* **209**, 367-372.

Kunkel, M.T. and Peralta, E.G. (1993) Charged amino acids required for signal transduction by the m3 muscarinic acetylcholine receptor. *EMBO J.* **12**, 3809-3815.

Kunkel, T.A. (1998) Rapid and efficient site-specific mutagenesis without phenotype selection. *Proc. Natl. Acad. Sci. USA* **82**, 488-492.

Kurtenbach, E., Curtis, C.A., Pedder, E.K., Aitken, A., Harris, A. and Hulme, E.C. (1990) Muscarinic acetylcholine receptors. Peptide sequencing identifies residues involved in antagonist binding and disulfide bond formation. *J. Biol. Chem.* **265**, 13702-13708.

Lambright, D.G., Noel, J.P., Hamm, H.E. and Sigler, P.B. (1994) Structural determinants for activation of the α-subunit of a heterotrimeric G protein. *Nature* **369**, 621-628.

Lambright, D.G., Sondek, J., Bohm, A., Skiba, N.P., Hamm, H.E. and Sigler, P.B. (1996) The 2.0 Å crystal structure of a heterotrimeric G protein. *Nature* **379**, 311-319.

Lazareno, S., Buckley, N.J. and Roberts, F.F. (1990) Characterization of muscarinic M_4 binding sites in rabbit lung, chicken heart, and NG108-15 cells. *Mol. Pharmacol.* **38**, 805-815.

Lazareno, S., Farries, T. and Birdsall, N.J.M. (1993) Pharmacological characterization of guanine nucleotide exchange reactions in membranes from CHO cells stably transfected with human muscarinic receptors M1-M4. *Life Sci.* **52**, 449-456.

Lazareno, S., Gharagozloo, P., Kuonen, D., Popham, A. and Birdsall, N.J.M. (1998) Subtype-selective positive cooperative interactions between brucine analogues and acetylcholine at muscarinic receptors: radioligand binding studies. *Mol. Pharmacol.* **53**, 573-589.

Lechleiter, J., Hellmiss, R., Duerson, K., Ennulat, D., David, N., Clapham, D. and Peralta, E. (1990) Distinct sequence elements control the specificity of G protein activation by muscarinic acetylcholine receptor subtypes. *EMBO J.* **9**, 4381-4390.

Lee, K.B., Pals-Rylaarsdam, R., Benovic, J.L. and Hosey, M.M. (1998) Arrestin-independent internalization of the m1, m3, and m4 subtypes of muscarinic cholinergic receptors. *J. Biol. Chem.* **273**, 12967-12972.

Lee, N.H., Earle-Hughes, J. and Fraser, C.M. (1994) Agonist-mediated destabilization of m1 muscarinic acetylcholine receptor mRNA. Elements involved in mRNA stability are localized in the 3'-untranslated region. *J. Biol. Chem.* **269**, 4291-4298.

Lee, N.H. and Fraser, C.M. (1993) Cross-talk between m1 muscarinic acetylcholine and beta 2- adrenergic receptors. cAMP and the third intracellular loop of m1 muscarinic receptors confer heterologous regulation. *J. Biol. Chem.* **268**, 7949-7957.

Leppik, R.A., Miller, R.C., Eck, M. and Paquet, J.-L. (1994) Role of acidic amino acids in the allosteric modulation by gallamine of antagonist binding at the m2 muscarinic acetylcholine receptor. *Mol. Pharmacol.* **45**, 983-990.

Levey, A.I. (1993) Immunological localization of m1-m5 muscarinic acetylcholine receptors in peripheral tissues and brain. *Life Sci.* **52**, 441-448.

Levey, A.I., Edmunds, S.M., Koliatsos, V., Wiley, R.G. and Heilman, C. (1995) Expression of m1-m4 muscarinic acetylcholine receptor proteins in rat hippocampus and regulation by cholinergic innervation. *J. Neurosci.* **15**, 4077-4092.

Levis, M.J. and Bourne, H.R. (1992) Activation of the alpha subunit of G_s in intact cells alters its abundance, rate of degradation, and membrane avidity. *J. Cell Biol.* **119**, 1297-1307.

Liu, J., Conklin, B.R., Blin, N., Yun, J. and Wess, J. (1995) Identification of a receptor/G-protein contact site critical for signaling specificity and G-protein activation. *Proc. Natl. Acad. Sci. USA* **92**, 11642-11646.

Liu, J., Schöneberg, T., van Rhee, M. and Wess, J. (1996) Mutational analysis of the relative orientation of transmembrane helices I and VII in G protein-coupled receptors. *J. Biol. Chem.* **270**, 19532-19539.

Lohse, M.J., Benovic, J.L., Codina, J., Caron, M.G. and Lefkowitz, R.J. (1990) β-Arrestin: a protein that regulates β-adrenergic receptor function. *Science* **248**, 1547-1550.

Lowry, O.H., Rosebrough, N.J., Farr, A.L. and Randall, R.J. (1951) Protein measurement with folin phenol reagent. *J. Biol. Chem.* **193**, 265-275.

Lu, Z.-L., Curtis, C.A.M., Jones, P.G., Pavia, J. and Hulme, E.C. (1997) The role of the aspartate-arginine-tyrosine triad in the m1 muscarinic receptor: mutations of aspartate 122 and tyrosine 124 decrease receptor expression but do not abolish signalling. *Mol. Pharmacol.* **51**, 234-241.

Lu, Z.-L. and Hulme, E.C. (1999) The functional topography of transmembrane domain 3 of the M_1 muscarinic acetylcholine receptor, revealed by scanning mutagenesis. *J. Biol. Chem.* **274**, 7309-7315.

Ma, J.C. and Dougherty, D.A. (1997) The cation-π interaction. *Chem. Rev.* **97**, 1303-1324.

Maeda, A., Kubo, T., Mishina, M. and Numa, S. (1988) Tissue distribution of mRNAs encoding muscarinic acetylcholine receptor subtypes. *FEBS Lett.* **239**, 339-342.

Mansour, A., Meng, F., Meador-Woodruff, J.H., Taylor, L.P., Civelli, O. and Akil, H. (1992) Site-directed mutagenesis of the human dopamine D_2 receptor. *Eur. J. Pharmacol. - Mol. Pharmacol. Sect.* **227**, 205-214.

Matsui, H., Lazareno, S. and Birdsall, N.J.M. (1995) Probing of the location of the allosteric site on m1 muscarinic receptors by site-directed mutagenesis. *Mol. Pharmacol.* **47**, 88-98.

McLatchie, L.M., Fraser, N.J., Main, M.J., Wise, A., Brown, J., Thompson, N., Solari, R., Lee, M.G. and Foord, S.M. (1998) RAMPs regulate the transport and ligand specificity of the calcitonin-receptor-like receptor. *Nature* **393**, 333-339.

Melchiorre, C., Minarini, A., Budriesi, R., Chiarini, A., Spampinato, S. and Tumiatti, V. (1995) The design of novel methoctramine-related tetraamines as muscarinic receptor subtype selective antagonists. *Life Sci.* **56**, 837-844.

Mery, P.F., Abi-Gerges, N., Vandecasteele, G., Jurevicius, J., Eschenhagen, T. and Fischmeister, R. (1997) Muscarinic regulation of the L-type calcium current in isolated cardiac myocytes. *Life Sci.* **60**, 1113-1120.

Mitchell, R., McCulloch, D., Lutz, E., Johnson, M., MacKenzie, C., Fennell, M., Fink, G., Zhou, W. and Sealfon, S.C. (1998) Rhodopsin-family receptors associate with small G proteins to activate phospholipase D. *Nature* **392**, 411-414.

Mixon, M.B., Lee, E., Coleman, D.E., Berghuis, A.M., Gilman, A.G. and Sprang, S.R. (1995) Tertiary and quaternary structural changes in $G_{i\alpha 1}$ induced by GTP hydrolysis. *Science* **270**, 954-960.

Mizobe, T., Maze, M., Lam, V., Suryanarayana, S. and Kobilka, B.K. (1996) Arrangement of transmembrane domains in adrenergic receptors. *J. Biol. Chem.* **271**, 2387-2389.

Monod, J., Wyman, J. and Changeux, J.-P. (1965) On the nature of allosteric transitions. *J. Mol. Biol.* **12**, 88-118.

Moro, O., Lameh, J., Högger, P. and Sadée, W. (1993) Hydrophobic amino acid in the i2 loop plays a key role in receptor-G protein coupling. *J. Biol. Chem.* **268**, 22273-22276.

Mumby, S.M., Kleuss, C. and Gilman, A.G. (1994) Receptor regulation of G-protein palmitoylation. *Proc. Natl. Acad. Sci. USA* **91**, 2800-2804.

Nardone, J. and Hogan, P.G. (1994) Delineation of a region in the B2 bradykinin receptor that is essential for high-affinity agonist binding. *Proc. Natl. Acad. Sci. USA* **91**, 4417-4421.

Noda, K., Saad, Y., Graham, R.M. and Karnik, S.S. (1994) The high affinity state of the β_2-adrenergic receptor requires unique interaction between conserved and non-conserved extracellular loop cysteines. *J. Biol. Chem.* **269**, 6743-6752.

Noel, J.P., Hamm, H.E. and Sigler, P.B. (1993) The 2.2 Å crystal structure of transducin-α complexed with GTPγS. *Nature* **366**, 654-663.

Nordvall, G. and Hacksell, U. (1993) Binding-site modeling of the muscarinic m1 receptor: a combination of homology-based and indirect approaches. *J. Med. Chem.* **36**, 967-976.

Northup, J.K., Smigel, M.D. and Gilman, A.G. (1982) The guanine nucleotide activating site of the regulatory component of adenylate cyclase. Identification by ligand binding. *J. Biol. Chem.* **257**, 11416-11423.

Ohara, K., Uchiyama, H., Haga, T. and Ichiyama, A. (1990) Interaction of deglycosylated muscarinic receptors with ligands and G proteins. *Eur. J. Pharmacol. - Mol. Pharmacol. Sect.* **189**, 341-346.

Okamoto, T. and Nishimoto, I. (1992) Detection of G protein-activator regions in M_4 subtype muscarinic, cholinergic, and α_2-adrenergic receptors based upon characteristics in primary structure. *J. Biol. Chem.* **267**, 8342-8346.

Okayama, H. and Berg, P. (1982) High-efficiency cloning of full-length cDNA. *Mol. Cell. Biol.* **2**, 161-170.

Okayama, H. and Berg, P. (1983) A cDNA cloning vector that permits expression of cDNA inserts in mammalian cells. *Mol. Cell. Biol.* **3**, 280-289.

Oldham, K.G. (1990) Polyphosphoinositide turnover. In: Hulme, E.C., (Ed.) *Receptor-effector coupling - a practical approach*, pp. 99-116. Oxford: IRL Press.

Onrust, R., Herzmark, P., Chi, P., Garcia, P.D., Lichtarge, O., Kingsley, C. and Bourne, H.R. (1997) Receptor and $\beta\gamma$ binding sites in the α subunit of the retinal G protein transducin. *Science* **275**, 381-384.

Ovchinnikov, Y.A., Abdulaev, N.G. and Bogachuk, A.S. (1988) Two adjacent cysteine residues in the C-terminal cytoplasmic fragment of bovine rhodopsin are palmitoylated. *FEBS Lett.* **230**, 1-5.

Page, K.M., Curtis, C.A.M., Jones, P.G. and Hulme, E.C. (1995) The functional role of the binding site aspartate in muscarinic acetylcholine receptors, probed by site-directed mutagenesis. *Eur. J. Pharmacol. - Mol. Pharmacol. Sect.* **289**, 429-437.

Palczewski, K., Hargrave, P.A., McDowell, J.H. and Ingebritsen, T.S. (1989b) The catalytic subunit of phosphatase 2A dephosphorylates phosphoopsin. *Biochemistry* **28**, 415-419.

Palczewski, K., McDowell, J.H., Jakes, S., Ingebritsen, T.S. and Hargrave, P.A. (1989a) Regulation of rhodopsin dephosphorylation by arrestin. *J. Biol. Chem.* **264**, 15770-15773.

Pals-Rylaarsdam, R., Gurevich, V.V., Lee, K.B., Ptasienski, J.A., Benovic, J.L. and Hosey, M.M. (1997) Internalization of the m2 muscarinic acetylcholine receptor. Arrestin-independent and -dependent pathways. *J. Biol. Chem.* **272**, 23682-23689.

Pals-Rylaarsdam, R. and Hosey, M.M. (1997) Two homologous phosphorylation domains differentially contribute to desensitization and internalization of the m2 muscarinic acetylcholine receptor. *J. Biol. Chem.* **272**, 14152-14158.

Parker, E.M., Kameyama, K., Higashijima, T. and Ross, E.M. (1991) Reconstitutively active G protein-coupled receptors purified from baculovirus-infected insect cells. *J. Biol. Chem.* **266**, 519-527.

Pemberton, K.E. and Jones, S.V.P. (1997) Inhibition of the L-type calcium channel by the five muscarinic receptors (m1-m5) expressed in NIH 3T3 cells. *Pflügers Arch. - Eur. J. Physiol.* **433**, 505-514.

Peralta, E.G., Ashkenazi, A., Winslow, J.W., Smith, D.H., Ramachandran, J. and Capon, D.J. (1987) Distinct primary structures, ligand binding properties and tissue-specific expression of four human muscarinic acetylcholine receptors. *EMBO J.* **6**, 3923-3929.

Pitcher, J.A., Payne, E.S., Csortos, C., DePaoli-Roach, A.A. and Lefkowitz, R.J. (1995) The G-protein-coupled receptor phosphatase: a protein phosphatase type 2A with a distinct subcellular distribution and substrate specificity. *Proc. Natl. Acad. Sci. USA* **92**, 8343-8347.

Pogozheva, I.D., Lomize, A.L. and Mosberg, H.I. (1997) The transmembrane 7-α-bundle of rhodopsin: distance geometry calculations with hydrogen bonding constraints. *Biophys. J.* **72**, 1963-1985.

Pollock, N.J., Manelli, A.M., Hutchins, C.W., Steffey, M.E., MacKenzie, R.G. and Frail, D.E. (1992) Serine mutations in transmembrane V of the dopamine D1 receptor affect ligand interactions and receptor activation. *J. Biol. Chem.* **267**, 17780-17786.

Porter, J.E., Hwa, J. and Perez, D.M. (1996) Activation of the α_{1b}-adrenergic receptor is initiated by disruption of an interhelical salt bridge constraint. *J. Biol. Chem.* **271**, 28318-28323.

Premont, R.T., Inglese, J. and Lefkowitz, R.J. (1995) Protein kinases that phosphorylate activated G protein-coupled receptors. *FASEB J.* **9**, 175-182.

Probst, W.C., Snyder, L.A., Schuster, D.I., Brosius, J. and Sealfon, S.C. (1992) Sequence alignment of the G-protein coupled receptor superfamily. *DNA Cell Biol.* **11**, 1-20.

Qian, N.-X., Russell, M. and Johnson, G.L. (1995) Acetylcholine muscarinic receptor regulation of the RAS/RAF/MAP kinase pathway. *Life Sci.* **56**, 945-949.

Rando, R.R. (1996) Chemical biology of isoprenylation/methylation. *Biochem. Soc. Trans.* **24**, 682-687.

Rao, V.R. and Oprian, D.D. (1996) Activating mutations of rhodopsin and other G protein-coupled receptors. *Annu. Rev. Biophys. Biomol. Struct.* **25**, 287-314.

Rechsteiner, M. and Rogers, S.W. (1996) PEST sequences and regulation by proteolysis. *Trends Biochem. Sci.* **21**, 267-271.

Ringdahl, B. (1989) Structural determinants of muscarinic agonist activity. In: Brown, J.H., (Ed.) *The muscarinic receptors*, pp. 151-218. Clifton, New Jersey: The Humana Press.

Ripoll, D.R., Faerman, C.H., Axelsen, P.H., Silman, I. and Sussman, J.L. (1993) An electrostatic mechanism for substrate guidance down the aromatic gorge of acetylcholinesterase. *Proc. Natl. Acad. Sci. USA* **90**, 5128-5132.

Robinson, P.R., Cohen, G.B., Zhukovsky, E.A. and Oprian, D.D. (1992) Constitutively active mutants of rhodopsin. *Neuron* **9**, 719-725.

Sadeghi, H.M., Innamorati, G., Dagarag, M. and Birnbaumer, M. (1997) Palmitoylation of the V_2 vasopressin receptor. *Mol. Pharmacol.* **52**, 21-29.

Sakuta, H., Sekiguchi, M., Okamoto, K. and Sakai, Y. (1991) Oscillatory muscarinic acetylcholine responses of *Xenopus* oocytes are desensitized by protein kinase C and sensitized by protein phosphatase 2B. *Eur. J. Pharmacol. - Mol. Pharmacol. Sect.* **208**, 297-305.

Samama, P., Cotecchia, S., Costa, T. and Lefkowitz, R.J. (1993) A mutation-induced activated state of the β_2-adrenergic receptor. *J. Biol. Chem.* **268**, 4625-4636.

Sanger, F., Nicklen, S. and Coulson, A.R. (1977) DNA sequencing with chain-terminating inhibitors. *Proc. Natl. Acad. Sci. USA* **74**, 5463-5467.

Savarese, T.M., Wang, C.-D. and Fraser, C.M. (1992) Site-directed mutagenesis of the rat m_1 muscarinic acetylcholine receptor: role of conserved cysteines in receptor function. *J. Biol. Chem.* **267**, 11439-11448.

Scheer, A. and Cotecchia, S. (1997) Constitutively active G protein-coupled receptors: potential mechanisms of receptor activation. *J. Recept. Signal Transduc. Res.* **17**, 57-73.

Scheer, A., Fanelli, F., Costa, T., De Benedetti, P.G. and Cotecchia, S. (1997) The activation process of the α_{1B}-adrenergic receptor: potential role of protonation and hydrophobicity of a highly conserved aspartate. *Proc. Natl. Acad. Sci. USA* **94**, 808-813.

Schmidt, M.F. (1989) Fatty acylation of proteins. *Biochim. Biophys. Acta* **988**, 411-426.

Schulman, J.M., Sabio, M.L. and Disch, R.L. (1983) Recognition of cholinergic agonists by the muscarinic receptor. 1. Acetylcholine and other agonists with the NCCOCC backbone. *J. Med. Chem.* **26**, 817-823.

Schwarz, R.D., Spencer, C.J., Jaen, J.C., Mirzadegan, T., Moreland, D., Tecle, H. and Thomas, A.J. (1995) Mutations of aspartate 103 in the Hm2 receptor and alterations in receptor binding properties of muscarinic agonists. *Life Sci.* **56**, 923-929.

Scrutton, N.S. and Raine, A.R.C. (1996) Cation-π bonding and amino-aromatic interactions in the biomolecular recognition of substituted ammonium ligands. *Biochem. J.* **319**, 1-8.

Shapiro, R.A. and Nathanson, N.M. (1989) Deletion analysis of the mouse m1 muscarinic acetylcholine receptor: effects on phosphoinositide metabolism and down-regulation. *Biochemistry* **28**, 8946-8950.

Shapiro, R.A., Wakimoto, B.T., Subers, E.M. and Nathanson, N.M. (1989) Characterization and functional expression in mammalian cells of genomic and cDNA

clones encoding a *Drosophila* muscarinic acetylcholine receptor. *Proc. Natl. Acad. Sci. USA* **86**, 9039-9043.

Sheikh, S.P., Zvyaga, T.A., Lichtarge, O., Sakmar, T.P. and Bourne, H.R. (1996) Rhodopsin activation blocked by metal-ion-binding sites linking transmembrane helices C and F. *Nature* **383**, 347-350.

Shiozaki, K. and Haga, T. (1992) Effects of magnesium ion on the interaction of atrial muscarinic acetylcholine receptors and GTP-binding regulatory proteins. *Biochemistry* **31**, 10634-10642.

Shortle, D. (1992) Mutational studies of protein structures and their stabilities. *Q. Rev. Biophys.* **25**, 205-250.

Smrcka, A.V., Hepler, J.R., Brown, K.O. and Sternweis, P.C. (1991) Regulation of polyphosphoinositide-specific phospholipase C activity by purified G_q. *Science* **251**, 804-807.

Solberg, Y. and Belkin, M. (1997) The role of excitotoxicity in organophosphorous nerve agents central poisoning. *Trends Pharmacol. Sci.* **18**, 183-185.

Sondek, J., Bohm, A., Lambright, D.G., Hamm, H.E. and Sigler, P.B. (1996) Crystal structure of a G_A protein $\beta\gamma$ dimer at 2.1 Å resolution. *Nature* **379**, 369-374.

Spalding, T.A., Birdsall, N.J.M., Curtis, C.A.M. and Hulme, E.C. (1994) Acetylcholine mustard labels the binding site aspartate in muscarinic acetylcholine receptors. *J. Biol. Chem.* **269**, 4092-4097.

Spalding, T.A., Burstein, E.S., Bräuner-Osborne, H., Hill-Eubanks, D. and Brann, M.R. (1995) Pharmacology of a constitutively active muscarinic receptor generated by random mutagenesis. *J. Pharmacol. Exp. Ther.* **275**, 1274-1279.

Spalding, T.A., Burstein, E.S., Henderson, S.C., Ducote, K.R. and Brann, M.R. (1998) Identification of a ligand-dependent switch within a muscarinic receptor. *J. Biol. Chem.* **273**, 21563-21568.

Spalding, T.A., Burstein, E.S., Wells, J.W. and Brann, M.R. (1997) Constitutive activation of the m5 muscarinic receptor by a series of mutations at the extracellular end of transmembrane 6. *Biochemistry* **36**, 10109-10116.

Sprang, S.R. (1997) G protein mechanisms: insights from structural analysis. *Annu. Rev. Biochem.* **66**, 639-678.

Strader, C.D., Candelore, M.R., Hill, W.S., Dixon, R.A.F. and Sigal, I.S. (1989) A single amino acid substitution in the β-adrenergic receptor promotes partial agonist activity from antagonists. *J. Biol. Chem.* **264**, 16470-16477.

Strader, C.D., Fong, T.M., Tota, M.R., Underwood, D. and Dixon, R.A.F. (1994) Structure and function of G protein-coupled receptors. *Annu. Rev. Biochem.* **63**, 101-132.

Strader, C.D., Sigal, I.S., Candelore, M.R., Rands, E., Hill, W.S. and Dixon, R.A. (1988) Conserved aspartic acid residues 79 and 113 of the β-adrenergic receptor have different roles in receptor function. *J. Biol. Chem.* **263**, 10267-10271.

Strader, C.D., Sigal, I.S. and Dixon, R.A. (1989) Structural basis of β-adrenergic receptor function. *FASEB J.* **3**, 1825-1832.

Strader, C.D., Sigal, I.S., Register, R.B., Candelore, M.R., Rands, E. and Dixon, R.A.F. (1987) Identification of residues required for ligand binding to the β-adrenergic receptor. *Proc. Natl. Acad. Sci. USA* **84**, 4384-4388.

Strange, P.G. (1996) The energetics of ligand binding at catecholamine receptors. *Trends Pharmacol. Sci.* **17**, 238-244.

Strnad, J. and Hadcock, J.R. (1995) Identification of a critical aspartate residue in transmembrane domain three necessary for the binding of somatostatin to the somatostatin receptor SSTR2. *Biochem. Biophys. Res. Commun.* **216**, 913-921.

Surratt, C.K., Johnson, P.S., Moriwaki, A., Seidleck, B.K., Blaschak, C.J., Wang, J.B. and Uhl, G.R. (1994) μ opiate receptor. Charged transmembrane domain amino acids are critical for agonist recognition and intrinsic activity. *J. Biol. Chem.* **269**, 20548-20553.

Szekeres, P.G., Koenig, J.A. and Edwardson, J.M. (1998) Involvement of receptor cycling and receptor reserve in resensitization of muscarinic responses in SH-SY5Y human neuroblastoma cells. *J. Neurochem.* **70**, 1694-1703.

Tesmer, J.J.G., Berman, D.M., Gilman, A.G. and Sprang, S.R. (1997) Structure of RGS4 bound to AlF_4^--activated $G_{i\alpha 1}$: stabilization of the transition state for GTP hydrolysis. *Cell* **89**, 251-261.

Tietje, K.M., Goldman, P.S. and Nathanson, N.M. (1990) Cloning and functional analysis of a gene encoding a novel muscarinic acetylcholine receptor expressed in chick heart and brain. *J. Biol. Chem.* **265**, 2828-2834.

Tietje, K.M. and Nathanson, N.M. (1991) Embryonic chick heart expresses multiple muscarinic acetylcholine receptor subtypes. *J. Biol. Chem.* **266**, 17382-17387.

Tränkle, C., Mies-Klomfass, E., Cid, M.H.B., Holzgrabe, U. and Mohr, K. (1998) Identification of a [^{3}H]ligand for the common allosteric site of muscarinic acetylcholine M_2 receptors. *Mol. Pharmacol.* **54**, 139-145.

Trumpp-Kallmeyer, S., Hoflack, J. and Hibert, M. (1992) Modeling of G-protein-coupled receptors: application to dopamine, adrenaline, serotonin, acetylcholine, and mammalian opsin receptors. *J. Med. Chem.* **35**, 3448-3462.

Tsuga, H., Kameyama, K., Haga, T., Honma, T., Lameh, J. and Sadée, W. (1998) Internalization and down-regulation of human muscarinic acetylcholine receptor m2 subtypes. *J. Biol. Chem.* **273**, 5323-5330.

Tucek, S. and Proska, J. (1995) Allosteric modulation of muscarinic acetylcholine receptors. *Trends Pharmacol. Sci.* **16** , 205-212.

Turcatti, G., Zoffmann, S., Lowe, J.A., III, Drozdal, S.E., Chassaing, G., Schwartz, T.W. and Chollet, A. (1997) Characterization of non-peptide antagonist and peptide agonist bindign sites of the NK1 receptor with fluorescent ligands. *J. Biol. Chem.* **272**, 21167-21175.

Umemori, H., Inoue, T., Kume, S., Sekiyama, N., Nagao, M., Itoh, H., Nakanishi, S., Mikoshiba, K. and Yamamoto, T. (1997) Activation of the G protein Gq/11 through tyrosine phosphorylation of the α subunit. *Science* **276**, 1878-1881.

Unger, V.M., Hargrave, P.A., Baldwin, J.M. and Schertler, G.F.X. (1997) Arrangement of rhodopsin transmembrane α-helices. *Nature* **389**, 203-206.

van Koppen, C.J. and Nathanson, N.M. (1990) Site-directed mutagenesis of the m2 muscarinic acetylcholine receptor. *J. Biol. Chem.* **265**, 20887-20892.

van Rhee, A.M. and Jacobson, K.A. (1996) Molecular architecture of G protein-coupled receptors. *Drug Dev. Res.* **37**, 1-38.

Vogel, W.K., Sheehan, D.M. and Schimerlik, M.I. (1997) Site-directed mutagenesis on the m2 muscarinic acetylcholine receptor: the significance of Tyr403 in the binding of agonists and functional coupling. *Mol. Pharmacol.* **52**, 1087-1094.

Wade, R.C., Gabdoulline, R.R., Lüdemann, S.K. and Lounnas, V. (1998) Electrostatic steering and ionic tethering in enzyme-ligand binding: insights from simulations. *Proc. Natl. Acad. Sci. USA* **95**, 5942-5949.

Wall, M.A., Coleman, D.E., Lee, E., Iñiguez-Lluhi, J.A., Posnér, B.A., Gilman, A.G. and Sprang, S.R. (1995) The structure of the G protein heterotrimer $G_{i\alpha1}\beta_1\gamma_2$. *Cell* **83**, 1047-1058.

Wang, C.-D., Buck, M.A. and Fraser, C.M. (1991) Site-directed mutagenesis of α_{2A}-adrenergic receptors: identification of amino acids involved in ligand binding and receptor activation by agonists. *Mol. Pharmacol.* **40**, 168-179.

Wang, C.D., Gallaher, T.K. and Shih, J.C. (1993) Site-directed mutagenesis of the serotonin 5-hydroxytrypamine$_2$ receptor: identification of amino acids necessary for ligand binding and receptor activation. *Mol. Pharmacol.* **43**, 931-940.

Wang, H., Lipfert, L., Malbon, C.C. and Bahouth, S. (1989) Site-directed anti-peptide antibodies define the topography of the β-adrenergic receptor. *J. Biol. Chem.* **264**, 14424-14431.

Wedegaertner, P.B., Chu, D.H., Wilson, P.T., Levis, M.J. and Bourne, H. (1993) Palmitoylation is required for signaling functions and membrane attachment of $G_{q\alpha}$ and $G_{s\alpha}$. *J. Biol. Chem.* **268**, 25001-25008.

Wedegaertner, P.B., Wilson, P.T. and Bourne, H.R. (1995) Lipid modification of trimeric G proteins. *J. Biol. Chem.* **270**, 503-506.

Weiner, D.M., Levey, A.I. and Brann, M.R. (1990) Expression of muscarinic acetylcholine and dopamine receptor mRNAs in rat basal ganglia. *Proc. Natl. Acad. Sci. USA* **87**, 7050-7054.

Wells, J.A. (1991) Systematic mutational analysis of protein-protein interfaces. *Methods Enzymol.* **202**, 390-411.

Wells, J.W. (1992) Analysis and interpretation of binding at equilibrium. In: Hulme, E.C., (Ed.) *Receptor-ligand interactions - a practical approach*, pp. 289-395. Oxford: IRL Press.

Wenkert, D., Schöneberg, T., Merendino, J.J.Jr., Rodriguez Pena, M.S., Vinitsky, R., Goldsmith, P.K., Wess, J. and Spiegel, A.M. (1996) Functional characterization of five V2 vasopressin receptor gene mutations. *Mol. Cell. Endocrinol.* **124**, 43-50.

Wess, J. (1996) Molecular biology of muscarinic acetylcholine receptors. *Crit. Rev. Neurobiol.* **10**, 69-99.

Wess, J., Bonner, T.I., Dorje, F. and Brann, M.R. (1990) Delineation of muscarinic receptor domains conferring selectivity of coupling to guanine nucleotide-binding proteins and second messengers. *Mol. Pharmacol.* **38**, 517-523.

Wess, J., Brann, M.R. and Bonner, T.I. (1989) Identification of a small intracellular region of the muscarinic m3 receptor as a determinant of selective coupling to PI turnover. *FEBS Lett.* **258**, 133-136.

Wess, J., Gdula, D. and Brann, M.R. (1991) Site-directed mutagenesis of the m3 muscarinic receptor: identification of a series of threonine and tyrosine residues involved in agonist but not antagonist binding. *EMBO J.* **10**, 3729-3734.

Wess, J., Maggio, R., Palmer, J.R. and Vogel, Z. (1992) Role of conserved threonine and tyrosine residues in acetylcholine binding and muscarinic receptor activation. *J. Biol. Chem.* **267**, 19313-19319.

Wess, J., Nanavati, S., Vogel, Z. and Maggio, R. (1993) Functional role of proline and tryptophan residues highly conserved among G protein-coupled receptors studied by mutational analysis of the m3 muscarinic receptor. *EMBO J.* **12**, 331-338.

Whaley, B.S., Yuan, N., Birnbaumer, L., Clark, R.B. and Barber, R. (1994) Differential expression of the β-adrenergic receptor modifies agonist stimulation of adenylyl cyclase: a quantitative evaluation. *Mol. Pharmacol.* **45**, 481-489.

Yang, J., Logsdon, C.D., Johansen, T.E. and Williams, J.A. (1993) Human m3 muscarinic acetylcholine receptor carboxyl-terminal threonine resides are required for agonist-induced receptor down- regulation. *Mol. Pharmacol.* **44**, 1158-1164.

Yang, K., Farrens, D.L., Altenbach, C., Farahbakhsh, Z.T., Hubbell, W.L. and Khorana, H.G. (1996) Structure and function in rhodopsin. Cysteines 65 and 316 are in proximity in a rhodopsin mutant as indicated by disulfide bond formation and interactions between attached spin labels. *Biochemistry* **35**, 14040-14046.

Yu, H., Kono, M., McKee, T.D. and Oprian, D.D. (1995) A general method for mapping tertiary contacts between amino acid residues in membrane-embedded proteins. *Biochemistry* **34**, 14963-14969.

Zeng, F.-Y. and Wess, J. (1999) Development of a disulfide cross-linking strategy to study muscarinic receptor structure. *Life Sci.* **64**, 565.

8. Appendix: SigmaPlot fitting routines.

8.1 Fitting saturation data.

```
[Parameters]                Initial values.
PKL=0.5                     -(Log (radioligand binding affinity in nM units)).
RT=0.0026                   Total concentration of receptor binding sites (pmol/ml).
NS=0.0009                   Non-specific binding.
BGD=15                      Background radioactivity.

[Variables]                 Assay data.
LTDPM=COL(1)                Total amount of radioligand in assay (dpm).
A=COL(2)                    Concentration of non-specific ligand (nM).
DPMTOT=COL(3)               Amount of radioligand bound to the receptor (dpm).
W=1/COL(4)^2                standard error of the mean of amount bound.

[Equations]
SPACT=51                    Radioligand specific activity (Ci/mmol).
PKA=1.0
KL=10^PKL
KA=10^PKA
LT=(LTDPM-BGD)/(2220*SPACT)
MU=NS
KAPP=KL/(1+KA*A)
C1=LT+RT+(1+MU)/KAPP
C2=RT*LT
ROOT=SQRT(C1*C1-4*C2)
RL=(C1-ROOT)/2
L=(LT-RL)/(1+MU)
BTOT=RL+MU*L
F=2220*SPACT*BTOT+BGD
FIT F TO DPMTOT  WITH WEIGHT W

[Constraints]
RT>0
NS>1e-5
BGD>0

[Options]
stepsize=1
```

8.2 Fitting competition assay data (The Hill Equation).

```
[Parameters]                Initial values.
BMAX=1400                   Maximum amount of radioligand bound (dpm).
BNS=100                     Non-specific binding of radioligand (dpm).
PK=6.0                      Apparent non-radioactive ligand affinity (pIC50).
NH=0.8                      Hill coefficient.

[Variables]                 Assay data.
A=COL(1)                    Log (non-radioactive ligand concentration).
Y=COL(2)                    Radioligand bound (dpm).
W=1/COL(3)^2                Standard error of the mean of radioligand bound.

[Equations]
KXN=(10^(PK+A))^NH
F=(BMAX-BNS)/(1+KXN)+BNS
FIT F TO Y WITH WEIGHT W

[Constraints]
NH>0.3

[Options]
```

8.3 Fitting competition assay data (The two-site model of binding).

```
[Parameters]                Initial values.
BTOT=4000                   Maximum amount of radioligand bound (dpm).
BNS=100                     Non-specific binding of radioligand (dpm).
FR1=0.5                     Fraction of high affinity binding-site.
PK1=6.0                     Apparent high affinity constant (pKH).
PK2=4.0                     Apparent low affinity constant (pKL).


[Variables]                 Assay data.
A=COL(1)                    Log (non-radioactive ligand concentration).
Y=COL(2)                    Radioligand bound (dpm).
W=1/COL(3)^2                Standard error of the mean of radioligand bound.

[Equations]
RT=1.0
TEMP1=RT*FR1/(1+10^(PK1+A))
TEMP2=RT*(1-FR1)/(1+10^(PK2+A))
F=(TEMP1+TEMP2)*(BTOT-BNS) +BNS
FIT F TO Y WITH WEIGHT W

[Constraints]
```

[Options]

8.4 Fitting PI experiment data.

[Parameters]	Initial values.
PK=7.0	Ligand affinity (pEC_{50}).
NH=1.0	Hill coefficient.
RMAX=1000	Maximum phosphoinositide response (dpm).
BASAL=400	Basal phosphoinositide response (dpm).
[Variables]	Assay data.
A=COL(1)	Log (agonist concentration)
Y=COL(2)	Phosphoinositide response measured (dpm).
W=1/COL(3)^2	Standard error of phosphoinositide response.

[Equations]
KXN=(10^(PK+A))^NH
F=KXN*(RMAX-BASAL)/(1+KXN) + BASAL
FIT F TO Y WITH WEIGHT W
[Constraints]

[Options]

8.5 Efficacy calculation.

[Parameters]	Initial values.
NH=1.0	Hill coefficient.
PP0=4.11	pIC_{50} corrected with Cheng-Prusoff correction factor.
PP4=5.0	proportional of pEC_{50}.
P2=0.0	proportional to basal receptor activity.
BMAX=100	Maximum ligand binding response.
BNS=0	Non-specific binding of ligand.
[Variables]	Data to be analysed.
PA=COL(1)	-Log(concentration of ligand).
Y=COL(2)	Contains both binding and PI response experimental data.
S1=COL(3)	Contains 1 to indicate PI data in row, else 0.
S2=COL(4)	Contains 1 to indicate binding data in row, else 0.
W=1/COL(5)^2	standard error of experimental data.
[Equations]	
MAXPI=100	Maximum PI response.
BASPI=0	Minimum PI response.
RT=20	Total concentration of receptors ($[\overline{Rt}]$) with wild-type = 20 and adjusted proportionally for mutant receptors (50 % expression = 10).

```
PKG=1.14                    pK̄G

A=10^PA
P0=10^PP0

P4=10^PP4
KG=10^PKG

T1=1+P2/(P4*A)
T2=P0/P4 + (P2/KG + 1)/(P4*A)    Full equation to determine efficacy values.
;T2=P0/P4 +1/(P4*A)              Approximation to determine efficacy values (see
                                 text).

TERM1=T1*T1
TERM2=T2 + T1*(1+RT)
TEMP=sqrt(TERM2*TERM2-4*TERM1*RT)

ARGgt=(TERM2-TEMP)/(2*TERM1)
RGgt= ARGgt*P2/(P4*A)

PI= (ARGgt + RGgt)*MAXPI + BASPI

X3= (P0*A)^NH/(1+(P0*A)^NH)
BIN=  (1-X3)*BMAX + BNS

F=PI*S1+BIN*S2

FIT F TO Y WITH WEIGHT W

[Constraints]
P2>0

[Options]
stepsize=1
```

Acknowledgements.

Firstly, I would like to thank my supervisor, Dr. Ed Hulme, for all of his help, advice and patience during this project. I would also like to thank Mrs. Carol Curtis, Miss. Marie Futter, Miss. Karen Allman and Dr. Zhi-Liang Lu for all of their help and useful conversation in the laboratory and Mr. Robin Munro, in the Division of Mathematical Biology, for his help with the receptor modelling.

I also must thank my industrial supervisor, Dr. Alan Fletcher, at Merck Sharp and Dohme for supporting this project and providing all of the L-compounds. I would also like to thank Dr. Stephen Freedman for originally developing this project idea along with Dr. Ed Hulme.

Special thanks go to Mrs. Carol Curtis, Miss. Amanda Martin and Dr. Barrie Ward for proof-reading this thesis.

Finally but not least, I would like to thank my wife, Lara, and my parents for their support and encouragement throughout this project.

This project was funded by a Medical Research Council and Merck Sharp and Dohme collaborative studentship.